UNIVERSIDAD MICHOACANA DE SAN NICOLÁS DE HIDALGO

INSTITUTO DE INVESTIGACIONES QUÍMICO BIOLÓGICAS

PROGRAMA INSTITUCIONAL DE DOCTORADO EN CIENCIAS BIOLÓGICAS

OPCIÓN BIOLOGÍA EXPERIMENTAL

TÍTULO DE TESIS:

"Dilucidación del mecanismo molecular involucrado en el efecto citotóxico de ciclodipéptidos producidos por *Pseudomonas aeruginosa* sobre células HeLa"

Autor: M.C. Laura Hernández Padilla

Grado Académico a obtener: Doctora en Ciencias Biológicas opción Biología Experimental

ASESOR: D.C. Jesús Campos García

Febrero del 2021

Contenido

ÍNDICE DE TABLAS Y FIGURAS

Página

RESUMEN

El cáncer es el resultado de una disfunción generalizada de procesos celulares fundamentales, en cuyos casos se involucran oncogenes, proto-oncogenes y genes supresores de tumores, que se ven frecuentemente relacionados en el desarrollo y la progresión de este. *Pseudomonas aeruginosa* PAO1 produce los ciclodipéptidos ciclo(L-Pro-L-Tyr), ciclo(L-Pro-L-Phe), ciclo(L-Pro-L-Val), y ciclo(L-Pro-L-Leu) (PAO1-CDPs), cuyos efectos han sido implicados en la inhibición de la proliferación de líneas celulares cancerosas. Esta propuesta se encaminó a investigar el mecanismo de inhibición de la proliferación de las células cancerosas por los PAO1-CDPs, en la que se utilizó como modelo de estudio la línea de adenocarcinoma cervicouterino humano HeLa. Los estudios realizados demostraron que los PAO1-CDPs inhiben la fosforilación de las proteínas cinasas Akt en el residuo Ser473 y S6K en el residuo Thr389, induciendo apoptosis en la línea celular HeLa. Adicionalmente se encontró que el efecto citotóxico de los PAO1-CDPs se efectúa a través de la vía de señalización PI3k/Akt/mTOR mediante los complejos mTORC1 y mTORC2, de una manera dependiente de la participación del complejo TSC1/TSC2. Los resultados obtenidos en el presente estudio indican que la desregulación y comunicación cruzada de las diferentes vías de señalización en la línea celular HeLa, las cuales se asocian con su agresividad y recurrencia, fueron impactadas como blancos moleculares por los PAO1-CDPs. Lo anterior sugiere que los PAO1-CDPs pueden ser considerados como potenciales drogas antineoplásicas.

Palabras clave: Antiproliferación, Adenocarcinoma de cérvix, Proteínas cinasa, Ciclodipéptidos, Apoptosis

ABSTRACT

Cancer results from dysfunction of fundamental cellular processes, in which oncogenes, proto-oncogenes, and tumor suppressor genes are frequently involved in cancer development and progression. *Pseudomonas aeruginosa* PAO1 produces the cyclodipeptides cycle(L-Pro-L-Tyr), cycle(L-Pro-L-Phe), cycle(L-Pro-L-Val) and cycle(L-Pro-L-Leu) (PAO1-CDPs), whose effects have been implicated in inhibition of the proliferation of cancer cell lines. Our proposal aimed to investigate the mechanism of inhibition of cancer cell proliferation by PAO1-CDPs, in which the adenocarcinoma human cervical line HeLa was used as study model. The studies performed showed that PAO1-CDPs inhibits the Akt protein kinase phosphorylation at residue Ser473 and S6K at residue Thr389, inducing apoptosis in the HeLa cell line. Additionally, it was found that the cytotoxic effect of PAO1-CDPs was achieved through the PI3k/Akt/mTOR signaling pathway by the mTORC1 and mTORC2 complexes, and in a dependent manner of the participation of the TSC1/TSC2 complex. The results obtained in this study indicate that the deregulation and cross-communication of the different signaling pathways in the HeLa cell line, which are associated with their aggressiveness and recurrence, were impacted as molecular targets by PAO1-CDPs. The foregoing suggests that PAO1-CDPs can be considered as potential antineoplastic drugs.

Keywords: Antiproliferation; Cervix adenocarcinoma; Protein kinases; Cyclodipeptides, Apoptosis

1. INTRODUCCIÓN

1.1. Cáncer

La Organización Mundial de la Salud (OMS) define al cáncer como un proceso de crecimiento y diseminación incontrolados de células, que puede aparecer prácticamente en cualquier lugar del cuerpo invadiendo el tejido circundante y puede provocar metástasis en puntos distantes del organismo. Normalmente, las células humanas crecen y se dividen para formar nuevas células a medida que el cuerpo las necesita. Cuando las células normales envejecen o se dañan, son reemplazadas por células nuevas. Sin embargo, en el cáncer, este proceso ordenado se altera; a medida que las células se hacen anormales, las células viejas o dañadas sobreviven, cuando deberían morir, y células nuevas se forman cuando no son necesarias. Estas células adicionales pueden dividirse sin interrupción y pueden formar masas que se llaman tumores.

El cáncer es un padecimiento multifactorial, donde las causas de su desarrollo son el resultado de la interacción entre los factores genéticos del paciente y tres categorías de agentes externos, a saber (www.cancer.gov, National Cancer Institute, NCI):

- Carcinógenos físicos, como las radiaciones ultravioletas e ionizantes;
- Carcinógenos químicos, como el amianto, los componentes del humo de tabaco, las aflatoxinas (contaminantes de los alimentos) y el arsénico (contaminante del agua de consumo), y
- Carcinógenos biológicos, como determinados virus, bacterias y parásitos.

Debido a que el cáncer es causado por alteraciones en la expresión de un grupo de genes, también se considera que el cáncer es una enfermedad genética compleja causada principalmente por factores ambientales que producen mutaciones que afectan a genes implicados en el crecimiento y la proliferación (Alison, 2011).

Desde hace varias décadas los tumores malignos se han posicionado en los primeros sitos como causa de mortalidad a nivel mundial representando un gran desafío para las economías y sistemas de salud. México no ha sido la excepción, desde la década de 1960 el cáncer se ubicó entre las diez principales causas de muerte (Reynoso-Noverón et al., 2016), siendo en 1960 y 1970 el sexto motivo de mortalidad ascendiendo diez años después al quinto puesto, para 1990 ocupó la segunda posición hasta 2004, periodo donde descendió un lugar, mismo que ocupó hasta 2014, únicamente por debajo de las enfermedades cardíacas y la diabetes mellitus. Así mismo, la mortalidad por neoplasias fue mayor en mujeres (13.97%) que en hombres (10.74%). El 43.7% de las muertes correspondieron a población en edad productiva (15-64 años) y 54.4% a población adulta mayor (65 años o más). Tumores como los provenientes de próstata, tráquea, bronquios, pulmón y estómago son los que más afectan al género masculino representando 36.1% de los fallecimientos; mientras que los cáncer de mama y cervicouterino constituyen el 25.7% de las defunciones en lo que se refiere a población femenina (Arrieta et al., 2015). En comparación con las cifras a nivel mundial, México parece tener bajas tasas de mortalidad anual por cáncer, considerando a toda la población (70 por 100 mil habitantes), siendo de las tasas más bajas del continente americano. Sin embargo, se ha estimado que las transiciones y estilos de vida llevarán al incremento de mortalidad por neoplasias en los próximos años, llegando a tasas superiores a las observadas en Europa (mayores de 200 por 100 mil habitantes) (Karimkhani et al., 2017). Según la OMS las proyecciones de muertes por neoplasias a nivel mundial indican que del 2007 a 2030 la mortalidad aumentará en 45%, pasando de 8 millones a 11.5; además, tumores de mama, próstata y pulmón, son los de mayor impacto tanto en países desarrollados como en vías de desarrollo (Silva, 1999). Sin embargo, en países desarrollados el cáncer colorrectal es la segunda causa de muerte en mujeres, a diferencia de países en vías de desarrollo, como es el caso de México, donde el cáncer cervicouterino (CCU) ocupa esta posición (Ferlay et al., 2015)**.** A nivel mundial, el CCU es el cuarto cáncer más frecuente en la mujer (Lin et al, 2016). Se calcula que en 2018 hubo 570 000 nuevos casos, que representaron el 7.5% de la mortalidad femenina por cáncer. De las aproximadamente 311 000 defunciones por CCU que se registran cada año, más del 85% se producen en las regiones menos desarrolladas (who.int, Organización Mundial de la Salud, OMS). En México, entre el periodo comprendido en los

años 2000 al 2010, se reportaron 82 090 nuevos casos de cáncer cervicouterino, dentro de los cuales se registraron 46 173 muertes (Anaya-Ruiz et al., 2014).

Como se puede observar, la mortalidad por tumores malignos presenta un comportamiento ascendente lo que conlleva una carga económico-social para el sistema de salud, para los pacientes y sus familias (Kuri-Morales, 2011; Ríos et al., 2015). El control del cáncer requiere un esfuerzo integral; México tiene el reto de mejorar el sistema de información en salud, así como la inversión en equipos e infraestructura para su correcto diagnóstico y tratamiento.

1.1.1. Aspectos moleculares del cáncer

Los cambios genéticos que contribuyen al desarrollo del cáncer tienden a afectar en tres tipos principales de genes, los proto-oncogenes, genes supresores de tumores y genes reparadores del ADN (Vogelstein et al., 2004; Cullen, 2002).

Los proto-oncogenes regulan el crecimiento y división celular normal. Sin embargo, cuando hay mutaciones en dichos genes, se potencian sus actividades provocando el crecimiento de las células, convirtiéndose en genes causantes de cáncer (u oncogenes), al permitir a las células crecer y sobrevivivir (Campbell et al.,2012). Por otra parte, cambios o mutaciones genéticos que inactivan los genes supresores de tumores liberan a la célula de las limitaciones impuestas por dichos genes, promoviendo la división de la célula sin control.

Estas dos alteraciones, la activación de proto-oncognes e inactivación de genes supresores de tumores son comúnmente detectados en el genoma de las células tumorales. Los supresores de tumores más estudiados codifican a las proteínas Rb (asociada a retinoblastoma) y TP53 (Weinberg, 1991), los cuales funcionan como nodos de control central que rigen las decisiones de las células ya sea para proliferar o activar programas de senescencia y apoptosis, respectivamente (Hanahan et al., 2011).

Los genes reparadores del ADN son aquellos encargados de corregir los posibles errores producidos en la replicación y de reparar las alteraciones producidas por cualquier agente mutagénico, además de que están involucrados en procesos como la segregación cromosomal. Si alguno de estos genes no funciona, aparecen múltiples mutaciones en el

genoma que acaban afectando a los dos tipos anteriores, desencadenando procesos tumorales (Wood et al., 2006).

1.1.2. Características distintivas del cáncer

A pesar de la gran diversidad y plasticidad de las células cancerosas, se han establecido una serie de características distintivas comunes a todos los tipos de cáncer, las llamadas "marcas" del cáncer, que se definen como capacidades que van adquiriendo las células a medida que evolucionan desde células normales a células tumorales (Figura 3), las cuales en conjunto constituyen un principio de organización celular; cada uno de estos cambios fisiológicos representa un mecanismo de defensa exitoso para el cáncer (Hanahan et al., 2011). Algunas de las características se mencionan a continuación:

1.-Inestabilidad genética y mutaciones.- La acumulación de mutaciones puede acelerar o comprometer la supervivencia de las células ya que normalmente se monitorea su integridad genómica y sí es el caso, se fuerza a las células dañadas a entrar en procesos de senescencia o apoptosis; la adquisición de múltiples habilidades de las células cancerosas depende en gran parte de una sucesión de alteraciones en el genoma, por ejemplo, la inactivación de genes supresores de tumores (Berdasco et al., 2010) como lo es TP53, el cual es llamado el "guardian del genoma"(Lane, 1992). El desarrollo de una alta inestabilidad genética genera un gran número de mutaciones, incluyendo rearreglos cromosomales, los cuales podrían ser los orquestadores de las "características distintivas del cáncer".

2.-Promoción de la inflamación.- Las células cancerosas asociadas a una respuesta inflamatoria tiene un efecto paradójico en donde gracias a esta respuesta inflamatoria se incrementa la tumorogénesis y progresión del cáncer a través del suministro de biomoléculas al microambiente tumoral, como factores de crecimiento que sustentan la señalización proliferativa (DeNardo et al., 2010), factores proangiogénicos (Grivennikov et al., 2010), modificación de enzimas de la matrix-extracelular que facilitan la angiogénesis, invasión y metástasis; induciendo la activación de transición epitelio-mesénquima y otras vías de señalización que coadyuvan las características distintivas del cáncer.

3.-Desregulación del metabolismo energético.- La proliferación celular sin control, representa la esencia del desarrollo del cáncer, en donde no sólo se ha perdido el control de la proliferación celular, sino que también ha ocurrido un cambio en el metabolismo energético para brindar la suficiente energía para el crecimiento y división celular. Bajo condiciones anaeróbicas, se favorece la glucólisis y se envía relativamente poco piruvato a las mitocondrias. Otto Warburg observó una característica anómala en el metabolismo energético de las células cancerosas (Warburg, 1930), que consta en que limitan su metabolismo energético en gran medida a la glucólisis, incluso en ausencia de oxígeno; las células cancerosas pueden reprogramar el metabolismo de la glucosa, y, por lo tanto, su producción de energía, lo que lleva a un estado que se ha denominado "glucólisis anaeróbica".

4.-Evasión del sistema inmune.- Las células del sistema inmune reconocen y eliminan células y tejidos dañados así como células cancerosas incipientes o de tumores nacientes. Lamentablemente, de alguna manera los tumores evitan ser detectados por el sistema inmune, evitando así ser eliminados. Éste hecho parece estar relacionado con el sistema inmunocomprometido del paciente (Vajdic et al., 2009).

5.-Resistencia a la muerte celular.- La muerte por apoptosis es un proceso homeostático fundamental para mantener regulada la población de células en los tejidos; se lleva a cabo cuando las células están dañadas, especialmente cuando el daño afecta al ADN (Hengartner et al., 1994). Los mecanismos de apoptosis son altamente complejos y sofisticados e involucran una cascada de eventos moleculares que son dependientes de energía. Existen dos principales vías que desencadenan la apoptosis: La vía extrínseca o vía de receptores de muerte y la vía intrínseca o vía mitocondrial (Elmore, 2007). Sin embargo, las dos vías están ligadas y las moléculas en una vía pueden influenciar a las otras (Igney et al., 2002). Existe una amplia variedad de estímulos y condiciones, tanto a nivel fisiológico como patológico, que pueden desencadenar la apoptosis, no todas las células necesariamente mueren en respuesta al mismo estímulo (Kerr, 2002); una de las ventajas de que se logre que células cancerosas de un tumor sean enviadas a muerte celular programada por apoptosis es que las células serán fagocitadas por macrófagos, de esta manera son eliminadaas del tejido, sin causar una respuesta inflamatoria (Kurosaka et al., 2003).

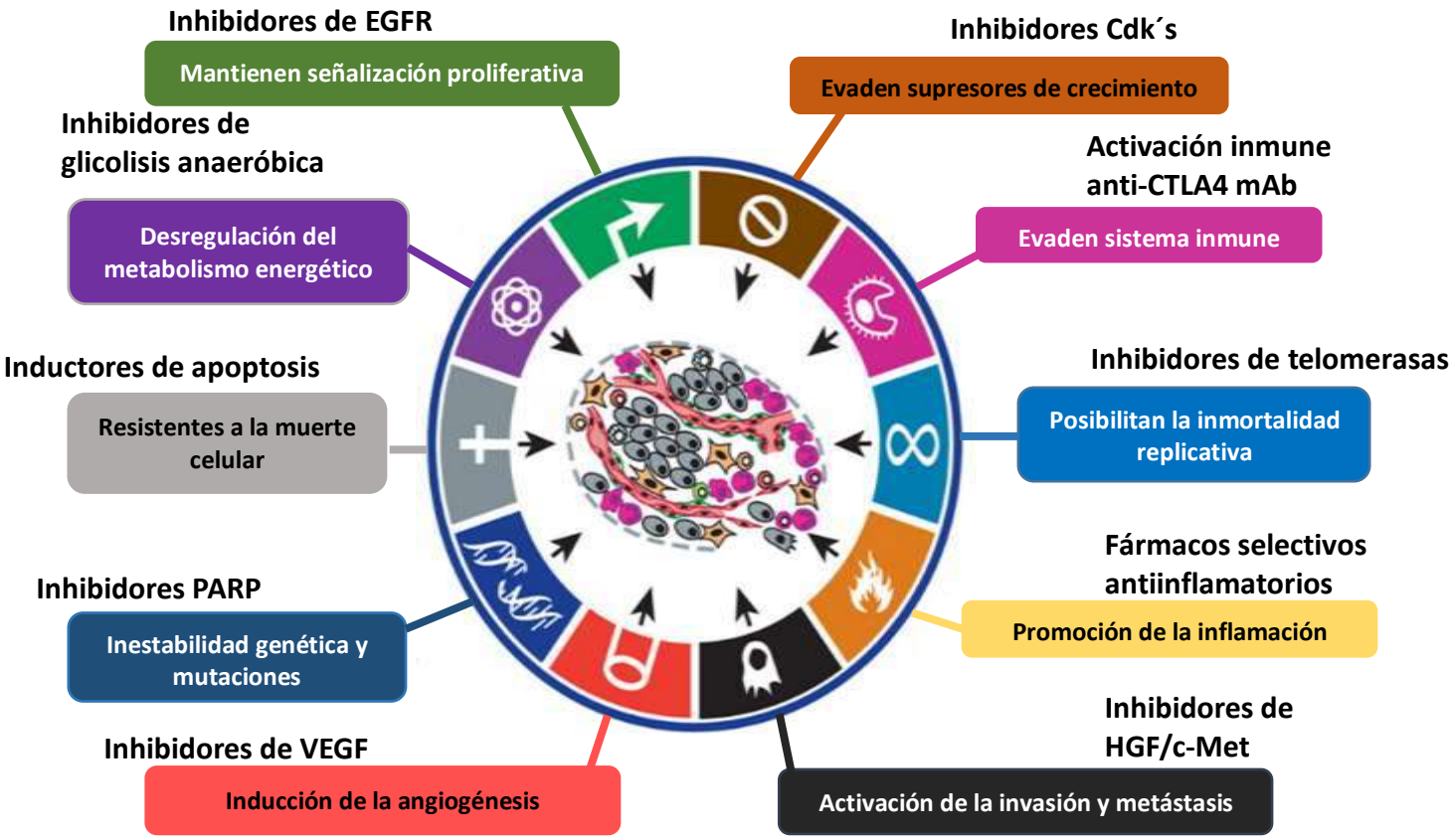

Figura 1. Características distintivas que permiten el desarrollo del cáncer

Posibles blancos terapeúticos (**Modificada de Hanahan et al., 2011**).

6.-Mantenimiento de señalización proliferativa.- Dentro de las características distintivas de las células cancerosas se encuentra su habilidad para mantener una proliferación constante (Zhu et al.,2019). Los tejidos normales controlan cuidadosamente la proliferación a través de la producción y liberación de señales promotoras del crecimiento que instruyen la progresión del ciclo celular, asegurando la homeostasis del número de células y, por lo tanto, el mantenimiento de la arquitectura y función normal del tejido. Por el contrario, las células cancerosas desregulan la señalización instruyendo a la progresión del ciclo celular constante, sin tomar en cuenta la homeostasis del número de células (Dai, et al.,2013). Las señales que activan la proliferación son transmitidas en gran parte por factores de crecimiento que se unen a los receptores de la superficie celular que típicamente contienen dominios intracelulares de tirosina cinasa.

Éstos últimos emiten señales a través de vías de señalización intracelulares que regulan la progresión del ciclo celular; a menudo estas señales influyen otras propiedades biológicas como supervivencia celular y metabolismo energético (Almendro et al.,2010).

Las células cancerosas pueden adquirir la capacidad de mantener la señalización proliferativa de formas alternas, ya sea mendiante la producción de sus propios ligandos de factores de crecimiento, a los que pueden responder mediante la expresión de receptores afines, lo que resulta en la estimulación proliferativa autocrina (Bhowmick et al., 2004).

El estudio de las "características distintivas del cáncer" brinda la oportunidad de identificar las alteraciones que permiten crecer a las células cancerosas, en este caso las vías de señalización y sus móleculas; existen varias moléculas que se encuentran en puntos control para regular las vías de señalización a los que se les conoce como biomarcadores del fenotipo canceroso, su estudio permite diseñar nuevas terapias específicas (Figura 3), siendo estos biomarcadores los posibles blancos terapéuticos.

1.1.3. Cáncer cervicouterino

El cáncer cervicouterino es una alteración celular que se origina en el epitelio del cérvix manifestándose inicialmente a través de lesiones precursoras de lenta y progresiva evolución, las cuales progresan a un cáncer *in situ* (confinado a la superficie epitelial) o un cáncer invasor, en donde las células con transformación maligna traspasan la membrana basal (Woodman et al., 2007).

El virus del papiloma humano (VPH) es el agente etiológico en el desarrollo del cáncer cervical. Sin embargo, no todas las mujeres infectadas con el VPH desarrollan cáncer cervicouterino, indicando que otros factores como alteraciones en oncogenes celulares, junto con una respuesta inmune inadecuada del hospedero (Chelimo et al., 2013) también están involucrados en la carcinogénesis cervical.

El desarrollo del cáncer cervicouterino es precedido por una serie de anomalías celulares caracterizadas citológica e histológicamente por variaciones en la maduración del citoplasma e irregularidades nucleares. La enfermedad comienza como una proliferación atípica de las células epiteliales que invaden el espesor del epitelio y degeneran en lesiones más graves

hasta invadir el estroma. La progresión de una lesión precancerosa del cuello uterino involucra varios eventos: la exposición a un VPH de alto riesgo (VPH-AR) produce una infección inicial del epitelio escamoso en la zona de transformación, seguido por alteraciones morfológicas y biológicas de las células infectadas por el VPH (Figura 2).

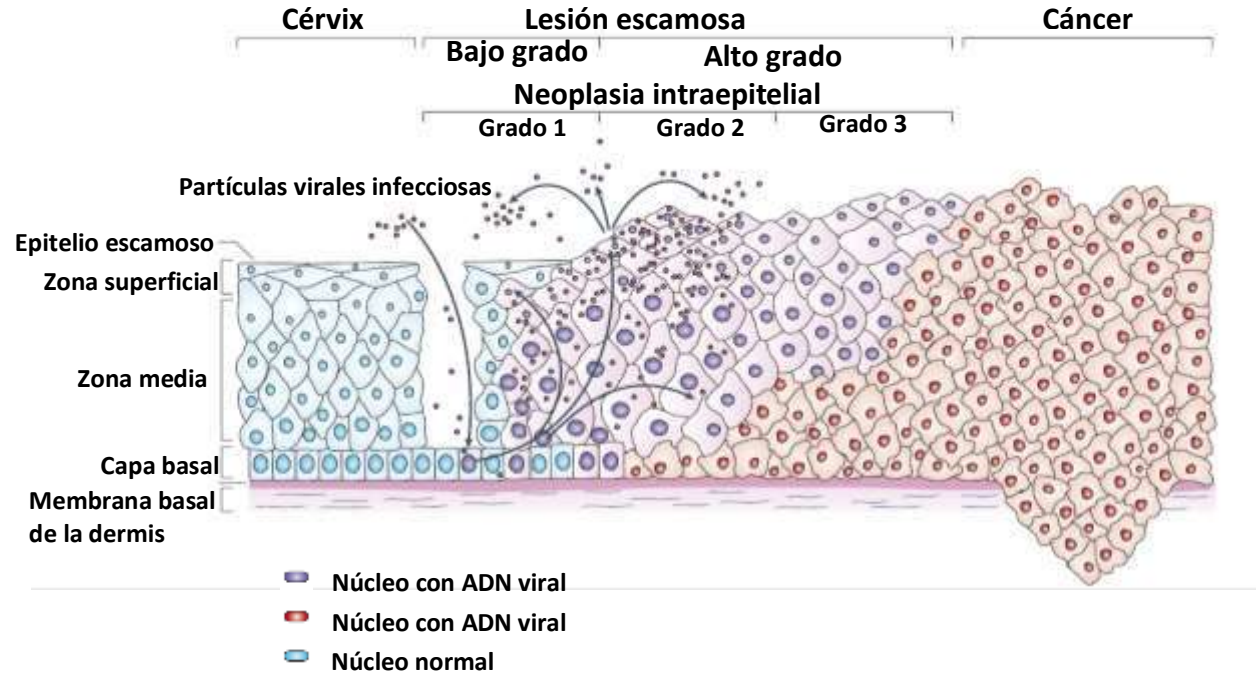

Figura 2. Desarrollo del cáncer cervicouterino

El VPH ingresa a las células basales a través de micro abrasiones en el epitelio del cuello uterino. Después de la infección, los genes tempranos del VPH E1, E2, E4, E5, E6 y E7 se expresan en las células infectadas, el genoma viral se mantiene de forma episomal (núcleos de color morado). En las capas superiores del epitelio (la zona media y la zona superficial), el genoma viral se replica con mayor intensidad, y los genes tardíos L1, L2, y E4 se expresan. La ruptura de la cápside permite la liberación del genoma viral, la formación de nuevos viriones y el inicio de una nueva infección. Las lesiones escamosas intraepiteliales de bajo grado (LEIBG) se caracterizan por una replicación viral productiva. Un número desconocido de infecciones por VPH-AR progresan a neoplasia intraepitelial cervical de alto grado. La progresión de las lesiones tratadas a cáncer microinvasor e invasivo se asocia con la integración del genoma del VPH en los cromosomas del hospedero (núcleos rojos), con la consiguiente pérdida o interrupción de E2, y la sobreregulación posterior de la expresión de los oncogenes E6 y E7. Modificado de (**Woodman et al., 2007**).

1.1.3.1. Biología molecular del cáncer cervicouterino

La integración del genoma viral al genoma celular provoca la proliferación de células epiteliales atribuyéndose esta a la expresión de los oncogenes virales, E6 y E7 (Cullen et al., 1991; Hopman et al., 2004). Las proteínas E6 estimulan la expresión de la subunidad catalítica de la telomerasa, una ADN polimerasa dependiente de ARN que mantiene los extremos cromosomales en las células somáticas proliferantes, provocando su inmortalización (Gewin et al., 2001). La influencia de la actividad de la telomerasa y la capacidad de las proteínas E6 y E7 de interferir con las funciones de p53 y pRb (proteína Retinoblastoma), respectivamente, representan las bases para el desarrollo del CCU (Oh et al., 2001; Veldman et al., 2001).

E6 se asocia con p53 (supresora de tumores) impidiendo la reparación normal de mutaciones en el genoma celular (Doorbar et al., 2006). Además, E6 se considera anti-apoptótica ya que se asocia con Bak (Thomas et al., 1998) y Bax (Li et al., 2000), dicha asociación permite que se comprometa la eficacia de la respuesta al daño en el ADN permitiendo la acumulación de mutaciones.

E7 se asocia con la proteína Rb (supresora de tumores) interrumpiendo la asociación entre la pRb y la familia de factores de transcripción E2F; el cual posteriormente transactiva a las proteínas celulares necesarias para la replicación del ADN viral, como las ciclinas A y E (Figura 2). E7 también se asocia con otras proteínas implicadas en la proliferación celular, como los inhibidores p21 y p27 de las cinasas dependientes de ciclina (CDK) (Funk et al., 1997); la capacidad de E7 para impulsar la proliferación celular depende de los niveles de p21y p27. Altos niveles de p21 y p27 puede conducir a la formación de complejos inactivos con E7 y ciclina, resultando en el bloqueo de la progresión del ciclo celular; en el caso de las células que expresan p21 y p27 a bajo nivel o que expresan suficiente E7 para superar el bloqueo a la progresión del ciclo celular progresan para desarrollar CCU (Noya et al., 2001) (Figura 2).

Si bien el mecanismo oncogénico inducido por el VPH se debe a la expresión conjunta de E6 y E7, existen otros factores que contribuyen al desarrollo carcinogénico entre los que destacan la sobreexpresión, amplificación o pérdida de función de genes.

El gen *c-myc* codifica para una proteína que actúa como regulador transcripcional y se encuentra amplificado en 32-34% de los cánceres de cérvix, lo cual se traduciría en un aumento en el crecimiento y división celular al inducir el paso de G0/G1 a S (Riou et al.,1987; Bourhis et al., 1990). Otra familia de genes que está involucrada en el desarrollo del cáncer es la familia Ras (*K-ras, H-ras y N-ras*). Ras codifica para una proteína (p21) que se localiza en la parte interna de la membrana y que actúa como un factor intercambiador de GTPasa. Las mutaciones en miembros de la familia Ras son muy frecuentes y provocan aumento en la capacidad de invasión y metástasis, así como disminución de la apoptosis. En cáncer cervical se han encontrado mutaciones en *K-ras y H-ras* del 10 al 15% (Dokianakis et al.,1998).

Otro gen supresor de tumores es el inhibidor de la apoptosis bcl-2 que se encuentra sobre expresado en linfomas y tumores epiteliales (Krajewski et al., 1993). Debido a la función de inhibir la apoptosis, la sobrexpresión de bcl-2 conlleva a la supervivencia celular y ha sido asociada con un fenotipo menos maligno. Dos estudios revelaron la sobrexpresión de bcl-2 en cáncer cervical en 61-63% y, en ambos casos, estuvo relacionado a una mayor supervivencia celular (Tjalma et al., 1997; Tjalma et al., 1998).

Además, la sobreexpresión o amplificación de diversos receptores de factores de crecimiento han sido implicados en el desarrollo del CCU. De manera particular, el receptor del factor de crecimiento epidérmico (EGFR) y Her2/neu han sido estudiados en cáncer cervical. El factor de crecimiento epidérmico es un miembro de la familia de receptores ErbB, una subfamilia relacionada con los receptores tirosina cinasa: EGFR (ErbB- 1), HER2/c-neu (ErbB-2), Her 3 (ErbB-3) y Her 4 (ErbB-4). El EGFR se encuentra en la superficie celular y se activa mediante la unión de sus ligandos, incluidos el factor de crecimiento epidérmico y el factor de crecimiento transformante alfa (TGFα) que inducen una cascada de transducción de varias señales, principalmente la Akt, MAPK y las vías de JNK, que conducen a diversos procesos celulares como la proliferación, adhesión y migración celular.

La sobreexpresión de EGFR usualmente está relacionada con la amplificación de su gen, y confiere una ventaja de crecimiento a las células. Este receptor se encuentra sobre expresado en una gran proporción de cáncer cervicouterino (Lakshmi et al., 1997). Además, el factor de crecimiento derivado de plaquetas (PDGF) es un fuerte estimulante para la formación de capilares sanguíneos y también ha sido asociado al desarrollo de cáncer cervicouterino debido a que sus ligandos se encuentran frecuentemente expresados en líneas celulares derivadas de CCU (Taja-Chayeb et al., 2006).

1.1.4. Tratamientos convencionales contra el cáncer

El diagnóstico correcto del cáncer es esencial para poder prescribir un tratamiento adecuado y eficaz, porque cada tipo de cáncer requiere un protocolo de tratamiento específico que puede abarcar una o más modalidades, tales como la cirugía, la radioterapia y la quimioterapia:

Cirugía

Consiste en la extirpación quirúrgica completa de un tumor sólido, en donde también se extrae una parte del tejido sano que rodea el tumor para garantizar que no queden remanentes de tumor que puedan seguir desarrollándose.

Radioterapia

Mediante el uso de radiaciones de alta energía como los rayos X, rayos gamma, haces de electrones o protones que pueden causar daño a las células cancerosas retrasando su división ó eliminándolas por completo. Generalmente es un tratamiento de aplicación local, sin embargo, puede administrarse de diferentes maneras, por ejemplo; radiación externa donde se usa una máquina que dirige los rayos desde fuera del cuerpo hacia el tumor; la radiación interna o braquiterapia en donde se coloca una fuente de radiación dentro o cerca del tumor en el cuerpo y; la radiación sistémica que administra medicamentos radiactivos vía oral o intravenosa.

Quimioterapia

Consiste en el uso de medicamentos para tratar cualquier enfermedad de manera sistémica. Actualmente se usan más de 100 medicamentos en el tratamiento contra el cáncer. Estos son diferentes en su composición química, administración y efecto y actúan sobre las células cancerosas en diferentes etapas del ciclo celular. Algunos ejemplos de quimioterapéuticos comúnmente empleados para tratar el cáncer cervicouterino son Topotecan, Paclitaxel, Vinorelbina, Gemcitabina, entre otros (Monk et al., 2009).

El problema de la radiación y la quimioterapia es que suelen ser altamente tóxicos con un amplio espectro de efectos secundarios (ej. anemia, alopecia, infertilidad, delirio, diarrea, dolor, edema, fatiga y nauseas) debido a que no son específicos, actuando en cualquier célula prolífica, sin diferenciar una célula sana de una maligna (Miller et al., 2019).

En la mayoría de los casos de cáncer se han encontrado múltiples alteraciones genéticas que los hacen difíciles de tratar con un solo tipo de fármaco. Dependiendo del mecanismo del efecto anticanceroso, los fármacos pueden ser categorizados como citotóxicos y citostáticos. Diversos tipos de fármacos han sido investigados para la terapia contra el cáncer, en el que sus blancos de acción incluyen genes, citocinas, anticuerpos y proteínas (Lengauer et al., 1998). Un ejemplo de ello son las tirosina cinasas, las cuales están frecuentemente desreguladas en células cancerosas, haciéndolos blancos terapéuticos atractivos; dentro de este contexto, el fármaco Wortmannin, un metabolito fúngico, es un potente inhibidor de la cinasa PI3-K (West, et al., 2002). Por el hecho de que Wortmannin es inestable en soluciones acuosas se necesitan desarrollar derivados más estables. Otro ejemplo es el StI571, el cual es un inhibidor de Akt que causa desregulación transcripcional de las proteínas antiapoptóticas Bcl-2 y c-IAP *in vitro* (West et al., 2002).

1.2. Mecanismos de muerte celular

Es de suma importancia caracterizar las vías involucradas en la muerte celular para poder entender las patologías que se presentan en el cáncer. Existen dos mecanismos principales de muerte, la necrosis y la apoptosis. Aunque, en realidad, el espectro biológico de los tipos de muerte es mucho más diverso como se describe abajo.

1.2.1. Necrosis

La necrosis es un tipo de muerte celular resultante de perturbaciones ambientales, se refiere a un proceso degradativo en el que la célula sufre cambios morfológicos como son formación de vacuolas citoplasmáticas, ruptura de la mitocondria, disgregación de los ribosomas y ruptura de los lisosomas con la posterior ruptura de la membrana celular (Fink et al., 2005). Esta pérdida de integridad de la membrana hace que se libere el contenido citoplasmático a la células vecinas, con lo que eventualmente se desencadena una respuesta inflamatoria en el tejido (Elmore, 2007).

1.2.2. Necroptosis

Desde el punto de vista morfológico se asemeja a la necrosis, ya que ambas se caracterizan por edema de la célula y los organulos, liberación de enzimas lisosómicas y, en último término, rotura de la membrana plasmática. El proceso de necroptosis se inicia de manera similar a la forma extrínseca de apoptosis, es decir, por la unió de un ligando a su receptor (TNFR1) (Holler et al., 2000). En la necroptosis intervienen al menos dos cinasas, llamadas cinasas asociadas a receptores 1 y 3 (RIP1 Y RIP3) las cuales son reclutadas por el TNFR1 desencadenándose la permeabilización de membranas lisosomicas, generación de especies reactivas de oxígeno y afectación mitocondrial (Christofferson et al., 2010).

1.2.3. Autofagia

El término autofagia fue introducido por De Duve y Wattiaux (1966), quienes definieron el proceso de vacuolización para el transporte del material intracelular a los lisosomas para su degradación. En estados de carencia de nutrientes, la célula desnutrida sobrevive canibalizándose a sí misma y reciclando el contenido digerido. La autofagia interviene en diversos estados fisiológicos (ej. ejercicio y envejecimiento) y en procesos patológicos (Chen

et al., 2016). En este proceso, los organelos intracelulares y porciones del citosol son primeramente secuestrados del citoplasma en vacuolas autofágicas formada por regiones del retículo endoplasmático rugoso libres de ribosomas, en donde ocurre elongación de la vesícula, maduración del autofagosoma, fusión de éste con los lisosomas, y por último degradación del contenido. Se han identificado más de una docena de genes relacionados con la autofagia; llamados Atg, cuyos productos son necesarios para formar el autofagosoma (Edinger et al., 2004; Yao et al., 2015).

1.2.4. Piroptosis

A diferencia de la apoptosis que inhibe la respuesta inflamatoria, la piroptosis es un tipo de muerte celular proinflamatoria, la cual depende de la caspasa 1, y no está involucrada en la muerte celular apoptótica. Una función importante de la caspasa 1 es el procesamiento de las proformas de citocinas inflamatorias IL-1β e IL-18 a sus formas activas (Maltez et al., 2015). Se ha visto la participación de la caspasa 1 durante la muerte celular en los sistemas inmunológico, nervioso central y cardiovascular (Liu et al., 2017; Fink et al., 2005).

1.2.5. Apoptosis

Kerr et al. en 1972 propusieron el término "apoptosis" (en griego "caída de hojas"), que se refiere al carácter "secuencial y ordenado" de este proceso, para describir una forma morfológicamente distinta de muerte celular, con características bioquímicas y genéticas específicas.

La muerte por apoptosis es un proceso homeostático fundamental para mantener regulada la población de células en los tejidos. Así mismo, la apoptosis ocurre cuando las células están dañadas sin remisión, especialmente cuando el daño afecta a su ADN (Hengartner et al., 1994). Existe una amplia variedad de estímulos y condiciones, tanto a nivel fisiológico como patológico, que pueden desencadenar la apoptosis, y no todas las células mueren necesariamente en respuesta al mismo estímulo (Kerr et al., 2002).

Desde el punto de vista morfológico, las células apoptóticas se caracterizan por la contracción celular, la ruptura de las uniones celulares por desmosomas, el incremento de la condensación del citoplasma, aparecen pequeñas evaginaciones esféricas surgidas a partir de la membrana que se denominan "blebs", se condensa la cromatina en la periferia del núcleo, la posterior fragmentación del mismo, el hinchamiento del retículo endoplasmático y de las mitocondrias

y, finalmente, la formación de cuerpos apoptóticos que serán fagocitados por macrófagos, de esta manera los cuerpos apóptoticos son eliminados del tejido, sin causar una respuesta inflamatoria. Estos cambios morfológicos son una consecuencia de los eventos bioquímicos que ocurren dentro de una célula apoptótica (Evan et al., 1998; Kurosaka et al., 2003).

Las características bioquímicas más destacadas de la apoptosis son: la activación de unas proteasas denominadas caspasas, la ruptura de ADN en fragmentos oligonucleosomales, el desacoplamiento de la cadena de transporte electrónico, generación de radicales libres, la disminución del potencial de membrana mitocondrial y la pérdida de la asimetría de la membrana citoplasmática, exponiéndose la fosfatidilserina en la superficie celular. El punto de no regreso en la apoptosis es cuando las caspasas comienzan a ser enzimáticamente activas uniéndose a sus proteínas blanco (las ejecutoras de la apoptosis) (Hengartner, 2000).

Los mecanismos de apoptosis son complejos y sofisticados, e involucran una cascada de eventos moleculares que son dependientes de energía. Existen dos vías principales de apoptosis: La vía extrínseca o vía de receptores de muerte y la vía intrínseca o vía mitocondrial (Elmore, 2007). Sin embargo, las dos vías están ligadas y las moléculas en una vía pueden influenciar a otras (Igney et al., 2002).

1.2.5.1. Caspasas

Las caspasas (proteasas específicas de aspartato dependiente de cisteína) son una familia de proteasas que contienen cisteína en sus sitios activos. Desde el descubrimiento de la primer caspasa en 1993, se han identificado al menos 10 caspasas en humanos. Todas las caspasas se unen específicamente justo en el carbono terminal del ácido aspártico. En la célula existen en forma de zimógenos que necesitan activación proteolítica para desencadenar la apoptosis (Fisher, 1994).

Las diez caspasas humanas (caspasas 2, 8, 9, 10, 3, 6, 7, 1, 4 y 5) identificadas han sido categorizadas como iniciadoras (caspasas 2, 8, 9, 10), las cuales tienen un pro dominio largo; las caspasas 8 y 10 poseen un dominio de muerte (DED) y un dominio de reclutamiento (CARD); en el caso de las caspasas 9 y 2, éstas son reclutadas por este pro dominio para luego ser activadas en complejos por la acción de un ligando en los receptores de muerte en

la superficie celular (Elmore, 2007). Las caspasas efectoras (3, 6, 7) tienen un pro dominio corto al igual que las caspasas inflamatorias (1, 4, 5) (Cohen, 1997).

Se considera que la caspasa efectora 3 es la más importante, ya que activa específicamente a la endonucleasa CAD. En células normales CAD se encuentra en complejo con su inhibidor ICAD. En células apoptóticas, la caspasa 3 en su forma activa se une a ICAD liberando a CAD. Posteriormente, CAD degrada el ADN cromosomal y causa condensación de la cromatina (Sakahira et al., 1998).

1.2.5.2. Vía extrínseca o mediada por receptor

La vía extrínseca de la apoptosis se origina con los receptores pertenecientes a la familia de los receptores del factor de necrosis tumoral (TNF), una superfamilia de genes que incluyen FAS/CD95, TNF-R1, DR-3, TRAIL-R1, TRAIL-R2, DR-6, EDA-R, DF-5 y p75NTR, denominados genéricamente receptores de muerte (DR). Esta familia de receptores presentan dominios extracelulares con motivos ricos en cisteína, una región transmembrana y una cola intracitoplasmática en la que destaca el dominio de muerte (DD) que le permite reconocer a su ligando con especificidad, dando como resultado la trimerización y activación del respectivo receptor de muerte (Naismith et al., 1998; Ashkenazi, 2002). Esta unión, conlleva a la interacción de los DD con otros dominios DD presentes en proteínas adaptadoras como FADD/MORT1 O TRADD (Chinnaiyan et al., 1995). Estas proteínas adaptadoras presentan a su vez dominios efectores de muerte (DED) que interaccionan con los DED de la procaspasa 8, generándose un complejo multimérico denominado complejo de la señal inductora de muerte (DISC), que permite la activación de la procaspasa y desencadena el comienzo de la apoptosis. Ésta última, procesa la caspasa efectora 3 la cual subsecuentemente ejecuta la muerte celular y las características bioquímicas usualmente observadas (Figura 4) (Kischkel et al., 1995).

1.2.5.3. Vía intrínseca o mediada por la mitocondria

En respuesta a señales apoptóticas, los miembros de la familia Bcl-2 alteran la permeabilidad de la membrana mitocondrial. Estas proteínas son capaces de formar canales en la membrana mitocondrial externa, produciendo cambios en el potencial de membrana mitocondrial, liberación de citocromo c y producción de especies reactivas de oxígeno (Salvesen et al., 2002).

La vía intrínseca o mediada por la mitocondria puede desencadenarse por varios factores como el daño al ADN, la hipoxia o la deprivación de factores de crecimiento, y en esta vía la mitocondria desempeña un papel crucial. Estos desencadenantes modifican el equilibrio entre miembros proapoptóticos (Bax o Bak) y antiapoptóticos (Bcl-2 o Bcl-x), se altera la permeabilidad de la membrana mitocondrial y se liberan diversos factores proapoptóticos como citocromo c, por lo que la proteína activadora de caspasas Apaf-1 se une al citocromo c y, en presencia de ATP o dATP, promueve la activación de la procaspasa 9 lo que desencadena la activación de otras caspasas efectoras como la caspasa 3 (Enari et al., 1998)

Además esta vía involucra a la procaspasa 9, la cual es activada por eventos proapoptóticos mitocondriales que forman el apoptosoma, el cual es un complejo proteico de señal de muerte dependiente de ATP, que se forma en el citosol debido a la liberación de citocromo c desde el espacio intermembranal de la membrana mitocondrial (Salvesen et al., 2002). En este caso, es la dimerización de la procaspasa 9 en este complejo que da como resultado la activación de la caspasa 9 (Denault et al., 2002). Una vez que la caspasa iniciadora es activada, puede activar proteolíticamente a caspasas efectoras como la procaspasa 3, la cual subsecuentemente proteoliza a diferentes sustratos proteicos como ICAD, y de esta manera amplifican la señal de muerte que finaliza con la ejecución de la muerte celular y sus características bioquímicas usualmente observadas (Earnshaw et al., 1999).

La apoptosis es un evento crítico para proteger la homeostasis tisular que asegura el estado de salud de los organismos, de manera que la supresión o sobreexpresión de la apoptosis está asociada con la presentación de algunas enfermedades como el cáncer (Björkerud et al., 1996; Thatte et al., 1997). Dado que en muchos tumores malignos la apoptosis está inhibida, la mayoría de las células malignas muestran cambios en la expresión, mutación o deleción de oncogenes y genes supresores de tumores como: bcl-2, p53, ras, Akt. Otras, en el ligando de

Fas y en los receptores TNF, o bien cambios en la actividad de las caspasas, lo que modifica el programa genético de muerte (Cory et al., 1999).

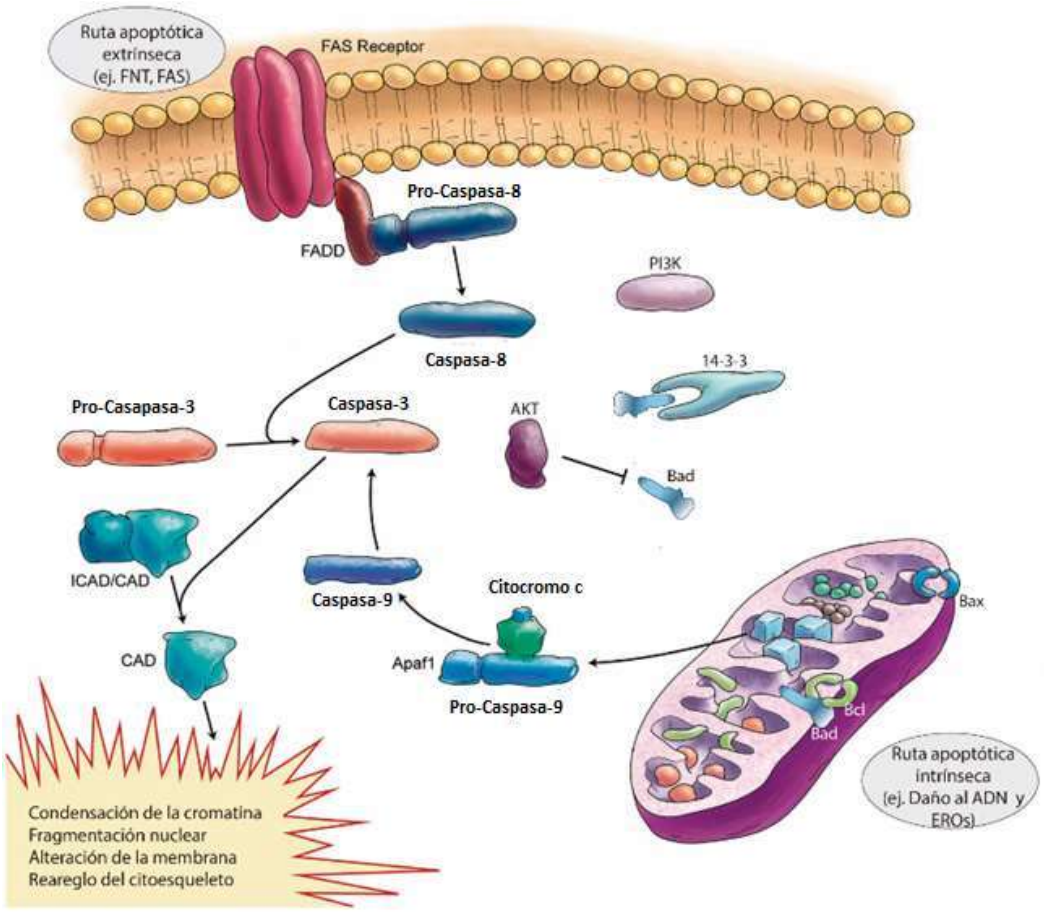

Figura 3. Vías de inducción de apoptosis

Vía extrínseca: Se puede observar la activación de receptores, así como la unión de un ligando de muerte (FasL) a su receptor específico (Fas) en la superficie celular. Los ligandos de muerte son constitutivamente homotriméricos y la unión a sus receptores conduce a la formación de un complejo homotrimérico mínimo ligando-receptor, que recluta factores citosólicos, tales como FADD y procaspasa 8. **Vía intrínseca**: En ausencia de un factor trófico, se inhibe la actividad cinasa de PI3K, que conduce a la inactivación de la cinasa Akt corriente abajo, que a su vez inactiva a Bad evitándose la formación del complejo con la proteína 14-3-3, por lo que Bad se une a las proteínas antiapoptóticas Bcl-2 y Bcl-xl, insertas en la membrana mitocondrial. La unión de Bad impide que las proteínas antiapoptóticas interactúen con Bax, una proteína proapoptótica unida a la membrana. Como consecuencia, Bax forma canales permitiendo la liberación de citocromo c al citosol, donde se une a la proteína adaptadora Apaf-1 estimulando la cascada de caspasas e induciendo muerte celular. Modificado de **Marzban, *et al.*, 2015**.

1.3. Vías de señalización implicadas en cáncer

El cáncer es causado por alteraciones en grupos de genes, por lo tanto, se considera que el cáncer es una enfermedad genética compleja causada principalmente por mutaciones que afectan a genes implicados en el crecimiento y proliferación (Alison et al., 2001). En este sentido, las señales supresoras de tumores y oncogénicas que están principalmente involucradas son PI3K, Akt, Ras, Raf, TRK, NF1, LKN1, PTEN, p53, TSC1 y TSC2 (Laplante et al., 2012; Borders et al., 2010) (Figura 5).

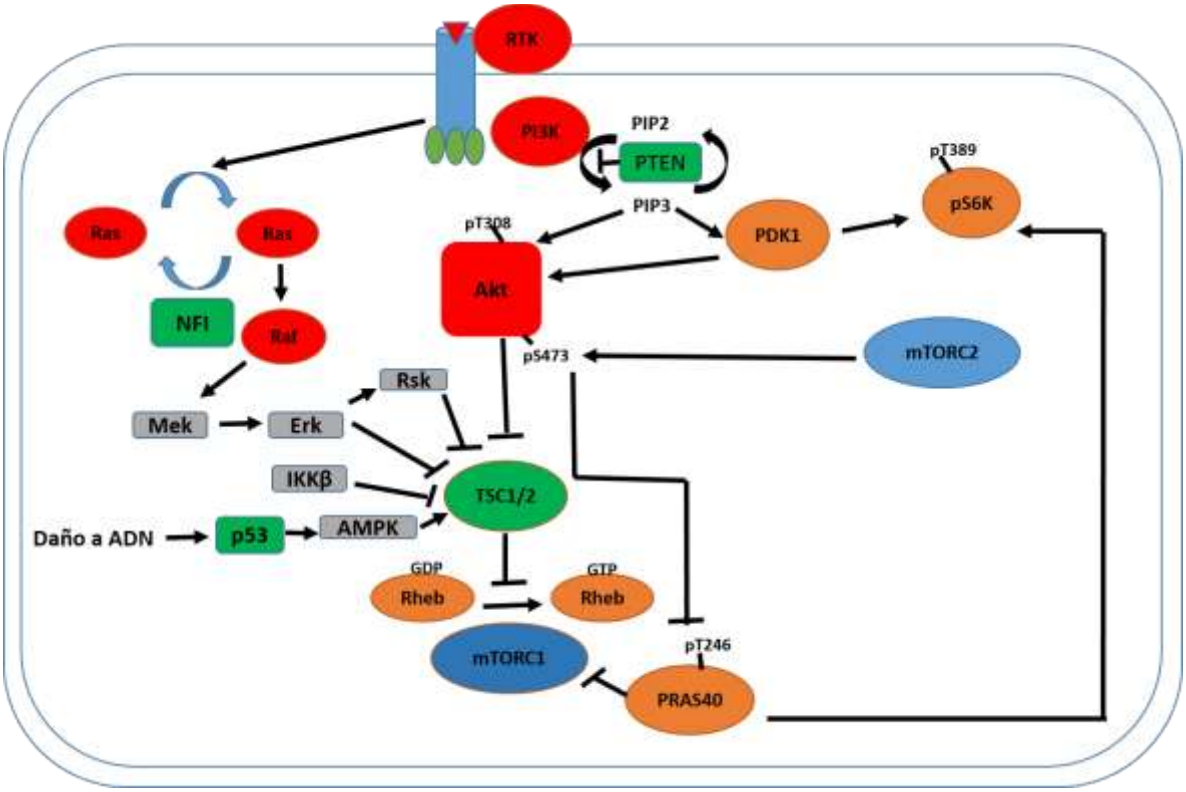

Figura 4. Nodos de señalización clave que regulan mTORC1 y mTORC2

En esta figura, las proteínas representadas en rojo son oncogenes, y las de color verde son supresores de tumores. Modificado de **Laplante et al., 2012**.

Los análisis de secuenciación de genomas de células cancerosas han revelado mutaciones somáticas en varios tipos de cáncer, que predicen la activación constitutiva de circuitos de señalización y esta activación es generalmente desencadenada por la activación de factores de crecimiento; por ejemplo, se han encontrado en distintos tipos de tumores mutaciones en la subunidad catalítica de las isoformas de fosfoinositol 3-cinasa (PI3K), lo que resulta en la hiperactivación de la vía de señalización PI3K, así como de la vía de señalización PI3K/Akt/mTOR (Ren et al., 2009; Yuan et al., 2008).

1.3.1. Vía de señalización PI3K/Akt/mTOR

La vía PI3K/Akt/mTOR regula diversos procesos celulares por lo que está implicada en un gran número de condiciones patológicas, incluyendo obesidad, diabetes, neurodegeneración y cáncer (Laplante et al., 2012). Se activa por diversas señales extracelulares, como factores de crecimiento (IGF-1, PDGF, IRS-1) que ejercen su acción a través de receptores con actividad de tirosina cinasa (RTKs) y otros, como PKC, SHP1, Rac, Rho y Src (Jiang et al., 2008). PI3K consta de dos subunidades; la subunidad regulatoria p85 y la subunidad catalítica p110. Cuando p85 es reclutada en la membrana, se une a p110 y cataliza la síntesis de PIP3, que se une a proteínas como Akt. Una vez en la membrana, Akt sufre un cambio conformacional que facilita la fosforilación en Thr308 por PDK1 y en Ser473 por mTORC2, para su completa activación (Toker, 2012). Una vez activada, AKT se trasloca al citoplasma y núcleo, donde ejerce sus funciones a través de numerosos efectores como GSK3β, PRAS40 eIF4E, TSC2, mTOR (mammalian Target of Rapamycin), entre otros (Hers et al. 2011) (Figura 6).

La rapamicina se descubrió inicialmente como un metabolito antimicótico producido por *Streptomices hygroscopicus* a partir de una muestra de suelo de la isla Rapa Nui. Posteriormente, se descubrió que la rapamicina posee propiedades inmunosupresoras y antiproliferativas en células de mamíferos, lo que produjo un interés en identificar el modo de acción de la rapamicina. A principios de la década de 1990, el análisis genético de células de levadura en gemación identificó los genes TOR1 y TOR2 como mediadores de los efectos tóxicos de la rapamicina en levadura (Cafferkey et al., 1993; Kunz et al., 1993). Posteriormente, se aisló e identificó mTOR en células animales como la diana molecular de la rapamicina (Laplante et al., 2012).

mTOR es una serina/treonina cinasa, que se considera como el regulador maestro del metabolismo celular pertenece a la familia de las cinasas relacionadas con la PI3K e interactúa con varias proteínas para formar dos complejos distintos denominados mTOR complejo 1 (mTORC1) y 2 (mTORC2). Cada uno de los complejos de mTOR contiene múltiples proteínas accesorias (mLST8, DEPTOR, y el complejo Ttil/Tel2 existen en ambos complejos, mTORC1 y mTORC2; por otra parte, RAPTOR y PRAS40 pertenecen a mTORC1, mientras que RICTOR, mSin1, y PROCTOR1/2 pertenecen a mTORC2). Los dos

complejos de cinasas tienen sustratos específicos, y por lo tanto desencadenan distintos eventos de señalización para modular funciones celulares (Laplante et al., 2012) (Figura 6).

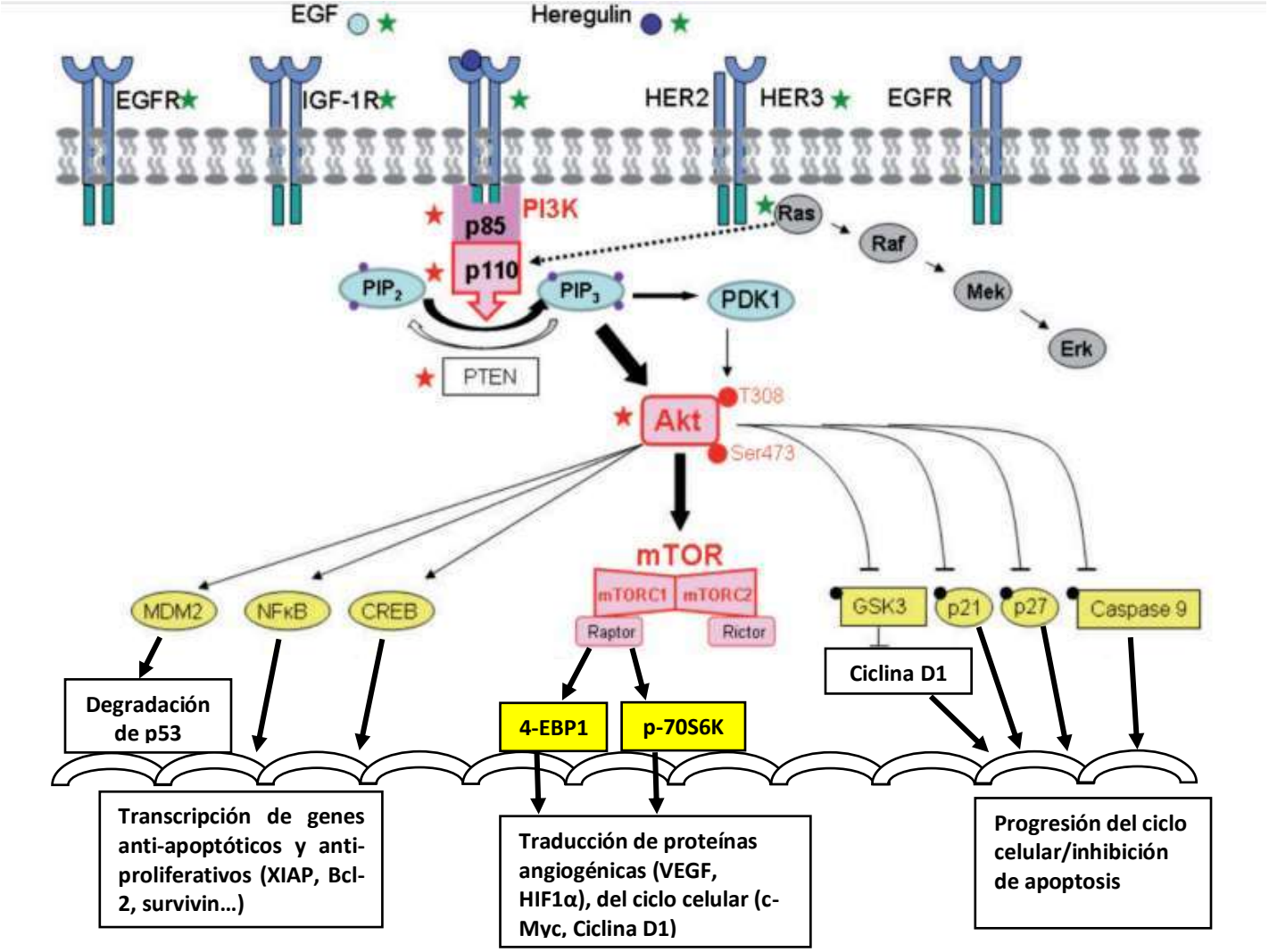

Figura 5. Vía de señalización PI3K/Akt/mTOR

Esta vía se encuentra desregulada en muchos tipos de cáncer, incluido el cáncer cervicouterino, ya sea a través de **a)** Estimulación directa de los receptores de factores de crecimiento y sus ligandos, **b)** Activación indirecta a través de la vía Ras y **c)** Activación vía intrínseca por alteraciones genéticas en PI3K, Akt, o por pérdida de función del supresor de tumores PTEN. En color verde se señala la activación de la vía PI3K mediante los RTK/ligandos o indirectamente mediante la vía Ras. En color rojo se señala la activación intrínseca de la vía que se lleva a cabo por las mutaciones de PI3K en p110 (*PIK3CA*) o p85 (*PIK3R*), mutaciones de Akt o por pérdida de PTEN. Modificado de **Leary et al., 2013**.

Una característica notable de mTORC1 es el número y la diversidad de las señales ascendentes que detecta; la vía mTORC1 integra al menos cinco señales extracelulares principalmente (factores de crecimiento, nutrientes (aminoácidos), estrés, estado energético, y oxígeno) para controlar procesos importantes, que incluyen la síntesis de proteínas, lípidos y la autofagia.

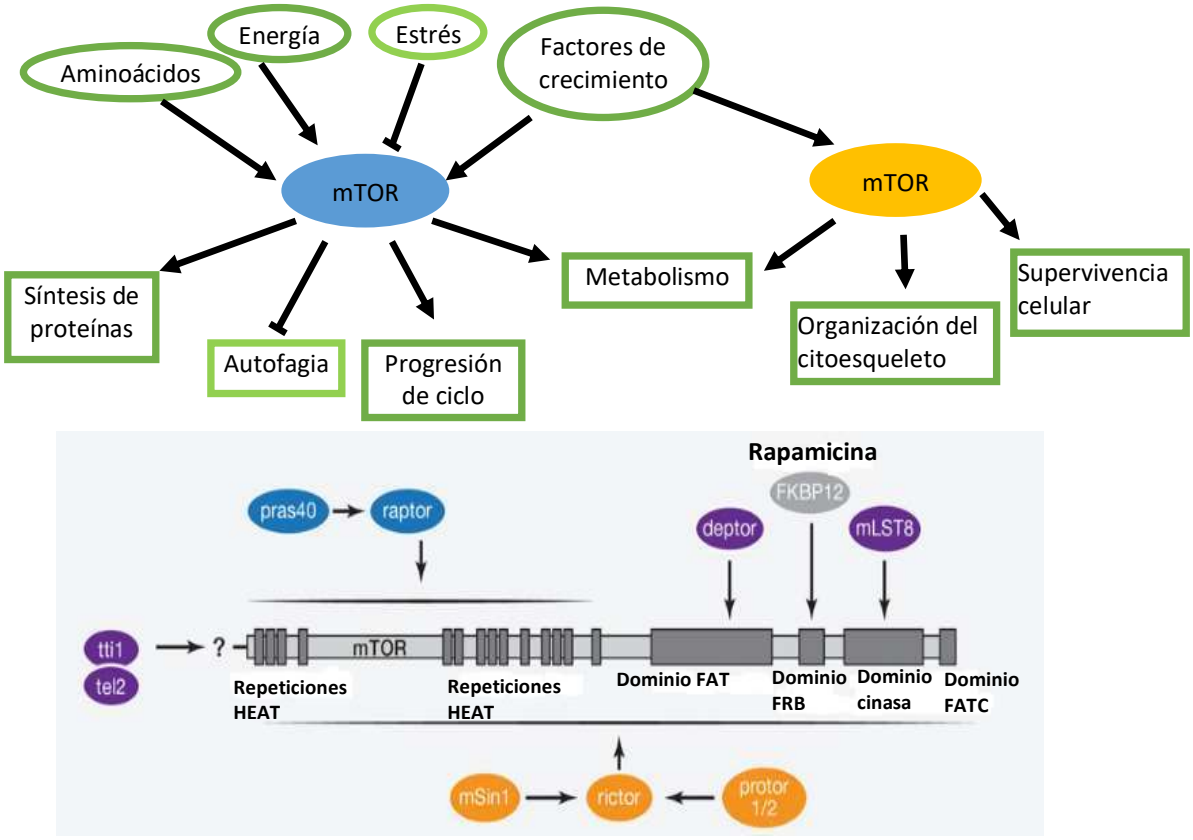

Figura 6. Complejos mTORC1 y mTORC2

Descripción de las abreviaciones: Dominio FAT, dominio terminal carboxi FAT; dominio FATC, dominio FRAP-ATM-TTRAP, dominio FRB, FKBP12-dominio de unión a rapamicina; repeticiones HEAT, Factor de Elongación 3 Huntingtin subunidad A de repeticiones PP2A-TOR1 Modificado de (Laplante et al., 2012).

1.3.2. mTORC1 en respuesta a factores de crecimiento

El heterodímero formado por TSC1 y TSC2 (esclerosis tuberosa 1, también conocida como Hamartina y esclerosis tuberosa 2 como Tuberina) es el regulador negativo más importante de mTORC1 (Inoki et al., 2002); su desregulación causa desarrollo de tumores en varios tejidos como angiofibromas, angiomiolipomas, y carcinoma de células renales. La pérdida

de función en las mutaciones ya sea de TSC1 o TSC2 provocan una activación constitutiva de mTORC1, el cual contribuye al crecimiento incontrolado de las células (Astrinidis et al., 2005).

El complejo TSC1/2 transmite muchas de las señales ascendentes que afectan a mTORC1, incluidos factores de crecimiento, como la insulina, y el factor de crecimiento similar a la insulina 1 (IGF1), que estimulan las vías de PI3K y Ras. Algunas de las cinasas efectoras de esta vía son, la proteína cinasa B (Akt/PKB), la cinasa ERK 1/2 (Extracellular signal Regulated Kinase 1/2) y la cinasa ribosomal S6 (RSK1), las cuales fosforilan directamente el complejo TSC1/TSC2 para inactivarlo y así activar a mTORC1 (Manning et al., 2002; Ma et al., 2005). Akt fosforila directamente e inhibe a TSC1/2, una proteína activada por GTPasa de Rheb (Ras homolog enriched in brain) (Potter et al., 2002). La fosforilación dependiente de Akt resulta en la disociación del complejo TSC1/TSC2 del lisosoma, donde se localiza Rheb, promoviendo su activación. Cuando Rheb se une a GTP es un potente activador de mTORC1, por lo que la inhibición de TSC1/2 por Akt dependiente de la fosforilación resulta en la activación de mTOR. Adicionalmente, Akt fosforila directamente a PRAS40, un componente de mTOR que regula negativamente la actividad cinasa del complejo, permitiendo la activación de mTORC1 (Inoki et al., 2003; Tee et al., 2003). Las citocinas proinflamatorias, como el factor de necrosis tumoral α (TNF α), activan mTORC1 a través de un mecanismo conceptualmente similar a los factores de crecimiento, ya que la cinasa IkB β (IKK β) fosforila a TSC1, causando la inhibición de TSC1/2 (Lee et al., 2007).

1.3.3. mTORC1 en respuesta a aminoácidos

Los aminoácidos, en particular la leucina y arginina, también activan mTORC1. Aunque, los aminoácidos actúan independientemente de TSC1/2, el mecanismo molecular a través del cual mTORC1 detecta los aminoácidos intracelulares es a través de las Rag GTPasas (Kim et al., 2003). Los mamíferos tienen cuatro proteínas Rag, RagA, RagB, RagC y RagD, los cuales forman heterodímeros entre ellos; los dos miembros de heterodímeros parecen tener estados de carga de nucleótidos opuestos, ya que cuando RagA/B se une a GTP, RagC/D se une al GDP y viceversa. A través de un mecanismo desconocido, los aminoácidos promueven la unión de RagA/B con GTP, lo que permite que el heterodímero interactúe con el

componente raptor de mTORC1 (Sancak et al., 2008). Esta interacción da como resultado la translocación de mTORC1 de una ubicación citoplasmática a la superficie lisosomal, donde las Rag GTPasas se acoplan en un complejo de subunidades múltiples llamado Ragulator, dicho complejo es esencial para la activación de mTORC1 por aminoácidos.

1.3.4. mTORC1 en condiciones de estrés

Algunos de los factores de estrés, como los niveles bajos de energía y oxígeno, o el daño del ADN también actúan a través del complejo TSC1/2 sobre mTORC1. De este modo, la proteína cinasa activada por monofosfato de adenosina (AMPK), en respuesta a la hipoxia o a un estado de baja energía, fosforila TSC2 y aumenta su actividad GAP hacia Rheb. Al igual que Akt, AMPK también se comunica directamente con mTORC1, fosforilando a Raptor, lo que lleva a la unión de la proteína 14-3-3 y la consecuente inhibición de mTORC1 (Gwinn et al., 2008). El daño al ADN induce la expresión de TSC2 y PTEN (del inglés, Phosphatase and tensin homolog deleted on chromosome 10), causando la infraregulación de todo el eje PI3K-mTORC1, activándose la vía AMPK a través de un mecanismo dependiente de Sestrin 1/2 (Stambolic, et al., 2001).

1.3.5. mTORC1 en el estado energético celular

mTORC1 también regula el metabolismo celular y producción de ATP, ya que aumenta el flujo glucolítico al activar la transcripción y la traducción de HIF1α (Hipoxia Inducible Factor 1), el cual es un regulador positivo de muchos genes glucolíticos. Además, HIF1α orquesta la adaptación celular a un ambiente con bajo oxígeno y sin nutrientes, impulsando la progresión de tumores (Iommarini et al., 2017).

1.3.6. Regulación de síntesis proteíca a través de mTORC1

El proceso por el cual mTORC1 regula la síntesis de proteínas esta bien caracterizado; mTORC1 fosforila directamente los reguladores de la traducción eIF4E (eukaryotic translation initiation factor 4E), 4E-BP1 (eIF4E binding protein 1) y S6K (S6 kinase 1), que a su vez, promueven la síntesis de proteínas. La fosforilación de 4E-BP1 impide su unión a la proteína eIF4E, lo que le permite participar en la formación del complejo eIF4F que es necesario para el inicio de la traducción. La activación de S6K y su sustrato, la proteína ribosomal S6 conducen a través de una variedad de efectores, a un aumento en la biogénesis de ARNm, así como a la iniciación de la traducción y la elongación. mTORC1 también regula la maquinaria de síntesis de proteínas a través de otras maneras, ya sea mediante la activación

de TIF-1A (regulatory element tripartite motif- containing protein-24), que promueve su interacción con la ARN polimerasa I (Pol I) y la expresión de ARN ribosómico (ARNr) y mediante la fosforilación de Maf1, un represor de Pol III, induciendo la transcripción (Mayer et al., 2004).

1.3.7. Regulación de síntesis de lípidos a través de mTORC1

Además de regular la producción de proteínas, mTORC1 también controla la síntesis de lípidos necesarios para que las células en proliferación generen membranas. mTORC1 actúa a través de los factores de transcripción sterol regulatory element binding proteins 1 and 2 (SREBP1/2), que controlan la expresión de numerosos genes implicados en la síntesis de ácidos grasos y colesterol. Los SREBP inactivos residen en el retículo endoplasmático (ER) y su procesamiento proteolítico en respuesta a la depleción de insulina o esterol libera su forma activa que viaja al núcleo para activar la transcripción. La inhibición de mTORC1 reduce los niveles de SREBP1/2 así como su procesamiento, disminuyendo marcadamente la expresión de genes lipogénicos (Düvel et al., 2010; Li et al., 2011).

1.3.8. Regulación de la autofagia a través de mTORC1

Uno de los papeles de mTOR es promover el metabolismo celular anabólico para suplir la energía o moléculas necesarias para el crecimiento celular y proliferación. mTOR integra varios estímulos y vías de señalización, como la síntesis de proteínas, lípidos y nucleótidos, y bloquea procesos catabólicos como la autofagia a niveles post-transcripcionales y transcripcionales. La autofagia permite a las células descomponer los orgánulos celulares, como los ribosomas y las mitocondrias, permitiendo que los catabolitos resultantes sean reciclados y por lo tanto utilizados para la biosíntesis y metabolismo energético. Como parte de este programa, las vesículas intracelulares llamadas autofagosomas envuelven los orgánulos intracelulares y luego se fusionan con lisosomas en los que se produce la degradación. De esta manera, se generan metabolitos de bajo peso molecular que brindan supervivencia en ambientes limitados por nutrientes. En el caso de las células cancerosas la activación de la autofagia les permitiría su supervivencia (Levine et al., 2008).

Al igual que la apoptosis, la maquinaria de la autofagia tiene biomoléculas que regulan su activación (Mizushima, 2007). Entre ellas se encuentran las proteínas que median la formación del autofagosoma y su liberación a los lisosomas. Cabe destacar que investigaciones recientes han revelado intersecciones entre los circuitos regulatorios que rigen la autofagia, la apoptosis y la homeostasis celular. Por ejemplo, la vía de señalización que involucra a las cinasas PI3K, AKT y mTOR, la cual es estimulada por señales que bloquean la apoptosis, también se encarga de inhibir de manera similar a la autofagia; cuando las señales de supervivencia son insuficientes, la vía de señalización PI3K activa señales para que la autofagia y/o la apoptosis puedan ser inducidas (Sinha et al., 2008; Mathew et al., 2007). Otra interconexión entre estos dos programas reside en la proteína Beclin-1, la cual es necesaria para la inducción de la autofagia (Levine et al., 2008). Beclin-1 es un miembro de la subfamilia de proteínas BH3 reguladoras de apoptosis, la característica es que su dominio BH3 les permite unirse a proteínas Bcl-2/Bcl-xL (Qu et al.,2003). Cuando se genera estrés celular las proteínas BH3 se acoplan provocando el desplazamiento de Beclin-1 de su asociación con Bcl-2/Bcl-xL, lo que permite la liberación de Beclin-1 y desencadenar la autofagia, así como la liberación de las proteínas proapoptóticas Bax y Bak para desencadenar la apoptosis (Pattingre et al.,2005).

Tras la inhibición de mTORC1, se forman autofagosomas que engullen a las proteínas citoplasmáticas y orgánulos fusionándose con los lisosomas, lo que conduce a la degradación de los componentes celulares. En mamíferos, mTORC1 fosforila y suprime directamente a ULK1/Atg13/FIP200 (unc-51- like kinase 1/mammalian autophagy-related gene 13/Focal adhesión kinase family-interacting protein of 200 kDa), un complejo cinasa requerido para iniciar la autofagia. Al igual que con el control de la síntesis de proteínas y lípidos, es probable que mTORC1 regule la autofagia a través de varios mecanismos. Por ejemplo, mTORC1 regula a la proteína DAP 1 (death associated protein 1). A través de un análisis fosfoproteómico se sabe que WIPI2 es efector de mTORC1 y que es esencial para la formación del autofagosoma (Hsu el al., 2011).

1.3.9. Procesos celulares regulados por mTORC2

mTORC2 ha sido considerado como insensible a nutrientes, pero responde a ciertos factores de crecimiento como la insulina a través de mecanismos no bien definidos, activando

principalmente a la cinasa Akt en su residuo Ser 473. mTORC2 controla varios miembros de la subfamilia de cinasas AGC, incluyendo Akt, SGK1 (serum-and glucorticoid-induced protein kinase 1) y PKC- α (Protein Kinase C-α). Akt regula procesos celulares como el metabolismo, la supervivencia, la apoptosis, el crecimiento y la proliferación a través de varios efectores. mTORC2 activa a Akt a través de la fosforilación de su dominio hidrofóbico Ser473. La fosforilación defectuosa de Akt-Ser473 causada por la depleción de mTORC2 disminuye la fosforilación de algunas dianas de Akt como FoxO1/3a (Forkhead box O1/3a), mientras que otras dianas de Akt como TSC2 y GSK3-β no se ven afectadas. mTORC2 también activa directamente SGK1, una cinasa que controla el transporte de iones y el crecimiento; en contraste con Akt, la actividad SGK-1 queda completamente bloqueada por la pérdida de mTORC2 (Jacinto et al., 2006). Debido a que SGK1 controla la fosforilación de FoxO1/3a en los mismos residuos fosforilados por Akt, la pérdida de la actividad de SGK1 es probablemente responsable de la reducción en la fosforilación de FoxO1/3a en células deficientes en mTORC2. Por otra parte, la activación de PKC-α por mTORC2 se encarga de regular el citoesqueleto de actina (Sarbassov et al., 2005).

1.3.10. Inhibidores de PI3K/Akt/mTOR en la terapia antitumoral

La activación oncogénica de la señalización de mTOR induce procesos requeridos para el crecimiento, supervivencia y proliferación de células cancerosas, por lo que se ha generado gran interés en blancos moleculares de la vía mTOR para el tratamiento del cáncer. Existen en el mercado más de 30 fármacos y 5 clases de inhibidores de la vía PI3K/AKT/mTOR, entre ellos, inhibidores de PI3K, inhibidores duales de PI3K y mTOR, inhibidores de Akt, inhibidores catalíticos de mTOR y análogos de la rapamicina. Estos agentes están siendo probados en ensayos clínicos como terapia contra distintos tipos de cáncer (Dienstmann et al., 2014). En la Tabla 1 se muestran algunos de los inhibidores.

Tabla 1 . Inhibidores de la vía PI3K/Akt/mTOR

Inhibidores de PI3K/AKT/mTOR en fase I, II y III		
Tipo de inhibidor	**Acción**	**Agente**/ensayo clínico/Tipo de cáncer
Pan-PI3K	Inhibe las 4 clases de subunidades p110 de PI3KIA: p110α, p110β, p110γ, p110δ	**-Buparlisib** (BKM120)/Cáncer de mama metástasico y de pulmón **-Pilaralisib** (XL147) **-Pictilisib** (GDC-0941)/Cáncer de mama
Pan-AKT	Inhibe las tres isoformas de AKT (AKT1, AKT2 y AKT3)	-MK-2206/Cáncer de mama -Uprosertib (GSK2141795) -Ipatasertib (GDC-0068, AZD5363)/Cáncer de mama y prostata
mTORC1	Se une alostéricamente inhibiendo a mTOR	-Everolimus/Cáncer de mama, riñón, pulmón y pancreas Ridaforolimus/Cáncer de endometrio -Temsirolimus/Cáncer de endometrio y de mama -Sirolimus/Sarcoma de Kaposi
mTORC1 y mTORC2	Se une al sitio de unión al ATP de mTOR e inhibe a ambos complejos	-AZD2014/Cáncer de mama metastásico -AZD8055/Cáncer de colon -INK128 (MLN0128), -CC-223
Inhibidor dual dePI3K y mTOR	Inhibe PI3K, mTORC1/ mTORC2	-Voxtalisib (XL765)/Glioblastoma y leucemia -Apitolisib (GDC-0980)/Cáncer de endometrio -Gedatolisib (PF-05212384)/Cáncer de endometrio y cáncer de colon -PI-103

Adaptada de **Chia et al., 2015**.

El uso de inhibidores como monoterapia en tumores sólidos no tuvo buenos resultados, debido al desarrollo de distintos mecanismos de resistencia (Brachmann et al., 2012). Dicha resistencia puede darse por reactivación de la vía, debido a mecanismos de retroalimentación negativa. Los mecanismos de retroalimentación negativa funcionan en múltiples nodos dentro de las vías de señalización, un ejemplo de ello es la activación de mTOR a través de fosfatidilinositol 3-cinasa (PI3K), la cual se lleva a cabo por vía retroalimentación lo que provoca que se active la vía de PI3K (Sudarsanam et al., 2010); por lo que cuando mTOR es farmacológicamente inhibido en células cancerosas (ej. con la rapamicina) la pérdida de la retroalimentación negativa provoca el incremento de la actividad de PI3K/Akt, debilitando los efectos antiproliferativos de la inhibición de mTOR.

La reactivación de la vía PI3K/Akt puede producirse con la administración de inhibidores de RTKs, PI3K o de Akt, por inhibición de la retroalimentación negativa que ejerce mTOR sobre los RTKs (Chandarlapaty et al., 2011; Chakrabarty et al., 2012). La inhibición de PI3K puede llevar con frecuencia a la activación de mecanismos alternativos como la MAPK (Carracedo, et al., 2008).

Los complejos que constituyen mTOR tienen diferentes sensibilidades a la rapamicina, así como a los reguladores upstream (río arriba) y downstream (río abajo). La rapamicina es un inhibidor alostérico de mTORC1 (Chiarini et al., 2015), formando un complejo con la proteína intracelular 12-kDa FK506-binding protein (FKBP12). Sin embargo, exposiciones prolongadas o altas concentraciones de rapamicina pueden resultar inhibitorias de mTORC2, probablemente porque secuestra moléculas recién sintetizadas de mTOR (Sarbassov et al., 2006; Efeyan et al., 2010).

Actualmente se han desarrollado los rapálogos Everolimus y Temsirolimus aprobados por la FDA. Aunque debido a la presencia de numerosos actores sobre la activación de mTOR contribuyen a la limitación de la eficacia terapéutica de los rapálogos (Laplante et al., 2013). Por lo que se tiene gran interés en desarrollar moléculas que inhiban la actividad cinasa de mTOR o en su caso buscar otros blancos moleculares que puedan inhibir esta vía de señalización.

1.4. Ciclodipéptidos como moléculas con potencial anticancerígeno

Debido a que la mayoría de los tratamientos convencionales para el cáncer radica en utilizar agentes citotóxicos, los cuales por lo general no son específicos para las células cancerosas, lo que desencadena un estado de citotoxicidad sistémica, resultando en efectos adversos indeseables, como alopecia, hepatotoxicidad, nefrotoxicidad y supresión del sistema inmunitario, sigue la búsqueda de nuevas alternativas de tratamiento, por lo que se está investigando el efecto anticancerígeno de biomoléculas producidas por una amplia gama de organismos (bacterias, plantas, hongos, etc).

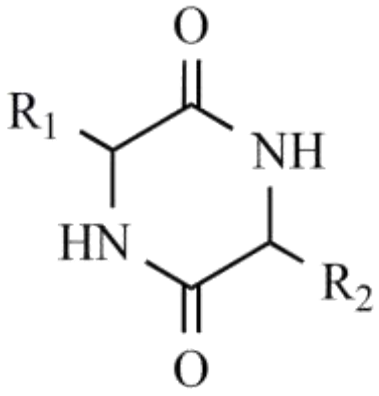

Figura 7. Estructura general de los ciclodipéptidos

Los ciclodipéptidos presentan dos aceptores y dos sitios donadores de puentes de hidrógeno importantes para la unión a receptores (**Borthwick, 2012**).

Dentro de las nuevas alternativas para contrarrestar el cáncer, tenemos a los ciclodipéptidos (Figura 8), una clase de moléculas pequeñas, derivadas de la condensación de dos aminoácidos, biosintetizadas por un amplio rango de microorganismos. Se sabe que el 90% de las bacterias Gram negativas los sintetizan. También han sido aislados de bacterias Gram positivas, hongos, plantas y organismos marinos (Carvalho et al., 2012). El anillo de la molécula de CDPs se compone de 6 átomos, los cuales orientan sus sustituyentes de manera espacial definida, y debido a sus características estructurales estables representa un importante farmacóforo, que se definen como la unidad central molecular para generaractividad biológica (Güner, 2000).

Los ciclodipéptidos son sintetizados por una familia de enzimas dependientes de los ARN de transferencia (tARN) llamadas ciclodipéptido sintasas no ribosomales (CDPS-NR); así como también por una familia de enzimas formadoras de enlace peptídico conocidas como ciclodipéptido sintasas no dependientes de ATP (CDPS) (Finking et al., 2004; Gondry et al., 2009). Aunque los CDPs son ampliamente obtenidos por extracción de fuentes naturales, éstos pueden ser fácilmente sintetizados, debido a su simplicidad estructural (Prasad, 1995).

Algunas de las actividades biológicas importantes de los ciclodipéptidos son antivirales, antifúngicas, antibacterianas, así como inductores de apoptosis (Kanoh et al., 1999; Sinha et al., 2004). Además de las actividades ya mencionadas, algunos CDPs inducen apoptosis en diferentes líneas celulares, como es el caso de ciclo(*L*-Pro-*L*-Tyr) y ciclo(*L*-Pro-*L*-Phe) aislado de especies de *Bacillus (*Hong et al., 2008); dichos CDPs inducen la disminución en la fosforilación de la cinasa serina/treonina (AKT1), la cual está involucrada en la vía de señalización PI3k/Akt/mTOR regulando mecanismos como la proliferación celular y la apoptosis (Laplante et al., 2013).

Además de la estructura rígida y quiral de los ciclodipéptidos, éstos se unen a una amplia variedad de receptores con una alta afinidad brindando un amplio rango de actividades biológicas. Por lo tanto, el estudio de ciclodipéptidos naturales y sintéticos contribuye a entender los requerimientos estructurales de las interacciones con los diversos receptores biológicos permitiendo la validación de blancos moleculares para así abrir nuevas perspectivas para el descubrimiento de nuevos fármacos anticancerosos. En este contexto se tiene que la plinabulina, un derivado semisintético del ciclo(*L*-Phe-*L*-His) es un fármaco anticanceroso en fase II, actuando como agente inhibidor de la polimerización de los microtúbulos (Okuyama et al., 2015).

2. ANTECEDENTES

La bacteria *Pseudomonas aeruginosa* cepa PAO1 produce los CDPs ciclo(L-Pro-L-Val), ciclo(L-Pro-LPhe) y ciclo(L-Pro-L-Tyr). En nuestro grupo de trabajo se reportó que los CDPs de *P. aeruginosa* (PAO1-CDPs) son sintetizados a través de las péptido sintetasas no ribosomales y se encontró que poseen actividad promotora del crecimiento en plantas (Ortíz-Castro et al., 2011). Además se determinó que los PAO1-CDPs influyen en la detección del quórum sensing (González et al., 2016). En 2019, Corona-Sánchez y colaboradores reportaron que los PAO1-CDPs promueven el crecimiento y desarrollo del maíz, a través de la vía de señalización TOR/S6K como un mecanismo de crecimiento de la planta y desarrollo de raíces en la interacción planta-microorganismo.

Se ha demostrado que los ciclodipéptidos producidos por una amplia gama de organismos tienen efectos citotóxicos en líneas celulares cancerosas (Hong et al., 2008; Fokas et al., 2010). En este contexto, se evaluó el efecto de la mezcla de los PAO1-CDPs en las líneas cancerosas humanas HeLa (cáncer cervico-uterino) y CaCo-2 (cáncer colorectal), los resultados mostraron que los PAO1-CDPs promueven muerte celular por apoptosis en ambas líneas celulares cancerosas, con una concentración inhibitoria 50 (IC50) de 0.53 y 0.66 mg/mL, respectivamente (Figura 9).

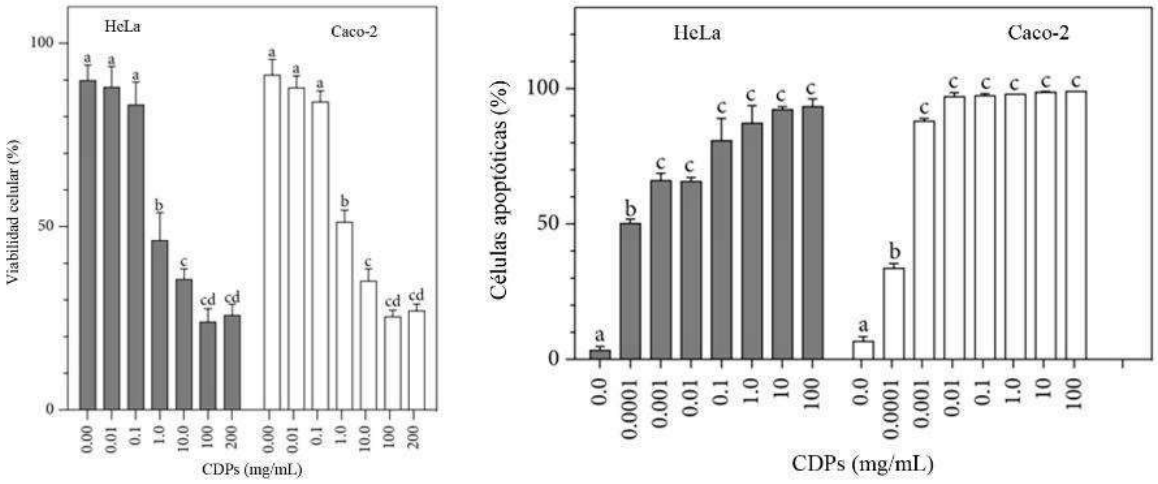

Figura 8. Efecto citotóxico de los PAO1-CDPs en células cancerosas

En la gráfica de la izquierda se muestra la viabilidad celular en forma dependiente de la dosis de los PAO1-CDPs sobre las líneas celulares cancerosas HeLa y CaCo-2. En la gráfica de la derecha se muestra la apoptosis en forma dependiente de la concentración de los PAO1-CDPs sobre las líneas celulares cancerosas HeLa y CaCo-2 (Modificado de **Vázquez-Rivera et al., 2015**).

Además se evaluó el efecto de los PAO1-CDPs en células no cancerosas, en células humanas NOVA (fibroblastos de pulmón humano obtenidas a partir de un cultivo primario de tejido de pulmón), y en células CEMB (Células de Epitelio Mamario Bovino), los resultados mostraron que los PAO1-CDPs no afectan la viabilidad de las células NOVA y CEMB (Vázquez-Rivera et al., 2015) (Figura 10).

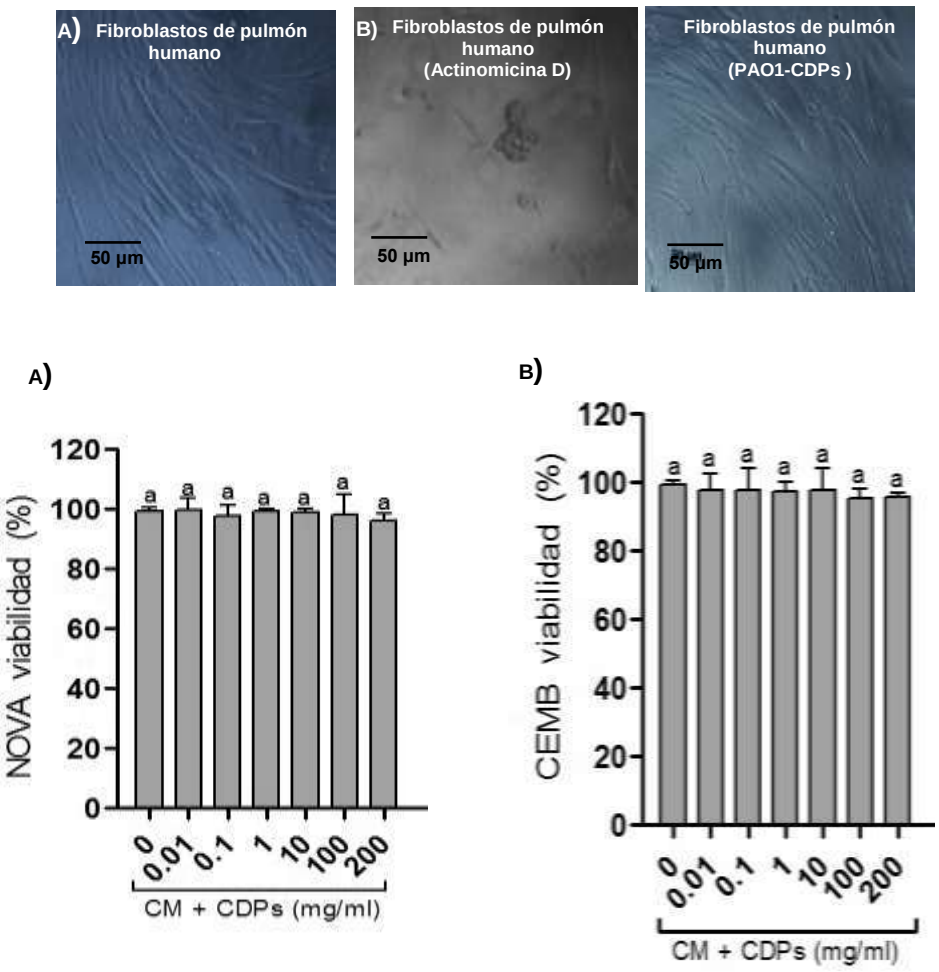

Figura 9. Efecto de los PAO1-CDPs en células NOVA y CEMB

En las fotografías A, B y C, se muestran células NOVA sin tratamiento, tratamiento con Actinomicina D y tratamiento con los PAO1-CDPs, respectivamente. En las gráficas A) muestra el efecto de los PAO1-CDPs en la viabilidad de fibroblastos de pulmón humano (NOVA) y en B) células de epitelio mamario bovino, respectivamente (Modificado de **Vázquez-Rivera, 2014**).

En 2020, Durán-Maldonado y colaboradores reportaron que los PAO1-CDPs disminuyeron el tamaño y la formación de tumores en un modelo *in vivo* de melanoma murino (Durán-Maldonado et al., 2020) (Figura 11).

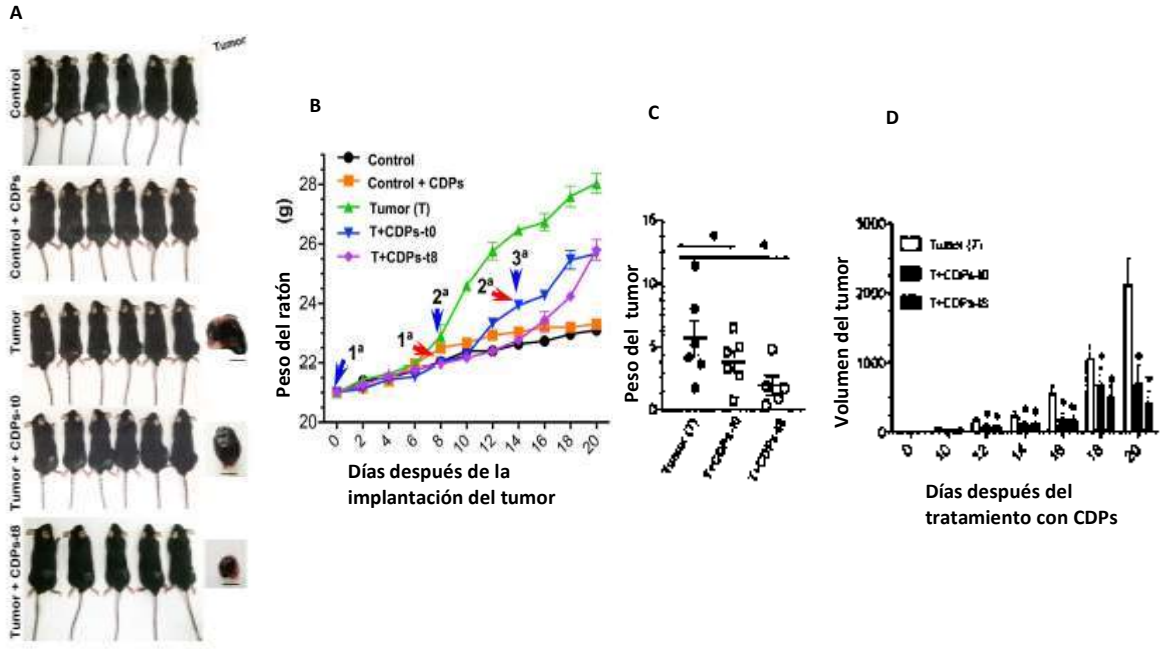

Figura 10. Efecto de los PAO1-CDPs en la formación de tumores en un modelo *in vivo* de melanoma murino

En el panel A) se muestra la fotografía de los grupos de ratones en el día 20 del procedimiento experimental antes de la eutanasia, se muestran fotografías representativas del tumor de cada grupo de ratones En el panel B), se muestra la determinación del peso del ratón durante un período de 20 días. Las puntas de flecha indican el tiempo de administración de los CDPs y el número de dosis. C) Peso del tumor. D) Volumen del tumor. (Modificado de Durán-Maldonado, et al., 2020).

La radiación y quimioterapia son los procedimientos más comunes para la terapia del cáncer, aunque estos métodos se asocian con daños colaterales serios. Por lo tanto, es necesario encontrar alternativas y tratamientos específicos para el cáncer, y en este aspecto, la vía de señalización PI3K-Akt-mTOR ha sido sugerida como blanco para el diseño de moléculas con propiedades farmacológicas anticancerosas que podrían ser utilizadas en el control y tratamiento de enfermedades humanas incluyendo el cáncer. En este sentido, dentro del

mismo grupo de trabajo, se reportó que el mecanismo por el cual los PAO1-CDPs inducen muerte celular por apoptosis es a través de la vía de apoptosis intrínseca, mediante la inhibición de la fosforilación de las proteínas Akt (Ser 473) y S6K (Thr 389) (Hernández-Padilla et al., 2017) (Figura 12).

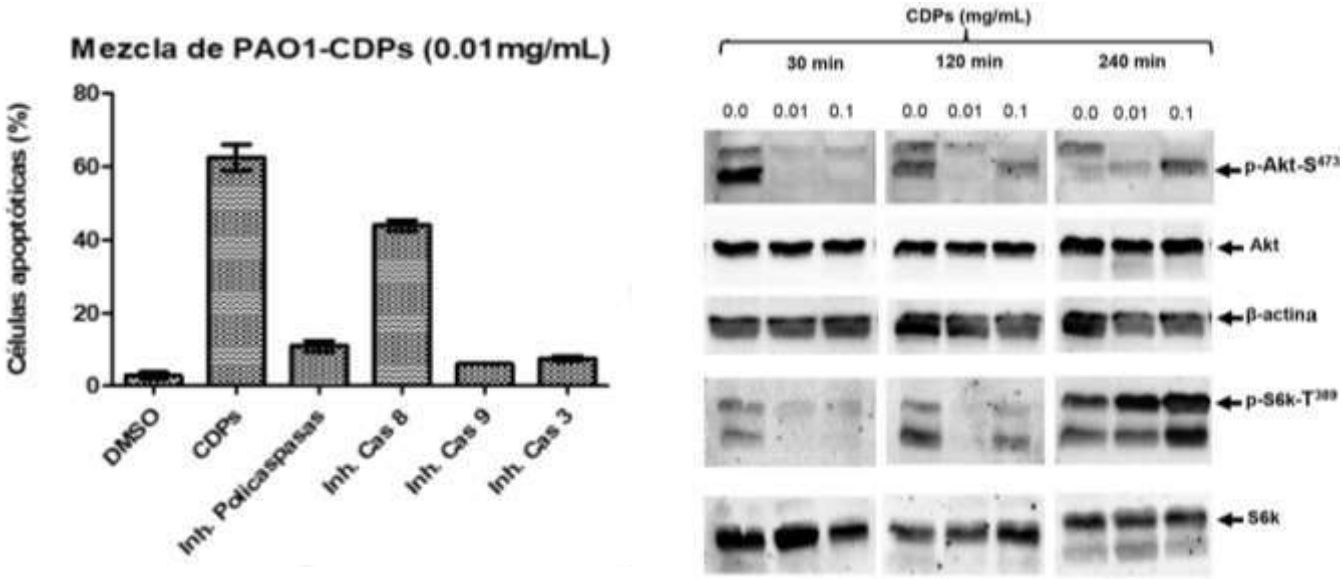

Figura 11. Inducción de apoptosis en células HeLa por los ciclodipéptidos producidos por *Pseudomonas aeruginosa*

A la izquierda; ensayo de inducción de apoptosis usando inhibidores de caspasas participantes en las diferentes vías apoptóticas. A la derecha, ensayo de inmunodetección por Western blot de las formas fosforiladas y desfosforiladas de las cinasas Akt y S6k a diferentes concentraciones de los PAO1-CDPs y tiempos de tratamiento. (Modificado de Hernández-Padilla et al., 2017).

mTORC2 es una cinasa que fosforila a Akt en su residuo Ser 473 causando su máxima activación; la fosforilación de Akt dependiente de mTORC2 conduce a la activación de mTORC1. Por lo tanto, mTORC2 puede inhibir indirectamente la autofagia (Kim el at., 2015). De esta forma el comportamiento de fosforilación cíclica de Akt-S473 observados durante el tratamiento con los PAO1-CDP de las células de HeLa sugiere que la actividad de mTORC2 puede estar involucrada posiblemente a través de mantener inhibida la autofagia asegurando la inducción de apoptosis como vía de muerte de las células cancerosas (Hernández-Padilla, et al., 2017). Además, mTORC2 está involucrado principalmente en reorganización del citoesqueleto de actina, y más recientemente, en la regulación del

crecimiento, la proliferación, el metabolismo energético y la resistencia a los medicamentos (Guri et al., 2017). Cabe resaltar que mTORC2 es fútil para epitelio de células sanas o fibroblastos de embrión, mientras que es muy necesario para células cancerosas que tienen hiperactivada la vía de señalización PI3K/Akt. Esto indica que la inhibición del complejo mTORC2 puede ser más deletérea para células cancerosas que para células normales, de forma que inhibidores de mTORC2 causarían menos toxicidad en células sanas.

En este sentido, se desconoce sí los PAO1-CDPs modulan otras vías relacionadas con los procesos requeridos para el crecimiento, supervivencia y proliferación de células cancerosas, los cuales son eventos importantes regulados por el complejo mTORC2, por lo que la caracterización de los mecanismos de acción de los PAO1-CDPs permitirá dilucidar sí éstos tienen capacidad multiblanco inhibiendo al complejo mTORC1 y mTORC2, proponiendo a los PAO1-CDPs como un fármaco con alto potencial anticanceroso.

3. JUSTIFICACIÓN

Una de las características ideales de un fármaco que causa efectos antiproliferativos es que no dañe a las células normales, pero que comprometa la proliferación y/o supervivencia de las células cancerosas. En este sentido, se sabe que mTORC2 es un blanco ideal en cáncer ya que se ha reportado que su inhibición provoca la muerte de células cancerosas, sin causar daño a células normales. Los estudios realizados hasta el momento demuestran que los PAO1-CDPs poseen efecto antiproliferativo inhibiendo la fosforilación de las proteínas cinasas Akt en el residuo Ser 473 y S6K en el residuo Thr 389, induciendo la apoptosis en la línea celular HeLa. Sin embargo, se desconoce la participación de los complejos mTORC1 y mTORC2 en este fenómeno, por lo que es de nuestro interés evaluar sí los PAO1-CDPs inducen la apoptosis en las células HeLa a través de la vía mTOR.

4. HIPÓTESIS

El efecto apoptótico causado por los ciclodipéptidos producidos por *Pseudomonas aeruginosa* PAO1 en la línea celular cancerosa humana HeLa se lleva a cabo a través de mTORC1 y mTORC2.

5. OBJETIVO GENERAL

Determinar el papel de la señalización de mTORC1 y mTORC2 implicada en el efecto apoptótico de los ciclodipéptidos producidos por *P. aeruginosa* PAO1 en la línea celular HeLa.

5.1. OBJETIVOS ESPECÍFICOS

1. Dilucidar la participación de los complejos mTORC2 y mTORC1 en el efecto de los PAO1-CDPs en la línea celular cancerosa humana HeLa.
2. Dilucidar la participación del complejo TSC1/TSC2 en el efecto de los PAO1-CDPs en la línea celular cancerosa humana HeLa.

6. RESULTADOS

6.1. Capítulo 1

Hernández-Padilla, L., Vázquez-Rivera, D., Sánchez-Briones, L. A., Díaz-Pérez, A. L., Moreno-Rodríguez, J., Moreno-Eutimio, M. A., & Campos-García, J. (2017). The antiproliferative effect of cyclodipeptides from Pseudomonas aeruginosa PAO1 on HeLa cells involves inhibition of phosphorylation of Akt and S6k kinases. *Molecules*, *22*(6), 1024.

molecules

MDPI

Article

The Antiproliferative Effect of Cyclodipeptides from *Pseudomonas aeruginosa* PAO1 on HeLa Cells Involves Inhibition of Phosphorylation of Akt and S6k Kinases

Laura Hernández-Padilla [1], Dolores Vázquez-Rivera [1], Luis A. Sánchez-Briones [1], Alma L. Diaz-Pérez [1], José Moreno-Rodriguez [2], Mario A. Moreno-Eutimio [2], Victor Meza-Carmen [1], Homero Reyes-De la Cruz [3] and Jesús Campos-García [1,*]

1 Laboratorio de Biotecnología Microbiana, Instituto de Investigaciones Químico-Biológicas, Universidad Michoacana de San Nicolás de Hidalgo, 58030 Morelia, Michoacán, Mexico; laura_1905898@hotmail.com (L.H.-P.); dolores_vazquez1001@hotmail.com (D.V.-R.); biol.luis.224@gmail.com (L.A.S.-B.); aldiaz078@yahoo.com (A.L.D.-P.); victor_meza2004@yahoo.com.mx (V.M.-C.)

2 División de Investigación, Hospital Juárez de México, 07760 Ciudad de México, Mexico; jmoreno49@gmail.com (J.M.-R.); marioadan@inmunoquimica.com (M.A.M.-E.)

3 Laboratorio de Control Traduccional, Instituto de Investigaciones Químico-Biológicas, Universidad Michoacana de San Nicolás de Hidalgo, 58030 Morelia, Michoacán, Mexico; delacruz@umich.mx

* Correspondence: jcgarcia@umich.mx; Tel.: +52-443326-5788

Received: 29 May 2017; Accepted: 16 June 2017; Published: 20 June 2017

Abstract: *Pseudomonas aeruginosa* PAO1, a potential pathogen of plants and animals, produces the cyclodipeptides cyclo(L-Pro-L-Tyr), cyclo(L-Pro-L-Phe), and cyclo(L-Pro-L-Val) (PAO1-CDPs), whose effects have been implicated in inhibition of human tumor cell line proliferation. Our purpose was to investigate in depth in the mechanisms of HeLa cell proliferation inhibition by the PAO1-CDPs. The results indicate that PAO1-CDPs, both purified individually and in mixtures, inhibited HeLa cell proliferation by arresting the cell cycle at the G0–G1 transition. The crude PAO1-CDPs mixture promoted cell death in HeLa cells in a dose-dependent manner, showing efficacy similar to that of isolated PAO1-CDPs (LD_{50} of 60–250 μM) and inducing apoptosis with EC_{50} between 0.6 and 3.0 μM. Moreover, PAO1-CDPs showed a higher proapoptotic activity ($\sim 10^3$–10^5 fold) than their synthetic analogs did. Subsequently, the PAO1-CDPs affected mitochondrial membrane potential and induced apoptosis by caspase-9-dependent pathway. The mechanism of inhibition of cells proliferation in HeLa cells involves inhibition of phosphorylation of both Akt-S473 and S6k-T389 protein kinases, showing a cyclic behavior of their expression and phosphorylation in a time and concentration-dependent fashion. Taken together our findings indicate that PI3K–Akt–mTOR–S6k signaling pathway blockage is involved in the antiproliferative effect of the PAO1-CDPs.

Keywords: biomolecule; cyclodipeptides; antitumoral activity; cell proliferation; apoptosis; Akt–S6k signaling; HeLa

1. Introduction

Pseudomonas aeruginosa colonizes several biological environments, such as soil, plants, and animal tissues, being an important opportunistic pathogen in humans, e.g., causing nosocomial infections [1,2]. Several mechanisms driving infection in the host have been attributed to the production of toxins, adhesins, siderophores, and a great number of virulence factors. Cyclodipeptides (CDPs) are cyclized

molecules comprising two amino acids attached by peptide bonds; they are produced by a wide range of organisms, from bacteria to fungi to animals [3]. CDPs represent a new class of quorum-sensing (QS) signals, and they may act as interkingdom signals; nonetheless, their mechanism of action and physiological relevance are poorly understood [4].

CDPs are structurally diverse and have been implicated in multiple biological effects. The CDP cyclo(L-Phe-L-Pro) isolated from *Lactobacillus plantarum* has an antifungal effect [5], whereas CDPs cyclo(L-Leu-L-Pro), cyclo(L-Phe-L-Pro), cyclo(L-Val-L-Pro), cyclo(L-Trp-L-Pro), and cyclo(L-Leu-L-Val) isolated from the deep-sea bacterium *Streptomyces fungicidicus* show antifouling effects [6]. In *Staphylococcus aureus*, aureusimines A/B, namely, CDPs cyclo(L-Val-L-Tyr) and cyclo(L-Val-L-Phe), respectively, are involved in the regulation of bacterial virulence factors in a murine host [7]. In addition, it was reported that CDPs cyclo(L-Leu-L-Pro) and cis-cyclo(L-Phe-L-Pro) isolated from *Lactobacillus* show antiviral activity against the influenza A (H3N2) virus [8]. In mammalian cells, CDPs induce DNA damage via reactive oxygen species (ROS) [9]. Cyclo(L-Phe-L-His) of *Aspergillus ustus* inhibits the cell cycle in various cancer cell lines [10], whereas cyclo(L-Phe-L-Pro) from *L. plantarum* induces apoptosis in colon cancer HT-29 cells [11]. On the other hand, synthetic CDPs such as cyclo(Phe-Pro) induce apoptosis in the HT-29 colon cancer cell line, and cyclo(L-Cys-L-Leu) has a potential for scavenging of free radicals [12]. The molecular mechanisms behind the induction of cell death in cancer cell lines by CDPs involve biological processes such as microtubule polymerization [13]. Cyclo(D-Tyr-D-Phe) isolated from *Bacillus* sp. induces apoptosis via caspase 3 activation in the A549 pulmonary adenocarcinoma cell line [14]. In addition, our group has demonstrated that a crude mixture of CDPs obtained from the *P. aeruginosa* PAO1 strain, mainly composed of cyclo(L-Pro-L-Tyr), cyclo(L-Pro-L-Val), and cyclo(L-Pro-L-Phe), promotes cell death in cultured HeLa and Caco-2 cells, pointing to an apoptotic pathway as the mechanism underlying the inhibition of cell proliferation [15].

Cancer results from malfunction of fundamental cellular processes that control cell number, including cellular growth, proliferation, survival and metabolism. In this sense, oncogenic and tumor suppressor signals such as PI3K, Akt, Ras, Raf, TRK, NF1, LKN1, PTEN, p53, and TSC1 and TSC2 have largely involved [16,17]. The phosphatidylinositol 3-kinase (PI3K) signal transduction pathway has been studied extensively and is known to be involved in growth control and in diseases [16,17]. The mTOR kinase is a master regulator of cellular metabolism, acting downstream of a more complex cell signaling network. The mTOR kinase exists in two complexes: mTORC1, which has been implicated in almost all cellular processes, such as anabolic metabolism, proliferation, protein, lipid, and nucleotide synthesis, cell survival, cell mobilization, oxygen supply, energy, proliferative signals, and tumorigenesis, and blocks catabolic processes such as autophagy at the post-translational and transcriptional levels; while mTORC2 is involved mainly in actin cytoskeleton reorganization [18]. The mTORC1 pathway is frequently up-regulated in cancer, particularly under increased PI3K signaling due to oncogenic activation of PI3K or mutagenic inactivation of the lipid phosphatase PTEN [16].

Radiation and chemotherapy are the most common procedures for cancer therapy, however, serious collateral damage is associated with these methods. Hence, is necessary to find alternative and specific cancer treatments, and in this regard, the PI3K–Akt–mTOR signaling pathway has been suggested as a target for the design of molecules with anticancer pharmacological properties that could be used in the control and treatment of human diseases including cancer. In this sense, CDPs have been shown to have toxic effects on tumor cell lines via an Akt-dependent mechanism [19], but the evidence is scarce.

2. Results

2.1. Purified CDPs from P. aeruginosa PAO1 Affect HeLa Cells Viability

Quantification of CDPs in the supernatant of *P. aeruginosa* cultures was conducted previously, identifying CDPs cyclo(L-Pro-L-Tyr), cyclo(L-Pro-L-Val), and cyclo(L-Pro-L-Phe) by GC-MS, RMN-H, and RMN-C [20]. During subsequent studies, an additional CDP was identified, corresponding to cyclo(L-Pro-L-Leu), whose mass fragmentation patterns showed >96% probability with respect to the NIST library. Therefore, the CDP mixture from the PAO1 strain (PAO1-CDPs) was composed of following proportions: cyclo(L-Pro-L-Tyr) ~25%, cyclo(L-Pro-L-Val) ~25%, cyclo(L-Pro-L-Phe) ~30%, cyclo(L-Pro-L-Leu) ~10%, and other compounds ~10% (Figure S1, Supplementary Material).

As previously described, we used this crude mixture of CDPs isolated from *P. aeruginosa* PAO1 cultures to evaluate the antiproliferative effect on HeLa and Caco-2 cells [15]. Moreover, to determine whether the most abundant CDPs in the mixture have differential antiproliferative activities, a preparative CDP purification procedure was carried out. After separation and concentration of the fractions, CDP structures were confirmed by GC-MS. The purified fractions with ~85–95% purity corresponding to the three major CDPs were used to determine the effect on HeLa cell viability, by the MTT assay. Additionally, the response to CDPs of bacterial origin was compared with that of the respective synthetic CDPs.

The results showed that PAO1-CDPs affected the viability of HeLa cells in a dose-dependent manner. Cell cultures showed 75% of dead cells after treatment with PAO1-CDPs, using either individual (purified) CDPs and the crude CDP mixture at 1.0 mg/mL after 24 h, being the cyclo(L-Pro-L-Phe) slightly more active against HeLa cells than the other CDPs (Figure 1a; Table 1). Moreover, the effect of synthetic CDPs on viability, separated or in the mixture, was significantly less active than PAO1-CDPs. At concentrations below 1.0 mg/mL, CDPs of bacterial origin showed HeLa cells viabilities below 20%, whereas the cell viability was ~80% with the synthetic CDPs at the same concentration (Figure 1b). For HeLa cells, the half-lethal dose (LD_{50}) for the individual and purified PAO1-CDPs was in the concentration range of 0.015–0.06 mg/mL (60–250 µM) after 24 h of treatment. Interestingly, the LD_{50} for the crude PAO1-CDP mixture was in the same range as for the purified PAO1-CDPs (Table 1). On the other hand, LD_{50} of individual synthetic CDPs was between 2 and 150 mg/mL (10–600 mM); furthermore, the mixture of synthetic CDPs was more bioactive (5- to 50-fold) than the individual synthetic compounds (Table 1). Remarkably, the LD_{50} data indicate that the PAO1-CDPs were ~1000-fold more bioactive inducing cellular death than their synthetic analogs.

Table 1. Induction of cellular dead and apoptosis on human tumor HeLa cells by the *P. aeruginosa* PAO1 cyclodipeptides.

Cyclodipeptide	Viability LD_{50} (mg/mL) [1]	Apoptosis EC_{50} (mg/mL) [1]
PAO1-Cyclo(L-Pro-L-Tyr)	0.061/0.053	$3.2 \times 10^{-4}/1.6 \times 10^{-4}$
PAO1-Cyclo(L-Pro-L-Val)	0.037/0.035	$2.7 \times 10^{-4}/2.8 \times 10^{-4}$
PAO1-Cyclo(L-Pro-L-Phe)	0.015/0.010	$5.0 \times 10^{-4}/4.1 \times 10^{-4}$
Crude PAO1-CDPs mix	0.060/0.062	$4.9 \times 10^{-4}/2.3 \times 10^{-4}$
Synthetic cyclo(L-Pro-L-Tyr)	10.7/11.4	ND
Synthetic cyclo(L-Pro-L-Val)	19.3/60.7	ND
Synthetic cyclo(L-Pro-L-Phe)	90.9/154	ND
Synthetic CDPs mix	2.90/2.04	100

[1] LD_{50}: Half lethal doses and EC_{50}: half effective concentration determined after 24 h of treatment with CDPs, being calculated using Nonlinear regression (curve fit), log(inhibitor/ inductor) vs response (variable slop), $R^2 = 0.95–0.99$ (GraphPad Prism 5.0). ND, not determined. Data obtained using: complete medium/incomplete medium.

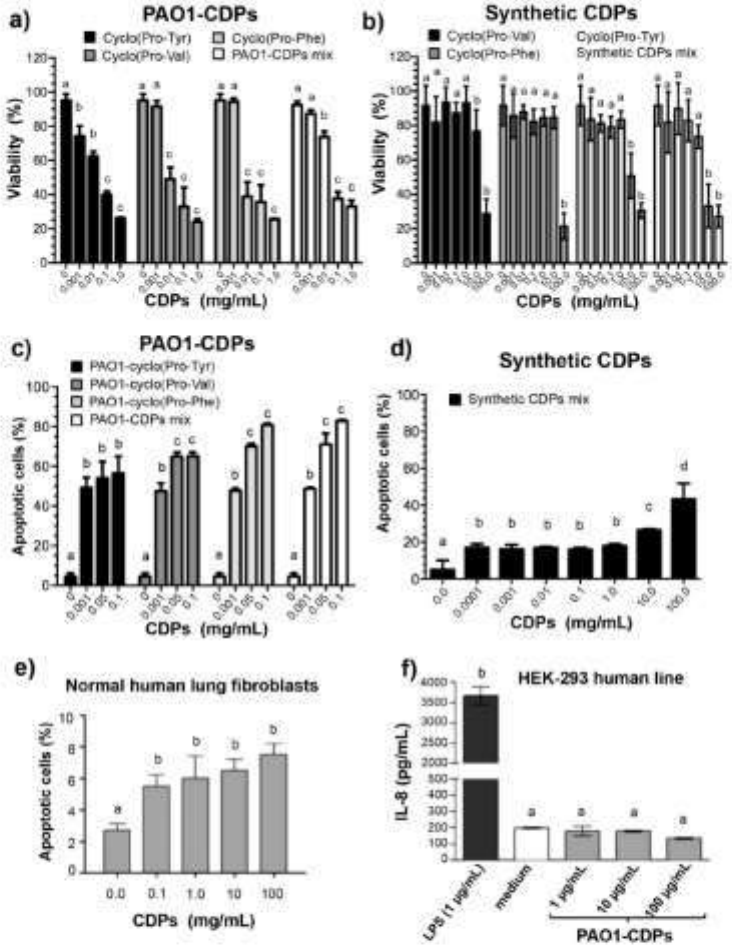

Figure 1. Effects of PAO1 and synthetic CDPs on HeLa cell viability and apoptosis induction. HeLa cells were incubated in CM medium and treated with CDPs for 24 h as described in Materials and Methods. Determination of viability of HeLa cells by an MTT assay treated with CDPs from *P. aeruginosa* PAO1 (**a**) and synthetic analogous CDPs (**b**). Induction of apoptosis in human HeLa cells by CDPs was analyzed in cultures grown in the CM medium and after treatment with CDPs for 24 h. Human cell lines were stained with annexin V and propidium iodide and analyzed by flow cytometry. The percentage of viability was determined by fluorescent cell quantitation in the dot plots, values were graphed as bars. Apoptosis induction in HeLa cells treated with PAO1-CDPs (**c**) and with the mixture of synthetic analogs of CDPs (**d**); (**e**) Apoptosis induction in normal human lung fibroblasts by the PAO1-CDP mixture at different concentrations determined as in (**c**); (**f**) IL-8 induction in HEK-293 cells by ELISA assay as described in Materials and Methods. Bars represent mean ± standard error (SE) of three independent experiments, $n = 6$. One-way analysis of variance (ANOVA) was carried out, with Tukey's *post hoc* test; statistical significance ($p < 0.01$) of differences between treatments is indicated with different lowercase letters.

2.2. Purified CDPs from P. aeruginosa PAO1 Induce Apoptosis in HeLa Cells

To determine whether some of the CDPs that constitute the PAO1-CDPs mixture are the compounds responsible of the induction of apoptosis in HeLa cells, the effect of PAO1-CDPs separately or in mixtures was determined by flow cytometry using annexin V and propidium iodide as probes. The percentage of fluorescent cells (PFC), corresponding to cells that were positive for the annexin V marker was ≤5% for HeLa cells without CDPs (Figure 1c). On the other hand, cells treated with the purified PAO1-CDPs added separately or in mixtures, showed ~50% of apoptotic HeLa cells at 1.0 μg/mL (4 μM) after 12 h of treatment (Figure 1c); interestingly, for the synthetic CDP mixture (that was more active than its individual compounds), the apoptosis induction was ~18% at the same concentration (Figure 1d). These results indicate that after 12 h of treatment, the PAO1-CDPs mixture induces apoptosis in ≥95% of HeLa cells, showing a half-effective concentration (EC_{50}) between $\sim 1.6 \times 10^{-3}$ and 5×10^{-4} mg/mL (~0.6–3 μM). However, no significant differences between isolated PAO1-CDPs and the crude PAO1-CDP mixture were observed, independently whether CM or SS mediums were used (Figure 1c; Table 1). Conversely, for the synthetic-CDP mixture, the EC_{50} values for apoptosis induction were higher than 100 mg/mL (400 mM; Table 1). These data indicate that PAO1-CDPs were at least three log units more active for apoptosis induction in HeLa cells than their synthetic analogs.

On the other hand, the crude PAO1-CDP mixture produced a slight apoptosis induction (~8%) in normal human lung fibroblasts, but at the highest concentration tested 100 mg/mL (400 mM); Figure 1e). Additionally, to rule out the possibility that the apoptotic effect caused by the crude PAO1-CDP mixture is due to the presence of lipopolysaccharides (LPS) as additional compounds of bacterial origin, the interleukin IL-8 presence was determined in the HEK-293 human cellular line. The data showed that the crude PAO1-CDP mixture obtained as described our procedure does not induce IL-8 production in the HEK-293 cell culture at concentrations over 0.5 mM (Figure 1f). These results indicate that the crude PAO1-CDP mixture does not contain LPS at concentrations that can to induce the biological response observed, and hence, the apoptotic response provoked in HeLa cells are indeed due to PAO1-CDPs.

In addition, the apoptosis induction in HeLa cells was confirmed by microscopic examination; the cells treated with the crude PAO1-CDP mixture at 0.01 mg/mL (40 μM) after 4 h of incubation, showed apoptotic cell morphology similar to the morphology of the cells treated with actinomycin D (10 mg/mL). Of note, apoptotic cell morphology was not observed in the normal human lung fibroblast line treated with high concentrations of the PAO1-CDP mixture (100 μM, Figure 2f)

2.3. CDPs from P. aeruginosa PAO1 Induce Apoptosis in HeLa Cells though a Caspase-9- and Caspase-3-Dependent Pathway

To identify the apoptotic pathway induced by the crude PAO1-CDP mixture, a more detailed study was carried out, determining apoptosis in HeLa cells at short response times. After 12 h of treatment with 6–60 μM of crude PAO1-CDP mixture, the cellular population was found mostly at early stages of apoptosis (~50% early with ~7% at late stages) (Figure 3a–d). Similar results were observed when tested in the concentration range of 1–100 μg/mL (6–600 μM; Figure 3e,f). Interestingly, cultures of normal human mononuclear blood cells treated with the crude PAO1-CDP mixture show minimal effect on apoptosis induction at early or late stages, with less than 10% of cell population at concentrations sufficient for apoptosis induction of ≥95% of HeLa cells (100 μg/mL; Figure 3g,h). These results indicate that the antiproliferative effect of the PAO1-CDP mixture in the HeLa cells was mediated by an apoptotic pathway instead of necrosis, indicating the participation of caspases as the molecular mechanism of cell death involved. To further elucidate this fact, the annexin V apoptosis-marker was used in the presence of caspase inhibitors. Data show that, although apoptosis was diminished (~20%) in the presence of the caspase-8 inhibitor (Z-IETD-FMK), it was strongly inhibited in HeLa cells treated with PAO1-CDPs plus the polycaspase inhibitor (Z-VAD-FMK), caspase-3 (Z-DEVD-FMK),

or caspase-9 (Z-LEHTD-FMK) inhibitors (Figure 3i), indicating that the PAO1-CDPs mixture induces apoptosis mainly by the caspase-9- and caspase-3-dependent pathway (intrinsic pathway).

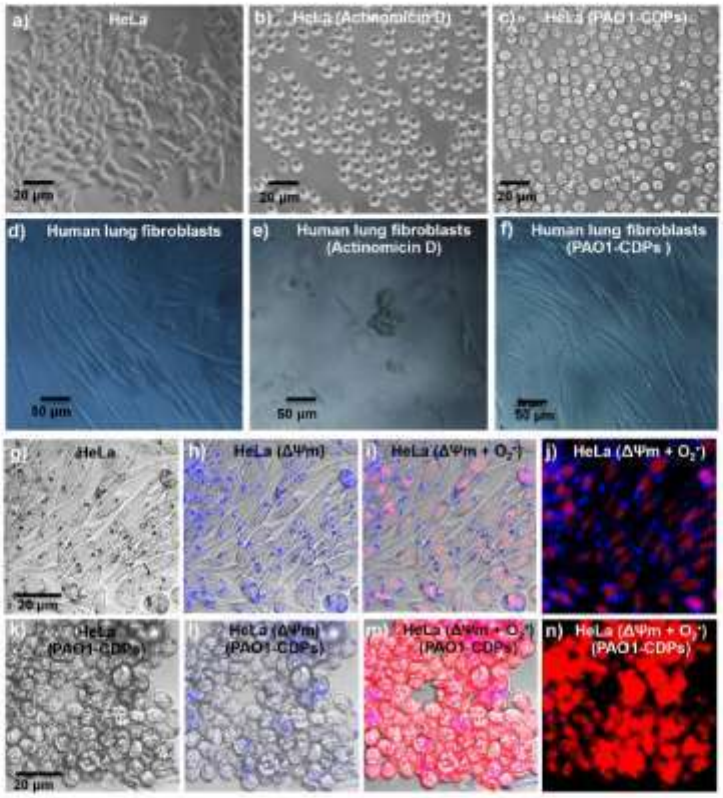

Figure 2. Morphological changes in human cell cultures stimulated with the CDP mixture from *P. aeruginosa* PAO1. (**a**–**n**) Images of human cells taken by means of phase contrast and confocal microscopy after treatment; (**a**–**c**) HeLa cell line; (**d**–**f**) Human lung fibroblast cell line. (**a**,**d**) DMSO (0.05%; negative control); (**b**,**e**) Actinomycin D (50 mg/mL; positive apoptosis control); (**c**,**f**) PAO1-CDP mixture (10 mg/mL) treatment for 2 h; (**g**) HeLa cells without treatment; (**h**) Determination of HeLa cells' membrane potential (ΔΨm) using Rhodamine 123 without treatment. (**i**) HeLa cell membrane potential (ΔΨm) and superoxide ($O_2^{\bullet-}$) quantification (using DHE probe) without treatment; (**j**) Same as in (**i**); but examination by dark field microscopy; (**k**–**n**) Conditions as in (**g**–**j**) but with treatment with the PAO1-CDP mixture. Images of the cells were taken at 40× magnification, using inverted phase-contrast microscope (HB0-50, Carl-Zeiss, San Diego, CA, USA) or confocal microscope (FV1000, Olympus, Center Valley, PA, USA).

2.4. *CDPs from P. aeruginosa PAO1 Arrest HeLa cells at the G0–G1 Transition*

The PAO1-CDPs antiproliferative mechanism was further explored by determining cell distribution in different phases of the cell cycle, through measuring the intracellular DNA content by flow cytometry. HeLa cells growing in a CM medium (medium with serum) showed ~25% of cells population at the G0–G1 stage, ~20% of cells at the G2–M stage, and ~55% of cells in the S phase.

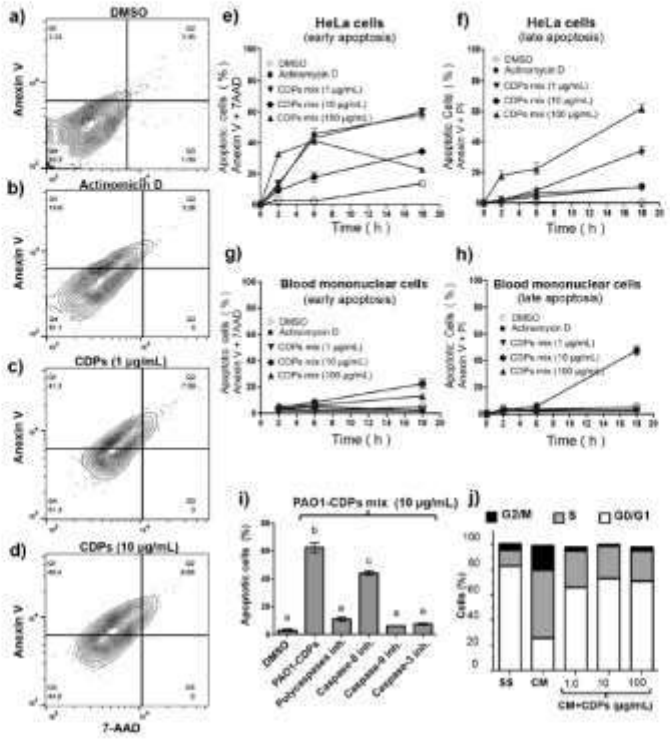

Figure 3. Apoptosis induction in HeLa cells by CDPs from *P. aeruginosa* PAO1. HeLa cells were incubated in the CM medium after treatment with PAO1-CDPs (various doses) as a function of time. Cells were stained with annexin V, 7-AAD, or propidium iodide and analyzed by flow cytometry. (**a**–**d**) The percentage of fluorescent cells determined in the dot plots is shown, corresponding to HeLa cells treated for 6 h with (**a**) DMSO; (**b**) actinomycin D (50 mg/mL), (**c**) PAO1-CDP mixture (1 µg/mL); (**d**) PAO1-CDP mixture (10 µg/mL). Q1, early apoptosis; Q2, late apoptosis; Q3, necrotic cells; Q4, viable cells; (**e**,**f**) Kinetic of induction early and late apoptosis stages in HeLa cells treated with the PAO1-CDP mixture; (**g**,**h**) Kinetics of induction of early and late apoptosis stages in blood mononuclear human cells treated with the PAO1-CDP mixture. Points of the plots represent mean ± standard error (SE) of three independent experiments; (**i**) Effects of inhibitors of apoptosis on HeLa cells in the presence of the PAO1-CDP mixture. The cells were incubated in the CM medium after treatment with 10 µg/mL PAO1-CDP mixture with the addition of caspases inhibitors. Cells were revealed with annexin V and analyzed by flow cytometry. The percentage of fluorescent cells (apoptotic cells) after each treatment was determined by means of the dot plots and is shown as bars in the graph. The inhibitors tested are indicated on the X-axis. Bars of the plots represent mean ± SE of three independent experiments, $n = 3$. One-way ANOVA was carried out, with Tukey's *post hoc* test; statistical significance ($p < 0.01$) of differences between treatments is showed with different lowercase letters; (**j**) Effects of the PAO1-CDP mixture on the cell cycle in HeLa cells. HeLa cells were incubated in serum-free medium (SS) and serum-enriched medium (CM) after treatment with various doses of the PAO1-CDPs for 24 h. Cells were fixed with paraformaldehyde (4%) for 10 min on ice. Then, the cells were incubated with DAPI (1:1000) for 10 min at room temperature and analyzed by flow cytometry for DNA quantitation.

Comparatively, cell cultures treated with the crude PAO1-CDP mixture (because no significant differences were observed in comparison with purified PAO1-CDPs) at 6–600 μM showed cell populations ~70% of cells at the G0–G1 stage, ~3% of cells at the G2–M stage, and ~25% of cells in the S phase (Figure 3j). Additionally, an arresting culture condition of HeLa cells such as SS medium (medium without serum by at least 4 h), showed proportions of cell populations similar to PAO1-CDPs treatment. These results suggest that the PAO1-CDPs diminish the proliferation of HeLa cells, blocking the DNA synthesis (S phase) and arresting the cultures at the G0–G1 stage.

2.5. CDPs from *P. aeruginosa* PAO1 Affect Membrane Potential and Induce Superoxide in HeLa Cells

Some toxic effects caused by CDPs in cell lines have been found to be associated with an increase in oxidative stress [9], or conversely, with beneficial effects of ROS scavenging [12]. Nevertheless, the mechanisms involved in ROS generation, accumulation, and type of ROS species generated by the CDPs are poorly known. So far, the findings indicate that the PAO1-CDP mixture induces apoptosis through an intrinsic pathway dependent on caspase-9 and caspase-3 activation, affecting the mitochondrial functionality prior to cytochrome *c* release, and therefore increased ROS generation is expected. The apoptotic pathway was confirmed by determining mitochondrial membrane potential ($\Delta\Psi m$) in cell cultures using the fluorescent marker Rhodamine 123. The findings showed that the fluorescence intensity of cells decreased ~70% after treatment with the crude PAO1-CDP mixture in comparison with untreated cells (Figure 4a). Real-time ROS quantification by flow cytometry and examination by confocal microscopy were carried out using the DHE fluorescent probe, which mainly identifies the mitochondrial superoxide radical. As described above, the crude PAO1-CDP mixture was able to decrease 80% cell survival at 60–250 μM; thus, this concentration range was used for superoxide determination in HeLa cells growing in CM or SS medium. The percentage of fluorescent cells (PFC) was increased in HeLa cells in a PAO1-CDP concentration-dependent and treatment time-dependent manner (Figure 4b). Cell suspensions without treatment showed PFC of ~10%, whereas with the PAO1-CDP mixture, the PFC increased significantly to 30–80% after 3 h of treatment (Figure 4b).

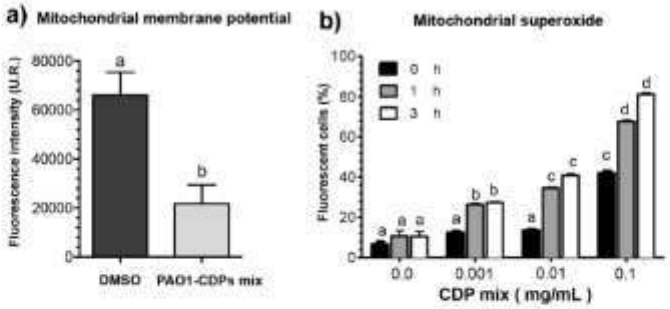

Figure 4. Membrane potential and superoxide quantification in HeLa cells treated with the CDP mixture from *P. aeruginosa* PAO1. Cell cultures were grown in the CM medium, harvested, and incubated in the CM or SS medium for 2 h. After that, the cell suspensions were incubated with or without PAO1-CDPs for 1 h at 37 °C. At the indicated time points, samples (100 μL) were resuspended in PBS and mixed with the Rhodamine 123 and DHE probes for quantitation of mitochondrial membrane potential and superoxide, respectively. The samples were incubated for 30 min and washed, and fluorescence was measured in real-time by flow cytometry. (**a**) Mitochondrial membrane potential and (**b**) superoxide quantification as percentage of fluorescent cells. Values are the mean of three independent experiments with 20,000 cells counted by flow cytometry per data point. SEM values are indicated as bars ($n = 3$), one-way ANOVA with Tukey's *post hoc* test, significant differences ($p < 0.01$) are indicated by different lowercase letters.

These results indicate that the crude PAO1-CDP mixture increased superoxide generation in HeLa cells in the same fashion, suggesting that the mechanism of antiproliferative effects (toxicity) could be related with ROS generation events, impairing mitochondrial functionality (such as $\Delta\Psi m$).

2.6. CDPs from *P. aeruginosa* PAO1 Modify the Akt and S6k Phosphorylation in HeLa Cells

Early studies on cell death regulation dependent on the caspase-9 protein have revealed the participation of Akt and small G protein p21-Ras kinases [21], and the PI3K–Akt–mTOR signaling pathway dysregulation has been extensively associated with cancer [22,23]. In this sense, our findings showed that the apoptotic caspase-9-dependent intrinsic pathway is involved in the antiproliferative effect of the PAO1-CDPs, and that HeLa cells are arrested in G0-G1 stages of the cell cycle. Accordingly, the participation of the PI3K–Akt–mTOR signaling pathway was analyzed next.

As described above, the results showed that the PAO1-CDP mixture induces apoptosis efficiently at short times; thus, analysis of Akt protein expression and phosphorylation was conducted by immunodetection procedures. The results showed that the phosphorylation of the Akt-S473 protein (p-Akt-S473) was decreased in the HeLa cells treated with 0.01 and 0.1 mg/mL (40 and 400 μM) of the crude PAO1-CDP mixture at 5 min of treatment, and was totally undetectable after 15 min (Figure 5a). On the other hand, the total Akt protein showed a strong level of expression with significant difference at 0.1 mg/mL by 5 min, but without significant differences at concentration (0.01 mg/mL) (Figure 5a). At longer periods of PAO1-CDPs treatment (30–240 min), the phosphorylation of p-Akt-S473 was induced again in function of time and PAO1-CDPs concentration, while total Akt protein and β-actin (protein load control) remained at high levels and without significant changes between treatments (Figure 5b).

The S6K (S6 ribosomal protein kinase) is one of the downstream targets of Akt protein in the PI3K–Akt–mTOR signaling pathway; thus, the effect of PAO1-CDPs on the S6K protein phosphorylation was determined in HeLa cells. We found that the phosphorylated S6K-T389 protein (p-S6K-T389) also was strongly inhibited after short periods of the PAO1-CDP treatment (≤30 min), whereas induction of p-S6K-T389 amount was detected after longer periods (≥120–240 min); however, total S6K protein expression was not modified at 30 min, but it showed an increased induction at 60 and 120 min post CDPs treatment (Figure 5b). These results showed that the crude CDP mixture from *P. aeruginosa* PAO1 modify the phosphorylation of Akt-S473 and S6K-T389 proteins, as well as their expression levels in a time- and concentration-dependent manner.

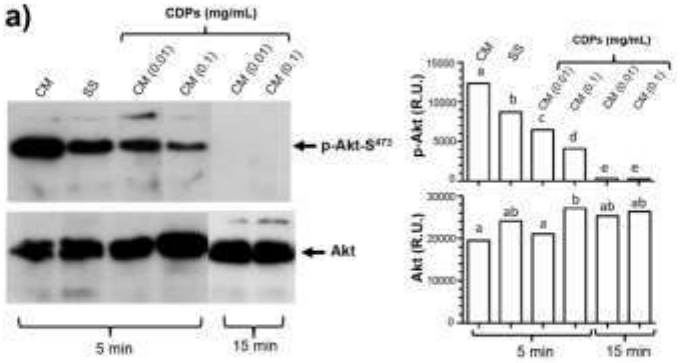

Figure 5. *Cont.*

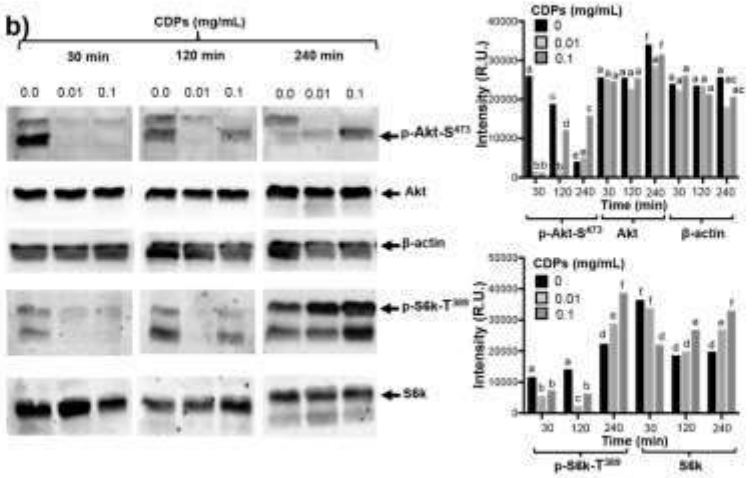

Figure 5. Effects of the CDP mixture from *P. aeruginosa* PAO1 on Akt and S6k phosphorylation and expression in HeLa cells. HeLa cells were incubated in SS and CM media and treated with 0.01 or 0.1 μg/mL PAO1-CDP mixture. At the indicated time points, cells were harvested and disrupted by sonication, and the solubilized proteins were separated by denaturing polyacrylamide gel electrophoresis (SDS-PAGE). Gels were electroblotted to PVDF membranes, and protein bands immunodetected using the indicated antibodies [anti-Akt (C-20-R), anti-Akt-phosphoryled 1/2/3 (Ser 473-R), anti-p70 S6 kinase α (H-160), anti-phosphoryled-p70 S6 kinase α (Thr 389)-R, and anti-β-actin] as the first antibody and a horseradish peroxidase (HRP)-conjugated goat anti-rabbit IgG antibody as the second antibody. Images correspond to representative gels from at least three independent treatments (left). Data correspond to the mean of three independent assays; the band intensity was determined by densitometry using the Image J software (right). (**a**) Immunodetection using the anti-phosphorylated Akt-S473 and anti-Akt antibodies after 5 and 15 min of treatment with the PAO1-CDP mixture; (**b**) HeLa cells extracts were obtained of cultures grown in CM media and treated with 0.01 or 0.1 mg/mL PAO1-CDP mixture. The same membranes reveled with anti-phosphorylated Akt-S473 were after immunodetected with the next antibodies: anti-Akt, anti-S6k, anti-phosphorylated-S6k-T389 and anti-β-actin. The assay was repeated at least three times using cell extracts from different cultures and treatments. A representative immunodetection assay is shown, and their plots of band intensity quantitation are shown to the right of the images. Bars represent mean of three densitometry determinations. Two-ways ANOVA was carried out, with Tukey's *post hoc* test; statistical significance ($p < 0.05$) of differences between treatments is indicated with different lowercase letters.

3. Discussion

The quest for novel molecules with properties related to inhibition of cancerous cell growth is a scientific field of major interest. Natural molecules with antiproliferative activity are considered more target-specific than their synthetic analogs. Besides, peptides constitute a diverse family of natural compounds that also have been implicated in diverse biological functions. Cyclic peptides or their derivatives diketopiperazines of microbial origin are believed to have a strong pharmaceutical potential as antimicrobial and antifungal agents, immunomodulators, antioxidants, or anticancer agents [13,24]. CDPs possess intrinsic physiological advantages over other molecules, for example, chemical and enzymatic stability and structural and conformational specificity. These properties make them more promising than their non-CDP counterparts. Several approaches to CDP synthesis have

been explored to discover synthetic analog molecules that can serve as novel drugs. Although CDPs have been discovered a long time ago and have been studied all this time, only recently have they aroused some interest because of their antiproliferative effects on cancerous cell lines [11,12,14,15].

P. aeruginosa is a pathogenic and opportunistic bacterium that produces a large number of virulence factors. CDPs can be considered the molecules that can regulate the production of virulence factors in a QS-dependent manner in this microorganism [25–28]. In the context of antiproliferative properties attributed to CDPs, we recently reported that a mixture of CDPs composed of cyclo(L-Pro-L-Tyr), cyclo(L-Pro-L-Val), and cyclo(L-Pro-L-Phe) isolated from the *P. aeruginosa* PAO1 strain can inhibit the proliferation of human tumor cell lines: HeLa and CaCo-2 [15]. In the present work, a CDP purification process was carried out with the aim to determine whether the antiproliferative effect previously observed in tumor cells are induced by some of the CDPs that constitute the PAO1-CDPs mixture or whether synergistic effects exit. We found that the CDP mixture from the PAO1 strain contains mainly the CDPs cyclo(L-Pro-L-Tyr), cyclo(L-Pro-L-Val), and cyclo(L-Pro-L-Phe) (≥80%) (Figure S1, Supplementary Material). When the effect of these isolated PAO1-CDP fractions on the viability or apoptosis of HeLa cells was tested, no significant differences were observed between them, except a slightly increased effect of cyclo(L-Pro-L-Phe) against HeLa cell viability than the other CDPs, but no over apoptosis induction (Figure 1a; Table 1). Furthermore, CDP synthetic analogs, though able to affect cell viability and to induce apoptosis, required a ~1000-fold higher concentration than PAO1-CDPs did. The LD_{50} of PAO1-CDPs was in the range between 0.010–0.03 mg/mL (60 and 250 μM) for HeLa cells; whereas this LD_{50} for the synthetic CDPs was between 10 and 400 mM (Table 1). Interestingly, we found that the PAO1-CDP mixture showed minimal apoptosis induction in blood mononuclear human cells cultures (<8%) at high concentrations such as 100 mg/mL (400 mM) and also in normal human lung fibroblasts cultures (<10%) at concentrations 100 μg/mL (4 μM) (Figures 1e and 3g–h). In addition, we previously have been reported that a crude PAO1-CDP mixture showed IC_{50} of 0.53 mg/mL [15], however in this work the LD_{50} dose was of 0.06 mg/mL; this discrepancy is attributed to a better extraction process that let us to eliminate compounds such as AHL, LPS, or pigments.

Previously, researchers have described the growth inhibition of colon cancer HT-29, HeLa, and MCF-7 cells in culture by seven synthetic proline-based CDPs, revealing that cyclo(Phe-Pro) causes growth inhibition at 10 mM and induction of apoptosis (15% cells population) at 5 mM after 72 h of treatment [11,12]. In agreement with these data, we observed an inhibitory effect of viability and apoptosis induction at the same concentration (10 mM) with the same synthetic CDPs in HeLa cells (Figure 1). However, PAO1-CDPs showed highest antiproliferative activity than synthetic CDPs such as apoptosis induction at 0.6 μM after 12 h of treatment (Table 1), whereas for the synthetic mixture, it was observed at 400 mM. Furthermore, these data showed that PAO1-CDPs were at least three log units more active than their synthetic analogs. The probable reason for the observed effects is that molecules isolated from living entities such as *P. aeruginosa* are produced with chiral specificity, ensuring stereochemical specificity and therefore strong activity, as described elsewhere [11].

The antiproliferative mechanism of the PAO1-CDP mixture was explored further by determining cell population distribution in different phases of cell cycle. The results indicate that proliferation of the HeLa cells was arrested at the G0–G1 stage and at the DNA synthesis stage (S phase; Figure 3j). Quantification of apoptotic cells indicates that PAO1-CDPs caused apoptosis in HeLa cells mostly at early apoptotic steps. This effect was not observed in normal blood mononuclear cells (Figure 3g). Furthermore, the utilization of caspase inhibitors allowed us to determine that the induction of apoptosis in HeLa cells was dependent of the caspase-9 and -3 pathway (Figure 3i). This pathway was verified by measuring $\Delta\Psi m$ in cell cultures, confirming that the intrinsic apoptotic pathway was implicated. In line with this finding, HeLa cells treated with the crude PAO1-CDP mixture showed an increase in superoxide generation in a dose-dependent manner, confirming that the mechanism of cellular death caused by PAO1-CDPs also involves ROS generation, with superoxide being one of the major produced and accumulated species (Figure 4). The cells showed increased superoxide levels at

the same times as the early stages of apoptosis induction with the PAO1-CDPs treatment, indicating that the strong ROS production occurs simultaneously with apoptotic events (Figures 3e and 4b).

Dysregulation of the PI3K–Akt–mTOR signal transduction pathway has been shown to be associated with some carcinomas and has been implicated in the apoptotic intrinsic pathway too; this pathway performs essential functions in cellular growth regulation [29]. Additionally, the regulation of the apoptotic intrinsic pathway involves caspase-9 and subsequent cytochrome *c* proteolysis, where phosphorylation of pro-caspase-9 is related to the Akt protein kinase [21]. In this context, studies have revealed that the possible pathway for apoptosis induction by the CDPs cyclo(prolyl-tyrosyl) and cyclo(prolyl-phenylalanyl) isolated from *Bacillus* sp., is associated with Akt phosphorylation (inhibition to ~3–18% with respect to untreated cell cultures) [19]. Nonetheless, those authors did not present sufficient evidence to implicate these CDPs in the mechanism of apoptosis induction. In this sense, our results clearly show that the PAO1-CDP mixture was able to abrogate phosphorylation of both Akt-S473 and S6k-T389 protein kinases in a time- and concentration-dependent manner in HeLa cells in short time periods (5–30 min) (Figure 5). Additionally, we found that the phosphorylation and dephosphorylation of Akt-S473 and S6k-T389 protein kinases showed a cyclic behavior in HeLa cells: after inhibition of phosphorylation by PAO1-CDPs treatment, phosphorylation of both proteins was detected again, but after longer periods of time (120–240 min). We also determined the phosphorylation of Akt-S473 protein in free cell extracts of HeLa cultures treated with the crude PAO1-CDP mixture at prolonged times (12–48 h), but it was impossible to detect the p-Akt-S473 or Akt protein isoforms, observing massive protein degradation on the SDS-PAGE gels.

Akt phosphorylation and dephosphorylation have been reported in HeLa cells subjected to serum starvation in a cyclic biphasic behavior. Incubation periods less than 12 h led to low levels of Akt-S473 phosphorylation, but after periods longer than 12 h, higher levels of p-Akt were observed involving endogenous insulinlike growth factor (IGF) synthesis under deficient culture conditions, such as serum deprivation [30]. It is interesting whether CDPs themselves also induce endogenous synthesis of molecules that can activate the Akt pathway, and more experiments are needed to explain this biphasic behavior of Akt phosphorylation.

mTORC1 controls the rate of protein synthesis through phosphorylation and activation of the S6k protein kinase and eukaryotic translation initiation factor 4E (eIF4E)-binding protein 1 (4E-BP1), promoting mRNA translation and protein synthesis [23]. In general, our findings confirm that PAO1-CDPs are capable of inducing apoptosis in human tumor HeLa cells involving the inhibition of Akt phosphorylation and subsequently the phosphorylation of the downstream S6k protein target. Because cell proliferation is associated with p-Akt/p-S6k levels, our findings suggest that the inactivation of the TORC1 complex probably participates in the antiproliferative effect of the PAO1-CDPs in HeLa cells, thereby pointing to inactivation of the PI3K–Akt–mTOR signal transduction pathway as PAO1-CDPs' mechanism of action.

Akt regulates metabolism, survival, apoptosis, growth, and proliferation, whereas mTORC2 directly activates Akt by phosphorylating its hydrophobic motif (Ser473), a site required for its maximal activation [16,31]. Hence, the cyclic phosphorylation behavior of Akt-S473 observed during PAO1-CDP treatment of HeLa cells suggests that mTORC2 activity may be involved. The mTORC2-dependent Akt phosphorylation leads to activation of mTORC1; thus, mTORC2 may indirectly suppress autophagy [18,32].

The heterodimer consisting of tuberous sclerosis 1 (TSC1; also known as hamartin) and TSC2 (also known as tuberin) is a key upstream regulator of mTORC1 and functions as a GTPase-activating protein (GAP) for Ras homolog enriched in brain (Rheb) GTPase. The GTP-bound form of Rheb directly interacts with mTORC1 and strongly stimulates its kinase activity. As a Rheb GAP, TSC1–2 heterodimer negatively regulates mTORC1 by switching Rheb to its inactive GDP-bound state [16]. Phosphorylated Akt disrupts the heterodimer by phosphorylating TSC1, thereby abrogating its GAP action on Rheb, leading to mTORC1 activation, thus promoting cell proliferation and inhibiting autophagy.

TSC1 or TSC2 dysfunction is also implicated in uncontrolled growth and cancer [18]. In contrast, low cellular energy levels or hypoxia induce TSC1/2 heterodimer formation inhibiting mTORC1 activation. Autophagy is a cellular process necessary for development and tissue homeostasis and participates in various physiological and pathologic processes (including exercise, metabolic adaptation, and disorders such as neurodegenerative diseases, infectious diseases, cardiovascular diseases, cancer, and aging) [18]. Because mTORC1 plays essential roles in autophagy, it is a potential pharmacological target. Therefore, identification of novel molecules with the capacity for modulation of autophagy via mTOR-dependent mechanisms is of great scientific interest in terms of treatment of human diseases.

4. Materials and Methods

4.1. Chemicals and Reagents

Dulbecco's modified Eagle's medium (DMEM), fetal bovine serum (FBS), antibiotic and antimycotic solution (100X) containing penicillin, streptomycin, amphotericin B, 4,6-diamidino-2-phenylindole (DAPI), 3-(4,5-dimethylthiazol-2-yl)-2,5-diphenyltetrazolium bromide (MTT) were purchased from Sigma-Aldrich Co. (St. Louis, MO, USA). Tissue-culture plasticware was acquired from Corning (New York, NY, USA), Alexa Fluor 488 Annexin V and the PI/dead cell apoptosis kits (Invitrogen, Life Technologies, Carlsbad, CA, USA), and synthetic CDPs cyclo(-Pro-Val), cyclo(-Pro-Tyr), and cyclo(-Phe-Pro) (G-4730, G-4715, and G-4720, respectively) were acquired from Bachem Co. (Torrance, CA, USA).

4.2. Bacterial Strains and Culture Conditions

The *P. aeruginosa* PAO1 wild type [33] was grown in Luria-Bertani (LB) broth at 37 °C, with shaking. Solid media were prepared by adding 1.5% (*w*/*v*) agar. Antibiotic concentrations used for the *P. aeruginosa* were 200 µg/mL streptomycin; all reagents were purchased from Sigma-Aldrich Co.

4.3. Solvent Extraction and Chemical Characterization of CDPs from the P. aeruginosa PAO1 Strain

A 2.5×10^8 CFU inoculum of *P. aeruginosa* WT was placed in 300 mL of LB broth and incubated in a growth cabinet 24 h at 37 °C for bacterial growth. Cell-free supernatants were prepared by centrifugation (10,000× *g* at 25 °C by 10 min; in an 5810R centrifuge (Eppendorf Hauppauge, NY, USA). The resulting supernatant was extracted twice with two volumes of ethyl acetate supplied with acetic acid (0.1 mL/L). The extract was evaporated to dryness using a rotavapor (Buchi-210 Lab, Buchi, Flawil, Switzerland) at 60 °C under vacuum. The residue was solubilized in methanol–acetonitrile (1:1), the undissolved residue was removed by centrifugation and the sample was evaporated to dryness, and finally dissolved in DMSO–water (1:3) rendering the crude PAO1-CDPs mixture. Analysis of extracts was carried out using High Performance Liquid Chromatography (HPLC, model 240, Varian, Santa Clara, CA, USA) using a Photodiode Array detector (Varian 410) and a reverse-phase HPLC column Sephasil-Peptide C18, 12 µm, 4.6 mm × 250 mm (Amersham, Pittsburgh, PA, USA). Fractions were eluted with water-acetonitrile, starting with a equilibration solvent mix of 0:100; followed by a gradient linear up 60:40, at flow of 1 mL/min by 15 min, following with return to 0:100 solvent mix in 3 min and an equilibrium phase during 2 min. The deionized water and HPLC-grade acetonitrile were filtered and degasified (J.T. Baker, Center Valley, PA, USA). The extract was also analyzed for CDPs identification by gas chromatography-mass spectrometry (GC-MS, GC-6850 Series II equipped with a MS-5973, Agilent Technologies Inc., Santa Clara, CA, USA) as previously described [20]. Relative CDP proportions were determined by area units showed in chromatograms of the GC-MS analysis. For dose-response assays, the crude PAO1-CDPs mix was evaporated to dryness, weighed out, and dissolved with DMSO-water 1:3 to prepare a 100 mg/mL concentration as stock solution.

4.4. Cell Line Growth

The human cancer cell line HeLa was obtained from the American Type Culture Collection (ATCC, Manassas, VA, USA), HEK-293/MD2/CD14 cell line used in IL-8 induction assay (InvivoGene, San Diego, CA, USA), peripheral blood mononuclear cells (PCMB) obtained from healthy volunteers by isolation through Ficoll gradient and human lung fibroblast cells were kindly provided by Dr. Moises Selman and Dr. Adan Moreno (Hospital Juárez de México, México City). Cell procedures were performed under class II biological safety cabinets. Cells were cultured in DMEM supplemented with 10% (v/v) FBS (complete medium, CM), and 1% antibiotic (10,000 units of penicillin, 10 mg streptomycin, and 25 g of amphotericin B per mL, Sigma-Aldrich Co.) solution. The cultures were fed twice a week and maintained at 37 °C under 80% humidity and incubated in an atmosphere of 5% CO_2. HeLa cells were collected by trypsinization using trypsin/EDTA buffered solution for 5 min at 30 °C, followed by the addition of serum-enriched complete medium (CM) to stop trypsin action. After trypsinization the cells were collected and washed with CM. Finally, cells were counted in a hemocytometer chamber and incubated in fresh CM media.

4.5. Cell Viability Assay

Cell viability was determined by the colorimetric method using MTT dye. Briefly, HeLa cells were seeded in 96-well flat-bottomed plates (Thermo Fisher Scientific, Grand Island, NY, USA) at a density of 3×10^4 cells per well in 200 µL of CM and incubated by 24 h at 37 °C with 5% CO_2 as described above. Then, the medium was removed and replaced with fresh CM or serum-free medium (SS). Then, cells were incubated with the CDPs solution at indicated concentrations. Cells were incubated for another 24 h at 37 °C with 5% CO_2. To determine cell viability, MTT 50 mg/mL in PBS was added to each well and incubated for 4 h at 37 °C. Finally, 100 µL of 2-propanol/1M HCl (19:1 v/v) was added to dissolve the formazan crystals. Absorbance measurements were conducted utilizing a microplate spectrophotometer reader (BioTek Instruments, Winooski, VT, USA) at 595 nm.

4.6. Necrosis and Apoptosis Assay

HeLa cell line was seeded in 96-well flat-bottomed plates at a density of 3×10^4 cells per well in 200 µL of CM and incubated for 24 h at 37 °C with 5% CO_2. Then, cells were synchronized with SS medium for 12 h under the same conditions and adding different concentrations of CDPs. DMSO was used as control at the same concentration used to dissolve the CDPs. To determinate the apoptotic effect, cells were collected by centrifugation at 2000× g for 10 min. The pellet was suspended in 20 µL of SS medium and treated with annexin V and propidium iodide (PI) (Dead Cell Apoptosis Kit; Molecular Probes, Invitrogen Life Technologies), or with 7-aminoactinomycin D (7-AAD; Molecular Probes, Invitrogen Life Technologies) following the indications recommended by the manufacturer. Fluorescence was immediately quantified by flow cytometry using an Accuri-C6 Flow Cytometer (BD Biosciences, San Jose, CA, USA). Cell populations from each treatment were gated in forward scatter and side scatter dot plots to eliminate cell debris. Populations corresponding to auto- or basal-fluorescence were located in the left quadrant, and cells with emission of fluorescence increasing at least one log unit value were located in the right quadrant of the dot plots. In addition, the percentage of fluorescent cells (PFC) and median fluorescence intensity (FI) were determined in monoparametric histograms of fluorescence emission obtained from the dot plots and labeled as PFC and as relative fluorescence units. The equipment was calibrated using Spherotech 8-peak (FL1-FL3) and 6-peak (FL-4) validation beads (BD Accuri, San Jose, CA, USA). For apoptosis and necrosis assays, fluorescence for annexin V in emission fluorescence channel FL1 at 495/519 nm, for propidium iodide in the FL2 channel at 535/617 nm, and for 7-AAD in the FL3 channel at 488/647 nm were monitored. At least 20,000 cellular events were analyzed for each determination point. Data were analyzed using FlowJo V12.1 software (Tree star, Stanford, CA, USA).

4.7. Caspases Inhibition Assays

HeLa cell line was seeded 2×10^5 cells per well in 24 flat bottom plates in 0.5 mL of CM medium. Cells were synchronized for 12 h in SS medium and after the caspases inhibitors: pan caspase (Z-VAD-FMK), caspase-3 inhibitor (Z-DEVD-FMK), caspase-8 inhibitor (Z-IETD-FMK), and caspase-9 inhibitor (Z-LEHTD-FMK) (BD Pharmigen, San Jose, CA, USA) at 10 mM concentration were added 120 min prior to the addition of crude PAO1-CDFs mix at 10 mg/mL, followed by 4 h of incubation. DMSO was used as negative control in absence of caspase inhibitor in the same condition as the crude PAO1-CDFs mix. Cells were collected by trypsinization, and washed with cold PBS. Apoptosis was monitored using anexin V-APC (allophycocyanin) conjugated (BD Pharmigen) and fluorescence was registered in Accuri-C6 flow cytometer by fluorescence emission (650/660 nm) determined in FL4 channel. At least 20,000 cellular events were analyzed in each determination point, data after were analyzed using FlowJo V12.1 software.

4.8. Determination of IL-8 by ELISA

HEK-293 TLR4/MD2/CD14 cell line that stably expressed TLR4 receptor were seeded into a 96-well plate at a concentration of 2×10^4 cells per well and treated with the crude PAO1-CDFs mix for 4 h. Cell supernatants were tested for IL-8 protein with the commercially available OptEIATM kit (BD Biosciences), absorbance was measure at 490 nm in ELISA reader (Dynex, Chantilly, VA, USA).

4.9. Mitochondrial Membrane Potential Determination

Membrane potential in HeLa cells suspension was determined using the fluorescent, cell-permeable indicator Rhodamine 123 (Sigma-Aldrich Co.). HeLa cell line was seeded in 96-well flat-bottomed plates at a density of 3×10^4 cells per well in 200 µL of CM and incubated for 24 h at 37 °C with 5% CO_2. Then, cells were synchronized with SS medium for 2 h under the same conditions and adding 0.1 mg/mL of the crude PAO1-CDFs mix. DMSO was used as control at the same concentration used to dissolve the CDFs. After, cells were loaded with Rhodamine 123 (5 µg/mL) and incubated at 37 °C for 30 min in darkness. Suspensions were washed and fluorescence was quantified using an Accuri-C6 Flow Cytometer monitoring the emission fluorescence in channel FL1 at 533/30 nm. At least 20,000 cellular events were analyze; or directly observed in a Confocal Microscopy (FV1000, Olympus, Center Valley, PA, USA) monitoring the emission fluorescence at 533/30 nm. Fluorescence intensity was quantified using the Image J software.

4.10. Real-Time Quantification of Superoxide in Human Tumor Cell Lines

Intracellular superoxide ($O_2^{\bullet-}$) in cell suspensions was determined using cell-permeant fluorescent probe dihydroethidium (DHE, Molecular Probes, Invitrogen) and fluorescence was quantified by flow cytometry using an Accuri-C6 Flow Cytometer. Human cell lines were grown as described above and samples (100 µL) were trypsinized and washed with PBS buffer. Cells suspensions (1×10^5 cells) were incubated with DHE (5 µg/mL) at 37 °C for 2 h in darkness. Then, human cells were harvested, washed, and re-suspended in PBS. The populations of fluorescent cells for each treatment were monitored by flow cytometry in the emission fluorescence channel FL1 (587/40 nm). At least 20,000 cellular events were analyzed in each determination point.

4.11. Immunodetection Assays

Human HeLa cell cultures were grown as described above and synchronized by 12 h in incomplete medium without serum (SS) incubating at 37 °C under 5% CO_2 atmosphere. 3×10^4 cells were seeded in each well (six-well plates) in total volume per well of 3 mL of fresh SS or CM mediums supplemented with respective compounds to test. After treatments, the medium was eliminated and cells were submitted to cellular trypsinization with CM/SS medium and harvested by centrifugation at 5000 × *g*, 4 °C by 10 min. Cellular lysis was carried out in phosphorylation buffer (PB) 300 µL composed by

]Hepes 50 mM pH 7.6, sodium-pyrophosphate 50 mM, sodium ortovanadate 1 mM, sodium molybdate 1 mM, EDTA, EGTA 20 mM, benzamidine 1 mM, NaF 20 mM, PMSF 0.2 mM, β-glycerophosphate 80 mM, mannitol 200 mM, protease inhibitor cocktails 1 µL/mL (all reagents from Sigma-Aldrich Co.)] Cell suspension was lysed (cell lysate) by two sonication pulses at low intensity by 30 sec each at 4 °C (Hielscher-US24 Utrasound Technol., Ringwood, NJ, USA). The protein extracts cell-free were obtaining by centrifugation of total cell homogenates at 7500 × *g*, 4 °C by 15 min. Protein was determined by Bradford method (BioRad, Hercules, CA, USA) and 30 µg of total protein was mixed with 10 µL of denaturing buffer (Tris-HCl 0.06M, pH6.8, 5% de glycerol, 4% SDS, 4% β-mercaptoethanol and 0.0025% bromophenol blue) during 5 min at 95 °C in a boiling water bath. Samples were run in a denaturing polyacrylamide gel electrophoresis at 10–12% (SDS-PAGE). The gels in one side were Coomassie blue stained and the other gel transferred to polyvinylidene difluoride (PVDF, Millipore, Billerica, MA, USA) membranes for western blot procedure.

For immunodetection, membranes were blocked using dry milk in TBS-T (Tris-HCL 10 mM; NaCl 0.9%; tween-20 0.1%, pH 7.8) and blotted with the anti-human antibodies: anti-Akt (C-20-R), anti-Akt-phosphoryled 1/2/3 (Ser 473-R), anti-p70 S6 kinase α (H-160), anti-phosphoryled-p70 S6 kinase α (Thr 389)-R, and anti-β-actin; all from Santa Cruz Biotechnology, Santa Cruz, CA, USA. The first antibody was blotted in blocking medium at 1:10,000 dilution for 12 h at 4 °C with light shaking. After washing, the membrane was incubated with the secondary antibody, Goat anti-Rabbit IgG HRP-conjugate (BioRad), in blocking medium at 1:10,000 dilution for 4 h at 4 °C; the membrane was twice washed with TBS-T and developed using hydrogen peroxide and Supersignal West Pico Luminol (Pierce, Thermo Fisher Scientific) and after exposing in light-sensitive films or ChemiDoc™ MP System (Bio-Rad). Assays were conducted by at least three independent assays and representative images are shown. Bands intensities in gels or films were quantified using the Image J1 software (NIH Image, Bethesda, MA, USA).

4.12. Cell Image Captures

HeLa cells was seeded in 12-well flat-bottomed plates at a density of 1×10^4 cells per well with 1 mL of CM and incubated for 24 h at 37 °C with 5% CO_2. Cells were incubated with serum-free medium (SS) for 12 h at 37 °C and an atmosphere of 5% CO_2 and incubated with different concentrations of the CDPs. After treatment, the cells were washed with PBS. Cells were fixed with paraformaldehyde (PFA at 4%) for 10 min on ice and collocated on cover glass, placed into a holder with a drop of PBS and glycerol 1:1 and photographed using an inverted phase-contrast microscope (Carl-Zeiss HB0-50, Gottingen, Germany) equipped with an AxioCam/Cc1 digital camera (Carl-Zeiss, Gottingen, Germany). Additionally cell cultures were observed directly using a confocal microscope (Olympus FV1000), Images of the HeLa cells were taken using 40 × magnification.

4.13. Ethical Considerations

The Hospital Juarez of Mexico Scientific Research Committee (composed of Scientific, Ethics, and Bio-security Committees) approved the project (projects number: HJM 2321/14-8, HJM2112/12-8), and in accordance with "Reglamento de la Ley General de Salud en Materia de Investigación para la Salud, Mexico", and the protocols that were used conformed to the ethical guidelines of the 1975 Declaration of Helsinki. All enrolled individuals provided written informed consent.

5. Conclusions

Our findings indicate that the antiproliferative effect of the PAO1-CDP mixture on HeLa cells involves inhibition of both Akt-S473 and S6k-T389 protein phosphorylation and activation of the caspase-9-dependent intrinsic apoptosis pathway and mitochondrial dysfunction. These data suggest that the antiproliferative effect of PAO1-CDPs involves the Akt–mTOR–S6k signalling pathway, pointing to the involvement of mTORC complexes.

Supplementary Materials: Supplementary materials are available online.

Acknowledgments: This study was funded by the Consejo Nacional de Ciencia y Tecnología (CONACYT) of México (grant numbers 256119, 167071, and 222405), the Marcos Moshinsky Foundation and Universidad Michoacana de San Nicolás de Hidalgo/C.I.C.2.14 grant. VR-D and PH-L received a scholarship from CONACYT.

Author Contributions: Conceived and designed the experiments: J.C.-G. Performed the experiments: L.H.-P., D.V.-R., L.A.S.-B., A.L.D.-P. Analyzed the data: H.R.-D.I.C., J.C.-G. Contributed reagents/materials/analysis tools: V.M.-C., J.M.-R., M.A.M.-E., H.R.-D.I.C., J.C.-G. Wrote the paper: H.R.-D.I.C., J.C.-G.

Conflicts of Interest: The authors declare that they have no conflict of interest.

References

1. Battle, S.E.; Meyer, F.; Rello, J.; Kung, V.L.; Hauser, A.R. Hybrid pathogenicity island pagi-5 contributes to the highly virulent phenotype of a *Pseudomonas aeruginosa* isolate in mammals. *J. Bacteriol.* **2008**, *190*, 7130–7140. [CrossRef] [PubMed]
2. De Abreu, P.M.; Farias, P.G.; Paiva, G.S.; Almeida, A.M.; Morais, P.V. Persistence of microbial communities including pseudomonas aeruginosa in a hospital environment: A potential health hazard. *BMC Microbiol.* **2014**, *14*, 118. [CrossRef] [PubMed]
3. Seguin, J.; Moutiez, M.; Li, Y.; Belin, P.; Lecoq, A.; Fonvielle, M.; Charbonnier, J.B.; Pernodet, J.L.; Gondry, M. Nonribosomal peptide synthesis in animals: The cyclodipeptide synthase of nematostella. *Chem. Biol.* **2011**, *18*, 1362–1368. [CrossRef] [PubMed]
4. Holden, M.T.; Ram Chhabra, S.; de Nys, R.; Stead, P.; Bainton, N.J.; Hill, P.J.; Manefield, M.; Kumar, N.; Labatte, M.; England, D.; et al. Quorum-sensing cross talk: Isolation and chemical characterization of cyclic dipeptides from *Pseudomonas aeruginosa* and other gram-negative bacteria. *Mol. Microbiol.* **1999**, *33*, 1254–1266. [CrossRef] [PubMed]
5. Strom, K.; Sjogren, J.; Broberg, A.; Schnurer, J. Lactobacillus plantarum milab 393 produces the antifungal cyclic dipeptides cyclo(L-phe-L-pro) and cyclo(L-phe-trans-4-oh-L-pro) and 3-phenyllactic acid. *Appl. Environ. Microb.* **2002**, *68*, 4322–4327. [CrossRef]
6. Li, X.; Dobretsov, S.; Xu, Y.; Xiao, X.; Hung, O.S.; Qian, P.Y. Antifouling diketopiperazines produced by a deep-sea bacterium, streptomyces fungicidicus. *Biofouling* **2006**, *22*, 201–208. [CrossRef] [PubMed]
7. Wyatt, M.A.; Wang, W.; Roux, C.M.; Beasley, F.C.; Heinrichs, D.E.; Dunman, P.M.; Magarvey, N.A. *Staphylococcus aureus* nonribosomal peptide secondary metabolites regulate virulence. *Science* **2010**, *329*, 294–296. [CrossRef] [PubMed]
8. Kwak, M.K.; Liu, R.; Kwon, J.O.; Kim, M.K.; Kim, A.H.; Kang, S.O. Cyclic dipeptides from lactic acid bacteria inhibit proliferation of the influenza a virus. *J. Microbiol.* **2013**, *51*, 836–843. [CrossRef] [PubMed]
9. Lee, K.; Jeong, J.E.; Kim, I.H.; Kim, K.S.; Ju, B.G. Cyclo(phenylalanine-proline) induces DNA damage in mammalian cells via reactive oxygen species. *J. Cell. Mol. Med.* **2015**, *19*, 2851–2864. [CrossRef] [PubMed]
10. Kanoh, K.; Kohno, S.; Asari, T.; Harada, T.; Katada, J.; Muramatsu, M.; Kawashima, H.; Sekiya, H.; Uno, I. (−)-phenylahistin: A new mammalian cell cycle inhibitor produced by aspergillus ustus. *Bioorg. Med. Chem. Lett.* **1997**, *7*, 2847–2852. [CrossRef]
11. Brauns, S.C.; Milne, P.; Naudé, R.; Van de Venter, M. Selected cyclic dipeptides inhibit cancer cell growth and induce apoptosis in ht-29 colon cancer cells. *Anticancer Res.* **2004**, *24*, 1713–1720. [PubMed]
12. Furukawa, T.; Akutagawa, T.; Funatani, H.; Uchida, T.; Hotta, Y.; Niwa, M.; Takaya, Y. Cyclic dipeptides exhibit potency for scavenging radicals. *Bioorg. Med. Chem.* **2012**, *20*, 2002–2009. [CrossRef] [PubMed]
13. Boyer, N.; Morrison, K.C.; Kim, J.; Hergenrother, P.J.; Movassaghi, M. Synthesis and anticancer activity of epipolythiodiketopiperazine alkaloids. *Chem. Sci.* **2013**, *4*, 1646–1657. [CrossRef] [PubMed]
14. Nishanth Kumar, S.; Dileep, C.; Mohandas, C.; Nambisan, B.; Ca, J. Cyclo(d-tyr-d-phe): A new antibacterial, anticancer, and antioxidant cyclic dipeptide from *Bacillus* sp. N strain associated with a rhabditid entomopathogenic nematode. *J. Pept. Sci.* **2014**, *20*, 173–185. [CrossRef] [PubMed]
15. Vázquez-Rivera, D.; González, O.; Guzmán-Rodríguez, J.; Díaz-Pérez, A.L.; Ochoa-Zarzosa, A.; López-Bucio, J.; Meza-Carmen, V.; Campos-García, J. Cytotoxicity of cyclodipeptides from *Pseudomonas aeruginosa* PAO1 leads to apoptosis in human cancer cell lines. *BioMed Res. Int.* **2015**, *2015*, 197608. [CrossRef] [PubMed]

16. Laplante, M.; Sabatini, D.M. mTor signaling in growth control and disease. *Cell* **2012**, *149*, 274–293. [CrossRef] [PubMed]
17. Borders, E.B.; Bivona, C.; Medina, P.J. Mammalian target of rapamycin: Biological function and target for novel anticancer agents. *Am. J. Health-Syst. Pharm.* **2010**, *67*, 2095–2106. [CrossRef] [PubMed]
18. Kim, Y.C.; Guan, K.L. Mtor: A pharmacologic target for autophagy regulation. *J. Clin. Investig.* **2015**, *125*, 25–32. [CrossRef] [PubMed]
19. Hong, S.; Moon, B.H.; Yong, Y.; Shin, S.Y.; Lee, Y.H.; Lim, Y. Inhibitory effect against akt of cyclic dipeptides isolated from *Bacillus* sp. *J. Microbiol. Biotechn.* **2008**, *18*, 682–685.
20. Ortiz-Castro, R.; Diaz-Pérez, C.; Martínez-Trujillo, M.; del Río, R.E.; Campos-García, J.; López-Bucio, J. Transkingdom signaling based on bacterial cyclodipeptides with auxin activity in plants. *Proc. Natl. Acad. Sci. USA* **2011**, *108*, 7253–7258. [CrossRef] [PubMed]
21. Cardone, M.H.; Roy, N.; Stennicke, H.R.; Salvesen, G.S.; Franke, T.F.; Stanbridge, E.; Frisch, S.; Reed, J.C. Regulation of cell death protease caspase-9 by phosphorylation. *Science* **1998**, *282*, 1318–1321. [CrossRef] [PubMed]
22. Ewald, F.; Grabinski, N.; Grottke, A.; Windhorst, S.; Norz, D.; Carstensen, L.; Staufer, K.; Hofmann, B.T.; Diehl, F.; David, K.; et al. Combined targeting of akt and mtor using mk-2206 and rad001 is synergistic in the treatment of cholangiocarcinoma. *Int. J. Cancer* **2013**, *133*, 2065–2076. [CrossRef] [PubMed]
23. Wang, Q.; Wei, F.; Li, C.; Lv, G.; Wang, G.; Liu, T.; Bellail, A.C.; Hao, C. Combination of mtor and egfr kinase inhibitors blocks mtorc1 and mtorc2 kinase activity and suppresses the progression of colorectal carcinoma. *PLoS ONE* **2013**, *8*, e73175. [CrossRef] [PubMed]
24. Borthwick, A.D. 2,5-diketopiperazines: Synthesis, reactions, medicinal chemistry, and bioactive natural products. *Chem. Rev.* **2012**, *112*, 3641–3716. [CrossRef] [PubMed]
25. Campbell, J.; Lin, Q.; Geske, G.D.; Blackwell, H.E. New and unexpected insights into the modulation of luxr-type quorum sensing by cyclic dipeptides. *Chem. Biol.* **2009**, *4*, 1051–1059. [CrossRef] [PubMed]
26. Galloway, W.R.J.D.; Hodgkinson, J.T.; Bowden, S.D.; Welch, M.; Spring, D.R. Quorum sensing in gram-negative bacteria: Small-molecule modulation of ahl and ai-2 quorum sensing pathways. *Chem. Rev.* **2011**, *111*, 28–67. [CrossRef] [PubMed]
27. Rojas Murcia, N.; Lee, X.; Waridel, P.; Maspoli, A.; Imker, H.J.; Chai, T.; Walsh, C.T.; Reimmann, C. The *Pseudomonas aeruginosa* antimetabolite L-2-amino-4-methoxy-trans-3-butenoic acid (AMB) is made from glutamate and two alanine residues via a thiotemplate-linked tripeptide precursor. *Front. Microbiol.* **2015**, *6*, 170. [CrossRef] [PubMed]
28. Dandekar, A.A.; Greenberg, E.P. Microbiology: Plan b for quorum sensing. *Nat. Chem. Biol.* **2013**, *9*, 292–293. [CrossRef] [PubMed]
29. Grabinski, N.; Ewald, F.; Hofmann, B.T.; Staufer, K.; Schumacher, U.; Nashan, B.; Jucker, M. Combined targeting of akt and mtor synergistically inhibits proliferation of hepatocellular carcinoma cells. *Mol. Cancer* **2012**, *11*, 85. [CrossRef] [PubMed]
30. Jo, H.; Jia, Y.; Subramanian, K.K.; Hattori, H.; Luo, H.R. Cancer cell-derived clusterin modulates the phosphatidylinositol 3'-kinase-akt pathway through attenuation of insulin-like growth factor 1 during serum deprivation. *Mol. Cell. Biol.* **2008**, *28*, 4285–4299. [CrossRef] [PubMed]
31. Sarbassov, D.D.; Guertin, D.A.; Ali, S.M.; Sabatini, D.M. Phosphorylation and regulation of akt/pkb by the rictor-mtor complex. *Science* **2005**, *307*, 1098–1101. [CrossRef] [PubMed]
32. Yang, G.; Murashige, D.S.; Humphrey, S.J.; James, D.E. A positive feedback loop between akt and mtorc2 via sin1 phosphorylation. *Cell Rep.* **2015**, *12*, 937–943. [CrossRef] [PubMed]
33. Li, L.L.; Malone, J.E.; Iglewski, B.H. Regulation of the *Pseudomonas aeruginosa* quorum-sensing regulator vqsr. *J. Bacteriol.* **2007**, *189*, 4367–4374. [CrossRef] [PubMed]

Sample Availability: Samples of the compounds PAO1-CDPS mixture is available from the authors.

6.2. Capítulo 2

Hernández-Padilla, L., de la Cruz, H. R., & Campos-García, J. (2020). Antiproliferative effect of bacterial cyclodipeptides in the HeLa line of human cervical cancer reveals multiple protein kinase targeting, including mTORC1/C2 complex inhibition in a TSC1/2-dependent manner. *Apoptosis*, *25*(9), 632-647.

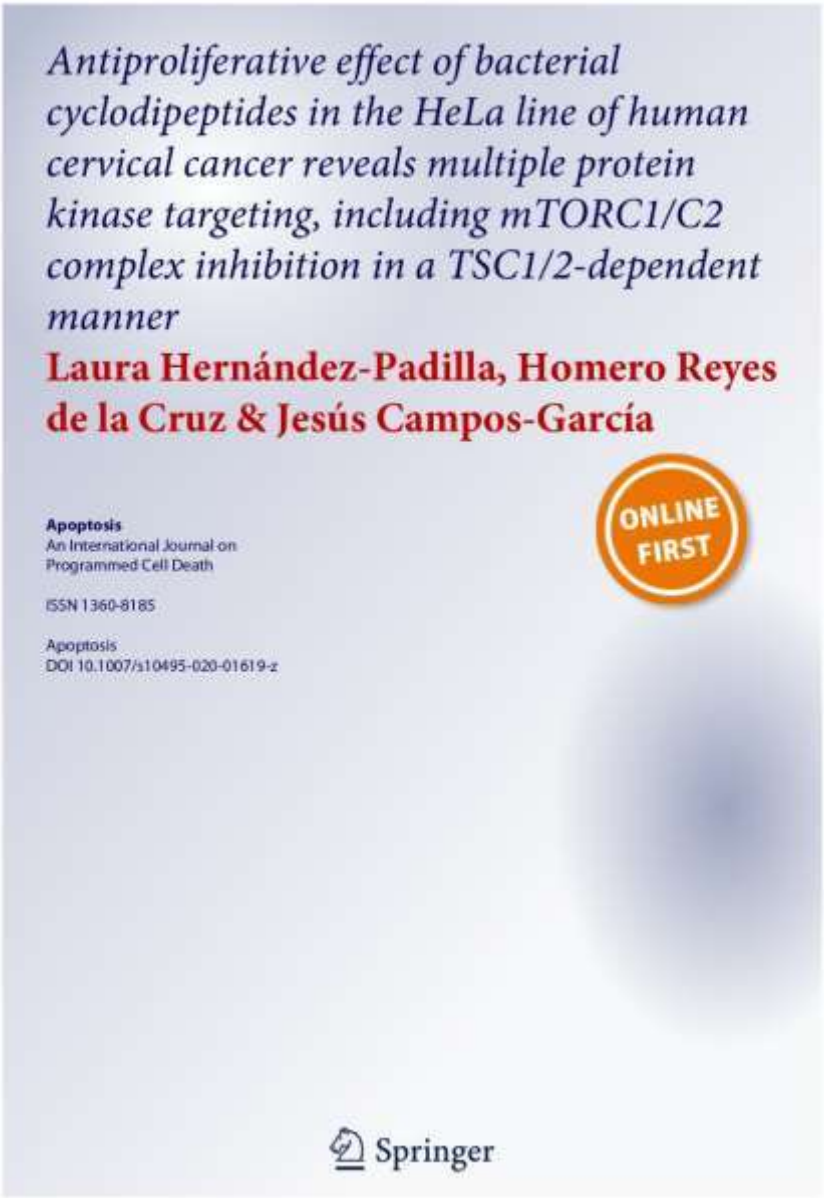

Apoptosis
https://doi.org/10.1007/s10495-020-01619-z

Antiproliferative effect of bacterial cyclodipeptides in the HeLa line of human cervical cancer reveals multiple protein kinase targeting, including mTORC1/C2 complex inhibition in a TSC1/2-dependent manner

Laura Hernández-Padilla[1] · Homero Reyes de la Cruz[2] · Jesús Campos-García[1]

Abstract
Cervix adenocarcinoma rendered by human papillomavirus (HPV) integration is an aggressive cancer that occurs by dysregulation of multiple pathways, including oncogenes, proto-oncogenes, and tumor suppressors. The PI3K/Akt/mTOR pathway, which cross-talks with the Ras–ERK pathway, has been associated with cervical cancers (CC), which includes signaling pathways related to carcinoma aggressiveness, metastasis, recurrence, and drug resistance. Since bacterial cyclodipeptides (CDPs) possess cytotoxic properties in HeLa cells with inhibiting Akt/S6k phosphorylation, the mechanism of CDPs cytotoxicity involved was deepened. Results showed that the antiproliferative effect of CDPs occurred by blocking the PI3K/Akt/mTOR pathway, inhibiting the mTORC1/mTORC2 complexes in a TSC1/TSC2-dependent manner. In addition, the CDPs blocked protein kinases from multiple signaling pathways involved in survival, proliferation, invasiveness, apoptosis, autophagy, and energy metabolism, such as PI3K/Akt/mTOR, Ras/Raf/MEK/ERK1/2, PI3K/JNK/PKA, p27Kip1/CDK1/survivin, MAPK, HIF-1, Wnt/β-catenin, HSP27, EMT, CSCs, and receptors, such as EGF/ErbB2/HGF/Met. Thus, the antiproliferative effect of the CDPs made it possible to identify the crosstalk of the signaling pathways involved in HeLa cell malignancy and to suggest that bacterial CDPs may be considered as a potential anti-neoplastic drug in human cervical adenocarcinoma therapy.

Keywords Antiproliferation · Anti-neoplastic drugs · Cervix adenocarcinoma · Cyclodipeptides · Malignancy · Protein kinases

Introduction

Cancer is caused by the malfunction of fundamental cellular processes modulating the number of cells, as well as cellular growth, proliferation, survival, and energy metabolism. In this sense, oncogenes and tumor suppressors, such as PI3K, Akt, Ras, Raf, TRK, NF1, LKN1, PTEN, P53, TSC1, and TSC2, have been widely documented in cancer diseases [1].

Cervical cancer (CC) is one common type of gynecologic cancer that is responsible for cancer-related death in women worldwide, which occurs due to the infection by certain types of the human papillomavirus (HPV), particularly types 16, 18, 33, and 42 [2, 3]. CC is characterized by poor diagnosis, high recurrence rates, and drug resistance. Consequently, CC patients have a relatively poor prognosis. In CC, the E6 and E7 oncoproteins targeted to the P53 and Retinoblastoma (Rb) tumor suppressor proteins are widely implicated in the regulation of cellular proliferation. In addition, mutations in the Ras family of genes or the dysregulation of EGFR and ERBB2 play important roles in the carcinogenesis and aggressiveness of CC [4]. Previous studies have reported that the spindle and kinetochore-associated complex subunit 3 (SKA3) participates in cancer pathogenesis and progression, and recently, it was also found to be associated with CC patients, with overexpression related to

✉ Jesús Campos-García
jcgarcia@umich.mx

[1] Laboratorio de Biotecnología Microbiana, Instituto de Investigaciones Químico-Biológicas, Universidad Michoacana de San Nicolás de Hidalgo, 58030 Morelia, Michoacán, México

[2] Laboratorio de Transducción de Señal, Instituto de Investigaciones Químico-Biológicas, Universidad Michoacana de San Nicolás de Hidalgo, Morelia, Michoacán, México

Published online: 02 July 2020

cell growth and migration by promoting cell cycle progression by the PI3K/Akt signaling pathway activation [2].

Human cervical cancer has been described in terms of the cross-talk of several signaling pathways, with the most common being the ERK/MAPK (RAF/MEK/ERK), PI3K/Akt/mTOR, EGFR/VEGFR, and Wnt/β-catenin pathways [4], though others pathways have recently been considered as potential participants, such as STAT, NOTCH [5], and HSPs (Hsp90, Hsp70, and Hsp27) [6].

From the PI3K/Akt/mTOR signaling pathway, the mTOR kinase is a master regulator that acts as two complexes. First, mTORC1 has been implicated in cellular processes, such as anabolic metabolism, oxygen supply, energy, proliferation, survival, mobilization, tumorigenesis, and autophagy, while mTORC2 is apparently involved mainly in actin cytoskeleton reorganization [7, 8], and more recently, in regulation of growth, proliferation, energy metabolism, and drug resistance [9, 10]. The mTORC1 complex (conformed by mTOR, Raptor, mLST8/GβL, PRAS40, Deptor, and KBP12-rapa) is frequently up-regulated in cancer, particularly under increased oncogenic activation of PI3K signaling or inactivation of the lipid phosphatase PTEN [11], whereas mTORC2 (conformed by mTOR, Rictor, mLST8, DEPTOR, mSin1, and Protor 1/2) is directly activated by Akt phosphorylation at Ser473, a site required for its maximal activation [8, 11, 12]. The mTORC2-dependent Akt phosphorylation leads to the activation of mTORC1. Thus, mTORC2 may indirectly suppress autophagy [7, 11, 13]. Hence, the cyclic phosphorylation behavior of Akt-S473 observed during PAO1-CDP treatment of HeLa cells suggests that mTORC2 activity may be involved [14].

The heterodimer, which consists of tuberous sclerosis 1 (TSC1; also known as hamartin) and TSC2 (also known as tuberin), is a key upstream regulator of mTORC1 and functions as a GTPase-activating protein (GAP) for Ras homologs, such as Rheb GTPase. The GTP-bound form of Rheb directly interacts with mTORC1 and strongly stimulates its kinase activity. As a Rheb GAP, the TSC1/2 heterodimer negatively regulates mTORC1 by switching Rheb to its inactive GDP-bound state [8]. Thus, the phosphorylated Akt protein disrupts the heterodimer by phosphorylating TSC1, thereby abrogating its GAP activity associated with Rheb. This leads to mTORC1 activation, which promotes cell proliferation and the inhibition of autophagy.

TSC1 or TSC2 dysfunction is also implicated in uncontrolled growth and cancer [7]. By contrast, low cellular energy levels or hypoxia induce TSC1/2 heterodimer formation, thereby inhibiting the activation of mTORC1. Autophagy is a cellular process necessary for development and tissue homeostasis, which participates in various physiological and pathologic processes, including exercise, metabolic adaptation, and certain disorders, such as neurodegenerative diseases, cardiovascular diseases, cancer, and aging [7]. Because mTORC1 plays essential roles in autophagy, it is a potential pharmacological target that may be associated with several malignances.

Therefore, identification of novel molecules that have the capacity to modulate cell proliferation, metastasis, drug resistance, and other processes, such as neurodegenerative diseases and autophagy, is of particular scientific interest in terms of treating human diseases. Our group has demonstrated that a mixture of CDPs obtained from the *Pseudomonas aeruginosa* PAO1 bacterium, which is mainly composed of cyclo(L-Pro-L-Tyr), cyclo(L-Pro-L-Val), and cyclo(L-Pro-L-Phe), promotes cell death (LD_{50} 15 μg/mL) and apoptosis induction (EC_{50} ~ 0.3 μg/mL) in cultures of HeLa cells, though not in normal human lung fibroblasts or peripherical blood cells [15]. The findings pointed to a mechanism underlying the inhibition of cell proliferation depending on mitochondrial functionality, while also implicating the Akt and S6k protein-kinases phosphorylation involvement [14, 15]. Thus, the objective of this study implies a deepening of the signaling pathways involved in the cytotoxicity effect of CDPs in the HeLa cell line, and as such, this knowledge may contribute to a better understanding of the malignancy and drug resistance as it occurs in human cervical cancer.

Materials and methods

Chemicals and reagents

Chemicals and reagents included Dulbecco's modified Eagle's medium (DMEM; Sigma-Aldrich), fetal bovine serum (FBS; Gibco Life Technology), and trypsin solution (Sigma Life Science), while Alexa Fluor 488 Annexin V was obtained from Invitrogen, Life Technologies, and 7-aminoactinomycin D (7-AAD) was from Molecular Probes, Invitrogen Life Technologies. Cyclodipeptides were obtained from *P. aeruginosa* PAO1 cells-free supernatant as previously described [16, 17]. CDPs were dissolved in a DMSO-water ratio of 1:3 to prepare stock solutions (100 mg/mL). AZD8055 and LY294002 inhibitors were purchased from LC Laboratories.

Cell line growth

The HeLa human cancer cell line was obtained from the American Type Culture Collection (ATCC, Manassas, VA, USA), which contained mutated the H-Ras oncogene and low-level expression of the P53 tumor suppressor protein. Cells were cultured in complete media [DMEM supplemented with 10% (v/v) FBS, 100 U/mL of penicillin, 40 μg/mL of streptomycin, and 1 μg/mL of amphotericin B (Sigma-Aldrich Co.)]. Cell culture media were changed

twice a week and maintained at 37 °C under 80% humidity and incubated in an atmosphere of 5% CO_2 to confluency; cells were then trypsinized, counted using a hemocytometer chamber, and used for subsequent assays. Cell cultures and other procedures were performed in class II biological safety cabinets.

Apoptosis and cellular cycle determination

Cellular apoptosis was determined using annexin V and 7-AAD reagents, and for cellular cycle phase determination, 7-AAD was used, both following the manufacturers' recommendations. Briefly, cells were seeded in 96-well flat-bottomed plates at a density of 3×10^4 cells per well in 200 µL of DMEM with FBS medium and incubated by 24 h at 37 °C with 5% CO_2. The culture media were then removed and replaced with serum-free DMEM medium. To quantify apoptosis, cell cultures were incubated using DMEM with FBS medium for 12 h prior to treatment with CDPs (0.1 mg/mL), DMSO (at the same concentration used to dissolve the CDPs) and Actinomycin D were used as the negative and positive controls, respectively. Following incubation, cells were trypsinized and collected by centrifugation at 2000×*g* for 10 min, and the pellet was suspended in 20 µL and incubated with annexin V and 7-AAD. Fluorescence was quantified by FACS using an Accuri-C6 Flow Cytometer (BD Biosciences). The percentages of fluorescent cells was determined from histograms of fluorescence emission in the plots. For apoptosis assays, fluorescence rendered by annexin V was measured in the fluorescence channel FL1 at 488/499 nm, and for 7-AAD, it was measured in the FL3 channel at 546/647 nm. At least 20,000 cellular events were used for each measurement. Stages of the cell cycle were determined for the HeLa cells using the 7-AAD reagent by FACS, and the data were analyzed using CFlow Plus software (Free star, Stanford).

Immunodetection assays

Human HeLa cell cultures were grown as described above and synchronized by 12 h in DMEM medium without fetal bovine serum incubated at 37 °C under 5% CO_2 atmosphere. Thereafter, 3×10^5 cells were seeded in each well (six-well plates) with a total volume per well of 3 mL of fresh DMEM medium with FBS, adding the CDPs at a concentration of 0.1 mg/mL. After treatments, the medium was eliminated and cells were submitted to cellular trypsinization in DMEM medium and harvested by centrifugation at 5000×*g*, 4 °C for 10 min. Cellular lysis was carried out in phosphorylation buffer (PB) 300 µL composed of Hepes (50 mM, pH 7.6), containing sodium-pyrophosphate (50 mM), sodium orthovanadate (1 mM), sodium molybdate (1 mM), EDTA (20 mM), EGTA (20 mM), benzamidine (1 mM), NaF (20 mM), PMSF (0.2 mM), β-glycerophosphate (80 mM), mannitol (200 mM), and protease inhibitor cocktails (1 µL/mL), with all reagents from Sigma-Aldrich Co. Cell suspension was lysed (cell lysate) by three cycles of sonication at low intensity (20 kHz, 5 W) for 30 s each at 4 °C with 5 min of resting between sonication cycles (Heelscher-UP524 Ultrasound Technol.). Cell-free protein extracts were obtaining by centrifugation at 7500×*g* and 4 °C for 15 min. Protein concentration was determined using the Bradford reagent (BioRad) and 30 µg of protein was mixed with 10 µL of denaturing buffer (Tris–HCl 0.06 M, pH 6.8, 5% glycerol, 4% SDS, 4% β-mercaptoethanol and 0.0025% bromophenol blue) for 5 min at 95 °C in a boiling water bath. Samples were separated under denaturing conditions using polyacrylamide gel electrophoresis at 10–12% (SDS-PAGE). Gels were stained with Coomassie blue, and proteins from replicate gels were transferred to polyvinylidene difluoride (PVDF, Millipore) membranes for immunodetection assays. Briefly, PVDF membranes were incubated with TBS-T (Tris–HCL 10 mM pH 7.8, 0.9% NaCl, 0.1% tween-20, 5% dry milk). PVDF membranes were cut according to a range of molecular weight markers and incubated with the indicated antibodies at the concentration suggested by the manufacturer. the antibodies used included p-mTOR (Ser2448), p-mTOR (Ser2481), mTOR, Raptor, Rictor, GβL, and anti-rabbit IgG-HRP from Cell Signaling Technology, as well as P-Akt (Ser473), Akt, Harmatin, p-tuberin, tuberin, p-p70S6k (Thr389), Rheb, H-Ras, HSP27, p-PTEN (Ser380), ULK, P53, and β-actin from Santa Cruz Biotechnology. Following 12 h of incubation (4 °C) for the primary antibody, membranes were washed and incubated with secondary antibody Goat anti-Rabbit IgG HRP-conjugate (1:10,000, BioRad) in blocking medium for 4 h at 4 °C; the membranes were washed twice with TBS-T buffer and developed using hydrogen peroxide and Supersignal West Pico Luminol (Pierce, Thermo Fisher Scientific). Images were then captured using a ChemiDoc™ MP System (Bio-Rad). Assays were conducted at least three times, representative images were obtained, and band intensities in gels images were quantified using the ImageJ software (NIH Image).

For antibody arrays immunodetection, 30 µg of total protein were added to each well with glass slides of an antibody array kit (PathScan Cancer Phenotype Antibody Array Kit #14821 and PathScan Intracellular Signaling Array Kit #7323; Cell Signaling Technology) following the instructions of the provider. The array glass slides were incubated overnight at 4 °C on an orbital shaker. Following immunoreactions and washes, slides were incubated with a biotinylated-antibody cocktail and HRP-linked Streptavidin for 1 h at room temperature. To detect immunoreactivity, LumiGlo®/Peroxide reagent was added and images were immediately captured using a digital imaging

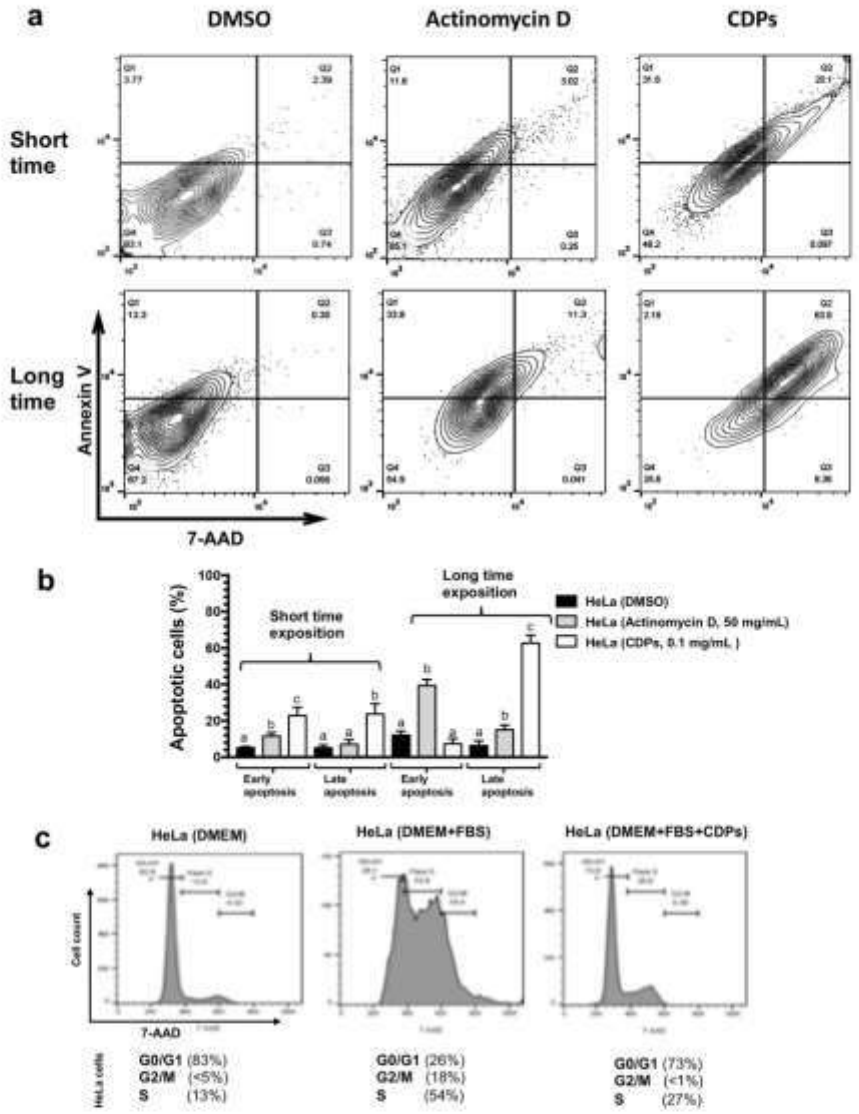

chemiluminescent system, ChemiDoc™ MP System (Bio-Rad). Determination of spot intensity from the micro-array was carried out by densitometric analysis using ImageJ software (NIH Image).

Statistic analysis

Correlation analysis of data obtained from antibody arrays was conducted utilizing response variables (treatments) versus data of signal intensity for each spot in the arrays (cases) with STATISTICA software (Data Analysis Software

◂**Fig. 1** Apoptosis induction and cell cycle arresting in HeLa cells by CDPs. HeLa cells were cultured in the DMEM + FBS medium and treated with CDPs. Cells were stained with annexin V and 7-AAD and analyzed by FACS. **a** The percentage of fluorescent cells determined in the dot plots is shown, which corresponds to HeLa cells treated for 2 h (short time) or 18 h (long time) with DMSO, actinomycin D (50 mg/mL), or CDPs (0.1 mg/mL). Q1, early apoptosis; Q2, late apoptosis; Q3, necrotic cells; Q4, viable cells. **b** Percentage of fluorescent cells (apoptotic cells) were determined by FACS after CDPs treatment. Bars of the plots represent means ± SE of three independent experiments. One-way ANOVA was carried out with a Bonferroni post hoc test; statistical significance ($P < 0.01$) of differences between treatments with respect to the control (DMSO) are denoted by different lowercase letters. **c** Effects of CDPs on the cell cycle in HeLa cells. HeLa cells were incubated in serum-free medium (DMEM) and serum-enriched medium (DMEM + FBS) after treatment with CDPs (10 µg/mL) for 18 h, which were stained with 7-AAD and analyzed by FACS. Proportion of cells in different stage of cell cycle are shown

System 8.0., Stat Soft, Inc.). Other data were statistically analyzed using GraphPad Prism 6.0 software (GraphPad Software, San Diego, CA).

Results

CDPs arresting HeLa cells on G0/G1 stage

In a previous study, we reported that the mixture of CDPs isolated from *P. aeruginosa* PAO1 cultures were cytotoxic and induced apoptosis in a dose-dependent manner on the HeLa cell line, which involved a mechanism that falls on the inhibition of phosphorylation of the Akt-S473 and S6k-T389 protein-kinases [14].

Exploration of apoptotic cells in the population of CDPs-treated HeLa cells (0.1 mg/mL) indicated that a population of cells responded at short times of CDP-exposure, inducing apoptosis (early and late apoptosis, ~ 20–30% of cells), while that other population of cells responded over long time periods (late apoptosis, ~ 60% of cells; Fig. 1a, b). This differential cell behavior was also observed when the phase of the cellular cycle was determined in HeLa cells after CDP-exposure (Fig. 1c). Regarding the control of cells with deprivation of nutrients [without fetal bovine serum (DMEM)], ~ 85% of cells were arrested at the G0–G1 stage, ~ 5% of cells at the G2–M stage, and ~ 10% of cells in the S phase. Comparatively, for HeLa cells in DMEM medium with fetal bovine serum (DMEM + FBS), major cell proportion was found in S phase (~ 55%), while a decreased proportion of cells was found in the G0/G1 stage (~ 25%; Fig. 1c). Interestingly, for the HeLa cultured in DMEM + FBS medium supplemented with CDPs (0.1 mg/mL), cell populations were arrested at the G0–G1 stage (~ 70% of cells), at the G2–M stage (< 1%), and in the S phase (~ 25% of cells). This indicates that HeLa cells meet in the S phase (~ 55%) and G2/M (~ 20%) were reprogramed by the addition of CDPs, changing the proportion of arrested cells at the G0/G1 stage (~ 70%). These results suggest that CDPs are targeted elements responsible for cell cycle control.

Effect of CDPs on cancer and intracellular signaling markers in HeLa cells

To deepen the intracellular mechanism involved in the antiproliferative effect of bacterial CDPs in the HeLa adenocarcinoma model, protein extracts obtained from HeLa cells cultures were used to immunodetect proteins involved in cancer [4]. These cancer markers were on a 21-antibody array (Fig. 2), which was blotted using the protein extract of HeLa cultures exposed to CDPs (at 0.1 mg/mL) for 15, 60, and 240 min of exposure. Results indicated that most of the antibodies contained on the array were turned on in the control HeLa protein extract, though in the HeLa CDP-exposed cell extract, a clear decrease in signals of the antibody signal spots were observed (at 15 min and 60 min of treatment; Fig. 2a). We found that at short times of CDP exposure (15 and 60 min), CDPs provoked a decrease in the expression of the cancer protein markers CD31 (PECAM-1), EpCAM, Vimetin, CD44, CD45, PCNA, Ki67, p27Kip1, E-Cadherin, N-Cadherin, VE-Cadherin, MUC1, Rb-Ser807, HIF-1α, Survivin, P53, HER2, Met, and EGF compared to the control HeLa protein extract (Fig. 2b). Interestingly, in proteins extracted from CDP-exposed HeLa cells during the longer treatment time (240 min), the spots of the antibody array were restored in the majority of proteins, which was similar to the control extract, except for P53, Met, and EGF, which remained with low protein expression (Fig. 2a, b). Additionally, the proteins EpCAM, CD45, p27Kip1, and VE-Cadherin showed a significant increase of expression level at 240 min of CDP exposure, comparing to the control.

Further, a second antibody array was used to monitor 20 intracellular signaling proteins subject to phosphorylation or cleaving, as being involved in cellular and cancer-related signaling pathways (Fig. 3). Results showed that Stat3-Tyr705, Akt-Thr308, Akt-Ser473, AMPKα-Thr172, S6-RP-Ser235/236, mTOR-Ser2448, HSP27-Ser78, Bad-Ser112, p70S6k-Thr389, PRAS40-Thr246, P53-Ser15, P38-Thr180/Tyr182, SAPK/JNK-Thr183/Tyr185, PARP-Asp214, Caspase 3-Asp175, and GSK-3β-Ser9 proteins diminished their immunoblot signal in HeLa cells exposed to CDPs at 30 min and 60 min (Fig. 3a, b), while restoration of immunoblot signal level was partially observed in the Akt (Ser473), Bad (Ser112), SAPK/JNK (Thr183/Tyr185), caspase-3 (Asp175), and GSK-3β (Ser9) proteins (Fig. 3a, b). Results showed that the expression/phosphorylation of proteins related to cancer and proteins involved in intracellular signaling pathways found dysregulated in HeLa cells were modified by the CDPs-exposure.

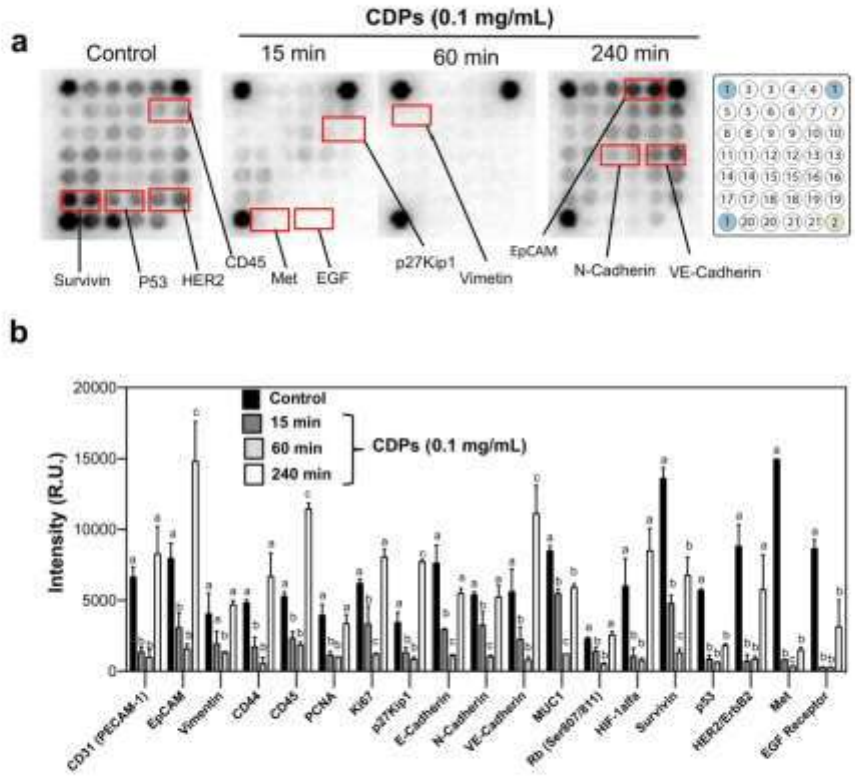

Fig. 2 Proteomic analysis of CDP effect on the expression of cancer markers in HeLa cells. HeLa cells were homogenized to obtain protein extracts used for immunodetection assays using antibody arrays as described in Materials and Methods. **a** Representative images correspond to antibody micro-array (PathScan Cancer Phenotype Antibody Array Kit). The array contains the following antibodies: (1) positive control, (2) negative control, (3) CD31, (4) EpCAM, (5) Vimentin, (6) CD44, (7) CD45, (8) PCNA, (9) Ki-67, (10) p27Kip1, (11) E-Cadherin, (12) N-Cadherin, (13) VE-Cadherin, (14) MUC1, (15) Rb Ser807/811, (16) HIF-1α, (17) Survivin, (18) P53, (19) HER2/ErbB2, (20) Met, (21) EGF. **b** Determination of spot signal intensity from micro-arrays **a** was conducted by densitometry using Image J software (NIH). Data represent the means ± SE of two independent assays with spot-duplication for each antibody. One-way ANOVA was carried out with a Bonferroni post-hoc test; statistical significance ($P<0.05$) of differences between treatments is denoted by lower-case letters

Correlation analysis of proteins expression on HeLa cells exposed to CDPs

Analysis of multiple proteins expression in the HeLa cells exposed to CDPs (using the numerical values of proteins expression/phosphorylation of the antibody arrays; Figs. 2, 3) were analyzed using statistical correspondence analysis (Fig. 4).

The plot clearly grouped the proteins in several correlation groups. First, a group of proteins that modified their expression in correlation with the CDP exposure at short time periods (15 min and 60 min), such as HSP27, AMPKα, PRAS40, JNK, ERK, mTOR, Akt-T, Akt-S, Stat1, Stat3, caspase-3, PARP, Bad, P38, P53, PARP, p70S6k, and S6-RP (black circle in Fig. 4). A second group of proteins was associated with the CDP exposure at the longer exposure time (240 min), including Vimetin, N-Cadherin, E-Cadherin, VE-Cadherin, MUC1, PCNA, CD31, CD44, CD45, EpCAM, Rb, p27Kip1, Ki67, and HIF-1α (green circle in Fig. 4). Finally, the third group of proteins that showed a behavior outside of the last two and near to control (HeLa cells without treatment), comprising the Survivin, HER2/ErbB2, P53, EGF, and Met proteins (red circle in Fig. 4). This analysis shows a clear effect of CDPs over the differential expression

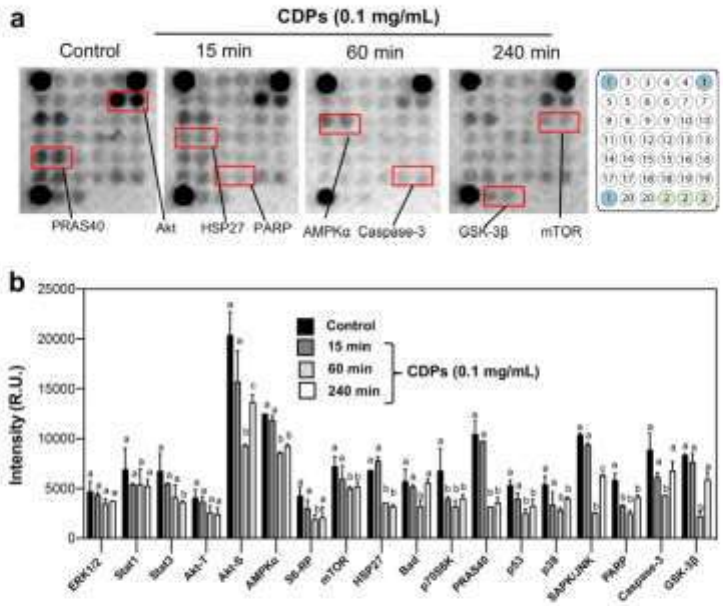

Fig. 3 Proteomic analysis of CDP effect on the expression of protein markers of intracellular signaling pathways in HeLa cells. HeLa cells were homogenized to obtain protein extracts used for immunodetection assays using antibody arrays as described in Materials and Methods. **a** Representative images correspond to antibody microarray (PathScan Intracellular Signaling Array Kit). The array contains the following antibodies: (1) positive control, (2) negative control, (3) ERK1/2-Thr202/Tyr204, (4) Stat1-Tyr701, (5) Stat3-Tyr705, (6) Akt-Thr308, (7) Akt-Ser473, (8) AMPKα-Thr172, (9) S6 Ribosomal Protein-Ser235/236, (10) mTOR-Ser2448, (11) HSP27-Ser78, (12) Bad-Ser112, (13) p70S6 Kinase-Thr389, (14) PRAS40-Thr246, (15) P53-Ser15, (16) P38-Thr180/Tyr182, (17) SAPK/JNK-Thr183/Tyr185, (18) PARP-Asp214, (19) Caspase-3-Asp175, (20) GSK-3β-Ser9. **b** Determination of spot signal intensity from micro-array **a** was conducted by densitometry using Image J software (NIH). Data represent the means ± SE of at two independent assays with spot-duplication for each antibody. One-way ANOVA was carried out with a Bonferroni post-hoc test; statistical significance ($P < 0.05$) of differences between treatments is indicated with lower-case letters

levels of multiple signaling and cancer-involved pathways. The result of the proteins that modified their expression at short time of CDPs exposition showed that several proteins belonging to the PI3K/Akt/mTOR pathway were grouped, suggesting that this pathway plays an important role in HeLa adenocarcinoma pathogenesis, which it can targeted by the bacterial CDPs.

CDPs inhibit the HeLa cells proliferation by blocking mTORC1/2 by TSC1/TSC2-dependent

To deepen the mechanism of signaling involved in the antiproliferation effect of the bacterial CDPs on HeLa cells, and to further confirm the antibody arrays findings, protein expression was determined by Western blot assays (Fig. 5). Results indicated that, as previously described [14], the Akt-Ser473 kinase showed a dramatic decrease of phosphorylation without modification in its total protein expression; and the P53-Ser15 protein, also widely described as a cancer marker, decreased its expression in response to CDP-treatment (Fig. 5). Remarkably, the phosphorylated form (p-mTOR-Ser^{2448}) showed strong levels of phosphorylation in untreated cells (control at 0 min), but was significantly diminished in its phosphorylation level in extracts from CDP-exposed HeLa cells at 15 min and 60 min, and total mTOR protein expression was unmodified by CDP exposure. Furthermore, the phosphorylation of mTOR-Ser^{2448} was recovery at a longer CDP exposure time (240 min, Fig. 5). With respect to the phosphorylation of the mTOR-Ser^{2481}form, it remained unaltered at 15 min and 60 min, but increased its phosphorylation at 240 min of CDP exposure, comparing with the control (Fig. 5).

With regard to the involvement of mTORC1 and mTORC2 complexes in the antiproliferative effect of CDPs in HeLa cells, our results showed that the protein expression of Rictor was decreased in the HeLa cells treated with CDPs

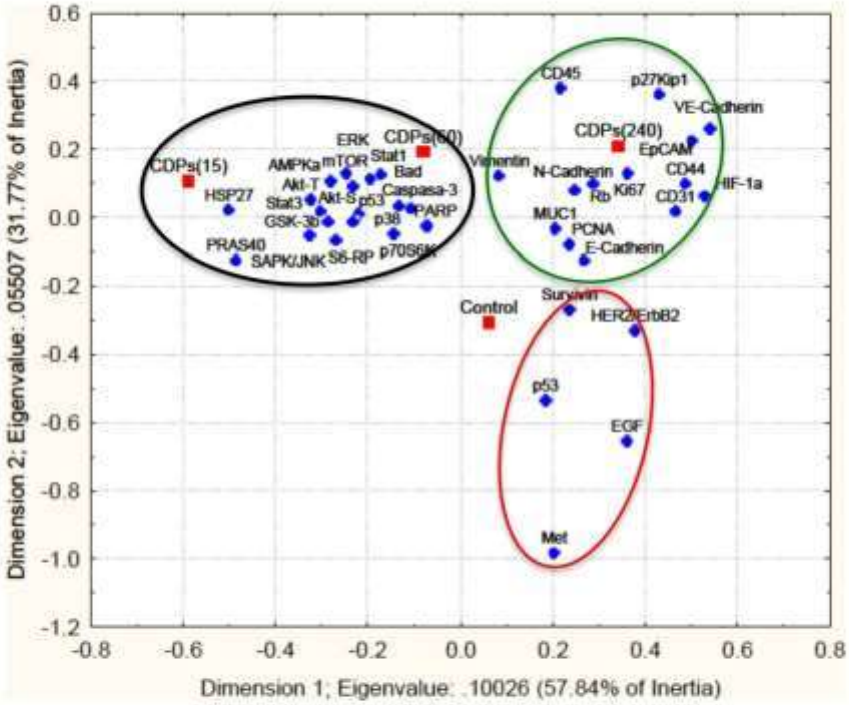

Fig. 4 Correlation analysis of proteomic approach of cancer and intracellular signaling pathways markers in HeLa cells treated with CDPs. Correlation analysis of densitometry data from microarrays (Figs. 2, 3) were analyzed by multivariate exploratory techniques, using the correspondence analysis (CA) with 2-D PCA correspondence analysis of frequencies w/out grouping variables using the STATISTICA Software System 8.0. Stat Soft. Inc. Response variables (independent) are indicated as: Control, HeLa cells without treatment; CDPs(15), HeLa cells treated with CDPs (0.1 mg/mL) by 15 min; and CDPs(60), HeLa cells treated with CDPs (0.1 mg/mL) by 60 min; and CDPs(240), HeLa cells treated with CDPs (0.1 mg/mL) by 240 min. Dependent variables are indicated as blue point and protein names in the graph

(Fig. 5); though, by contrast, the Raptor protein showed an increased expression depending of the exposure time. Interestingly, harmatin (TSC1) also diminished its expression by CDP-exposure and as a function of exposure time, while the phosphorylated-tuberin form (p-tuberin-Ser1798; TSC2) showed decreased phosphorylation at 15 min and 60 min. Nevertheless, the p-tuberin-Ser1798 exhibited a partial recovery of its phosphorylation at 240 min of CDP exposure, but no changes for the tuberin total protein expression were shown (Fig. 5). Similar behavior was observed for the mTORC1-modulator protein, mLST8/GβL (Fig. 5).

Further implication of the PI3K/AKT/mTOR pathway was confirmed with the utilization of the AZD8055 mTOR inhibitor and LY294002 PI3K inhibitor (Fig. 6). Our findings showed that the CDP-treated HeLa cells at 60 min inhibited the phosphorylation of p-mTOR-S2448, which was similar to HeLa cells exposed to AZD8055 (Fig. 6a). As mentioned above, the cyclic overexpression of p-mTOR-S2448 phosphorylation at 240 min was observed for CDP treatment but not in the HeLa cells treated with the AZD8055 inhibitor. Importantly, the combination of AZD8055 with CDPs showed a decrease of p-mTOR-S2448 phosphorylation at 240 min of CDP exposure. This result indicated a similar mechanism of inhibition of CDPs and AZD8055, also as an interference in the hyper-phosphorylation at 240 min of the CDPs by AZD8055. With respect to the PI3K inhibition, the LY294002 inhibitor caused a decrease in phosphorylation of the p-mTOR-S2448 protein induced by the addition of CDPs at 240 min of exposure with respect to the control (Fig. 6b), indicating that the CDP mechanism involves the interaction with the mTOR complexes and also at the PI3k blocking level.

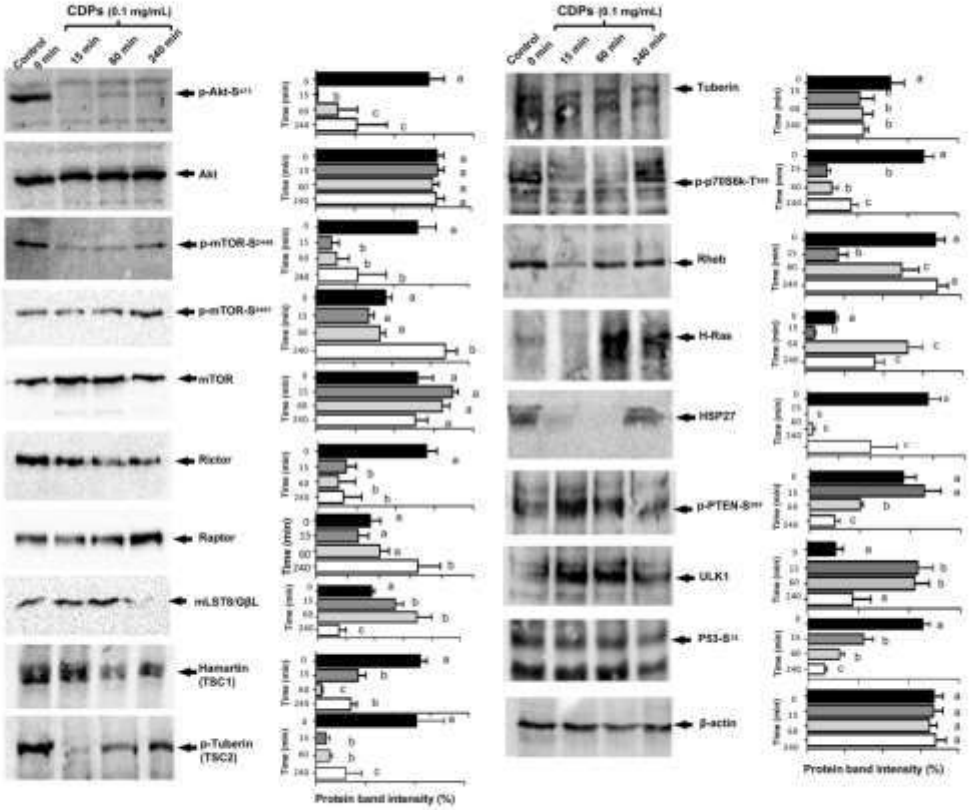

Fig. 5 Effects of CDPs on the expression of proteins involved in mTOR signaling pathway in HeLa cells. HeLa cells were homogenized to obtain protein extracts used for Western blot assays as described in Materials and Methods. Representative images correspond to western blot using protein extracts of at least three independent assays using the indicated antibody. The antibodies used were as follows; p-Akt-S473, Akt, p-mTOR-S2481, p-mTOR-S2448, mTOR, Rictor, Raptor, Harmatin (TSC1), p-Tuberin (TSC2), Tuberin, p-p70S6k-T389, Rheb, H-Ras, HSP27, p-PTEN-S380, GβL, ULK, P53-S15, and β-actin. On the right, graphs correspond to the determination of the band intensity from the Western blot assay (left), which were analyzed by densitometry using the Image J software. Data represent the means ± SE of densitometry determinations using protein extracts obtained from at least three independent assays. One-way ANOVA with a Bonferroni post-hoc test was used to compare treatment-times with respect to control. Significant differences ($P < 0.05$) vs. control is denoted by lower-case letters

The protein expression of downstream target proteins to TSC1/TSC2 or TOR, such as Rheb and p70S6k, respectively, or upstream proteins, such as H-Ras and PTEN, were evaluated in HeLa cells exposed to CDPs. Western blot results showed that the Rheb expression and phosphorylation of p-p70S6k-Thr389 were decreased by CDP treatment at short exposure times, but reverted at the longer time of 240 min (Fig. 5). Additionally, H-Ras was inhibited at 15 min, but overexpressed at 60 min and 240 min of CDP exposure. While the HSP27 protein showed inactivation at 15 min and 60 min, it recovered at 240 min. By contrast, p-PTEN-S380 showed increased phosphorylation at 15 min and 60 min, though it was diminished at 240 min of CDPs exposure, and similar behavior was observed for the ULK1 and P53 proteins (Fig. 5). These findings indicate that in addition to the PI3k/Akt/mTOR pathway, other important signaling pathways involved in tumorigenesis were targeted by CDPs.

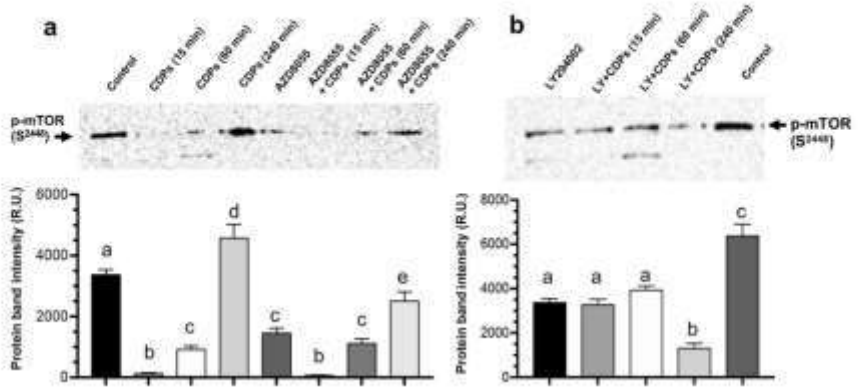

Fig. 6 Effect of the AZD8055 and LY294002 inhibitors over the mTOR-S2448 phosphorylation in CDP-treated HeLa cells. HeLa cells were homogenized to obtain protein extracts used for Western blot assays as described in Materials and Methods. Representative images correspond to western blot using protein extracts of at least three independent assays using the p-mTOR-S2448 antibody. **a** Effect of AZD8055 inhibitor. **b** Effect of LY294002 inhibitor. At below are showed the plots that correspond to the determination of the bands intensity from Western blot assay, analyzed by densitometry using the ImageJ software. Data represent the means ± SE of densitometry determinations using protein extracts obtained from at least three independent assays. One-way ANOVA with a Bonferroni post-hoc test was used to compare treatment-times with respect to control. Significant differences ($P < 0.05$) versus control is indicated with lower-case letters

Discussion

Antiproliferative effect of the CDPs involves mTORC1 and mTORC2 blocking

Cervical adenocarcinoma is one of the most aggressive types of cancer and presents resistance to chemotherapeutics, and this cancer type has been described with the participation and cross-talk of several signaling pathways. One of the more studied pathways is the PI3K/Akt/mTOR signaling pathway, being upregulated 73% in different types of cancers [18]. Previously, we described the antiproliferative properties of bacterial CDPs in the human HeLa line involving the abrogation of phosphorylation of Akt-S473 and S6k-T389 protein kinases [14]. Interestingly, the phosphorylation of these proteins showed cyclic behavior, the inhibition of phosphorylation by CDPs at short time of exposures (5 min to 60 min), then recovering at longer exposure times (120–240 min) [14]. Thus, this cyclic phosphorylation behavior may first suggest that the antiproliferative effect of CDPs occurs at a level of inhibition of phosphorylation of elements of the PI3K/Akt/mTOR signaling pathway. Secondly, the induction at the genetic level of master modulators constitutes signaling pathways associated with recurrence and drug resistance of the HeLa line that this study was designed to discern. The third reason, similar to the Mnk1 pathway, which has been implicated with exposure to rapamycin or prolonged mTORC1 inhibition status, leading to feedback loop of rescue of the eIF4E phosphorylation through Mnk1 activation [19]; mechanisms that could be implicated on long time CDP exposure in our followed HeLa cells model.

The apoptosis and cell cycle stage results of the HeLa cells exposed to CDPs (Fig. 1), revealed that a HeLa cells population was susceptible to induce early apoptosis, arresting the cells mainly in the G0/G1 stage. Consistent with its antiproliferative effect, this finding suggests inhibition of quick response elements from signaling pathways associated with the S phase control and nutrients, while a second cell population's response could be associated with mechanisms that modulate apoptosis and autophagy. Thus, the antibody array approach utilized in this work with the cervix adenocarcinoma HeLa line model made it possible to evaluate elements of several signaling pathways related to cancer and protein kinases involved in intracellular signaling pathways.

In the HeLa model, we further confirmed that signaling pathways are upregulated and related to noncontrolled cell proliferation. Hyperphosphorylation of proteins, such as p-Akt-Ser473, p-mTOR-Ser2448, and p-p70S6K-Thr389, clearly confirmed the malignancy in HeLa cells line, which were inactivated after CDP exposure (Figs. 2, 3). In our antiproliferative study, the cyclic behavior of phosphorylation/dephosphorylation over several proteins involved in carcinogenic pathways was an important observation. On one hand, inhibition of phosphorylation by CDPs was observed at short times of exposure (15 min and 60 min), but recovered at

longer exposure times (240 min). By contrast, we found hyper-phosphorylation of p-mTOR-Ser2481 at longer times of CDPs exposure (Fig. 5). This finding shows that CDPs are actuated over mTOR complexes at different sites of phosphorylation, and therefore, they are actuated over different signaling pathway targets. CDPs reduced the amount of the p-p70S6K-Thr389 isoform (Fig. 5), which correlates with a decrease in the p-mTOR-Ser2448 isoform, a phosphorylation target site mainly associated with the mTORC1 complex [20], while the p-mTOR-Ser2481 isoform is mainly associated with the mTORC2 complex [20]. Interestingly, reduction in phosphorylation of the Ser-2448 residue was also observed, confirming the involvement of both the mTORC1 and mTORC2 complexes in the antiproliferative effect of the bacterial CDPs (Fig. 5).

Deepening of the signaling mechanism of the antiproliferative effect of CDPs, our findings showed that both the mTORC1 and mTORC2 complexes are involved in the malignancy of the HeLa line. The Rictor protein was decreased by CDP treatment, which indicates that the mTORC2 complex decreased, while the Raptor protein expression was increased by CDPs treatment, indicating that mTORC1 complex formation was favored (Fig. 5). In addition, the positive regulator mLST8 associated with mTOR activity favors the interaction with Raptor, and in mammalians, mLST8 is a shared constituent of both mTORC1 and mTORC2, which has been found in high levels of expression in certain types of carcinoma. Thus, mLST8 overexpression is positively correlated with tumor size, differentiation, and invasiveness [21]. Interestingly, nutrients and rapamycin only regulate the association between mTOR and Raptor in complexes that also contain mLST8. This suggests that the opposing effects of the mLST8- and Raptor-mediated interactions on mTOR activity, regulate the AKT pathway. In our study, mLTS8 was increased at short times of CDP exposure, but was inhibited at longer times. These results suggest that the antiproliferative effect of the CDPs in HeLa cells favor the mTORC1 complex integration at short times of CDP exposure and the prevalence of mTORC2 at longer times of CDPs exposure, confirming the essential role of mLST8 in the function of mTOR, as described elsewhere [11].

Some neurodegenerative and tumor diseases have been described as being associated with the tuberous sclerosis complex (TSC) in any of its forms, and both the hamartin (TSC1) and the tuberin (TSC2) levels are upregulated and have been found to be mutation-associated [22]. We found that in HeLa cells, the TSC1 and TSC2 protein levels were overexpressed (Fig. 5), though the TSC1 expression was decreased by the addition of CDPs (indicating that mTORC1 is down-activated). Interestingly, the phosphorylation of TSC2-Thr1462 showed a cyclic behavior of phosphorylation, and similar to others elements of the PI3K/Akt/mTOR pathway, it was inhibited at short times of CDP treatment (15 min and 60 min) and recovered at a longer time (240 min), indicating that the phosphorylation on TSC2 is responsible for mTORC1 activation and correlated with an increase of the Raptor expression. These results further confirm that in HeLa cells, both the mTORC1 and mTORC2 complexes can be modified in conformation/activation by the bacterial CDPs effect, implicating both TSC1 and TSC2 elements in the transduction signaling mechanism, and therefore, in the conformation/activation of the mTORC1 and mTORC2 proportions, rendering it in the on/off switching of proteinic elements of diverse signaling pathways.

Regarding the proteins that showed modification in expression or phosphorylation level belonging to the PI3K/Akt/mTOR pathway included Akt, mTOR, TSC1, TSC2, Rictor, Raptor, mLST8, Rheb, PTEN, S6K, and S6RP. This finding further confirms that the PI3K/Akt/mTOR pathway is one of the main pathways implicated in the HeLa line malignancy. TOR kinase inhibitors, such as AZD8055, have been proposed as anti-neoplastic drugs [23]. We used this mTOR ATP-binding site inhibitor to test whether the bacterial CDPs show similar mechanisms of inhibition of HeLa cells proliferation. Importantly, the bacterial CDP treatment (15 min) showed a similar effect to AZD8055 on the p-mTOR-Ser2448 isoform; but at longer times of exposure, the CDPs caused hyperphosphorylation of the p-mTOR-Ser2448 (Fig. 6). Additionally, treatment with AZD8055 plus CDPs resulted in diminished phosphorylation levels of the p-mTOR-Ser2448 isoform compared to CDP-only exposure. These results indicated that the CDPs molecular mechanism involves the mTOR inhibition, like AZD8055. The efficacy of mTORC1 inhibitors is limited because they suppress the mTORC1-dependent negative feedback loop and paradoxically activate Akt signaling, resulting in resistance. By contrast, mTORC2 directly phosphorylates Akt at a regulatory site critical to maximal Akt-kinase activity. Thus, targeting both mTORC1 and mTORC2 would seem to be necessary to completely block the PI3K/Akt/mTOR signaling pathway, which has been suggested elsewhere [24]. Dual mTOR inhibitors represent promising therapeutic agents by arresting cells in G0/G1 stage, conducive to apoptosis by blocking the phosphorylation of Akt-Ser473. The PI3K inhibitor (LY294002) and the dual mTORC1/2 inhibitor (AZD8055) inhibits the phosphorylation of Akt-Ser473 and consequently exert affectation in phosphorylation on PRAS40, TSC2, GSK3b, and Fox01. When this occurs, inhibition of PRAS40 and TSC2, mTORC1 will be affected, as well as the activity of P70S6K [24]. Interesting results were also obtained with the LY294002 PI3K-inhibitor, as the phosphorylation of the p-mTOR-Ser2448 isoform was diminished by effects associated with the presence of LY294002, but were totally abrogated when CDPs were added jointly with LY294002 (Fig. 6). These results indicated that the CDPs were competing with target proteins of

the AZD8055 and LY294002 inhibitors, confirming that the PI3K/Akt/mTOR/S6K pathway was targeted by the bacterial CDPs; however, the lack of total inhibition of the phosphorylation of the element from this pathway (at longer time periods of exposure) suggest the involvement of additional signaling pathways and additional targets.

Involvement of multiple signaling pathways in HeLa carcinogenesis and CDPs blocking

Our data obtained by the antibody arrays showed that the epidermal growth factor (EGF) family of receptor tyrosine kinases, EGF-R and ErbB2, also as the HGF/Met receptor modified their expression levels by CDPs exposure (Figs. 2, 3). These receptors can lead to modified downstream signaling pathways, such as the RAS/RAF/MEK/ERK, JAK/STATs/Bcl-xL, the PI3K/Akt/mTOR, PAK1/MEKK1/MKK4-7/JNKs, Wnt/β-catenin/GSK3β, PKC, MAPK, CSC (STAT1/3, CD44), and EMT (Snail, E-Cad, Vimetin) pathways. In this sense, factors belonging to these pathways were clearly modified in protein expression or phosphorylation levels by CDP exposure (Figs. 2, 3), confirming multiple signaling pathway participation in the carcinogenesis of the HeLa line and suggesting cross-talk between these signaling pathways (Fig. 7).

When the Ras/Raf/MEK/ERK1/2 pathway is activated by prolonged times of drugs exposure, it leads to altered gene expression and contributes to cancer and chemotherapy resistance. Several MEK inhibitors have shown promising pre-clinical activity in adenocarcinoma types; however, the frequent development of resistance to kinase inhibitors occurs through a variety of mechanisms. Our

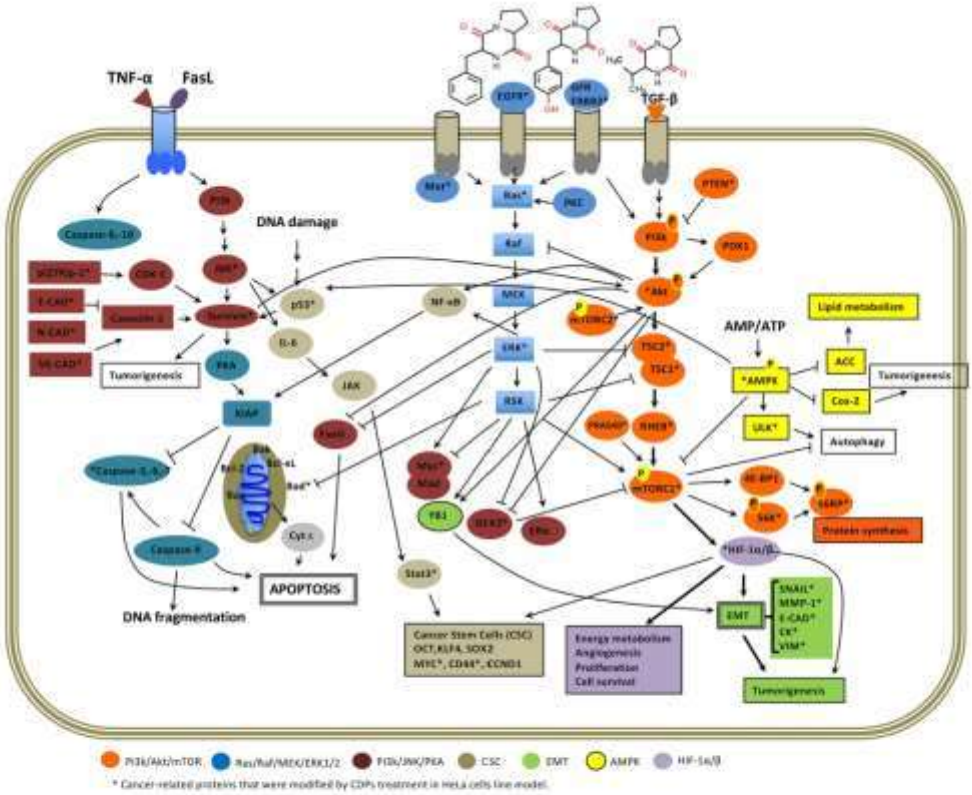

Fig. 7 Scheme of the proposed mechanisms involved in the antiproliferative effect of the bacterial CDPs in HeLa cells. Proteins identified in this study are indicated with an asterisk (*). Different color were used for protein elements of each signaling pathway

work indicates that the Ras/Raf/MEK/ERK1/2 pathway is strongly modulated by CDPs, indicating that it can be considered as an additional targeted pathway of CDP action (Fig. 7).

Other findings also included the observation of an over-expression of the HIF-1α protein (Fig. 2). The HIF-1 suppressor is a master regulator of elements involved in glycolysis, which has been found to be dysregulated in tumorigenesis and invasiveness. It is known that the regulation of HIF-1 is closely related to the PI3K/Akt/mTOR pathway, and it has even been shown that Akt and HIF-1 interact synergistically during the development of adenocarcinoma [25], as shown in Fig. 7.

Our findings show that the protein expression of the E-CAD and VIM markers was decreased in the extracts from HeLa cells CDPs-treated, and these findings suggest that CDPs are targeted elements of the EMT signaling pathway, such as those found in a xenografted melanoma mouse model [26]. EMT-related protein markers, such as MMP-1, E-CAD, VIM, SNAIL, and CK, showed a significant up-regulation in cancer [27–29]. Evidence from many clinical studies prompts further investigation of the pathophysiologic role of EMT in metastatic progression. Increased expression of EMT components has been associated with the incidence or invasiveness of various types of cancer, including colorectal, esophageal, pancreatic, gastric, breast, and malignant melanoma [30]. Tumor progression correlates with an overall loss E-cadherin expression or loss of its normal localization at cell–cell contacts. High levels of VIM expression in cancer patients have been correlated with a poor prognosis in breast cancer, also correlating with a high histological grade and the triple-negative phenotype [31]. In our model, inhibition associated with short times of exposure of the CD44 receptor and E-CAD was observed, also suggesting their participation in antiproliferative effects of bacterial CDPs (Fig. 7). Vimentin has been implicated in many aspects of cancer initiation and progression. In tumorigenesis, vimentin forms a complex with 14-3-3 and beclin-1 to inhibit autophagy via an Akt-dependent mechanism. In this regard, our results suggest that CDPs diminish the expression of VIM protein, which is also indicative of a potential target.

Differential protein expression of the CD44 and cadherins indicated that the cancer stem cell (CSCs) system is also involved in HeLa malignancy and the antiproliferative effect of CDPs (Fig. 7). CD44 is a cell surface adhesion receptor that is highly expressed in many cancers and regulates metastasis via recruitment of CD44 to the cell surface [32]. In our study, the CD44 was decreased in the protein extracts of HeLa cells from CDPs treated with short times of exposure, suggesting that the antiproliferative effect of CDPs involves the CD44 receptor, and consequently, actuation over the CSCs pathways, such as those found in the xenografted melanoma mouse model [26].

On the other hand, the Ras–ERK pathway was also dysregulated in adenocarcinoma types, as previously shown [33, 34]. Interestingly, we found that proteins involved in the Ras–ERK pathway (Met and Bad) were overexpressed in HeLa cells and down-expression by CDP addition was found (Fig. 2). Met is a receptor that is generally related to its main ligand hepatocyte growth factor (HGF) during embryonic development, though it is also known as an oncogene that may participate in invasiveness. Met can activate various signaling pathways, including PI3K either directly or through Ras-p. Therefore, in cancer, the Ras–ERK pathway is implicated as an alternative via signaling dysregulation.

Other protein tumor suppressors belonging to the TNF-α/FasL pathway were found to have modified their expression in the HeLa-CDPs model, which could be considered independent of the mTOR and Ras pathways. The proteins that showed differential expression included JNK, E-CAD, N-CAD, p27Kip1, survivin, Stat-3, and Cas-3 (Figs. 2, 3). The p27kip1 is an universal cyclin-dependent kinase inhibitor that regulates cell cycle progression by acting over nuclear CDK proteins, and it has been related to tumor suppression, apoptosis promotion, drug resistance in solid tumors, cell differentiation, and safeguarding against inflammatory injury [35]. We also found that p27Kip1 was inhibited in the HeLa cells treated with CDPs for short time exposures (Fig. 2).

The promotion of malignancy involving the increment of N-Cadherin and the activation of PI3K/Akt pathway suggested that the N-Cadherin could be also a therapeutic target in cancer [36]. On the other hand, N-Cadherin can promote cell survival, migration/invasion, and induction of the epithelial to mesenchymal transition (EMT) process by direct recruitment of signaling molecules. The modulation of the phosphorylation state of catenins also regulates their binding to N-Cadherin and other effector molecules, contributing to N-Cadherin signaling. The N-CAD inhibition found in our model indicates that the EMT signaling pathway participates in HeLa malignancy and also as the Wnt/β-catenin pathway.

In the correlation analysis utilizing data of the antibody arrays in our study revealed a group of proteins that were outside of all other cancer and intracellular signaling proteins (Fig. 4, red circle). From this group, we identified the Met, EGF, and HER2/ErbB2 receptors, which were differentially located far from other 35 CDPs-associated proteins (Fig. 4), suggesting they play important roles in the antiproliferative effect on the HeLa line by CDPs, though their participation requires more clarification.

In cancerous cells, PTEN loss correlates with an increase in transcription and activation of CREB regulators, and CREB phosphorylation restores the effect of MEK inhibitors [37]. Our results showed decreased phosphorylation levels of p-PTEN by CDPs treatment with long time exposure (Fig. 5), suggesting that in addition to the effect over the

PI3K/Akt/mTOR pathway, it could has also have an effect on the CREB regulator and consequently on the MEK pathway (Fig. 7).

With respect to the HSP27 protein, it has been widely associated with apoptosis control, ROS damage, and also in actin remodeling and protein folding. High intracellular levels of HSP27 have been found in many cancer types and association with promoting drug resistance [6]. HSP27 phosphorylation also regulates its interaction with other proteins such as Akt and MAPKa, and its phosphorylation dissociates from Akt, and thus promoting apoptosis [6]. In our study, the HSP27 was inhibited its expression by CDPs treatment in HeLa cells for short treatment times and recovery at longer times (Fig. 5). This suggests that the CDPs also targets the HSP70 protein kinase and probably renders effects over downstream and upstream elements, such as Akt, promoting induction of apoptosis in the HeLa line (Fig. 7).

Finally, ULK (unc-51-like autophagy activating kinase) participation in HeLa cell malignancy, which includes expression also induced and repressed by CDPs treatment, suggests that it could be an important target element in therapeutic processes. In the lysosomal degradative pathway (autophagy), which is essential to development and homeostasis, its dysregulation is closely associated with a variety of human diseases and cancers [38]. The major autophagy pathway involves the activation of the ULK1/ATG13/FIP200 complex, the PI3K complex, and the mATG9 cycling machinery to initiate the formation of a phagophore/isolation membrane, leading to subsequent expansion and maturation of the autophagosome [39]. Alteration of ULK1-mediated phosphorylation has effects on downstream elements of autophagy stimuli, such as ATG14 and ATG9 proteins. Induction of autophagy is triggered in response to nutrient deprivation or stresses to efficiently degrade and recycle cytoplasmic components for homeostasis and cell survival. Defects in autophagy have been causally linked to degenerative, inflammatory, metabolic, and neoplastic diseases [39]. Thus, our results indicate that CDPs can also target ULK1 kinase and consequently induce autophagy in HeLa cells as a cytotoxicity mechanism, which was previously found to exacerbate ROS generation and cellular disintegration in the cultures of HeLa cells treated with CDPs [14].

In our work, the HeLa cell line was treated with CDPs as an antiproliferative study model, revealing a significant decrease in protein expression/phosphorylation of pathways involved in survival, proliferation, invasiveness, autophagy, and energy metabolism. Thus, our data suggests that bacterial CDPs block or suppress the activation of the signal transduction pathways associated with the onset of tumorigenesis governed by PI3K/Akt/mTOR, Ras/Raf/MEK/ERK1/2, PI3K/JNK/PKA, p27Kip1/CDK1/survivin, MAPK, HIF-1, Wnt/β-catenin, HSP27, EMT, and CSCs signaling pathways and receptors, such as EGF/ErbB2/HGF/Met, in which the molecular mechanism involved could be the targeting of ATP-binding site of protein kinases. Findings further indicated that the multiple signaling pathways were implicated in adenocarcinoma aggressiveness, which were impacted by the CDPs on the HeLa line, which suggests that bacterial CDPs may be considered as a potential antineoplastic drug in human cervical adenocarcinoma therapy.

Acknowledgements This study was funded by the Consejo Nacional de Ciencia y Tecnología (CONACYT) of México (Grant Numbers 256119 and 222405), the Marcos Moshinsky Foundation, and Universidad Michoacana de San Nicolás de Hidalgo/C.I.C.2.14 Grants. L.H.-P. received a scholarship from CONACYT. We thank Alejandra Ochoa for HeLa cell line donation.

Author contributions Conception and design: JC-G, LH-P. Analysis and interpretation of data: LH-P, JC-G. Writing, review, and/or revision of the manuscript: JC-G, LH-P, HR-C. Administrative, technical, or material support: JC-G, HR-C.

Compliance with ethical standards

Conflict of interest The authors declare no potential conflicts of interest.

References

1. Borders EB, Bivona C, Medina PJ (2010) Mammalian target of rapamycin: biological function and target for novel anticancer agents. Am J Health Syst Pharm 67(24):2095–2106. https://doi.org/10.2146/ajhp100020
2. Hu R, Wang MQ, Niu WB, Wang YJ, Liu YY, Liu LY, Wang M, Zhong J, You HY, Wu XH, Deng N, Lu L, Wei LB (2018) SKA3 promotes cell proliferation and migration in cervical cancer by activating the PI3K/Akt signaling pathway. Cancer Cell Int 18(1):183. https://doi.org/10.1186/s12935-018-0670-4
3. Yang M, Wang M, Li X, Xie Y, Xia X, Tian J, Zhang K, Tang A (2018) Wnt signaling in cervical cancer? J Cancer 9(7):1277–1286. https://doi.org/10.7150/jca.22005
4. Manzo-Merino J, Contreras-Paredes A, Vazquez-Ulloa E, Rocha-Zavaleta L, Fuentes-Gonzalez AM, Lizano M (2014) The role of signaling pathways in cervical cancer and molecular therapeutic targets. Arch Med Res 45(7):525–539. https://doi.org/10.1016/j.arcmed.2014.10.008
5. Campos-Parra AD, Padua-Bracho A, Pedroza-Torres A, Figueroa-González G, Fernández-Retana J, Millan-Catalan O, Peralta-Zaragoza O, Cantú de León D, Herrera LA, Pérez-Plasencia C (2016) Comprehensive transcriptome analysis identifies pathways with therapeutic potential in locally advanced cervical cancer. Gynecol Oncol 143(2):406–413. https://doi.org/10.1016/j.ygyno.2016.08.327
6. Wang X, Chen M, Zhou J, Zhang X (2014) HSP27, 70 and 90, anti-apoptotic proteins, in clinical cancer therapy (Review). Int J Oncol 45(1):18–30. https://doi.org/10.3892/ijo.2014.2399
7. Kim YC, Guan KL (2015) mTOR: a pharmacologic target for autophagy regulation. J Clin Invest 125(1):25–32. https://doi.org/10.1172/jci73939
8. Laplante M, Sabatini DM (2012) mTOR signaling in growth control and disease. Cell 149(2):274–293. https://doi.org/10.1016/j.cell.2012.03.017

9. Gaubitz C, Prouteau M, Kusmider B, Loewith R (2016) TORC2 structure and function. Trends Biochem Sci 41(6):532–545. https://doi.org/10.1016/j.tibs.2016.04.001
10. Guri Y, Colombi M, Dazert E, Hindupur SK, Roszik J, Moes S, Jenoe P, Heim MH, Riezman I, Riezman H, Hall MN (2017) mTORC2 promotes tumorigenesis via lipid synthesis. Cancer Cell 32(6):807–823.e812. https://doi.org/10.1016/j.ccell.2017.11.011
11. Saxton RA, Sabatini DM (2017) mTOR signaling in growth, metabolism, and disease. Cell 168(6):960–976
12. Sarbassov DD, Guertin DA, Ali SM, Sabatini DM (2005) Phosphorylation and regulation of Akt/PKB by the rictor-mTOR complex. Science 307(5712):1098–1101. https://doi.org/10.1126/science.1106148
13. Yang G, Murashige DS, Humphrey SJ, James DE (2015) A positive feedback loop between Akt and mTORC2 via SIN1 phosphorylation. Cell Rep 12(6):937–943. https://doi.org/10.1016/j.celrep.2015.07.016
14. Hernandez-Padilla L, Vazquez-Rivera D, Sanchez-Briones LA, Diaz-Perez AL, Moreno-Rodriguez J, Moreno-Eutimio MA, Meza-Carmen V, Cruz HR, Campos-Garcia J (2017) The antiproliferative effect of cyclodipeptides from *Pseudomonas aeruginosa* PAO1 on HeLa cells involves inhibition of phosphorylation of Akt and S6k kinases. Molecules. https://doi.org/10.3390/molecules22061024
15. Vázquez-Rivera D, González O, Guzmán-Rodríguez J, Díaz-Pérez AL, Ochoa-Zarzosa A, López-Bucio J, Meza-Carmen V, Campos-García J (2015) Cytotoxicity of cyclodipeptides from *Pseudomonas aeruginosa* PAO1 leads to apoptosis in human cancer cell lines. BioMed Res Int 2015:197608. https://doi.org/10.1155/2015/197608
16. Ortiz-Castro R, Díaz-Pérez C, Martínez-Trujillo M, del Río RE, Campos-García J, López-Bucio J (2011) Transkingdom signaling based on bacterial cyclodipeptides with auxin activity in plants. Proc Natl Acad Sci USA 108(17):7253–7258. https://doi.org/10.1073/pnas.1006740108
17. Gonzalez O, Ortiz-Castro R, Diaz-Perez C, Diaz-Perez AL, Magana-Duenas V, Lopez-Bucio J, Campos-Garcia J (2017) Non-ribosomal peptide synthases from *Pseudomonas aeruginosa* play a role in cyclodipeptide biosynthesis, quorum-sensing regulation, and root development in a plant host. Microbial Ecol 73(3):616–629. https://doi.org/10.1007/s00248-016-0896-4
18. Karbowniczek M, Spittle CS, Morrison T, Wu H, Henske EP (2008) mTOR is activated in the majority of malignant melanomas. J Invest Dermatol 128(4):980–987. https://doi.org/10.1038/sj.jid.5701074
19. Batool A, Majeed ST, Aashaq S, Majeed R, Bhat NN, Andrabi KI (2020) Eukaryotic initiation factor 4E is a novel effector of mTORC1 signaling pathway in cross talk with Mnk1. Mol Cell Biochem 465(1):13–26. https://doi.org/10.1007/s11010-019-03663-z
20. Copp J, Manning G, Hunter T (2009) TORC-specific phosphorylation of mammalian target of rapamycin (mTOR): phospho-Ser2481 is a marker for intact mTOR signaling complex 2. Cancer Res 69(5):1821–1827. https://doi.org/10.1158/0008-5472.CAN-08-3014
21. Yu XN, Zhang GC, Sun JL, Zhu HR, Shi X, Song GQ, Weng SQ, Dong L, Liu TT, Shen XZ, Guo HY, Zhu JMA, Oboo X (2020) Enhanced mLST8 expression correlates with tumor progression in hepatocellular carcinoma. Ann Surg Oncol 27(5):1546–1557
22. Habib SL, Michel D, Masliah E, Thomas B, Ko HS, Dawson TM, Abboud H, Clark RA, Imam SZ (2008) Role of tuberin in neuronal degeneration. Neurochem Res 33(6):1113–1116. https://doi.org/10.1007/s11064-007-9558-8
23. Chresta CM, Davies BR, Hickson I, Harding T, Cosulich S, Critchlow SE, Vincent JP, Ellston R, Jones D, Sini P, James D, Howard Z, Dudley P, Hughes G, Smith L, Maguire S, Hummersone M, Malagu K, Menear K, Jenkins R, Jacobsen M, Smith GC, Guichard S, Pass M (2010) AZD8055 is a potent, selective, and orally bioavailable ATP-competitive mammalian target of rapamycin kinase inhibitor with in vitro and in vivo antitumor activity. Cancer Res 70(1):288–298. https://doi.org/10.1158/0008-5472.can-09-1751
24. Kawata T, Tada K, Kobayashi M, Sakamoto T, Takiuchi Y, Iwai F, Sakurada M, Hishizawa M, Shirakawa K, Shindo K, Sato H, Takaori-Kondo A (2018) Dual inhibition of the mTORC1 and mTORC2 signaling pathways is a promising therapeutic target for adult T-cell leukemia. Cancer Sci 109(1):103–111. https://doi.org/10.1111/cas.13431
25. Sanchez-Hernandez I, Baquero P, Calleros L, Calleros L, Chiloeches A (2011) Dual inhibition of (V600E)BRAF and the PI3K/AKT/mTOR pathway cooperates to induce apoptosis in melanoma cells through a MEK-independent mechanism. Cancer Lett 314(2):244–255
26. Duran-Maldonado MX, Hernández-Padilla L, Gallardo-Pérez JC, Díaz-Pérez AL, Martínez-Alcantar L, Reyes-De La Cruz H, Rodríguez-Zavala JS, Pacheco-Rodríguez G, Moss J, Campos-Garcia J (2020) Bacterial cyclodipeptides target signal pathways involved in malignant melanoma. Front Oncol. https://doi.org/10.3389/fonc.2020.01111
27. Derksen PW, Liu X, Saridin F, van der Gulden H, Zevenhoven J, Evers B, van Beijnum JR, Griffioen AW, Vink J, Krimpenfort P, Peterse JL, Cardiff RD, Berns A, Jonkers J (2006) Somatic inactivation of E-cadherin and p53 in mice leads to metastatic lobular mammary carcinoma through induction of anoikis resistance and angiogenesis. Cancer Cell 10(5):437–449. https://doi.org/10.1016/j.ccr.2006.09.013
28. Tinkle CL, Lechler T, Pasolli HA, Fuchs E (2004) Conditional targeting of E-cadherin in skin: insights into hyperproliferative and degenerative responses. Proc Natl Acad Sci (USA) 101(2):552–557. https://doi.org/10.1073/pnas.0307437100
29. Tunggal JA, Helfrich I, Schmitz A, Schwarz H, Gunzel D, Fromm M, Kemler R, Krieg T, Niessen CM (2005) E-cadherin is essential for in vivo epidermal barrier function by regulating tight junctions. EMBO J 24(6):1146–1156. https://doi.org/10.1038/sj.emboj.7600605
30. McGowan PM, Duffy MJ (2008) Matrix metalloproteinase expression and outcome in patients with breast cancer: analysis of a published database. Ann Oncol 19(9):1566–1572. https://doi.org/10.1093/annonc/mdn180
31. Jeong H, Ryu YJ, An J, Lee Y, Kim A (2012) Epithelial-mesenchymal transition in breast cancer correlates with high histological grade and triple-negative phenotype. Histopathology 60(6B):E87–95. https://doi.org/10.1111/j.1365-2559.2012.04195.x
32. Senbanjo LT, Chellaiah MA (2017) CD44: a multifunctional cell surface adhesion receptor is a regulator of progression and metastasis of cancer cells. Front Cell Dev Biol 5:18. https://doi.org/10.3389/fcell.2017.00018
33. Mendoza MC, Blenis J, Blenis J (2011) The Ras-ERK and PI3K-mTOR pathways: cross-talk and compensation. Trends Biochem Sci 36(6):320–328. https://doi.org/10.1016/j.tibs.2011.03.006
34. Bedogni B, Welford SM, Cassarino DS, Nickoloff BJ, Giaccia AJ, Powell MB (2005) The hypoxic microenvironment of the skin contributes to Akt-mediated melanocyte transformation. Cancer Cell 8(6):443–454. https://doi.org/10.1016/j.ccr.2005.11.005
35. Lloyd RV, Erickson LA, Jin L, Kulig E, Qian X, Cheville JC, Scheithauer BW (1999) p27(kip1): A multifunctional cyclin-dependent kinase inhibitor with prognostic significance in human cancers. Am J Pathol 154(2):313–323
36. Mariotti A, Perotti A, Sessa C, Ruegg C (2007) N-cadherin as a therapeutic target in cancer. Exp Opin Invest Drugs 16(4):451–465. https://doi.org/10.1517/13543784.16.4.451

37. Smith AM, Zhang CRC, Cristino AS, Grady JP, Fink JL, Moore AS (2019) PTEN deletion drives acute myeloid leukemia resistance to MEK inhibitors. Oncotarget 10(56):5755–5767. https://doi.org/10.18632/oncotarget.27206
38. Ding X, Jiang X, Tian R, Zhao P, Li L, Wang X, Chen S, Zhu Y, Mei M, Bao S, Liu W, Tang Z, Sun Q (2019) RAB2 regulates the formation of autophagosome and autolysosome in mammalian cells. Autophagy 15(10):1774–1786. https://doi.org/10.1080/15548627.2019.1596478
39. Zhou C, Ma K, Gao R, Mu C, Chen L, Liu Q, Luo Q, Feng D, Zhu Y, Chen Q (2017) Regulation of mATG9 trafficking by Src- and ULK1-mediated phosphorylation in basal and starvation-induced autophagy. Cell Res 27(2):184–201. https://doi.org/10.1038/cr.2016.146

7. DISCUSIÓN

En la actualidad se tiene un gran interés en encontrar moléculas novedosas que posean propiedades para inhibir el crecimiento de células cancerosas y/o tumores cancerosos. Dentro de este contexto, los péptidos constituyen una familia diversa de compuestos naturales que han sido implicados en diversas funciones biológicas. Se sabe que los ciclodipéptidos (CDPs) de origen microbiano tienen un gran potencial farmacéutico como agentes antifúngicos, antimicrobianos, inmunomoduladores, antioxidantes y anticancerosos (Kanoh et al., 1999; Sinha et al., 2004). Los CDPs poseen ventajas fisiológicas intrínsecas en sus moléculas, por ejemplo, su estabilidad fisiológica y química y su especificidad conformacional y estructural. Estas propiedades los hacen más estables que los péptidos no cíclicos. Se han explorado muchos aspectos de la síntesis de CDPs para descubrir moléculas análogas sintéticas que puedan servir como fármacos novedosos. Aunque ha pasado mucho tiempo desde que se descubrieron los CDPs y han sido estudiados desde entonces, recientemente se ha incrementado el interés en sus efectos antiproliferativos y citotóxicos en líneas celulares cancerosas, así como en tumores *in vivo*.

En este sentido, se ha reportado que los CDPs producidos por *Pseudomonas aeruginosa* poseen efecto citotóxico en las líneas cancerosas HeLa y CaCo-2 (Vázquez-Rivera et al., 2015), mediante inducción de apoptosis intrínseca a través de la vía PI3K/Akt/S6k mostrando especificidad por células cancerosas a través de la disminución de la fosforilación de p-Akt y p-S6k en células HeLa, dependiente del tiempo y concentración (Hernández-Padilla et al., 2017).

Debido a la inactivación de la vía de transducción de señales PI3K-Akt causada por los PAO1-CDPs, se posiciona a estas moléculas como potencial opción terapéutica contra el cáncer (Hernández-Padilla et al., 2017). Curiosamente, como se muestra en la figura 5 panel (b) del capitulo 1 la fosforilación de las proteínas p-Akt y p-S6k mostraron un comportamiento cíclico, debido a la inhibición de la fosforilación por los PAO1-CDPs a tiempos de exposición cortos (5 a 60 min), luego recuperándose a tiempos de exposición largos (120-240 min).

Akt regula el metabolismo, supervivencia, apoptosis, crecimiento, y proliferación, al estar fosforilada. El residuo de Akt Thr 308 es fosforilado por PI3K, mientras que mTORC2 fosforila directamente a Akt en su residuo Ser473, un sitio requerido para su máxima activación (Toker, 2012). El fenómeno de fosforilación cíclica observado en Akt-S473 y S6k-T389 durante el tratamiento de células HeLa con los PAO1-CDP sugiere que la actividad de mTORC2 podría estar involucrada. Otra causa del fenómeno de fosforilación cíclica puede estar vinculada con la participación de la vía Mnk1, la cual se relaciona con la exposición prolongada de rapamicina para inhibir mTORC1, provocando la retroalimentación de la fosforilación a través de eIF4E (Batool et al., 2020), donde este mecanismo se podría relacionar con los PAO1-CDPs. Por último, otra alternativa es que haya inducción a nivel genético de moduladores de vías de señalización asociadas con la recurrencia y/o resistencia a fármacos anticancerosos en la línea celular HeLa, aunque se deben hacer más experimentos para descartar este raciocinio.

Por todo lo anterior, en este estudio se evaluó el efecto de los PAO1-CDPs en el complejo mTOR y las vías de señalización que lo regulan, usando como modelo células de cáncer cervicouterino humano (HeLa); donde el enfoque de inmunodetección en tándem utilizado, hizo posible evaluar elementos de vías de señalización y proteínas cinasas implicadas en vías de señalización intracelular relacionadas con el cáncer.

La fosforilación de Akt dependiente de mTORC2 permite la activación de mTORC1; por lo que mTORC2 puede inhibir indirectamente la autofagia (Kim el at., 2015). Adicionalmente, Akt fosforila directamente e inhibe a PRAS40, un componente de mTORC1 que regula negativamente su actividad cinasa permitiendo la activación de mTORC1 (Sancak, et al 2007). En este contexto, en la figura 3 del capitulo 2 se muestra que los PAO1-CDPs inhiben la fosforilación de PRAS40 (Thr 246) dependiente del tiempo de tratamiento. Además, los PAO1-CDPs no afectan la fosforilación de la cinasa Akt en su residuo Thr308, por el contrario, los PAO1-CDPs disminuyen la fosforilación de la cinasa Akt en su residuo Ser473, (figura 3 del capitulo 2).

AMPKa (proteína cinasa activada por AMP) es una proteína que tiene un papel importante en la regulación de la homeostasis de energía, cuando es activada por un incremento en los niveles de AMP/ATP en la célula, la subunidad catalítica de AMPKa (Thr 172) es el mejor sitio de fosforilación para que se lleve a cabo ésta regulación. AMPKa responde a señales de

energía y/o estrés a través de p53 (daño al DNA) y LKB1 (déficit de energía), teniendo como blanco la activación/inactivación del complejo mTOR. Se ha reportado que AMPK y mTOR son sensores de energía que activan la autofagia a través de ULK1 (Dengler et al., 2020). En la figura 3 del capitulo 2 se muestra que los PAO1-CDPs disminuyen la fosforilación de AMPKa (Thr172) dependiente del tiempo, por lo que disminuyen la activación de la cinasa mTOR. Los resultados demuestran que los PAO1-CDPs disminuyen la fosforilación de la cinasa mTOR en su residuo Serina 2448, esto indica que los PAO1-CDPs podrían estar disminuyendo la proliferación celular y la expresión de proteínas en las células HeLa a través del complejo mTOR(figura 3 del capitulo 2). Esto concuerda con los resultados de la cinasa p70S6K (Thr 389), en dónde los PAO1-CDPs disminuyen la fosforilación de la cinasa p70S6K en su residuo Thr 389, por lo que se disminuye la síntesis de proteínas.

Interesantemente, entre las proteínas que mostraron una disminución significativa en los niveles de expresión por los tratamientos con los CDPs dependiente del tiempo, están dos receptores: el receptor tirosina Cinasa Met y el Receptor EGF (figura 2 del capitulo 2). Dichos receptores han sido reportados como receptores involucrados en la vía de AKT/mTOR/S6K (Kang et al., 2013) y son claves en la supervivencia, progresión y migración celular en distintos tipos de cáncer (Engelman et al., 2008), por ejemplo en cáncer cervicouterino (Liu et al., 2016). Los primeros estudios de la acción de los oncogenes alentaron la noción de que la expresión cada vez mayor de tales genes, y las señales que se multiplicaron por sus productos proteicos, darían lugar a un aumento correspondiente de la proliferación de células cancerosas y, por lo tanto, al crecimiento tumoral. Investigaciones más recientes han debilitado esta noción, y han demostrado que la señalización excesivamente elevada por oncoproteínas como RAS, MYC y RAF puede provocar respuestas contrarias como inducción de senescencia celular y/o apoptosis (Collado and Serrano, 2010; Evan and d'Adda di Fagagna, 2009; Lowe et al., 2004). Los resultados mostraron que los PAO1-CDPs provocan la expresión de Ras a los 60 y 240 min de exposición (Figura 5 del capitulo 2).

Sorprendentemente, en este trabajo se observó un decremento significativo de la fosforilación en la mayoría de las proteínas evaluadas, cuando las células fueron tratadas con los ciclodipéptidos, durante las primeras horas. Estos hallazgos concuerdan con los resultados descritos anteriormente en donde la disminución de los receptores Met y EGF (Figura 2 del

capitulo 2) traerían como consecuencia la desregulación de proteínas río abajo de la vía de mTOR. Interesantemente, la fosforilación de Akt-Ser473 fue diferencial; mientras que la fosforilación en el residuo Thr308 no mostró cambio con los tratamientos, la fosforilación en el residuo Ser 473 disminuyó significativamente en las primeras horas de tratamiento (Figura 3 del capitulo 2). Los hallazgos recientes de Fontoura y col., 2017, mostraron que la fosforilación del residuo Ser-473 es llevado a cabo directamente y exclusivamente por el complejo mTORC2, lo cual activa río abajo a mTORC1 que promueve la fosforilación de la proteína S6K y dicha fosforilación-desfosforilación está involucrada en la vía de apoptosis. Por lo tanto, los resultados sugieren que la fosforilación del residuo Ser-473 de AKT es llevada a cabo por mTORC2, y que cuando las células son tratadas con los CDPs, ésta se ve inhibida. En concordancia a esto y en el mismo sentido, la proteína AMPK también mostró una disminución en la fosforilación en el residuo Thr172 (figura 3 del capitulo 2). Se ha reportado que la fosforilación de AMPK es inducida por p53, que a su vez induce la fosforilación de TSC2, y como consecuencia la activación de mTORC1 (Inoki et al., 2003), promoviendo la supervivencia y proliferación celular. Los resultados en este trabajo también sugieren que cuando las células HeLa son tratadas con los PAO1-CDPs en la primera hora de tratamiento, hay una disminución de p53, una disminución de la fosforilación de AMPK, una disminución en la fosforilación del residuo Thr240 en la proteína PRAS40 (mTORC1), y una disminución en la fosforilación del residuo Ser112 en la proteína BAD (Figura 3 del capitulo 2); esta última involucrada también en la vía de apoptosis (Wang et al.,1999). Adicionalmente, se ha reportado que la activación de Akt por si sola es suficiente para promover la fosforilación en el residuo 246 del represor PRAS40, lo que causa su disociación del complejo mTORC1 y permite su actividad (Kovacina et al., 2003). En concordancia con esto, los resultados sugieren que la disminución de la fosforilación del residuo 246 del represor PRAS40 por el tratamiento de las células con los PAO-CDPs podría desactivar al complejo mTORC1.

PECAM-1 es una molécula de adhesión en células hematopoyéticas (Bergom et al., 2005), y en el caso de las células endoteliales y epiteliales PECAM-1 funciona como molécula inhibidora de la muerte celular programada (Gao et al.,2003) . Los PAO1-CDPs disminuyen la presencia de PECAM-1 en las células HeLa a los 15 y 60 min de tratamiento (figura 2 del capitulo 2), y esto podría deberse a que los PAO1-CDPs provocan que las moléculas de

PECAM-1 se degraden o cambien su configuración. Los PAO1-CDPs disminuyen la presencia de EpCAM en las células HeLa a los 15 y 60 min de tratamiento, lo que se correlaciona con los resultados anteriores de Hernández-Padilla y col. 2017 en donde a estos tiempos se disminuye la proliferación celular, además, de que se puede inferir que los PAO1-CDPs promueven la agregación celular a los 240 min a través de EpCAM. La pérdida de expresión de E-Cadherina provoca la pérdida de polaridad e inhibe el contacto celular, promoviendo crecimiento no controlado e invasión de células tumorales a tejido adyascente (Münz et al., 2004). La expresión de E-Cadherina es baja en células HeLa (Chen et al., 2003), como los PAO1-CDPs restauran la expresión de E-Cadherina a los 240 min comparado con el control, se puede proponer que los PAO1-CDPs disminuyen la invasividad de las células HeLa.

Así mismo se puede inferir que los PAO1-CDPs inhiben interacciones célula-célula y célula matriz ya que disminuyen la presencia de la proteína CD44 a los 15 y 60 min de tratamiento, interesantemente, se restaura su expresión a los 240 minutos. Se ha reportado que cuando Merlin (inhibidor de CD44) se desfosforila y se une a CD44, esta no puede unirse a actina y por lo tanto, no interactúa con proteínas de superficie como PI3K (Al-Othman et al., 2019). Las interacciones de CD44 con proteínas de señalización conducen a la inducción de diversas vías como PI3K, que activan una serie de procesos, incluyendo la supervivencia y e invasión celular (Bourguignon et al., 2010). Por lo que se puede sugerir que CD44 se encuentra secuestrado por la proteína Merlin inhibiendo el crecimiento celular, ya que se sabe que los PAO1-CDPs inhiben la vía de señalización PI3K/Akt (Hernández-Padilla et al., 2017) y que además los PAO1-CDPs restauran la expresión de CD44 a los 240 min de tratamiento probablemente contribuyendo a la agregación celular.

El complejo TSC1/TSC2 funciona como un regulador negativo de la actividad de mTORC1 (Inoki et al.,2002). La señalización a través de mTORC1 dirige la síntesis proteica, esencial para la proliferación celular. Otros procesos como autofagia y apoptosis están íntimamente ligados a la ruta TSC/mTORC1 y tienen un papel importante en la muerte o supervivencia de las células (McManus et al.,2002). En este sentido, y como se describió previamente en este trabajo, se observó una disminución en la fosforilación del residuo Thr172 de la proteína AMPK con los PAO-CDPs (Figura 3 del capitulo 2). Se ha reportado que la fosforilación de AMPK es promovida por p53, que a su vez fosforila a a TSC2 en el residuo Thr1271

incrementando su actividad, provocando disminución de supervivencia y proliferación celular a través de mTORC1. Contrariamente, se ha reportado que la cinasa RSK1 fosforila a TSC2 en el residuo Ser1798 para inhibir la actividad del complejo TSC1/TSC2 y así promover proliferación celular a través de mTORC1(Inoki, et al 2003). La evaluación del efecto de los PAO1-CDPs sobre la fosforilación de TSC2 (Ser 1798) mostró primeramente una disminución a los 15 y 60 minutos de tratamiento, y posteriormente, un incremento a los 240 minutos, comparado con el control de carga, β-actina, que se mantuvo sin cambios significativos entre los tratamientos (Figura 5 del capitulo 2). Éstos resultados sugieren que la mezcla de los CDPs de *P. aeruginosa* PAO1 promueve la fosforilación de la proteína TSC2 en el residuo Ser1798, para inhibir el complejo mTORC1.

mTORC2 es una cinasa que fosforila a Akt en su residuo Ser 473 causando su máxima activación (Sarbassov et al., 2005), además, mTORC2 puede activar la señalización de mTORC1 a través de Akt Ser 473, un activador de mTORC1 a través de TSC2 (Li et al.,2015). La activación de mTORC2 es fútil para epitelio de células sanas o fibroblastos de embrión, mientras que es necesario para células cancerosas que mantienen activa la vía PI3K. Esto indica que la inhibición de Rictor/mTORC2 puede ser más deletérea para células cancerosas que para células normales, de forma que inhibidores de mTORC2 causarían menos toxicidad en células normales (Guertin et al., 2009).

En este trabajo se confirmó que las vías de señalización están desreguladas en células HeLa y que esto se relaciona con su alta capacidad prolífica, ya que se detectó hiperfosforilación de las proteínas, p-Akt-Ser473, p-mTOR-Ser2448 y p-p70S6K-Thr389, confirmando claramente la neoplasia maligna en estas células, las cuales disminuyeron su fosforilación después de la exposición con los PAO1-CDPs (Figura 5 del capitulo 2). mTOR participa en la vía PI3K/ AKT, y está involucrado en la proliferación de tumor y en la angiogénesis (Karar, et al., 2011).

La alta expresión de p-mTOR está asociada con resistencia a radioterapia (Wang et al., 2016); por lo tanto, inhibir mTOR podría ser un blanco terpéutico en cáncer cervico-úterino (Kim MK, et al., 2010). A este respecto, se encontró que los PAO1-CDPs disminuyen la fosforilación de p-mTOR-Ser2481 a los 15 y 60 min de exposición y provocan la restauración de la fosforilación a tiempos de exposición de 240 min (Figura 5 del capitulo 2). Así mismo, los PAO1-CDPs redujeron la fosforilación de p70S6K-Thr389 (Figura 5 panel

(b) del capitulo 1), que se correlaciona con la disminución de la fosforilación de p-mTOR-Ser2448 a los 15 y 60 min de exposición (Figura 5 del capitulo 2), este sito de fosforilación se encuentra asociado principalmente con el complejo mTORC1, mientras que la isoforma p-mTOR-Ser2481 se asocia principalmente con el complejo mTORC2 (Copp et al., 2009). Este hallazgo demuestra que los PAO1-CDPs actúan en los complejos mTOR en diferentes sitios de fosforilación, y por lo tanto, se modulan diferentes elementos de la vía de señalización. Estos resultados demuestran que en el efecto antiproliferativo de los PAO1-CDPs participan los complejos mTORC1 y mTORC2. Por lo que se evaluó el efecto de los PAO1-CDPs en las proteínas Raptor (mTORC1) y Rictor (mTORC2).

Los PAO1-CDPs provocan la disminución de la expresión de la proteína Rictor, lo que indica que disminuyó la formación del complejo mTORC2, mientras que la expresión de la proteína Raptor se incrementó con el tratamiento, lo que indica que se favoreció la formación del complejo mTORC1 (Figura 5 del capitulo 2). En este sentido, la proteína mLST8 (mammalian lethal with sec-13 protein 8 (mLST8 o GβL) es un componente de mTORC1 y mTORC2, funciona estabilizando la interacción entre raptor y mTORC1 así como la interacción entre rictor y mTORC2, mLST8 se ha encontrado en altos niveles de expresión en ciertos tipos de carcinoma (Kakumoto etal.,2015). La sobreexpresión de mLST8 se correlaciona positivamente con el tamaño del tumor, la diferenciación e invasividad (Yu et al., 2020). En este estudio, los PAO1-CDPs provocan el incremento de la expresión de mLTS8 a tiempos cortos de exposición, pero se inhibe a los 240 min (Figura 5 del capitulo 2). Estos resultados sugieren que el efecto antiproliferativo de los PAO1-CDPs en las células HeLa favorecen la integración del complejo mTORC1 a tiempos largos de exposición y la disminución del complejo de mTORC2 en tiempos largos de exposición (240 min), confirmando la participación esencial de mLST8 en la función de mTOR (Figura 5 del capitulo 2).

AZD8055 es un inhibidor competitivo del sitio de unión a ATP de la cinasa de mTOR, el cual inhibe la fosforilación de sustratos de mTORC1 y de mTORC2, y ha sido propuesto como un fármaco anti-neoplásico (Chresta et al., 2010). En este estudio se usó el inhibidor AZD8055 para saber si los PAO1-CDPs tienen mecanismos similares de inhibición en células HeLa. Es importante destacar que el tratamiento con los PAO1-CDPs a los 15 min de

exposición en las células, mostró un efecto similar al de AZD8055 en la fosforilación de p-mTOR-Ser2448; pero a tiempos de exposición de 240 min, los PAO1-CDPs causaron un incremento de la fosforilación de p-mTORSer2448 (Figura 6 del capítulo 2). Además, el tratamiento con AZD8055 y PAO1-CDPs dió lugar a una mayor disminución de los niveles de fosforilación de p-mTOR-Ser2448, comparado con el efecto del tratamiento solamente con los PAO1-CDPs en células HeLa (Figura 6 del capítulo 2). Estos resultados indican que el mecanismo molecular por el cual los PAO1-CDPs inhiben a la cinasa mTOR es parecido al del inhibidor AZD8055.

La eficacia de los inhibidores de mTORC1 es limitada porque al inhibir mTORC1 se disocian los mecanismos de retroalimentación negativa dependiente de mTORC1 y paradójicamente se activa la señalización Akt, lo que resulta en resistencia. Por el contrario, mTORC2 fosforila directamente Akt en un sitio regulatorio crítico para la actividad máxima de la cinasa Akt. Por lo tanto, parece necesario inhibir ambos complejos, tanto a mTORC1 y mTORC2 para bloquear completamente la vía de señalización PI3K/Akt/mTOR (Kawata et al., 2018). Los inhibidores duales de mTOR representan agentes terapéuticos promisorios, mediante la inhibición del ciclo celular en la etapa G0/G1, induciendo apoptosis y bloqueando la fosforilación de Akt-Ser473. El inhibidor de PI3K LY294002 y el inhibidor dual de mTORC1-2 AZD8055 inhiben la fosforilación de Akt- Ser473 y, en consecuencia, ejercen afectación en la fosforilación en PRAS40, TSC2, GSK3b y FoxO1. Cuando esto ocurre, se afecta la inhibición de PRAS40, TSC2, mTORC1, así como la actividad de P70S6K (Kawata et al., 2018). Interesantemente, se obtuvieron resultados similares con el inhibidor de PI3K LY294002, en donde se disminuyó la fosforilación de p-mTOR-Ser2448 por efectos asociados con la presencia de LY294002, pero cuando se agregaron los PAO1-CDPs conjuntamente con LY294002 se potenció la inhibición de p-mTOR-Ser2448 (Figura 6 del capítulo 2). Estos resultados indican que los PAO1-CDPs están compitiendo con proteínas blanco de los inhibidores AZD8055 y LY294002, en el que el mecanismo molecular involucrado podría ser el sitio de unión a ATP de las proteínas cinasas mTORC1 y mTORC2. Lo que sugiere que los PAO1-CDPs pueden considerarse como un potencial antineoplásico en la terapia de adenocarcinoma cervical humano.

8. CONCLUSIÓN

La mezcla de ciclodipéptidos ciclo(*L*-Pro-*L*–Tyr), ciclo(*L*-Pro-*L*–Val) y ciclo(*L*-Pro-*L*-Phe) producidos por *Pseudomonas aeruginosa* PAO1 inducen apoptosis en células de cáncer cervicouterino HeLa a través de la inhibición de los complejos mTORC1 y mTORC2.

9. ARTICULO DE DIVULGACION

ARTÍCULO

Cáncer: apocalipsis zombi en el cuerpo

Laura Hernández-Padilla y Jesús Campos-García

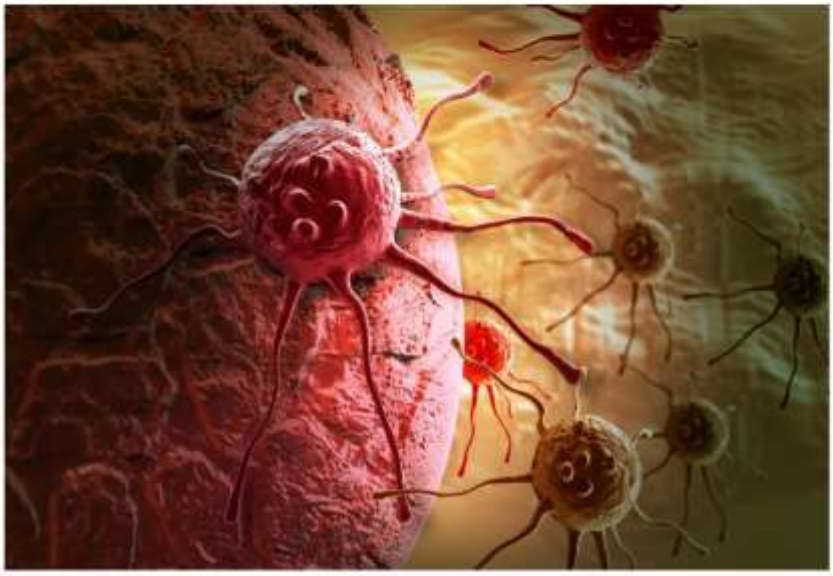

M.C. Laura Hernández-Padilla es estudiante del Programa Institucional de Doctorado en Ciencias Biológicas opción en Biología Experimental del Instituto de Investigaciones Químico Biológicas de la Universidad Michoacana de San Nicolás de Hidalgo.
laura_190589@hotmail.com

D.C. Jesús Campos-García es Profesor e Investigador del Instituto de Investigaciones Químico Biológicas de la Universidad Michoacana de San Nicolás de Hidalgo.
jcgarcia@umich.mx

La ciencia ficción nos ha permitido ver un panorama apocalíptico hipotético en el que los seres humanos se convierten en zombis, entes reanimados después de su muerte, sin voluntad propia, que buscan a otros humanos para transformarlos en uno de ello. En este escenario, el mundo teóricamente termina con la extinción total de la raza humana, pero como en toda película de zombis, siempre hay sobrevivientes en busca de una cura que logre salvar a la humanidad.

En este artículo te describimos, cómo la vida cotidiana supera la ciencia ficción, ya que te explicaremos que hay células que asemejan a un zombi: las cancerosas. Para ello, también revisaremos el comportamiento, la invasión, así como las alternativas de tratamientos actuales para la erradicación

de estas células, a las que denominamos **«células zombis»**.

Estas no pueden morir, son incapaces de realizar las funciones de una célula normal, lo que provoca el descontrol y/o desregulación de la división celular. En general, los zombis son, como dice «The Ghost Breakers», esta comedia norteamericana de terror: «Los verás, caminando ciegamente con los ojos muertos, siguiendo órdenes, sin saber lo que hacen». Los zombis se alimentan de carne humana, lo cual les garantiza la vitalidad y la vida eterna, se distinguen de los humanos en que son incapaces de dominar su voluntad, y esto mismo ocurre con una célula cancerosa, que al parecer inmortal, convierte las células sanas en cancerosas.

Invasión zombi: el terror que implica

El cáncer es un conjunto de más de 200 enfermedades diferentes que comparten ciertas características, entre ellas, que mantienen un crecimiento celular incontrolado «células inmortales», que al igual que un zombi, no mueren y son **capaces de infectar células sanas.**

Los seres humanos **estamos predispuestos a desarrollar cáncer** debido a diversos factores como el tabaquismo, la alimentación, la exposición a sustancias químicas tóxicas, entre otros más. En general, estos factores dañan nuestro ADN, específicamente en sitios llamados genes, de los cuales existen dos grupos que al estar dañados o desregulados, puedan promover el crecimiento celular descontrolado y provocar el desarrollo de esta enfermedad.

La transformación de un humano a zombi se da por mordidas u otra lesión por estar en contacto con otro zombi. Las células cancerosas tienen un método similar para transformar a las células sanas, esto es conocido como **«metástasis»**, que es la capacidad invasora que tiene una célula cancerosa de entrar en el torrente sanguíneo para desarrollar cáncer en lugares distintos del cuerpo donde se originó. Cabe mencionar que cuanto más capacidad de metástasis tenga un tipo celular de cáncer, más difícil resultará erradicarlas.

Lo anterior tiene analogía a lo que hacen los zombis de la serie «The walking dead», su característica es ser lentos y torpes, pero también están los que corren a gran velocidad como los que hemos visto en la película «Guerra mundial Z». Un zombi hambriento y veloz será más peligroso que uno lento y menos voraz, un cáncer con las características de «Guerra mundial Z» será más agresivo.

Así como los zombis son muy invasores, ya que con un solo rasguño convierten a sus víctimas en cientos o miles de zombis, **una célula cancerosa es capaz de convertir una célula sana en inmortal,** de la cual podrían formarse un número inmenso de células cancerosas. Un caso particular, es el de una mujer estadounidense llamada Henrietta Lacks que alcanzó literalmente la inmortalidad, ya que sus células se transformaron en cancerosas, de aquí que científicos pudieron aislar la primera línea

Oncogenes

Genes que generalmente están dormidos, pero cuando son expresados (despiertan), provocan de manera directa la aparición de cáncer. Un ejemplo de ello es que pueden hacer que se produzca un exceso de proteína estimuladora del crecimiento, lo que conlleva a un crecimiento celular incontrolado). Entre los oncogenes más estudiados tenemos a: *PI3K, AKT, RAS, RAF.*

Genes supresores de tumores

Son los genes que normalmente se encuentran despiertos y su función es evitar la aparición de cáncer. Si éstos no se pueden expresar por alguna anomalía, privan a la célula de los mecanismos de defensa contra el crecimiento desmesurado de los tumores formados por las células cancerosas. Entre los más estudiados de este tipo de genes, se encuentran *NF1, PTEN, P53, TSC1, TSC2.*

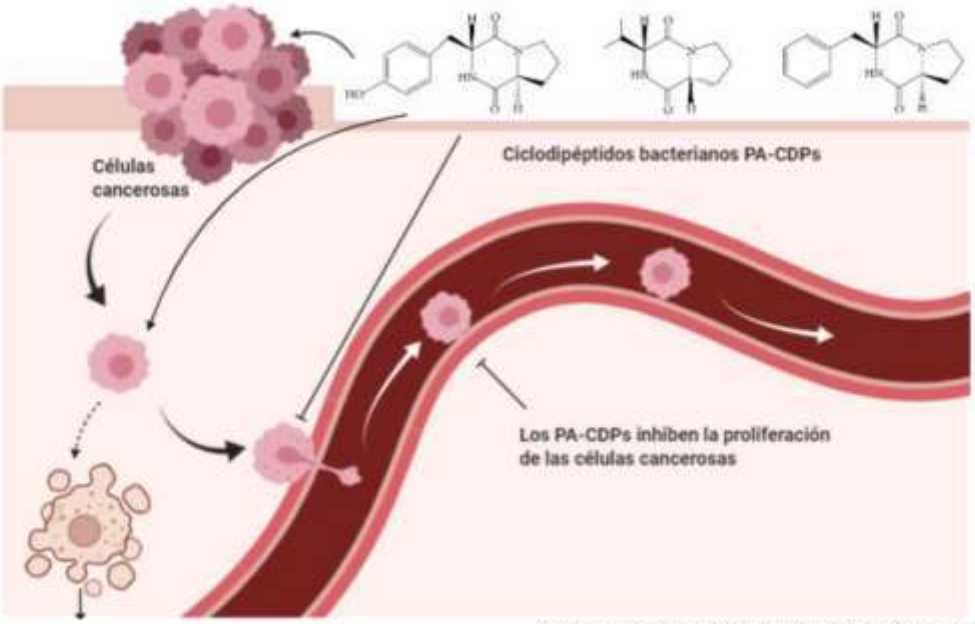

Muerte de las células cancerosas, provocada por los PA-CDPs

celular cancerosa humana llamada HeLa (derivado de las dos primeras letras de su nombre y apellido), lo que permitió conocer cómo actúan este tipo de células cancerosas. Irónicamente, este cáncer permitió que Henrietta sea inmortal, ya que actualmente sus células se encuentran deambulando en importantes laboratorios de investigación, donde están bajo constantes estudios con el fin de modificar su comportamiento, y así detener su crecimiento descontrolado.

¿Cómo se alimentan los zombis?

La obtención de energía en las células se lleva a cabo por la completa oxidación de la glucosa, empleando tres vías metabólicas: glicólisis, ciclo de Krebs y fosforilación oxidativa. El aumento descontrolado de la glicólisis, es una característica en tumores cancerosos; típicamente las células tumorales se caracterizan por un aumento de captación de glucosa para generar energía; sin embargo, no usan la respiración, este fenómeno es conocido como efecto **Warburg.**

Cuando se infectan las células cambian de metabolismo, disminuyendo el metabolismo oxidativo, ¡similar a lo que ocurre en los zombis!, que cambian la dieta del ser humano por el canibalismo. Estas alteraciones en el metabolismo confieren una ventaja selectiva para la supervivencia zombi.

Principales armas contra los zombis o tratamiento contra el cáncer

Actualmente, las principales terapias contra el cáncer son la cirugía, la quimioterapia y la radioterapia, este **tratamiento multidisciplinario** resulta efectivo matando a las células cancerosas, pero estas armas traen consigo efectos secundarios nocivos como anemia, fallo renal, entre otros. Varios estudios han identificado subpoblaciones de células que son resistentes a tratamientos de quimioterapia y radioterapia, lo que explica el origen de las recaídas y la reaparición del tumor con el paso del tiempo, haciendo difícil erradicar al «zombi invasor», por lo que la investigación sobre nuevas estrategias es uno de los grandes retos.

Los medicamentos contra el cáncer son sin duda unos de los más agresivos que se conocen, ya que aunque tienen la función de matar las células cancerosas, también envenenan a las otras células sanas de nuestro organismo. Una de las diferencias, es que las células cancerosas se reproducen rápidamente, y eso es una ventaja, ya que los tejidos que se reproducen a mayor velocidad se envenenan

primero. Por lo que, encontrar un fármaco que identifique y mate a la célula zombi sin que afecte a las células sanas, es vital para contrarrestar los efectos secundarios mencionados.

Los ciclodipéptidos de origen bacteriano: una nueva esperanza

Los ciclopéptidos o ciclodipéptidos (CDPs), son moléculas sintetizadas por bacterias como *Pseudomonas aeruginosa* (PA-CDPs) que tienen la capacidad de evitar la proliferación de diferentes tipos de células cancerosas. En nuestro grupo de trabajo, en el laboratorio de Biotecnología Microbiana del Instituto de Investigaciones Químico Biológicas de la Universidad Michoacana de San Nicolás de Hidalgo, realizamos estudios con los **PA-CDPs** y los avances indican que estos inducen la muerte celular (apoptosis) de las células cancerosas, e interesantemente, **no afectan a las células sanas**. Incluso, sabemos cómo actúan, los PA-CDPs: provocan la muerte de las células cancerosas a través del bloqueo de la activación de una de las principales vías de supervivencia celular «*PI3K/AKT*», oncogenes de los que mencionamos al inicio del artículo.

El hecho de que las células cancerosas sean eliminadas del huésped mediante fármacos como los PA-CDPs, tiene gran relevancia en la práctica clínica, ya que los resultados experimentales brindan la posibilidad **de mejorar el tratamiento y pronóstico del cáncer.** De hecho, los PA-CDPs tienen el potencial, si no de ganar la guerra zombi, sí alguna de las batallas, evitando el inminente final de un ser humano con esta terrible enfermedad. Con estas nuevas armas, comienza una era muy alentadora donde existirán más finales felices en las líneas de batalla, los hospitales.

Nos queda esperar para ver si esta es la década en la que por fin comprendamos el efecto que tienen ciertos fármacos en las vías de señalización que gobiernan una célula para permitirle crecer, multiplicarse, dividirse o morir. Estaremos ante el arma poderosa que elimine solo a las células zombis y no mate a las sanas, así como el final de una película.

¿Cómo evitar el contagio?

Dar la noticia a un paciente de que tiene cáncer, resulta muy alarmante, de igual manera que si en el noticiario de las 3:00 p. m. informara de una invasión zombi. ¿Qué haríamos si esto sucediera? Seguir las recomendaciones y tratamientos para sobrevivir.

Algunas recomendaciones para disminuir la probabilidad de adquirir cáncer son tener buenos hábitos alimenticios y de ejercicio, hacer deporte, no fumar y no exponerse al sol por largos periodos. Además, el tener revisiones médicas al menos una vez al año, garantizaría tener una vida saludable para... ¡No convertirnos en zombis!

sabermás

Boticano C.B. y Angosto M.C. (2009). Innovaciones en cáncer. Madrid: Editorial UNED, 2012. https://books.google.com.mx/books?id=uL2RO-FbshOsC&pg=PT352&dq=biomoleculas+y+cancer&hl=es-419&sa=X&ved=0ahUKEwihLn58fzpAhVEG80KHWIDD3wQ6AEIPDAC#v=onepage&q=biomoleculas%20y%20cancer&f=false

Hernández-Padilla L., Vázquez-Rivera D., Sánchez-Briones L.A., et. al. (2017). «The antiproliferative effect of cyclodipeptides from Pseudomonas aeruginosa PAO1 on HeLa cells involves inhibition of phosphorylation of Akt and S6k kinases». Molecules, 22(6):1024 https://www.mdpi.com/1420-3049/22/6/1024

Mercade T.M. y Pascual F.J.R. (2009). Comprender el cáncer. Barcelona: Editorial AMAT, 2009. https://books.google.com.mx/books?id=trOvNJDjUdoC&pg=PA21&dq=cancer&hl=es-419&sa=X&ved=0ahUKEwjNoZWw8PzpAhVBXqwKHVgRDPcQ6AEIaTAI#v=onepage&q=cancer&f=false

10. ANEXOS

10.1. Artículo de colaboración

Durán-Maldonado, M. X., Hernández-Padilla, L., Gallardo-Pérez, J. C., Díaz-Pérez, A. L., Martínez-Alcantar, L., Reyes De la Cruz, H., & Campos-García, J. (2020). Bacterial cyclodipeptides target signal pathways involved in malignant melanoma. *Frontiers in oncology*, *10*, 1111.

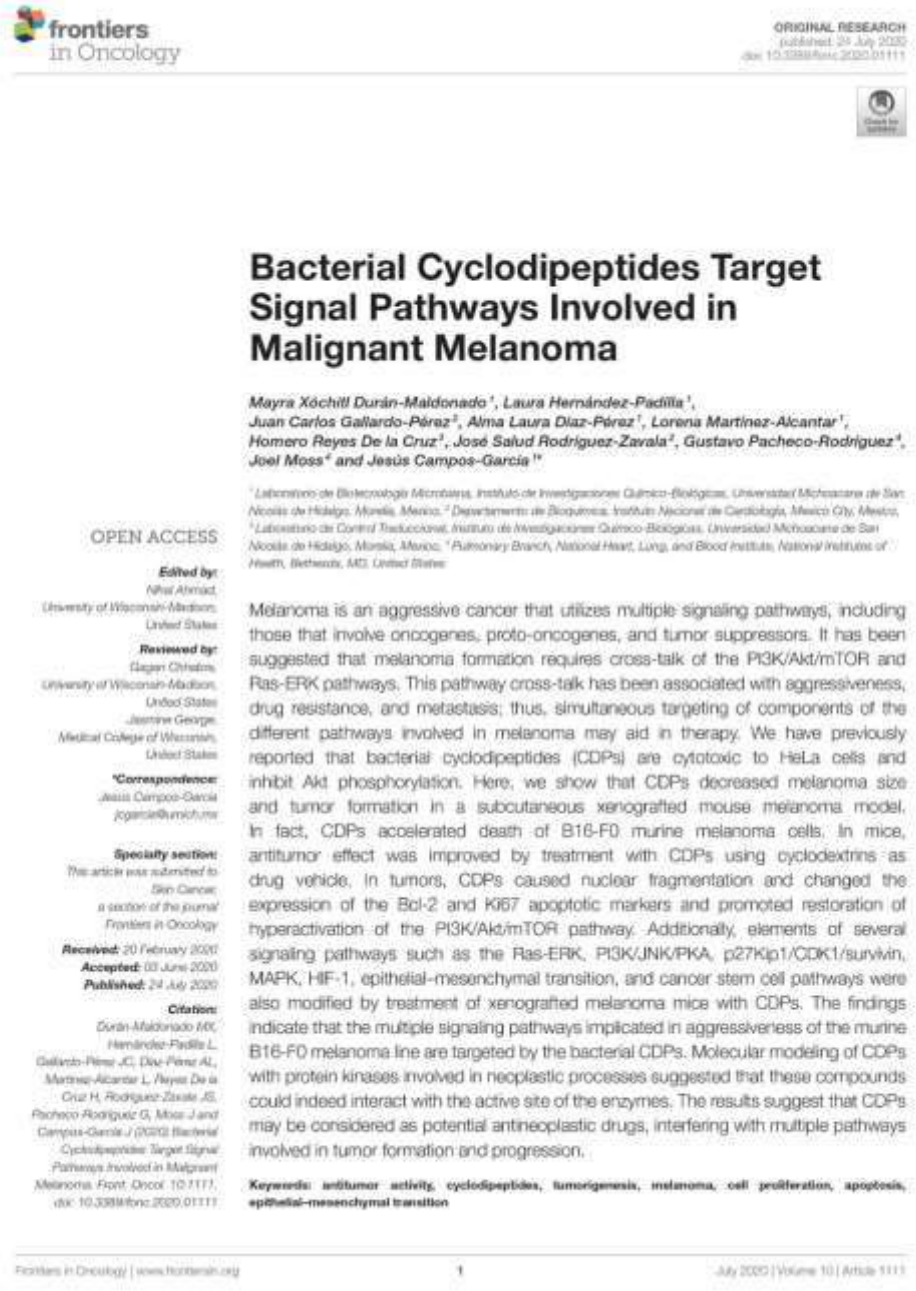

frontiers in Oncology

ORIGINAL RESEARCH
published: 24 July 2020
doi: 10.3389/fonc.2020.01111

Bacterial Cyclodipeptides Target Signal Pathways Involved in Malignant Melanoma

Mayra Xóchitl Durán-Maldonado[1], *Laura Hernández-Padilla*[1], *Juan Carlos Gallardo-Pérez*[2], *Alma Laura Díaz-Pérez*[1], *Lorena Martínez-Alcantar*[1], *Homero Reyes De la Cruz*[3], *José Salud Rodríguez-Zavala*[2], *Gustavo Pacheco-Rodríguez*[4], *Joel Moss*[4] *and Jesús Campos-García*[1]*

[1] Laboratorio de Biotecnología Microbiana, Instituto de Investigaciones Químico-Biológicas, Universidad Michoacana de San Nicolás de Hidalgo, Morelia, Mexico, [2] Departamento de Bioquímica, Instituto Nacional de Cardiología, Mexico City, Mexico, [3] Laboratorio de Control Traduccional, Instituto de Investigaciones Químico-Biológicas, Universidad Michoacana de San Nicolás de Hidalgo, Morelia, Mexico, [4] Pulmonary Branch, National Heart, Lung, and Blood Institute, National Institutes of Health, Bethesda, MD, United States

OPEN ACCESS

Edited by:
Nihal Ahmad,
University of Wisconsin-Madison, United States

Reviewed by:
Gagan Chhabra,
University of Wisconsin-Madison, United States
Jasmine George,
Medical College of Wisconsin, United States

***Correspondence:**
Jesús Campos-García
jcgarcia@umich.mx

Specialty section:
This article was submitted to Skin Cancer, a section of the journal Frontiers in Oncology

Received: 20 February 2020
Accepted: 03 June 2020
Published: 24 July 2020

Citation:
Durán-Maldonado MX, Hernández-Padilla L, Gallardo-Pérez JC, Díaz-Pérez AL, Martínez-Alcantar L, Reyes De la Cruz H, Rodríguez-Zavala JS, Pacheco-Rodríguez G, Moss J and Campos-García J (2020) Bacterial Cyclodipeptides Target Signal Pathways Involved in Malignant Melanoma. Front. Oncol. 10:1111. doi: 10.3389/fonc.2020.01111

Melanoma is an aggressive cancer that utilizes multiple signaling pathways, including those that involve oncogenes, proto-oncogenes, and tumor suppressors. It has been suggested that melanoma formation requires cross-talk of the PI3K/Akt/mTOR and Ras-ERK pathways. This pathway cross-talk has been associated with aggressiveness, drug resistance, and metastasis; thus, simultaneous targeting of components of the different pathways involved in melanoma may aid in therapy. We have previously reported that bacterial cyclodipeptides (CDPs) are cytotoxic to HeLa cells and inhibit Akt phosphorylation. Here, we show that CDPs decreased melanoma size and tumor formation in a subcutaneous xenografted mouse melanoma model. In fact, CDPs accelerated death of B16-F0 murine melanoma cells. In mice, antitumor effect was improved by treatment with CDPs using cyclodextrins as drug vehicle. In tumors, CDPs caused nuclear fragmentation and changed the expression of the Bcl-2 and Ki67 apoptotic markers and promoted restoration of hyperactivation of the PI3K/Akt/mTOR pathway. Additionally, elements of several signaling pathways such as the Ras-ERK, PI3K/JNK/PKA, p27Kip1/CDK1/survivin, MAPK, HIF-1, epithelial–mesenchymal transition, and cancer stem cell pathways were also modified by treatment of xenografted melanoma mice with CDPs. The findings indicate that the multiple signaling pathways implicated in aggressiveness of the murine B16-F0 melanoma line are targeted by the bacterial CDPs. Molecular modeling of CDPs with protein kinases involved in neoplastic processes suggested that these compounds could indeed interact with the active site of the enzymes. The results suggest that CDPs may be considered as potential antineoplastic drugs, interfering with multiple pathways involved in tumor formation and progression.

Keywords: antitumor activity, cyclodipeptides, tumorigenesis, melanoma, cell proliferation, apoptosis, epithelial–mesenchymal transition

INTRODUCTION

Communication between the microbiome and host cells plays important roles in health and disease [1]. Microbes produce metabolites capable of affecting cellular signaling pathways and thus could become potent therapeutics [2]. For instance, structurally diverse cyclodipeptides (CDPs) of bacterial [3, 4] and with less efficiency of synthetic origin [5] are cytotoxic to human cancer cell lines. In fact, we have shown that CDPs [cyclo(L-Pro-L-Tyr), cyclo(L-Pro-L-Val), and cyclo(L-Pro-L-Phe)] from *Pseudomonas aeruginosa* PAO1 promoted apoptosis and cell death of human cervical (HeLa) and colorectal adenocarcinoma (CaCo-2) cells, whereas normal human lung fibroblasts were insensitive [6]. The molecular mechanisms used by CDPs to trigger cytotoxicity, leading to death of cancer cells, appear to involve microtubule polymerization [7] and caspase-3 activation [3, 6].

Cancer results from dysfunction of fundamental cellular processes. In fact, pathways involving oncogenes and tumor suppressors are frequently involved in cancer development and progression [8, 9]. Interestingly, the mechanistic target of rapamycin (mTOR) serine/threonine kinase is a master regulator that participates in two complexes (mTORC1 and mTORC2), and its dysregulation has been implicated in cancer. mTORC1 has been implicated in cellular processes, such as, energy metabolism, proliferation, tumorigenesis, and autophagy, whereas the mTORC2 complex is involved in actin cytoskeleton reorganization and survival [10]. mTORC1 activity is frequently up-regulated in cancer, particularly following increased oncogenic activation of phosphoinositide 3-kinase (PI3K) signaling or inactivation of the lipid phosphatase PTEN (phosphatase and tensin homolog) [9, 11].

Multiple biomarkers characterize a neoplasm/cancer and metastasis [9, 10, 12], which in many cases is initiated by cancer stem cells (CSC) and may involve epithelial–mesenchymal transition (EMT). Epithelial–mesenchymal transition has been associated with action of N-cadherin, a membrane protein involved in cell attachment, which is up-regulated during metastasis and invasion, and promotes tumorigenesis. Additionally, direct interaction of N-cadherin with PI3K may enable activation of the PKB/Akt pathway, suggesting that it could be a therapeutic target in cancer [13]. N-cadherin can also promote cell survival, migration/invasion, and the EMT process by direct cross-talk with other signaling pathways [e.g., nuclear factor κB (NFκB)–mediated, mitogen-activated protein kinase (MAPK), receptor tyrosine kinase (RTK), Ras homolog family member A small GTPase protein (RhoA GTPase), PI3K [14]]. Otherwise, EMT is a crucial regulatory pathway with links to embryogenesis and cancer development.

In melanoma, multiple signaling pathways are dysregulated, involving oncogenes and tumor suppressors (i.e., PI3K/AKT/mTOR, MAPK, RAS/MEK/ERK, BRAF, and CDK), the multiple dysregulation of these signaling pathways favors tumor invasiveness, progression, drug resistance, and recurrence. Current therapeutic procedures for melanoma include chemotherapy, immunotherapy, biochemotherapy, and gene therapy [15, 16]. However, participation of multiple signaling pathways in melanoma pathology complicates its treatment. Then, the elucidation of the involvement of EMT and CSC pathways in melanoma invasiveness, drug resistance, and recurrence is crucial. The main goal of this study was to evaluate the effects of CDPs on a xenografted melanoma tumor model and elucidate the molecular mechanisms involved in CDP action. We observed that CDPs killed melanoma cells and decreased tumor burden. During melanoma development, multiple cell-signalling pathways were targeted and restored by bacterial CDPs, suggesting that these molecules have the potential for use as antiproliferative drugs.

MATERIALS AND METHODS

Chemicals and Reagents

Dulbecco modified Eagle medium (DMEM), fetal bovine serum (FBS), 3-(4,5-dimethylthiazol-2-yl)-2,5-diphenyltetrazolium bromide (MTT), and β-cyclodextrin (β-cyclodextrin hydrate were purchased from Sigma-Aldrich Co., St. Louis, MO, USA). Alexa Fluor 488 annexin V and the propidium iodine (PI)/dead cell apoptosis kits were from Invitrogen Life Technologies, Carlsbad, CA, USA. Cyclodipeptides were obtained from *P. aeruginosa* PAO1 and characterized as previously described [17, 18].

Cell Culture

Mouse B16-F0 melanoma cells line was obtained from the American Type Culture Collection (ATCC, Manassas, VA, USA). Cells were cultured in complete media (CM) [DMEM supplemented with 10% (vol/vol) FBS, 100 U/mL of penicillin, 40 μg/mL of streptomycin, and 1 μg/mL of amphotericin B (Sigma-Aldrich Co., St. Louis, MO, USA)]. Cell culture media were changed twice a week and maintained at 37 °C under 80% humidity and incubated in an atmosphere of 5% CO_2. Following trypsinization, cells were grown to confluency; cells were counted using a hemocytometer chamber.

Cell Viability, Necrosis, and Apoptosis Assays

Cell viability was determined colorimetrically with MTT. Briefly, cells were seeded in 96-well flat-bottomed plates at a density of 1×10^4 cells per well in 200 μL of CM medium and incubated for 24 h at 37 °C with 5% CO_2 as described above. Then, cell culture media were removed and replaced with serum-free DMEM. Following incubation in DMEM with FBS for 24 h, cells were incubated in the presence or absence of the indicated amounts of CDPs for 24 h at 37 °C with 5% CO_2. To determine cell viability, MTT, 50 mg/mL in phosphate-buffered saline (PBS), was added to each well and incubated for 4 h at 37 °C. Finally, 100 μL of 2-propanol/0.1 M HCl (19:1 vol/vol) was added to dissolve formazan crystals, and absorbance was measured at 595 nm using a microplate reader (BioTek Instruments, Winooski, VT, USA).

To quantify necrosis and apoptosis, cell cultures were incubated with DMEM with FBS for 12 h prior to treatment with CDPs. Dimethyl sulfoxide (DMSO) was used as a control at the same concentration used to dissolve the CDPs. Following incubation, cells were collected by centrifugation at 2,000 g for

10 min. The pellet was suspended in 20 µL and incubated with annexin V and propidium iodide (PI) (Dead Cell Apoptosis Kit, Molecular Probes, Invitrogen Life Technologies, Carlsbad, CA, USA). Fluorescence was immediately quantified by fluorescence-activated cell sorting (FACS) using an Accuri C6 Flow Cytometer (BD Biosciences, San Jose, CA, USA). The percentages of fluorescent cells (PFC) and median fluorescence intensity were determined from histograms of the fluorescence emission in the plots, labeled as PFC or as relative fluorescence units. For apoptosis and necrosis assays, annexin V fluorescence was measured with fluorescence channel FL1 at 495/519 nm and for PI in FL3 channel at 535/617 nm. At least 20,000 cellular events were used for calculations.

Subcutaneous Xenografted Melanoma Mouse Model

All the experiments using mice complied with standard guidelines for the welfare of animals with experimental neoplasia in accordance with the recommendations of the Mexican Official Regulations for the Use and Care of Animals (NOM-062-ZOO-1999; Ministry of Agriculture, Mexico). This research was also approved by the Institutional Committee for Use of Animals of the Universidad Michoacana de San Nicolás de Hidalgo. Male C57BL/6 mice between the ages of 4 and 6 weeks were purchased from Envigo RMS S.A. (Mexico City, Mexico). Animals were hosted in cycling for 2 weeks before experiments were started, afterward, the xenograft melanoma procedure was conducted as described below. The mice were housed separately in ventilated cages under a controlled light cycle (12-h light/12 h dark) at room temperature (22–26°C) and were fed with a standard rodent diet and water *ad libitum* in accordance with NOM 062-ZOO-1999; Ministry of Agriculture, Mexico.

Melanoma cells were injected subcutaneously in place of the right flank with 2×10^4 B16-F0 murine melanoma cells. Tumor size was measured every 2 days. Two bisecting diameters of each tumor were measured with calipers. The volume was calculated using the formula (0.4) (ab^2), with "a" being the larger diameter and "b" being the smaller diameter [19]. All mice injected with melanoma cells developed tumors of 20–50 mm^3 8 days from the day of injection. The CDPs were administered at a dose of 0.1 mg/g of mice weight, which was determined assuming that the corporal volume of mice is ~50 cm^3. A concentration of 50 µg/ml (50% apoptotic cells in the assay) was used, rendering 2.5 mg per mouse per dose. In addition, two additional doses of CDPs were tested in a pilot study, with CDP treatment at 10, 50, and 200 µg/ml of CDPs. The results showed similar antitumorigenic effect at 50 and 200 µg/mL of CDPs, but no significant results with 10 µg/mL of CDPs; thus, we decided to use 50 µg/mL of CDPs for this study. A 50 mg/mL stock solution of CDPs was prepared by dissolving the compounds in sterile saline solution containing DMSO (0.1 %), or β-cyclodextrin (50 mg/mL). All liquid treatments of the mouse model were injected in the caudal vein as authorized by NOM 062-ZOO-1999; Ministry of Agriculture, Mexico. Seven different groups of six mice each were randomly assigned: (1) control, healthy mice were injected with 50 µL of sterile saline solution with DMSO (0.1%); (2) control + CDPs, healthy mouse group injected with 50 µL of CDP stock solution; (3) tumor (T), mice with melanoma tumors were injected with 50 µL of sterile saline solution with DMSO (0.1%); (4) T + CDPs-t0, mice with melanoma cell injections were treated from the beginning with a weekly injection with 50 µL of CDP stock solution (three total doses); (5) T + CDPs-t8, mice with melanoma tumors (with volume of ~20–50 mm^3 after 8 days) were injected weekly with 50 µL of CDP stock solution (two total doses); (6) T + CDPs-cdx40, mice as in group 4 were injected weekly with 50 µL of CDP stock solution in β-cyclodextrin (50 mg/mL, three total doses); and (7) T + CDPs-cdx80 mice as in group 5 were treated weekly with 50 µL of CDP stock solution in β-cyclodextrin (50 mg/mL, two total doses). The mice were examined every 2 days and weighed, and tumor size was measured until they were euthanized (20 days) as authorized by the Institutional Committee for Use of Animal of the Universidad Michoacana de San Nicolás de Hidalgo in accord to the NOM 062-ZOO-1999, Ministry of Agriculture, Mexico. Then, organs were removed, tumor area was determined, and dissected tumors and organs were stored at −80 C prior to histopathological studies. Mice that died of causes unrelated to the neoplasm and CDP treatment were not considered in the analysis.

Blood Parameters Evaluation

Blood was obtained by cardiac puncture prior to euthanizing as recommended (NOM 062-ZOO-1999; Ministry of Agriculture, Mexico) and collected in tubes containing heparin. Blood was centrifuged at 3,500 g for 10 min to obtain plasma. Hematocrit was measured by centrifugation (10,000 g for 5 min) using a hematocrit capillary tube. Hemoglobin was determined as follows: Hb = (hematocrit value) (3.3 factor). Plasma was utilized to measure lactate dehydrogenase (LDH), aspartate aminotransferase (AST), and alanine aminotransferase (ALT) activities using the Dry Chemical Analyzer Vitros 350 (Ortho Clinical Diagnostics, Woodburn Green, Buckinghamshire, UK).

Histological Analysis of Tumor Tissue

Tumors and tissues from mice were excised and fixed in 10% neutral-buffered formaldehyde solution and embedded in paraffin. Tissue sections (0.2 mm × 10 µm) were obtained using a Cryostat (Leica CM1850, Leica Biosystems Inc., Buffalo Grove, IL, USA) and stained with hematoxylin-eosin. For immunohistochemical analyses, formalin-fixed tissue sections were dehydrated in a sucrose gradient (10–30%) in PBS buffer for 48 h each. Slides were treated with 10 mM citrate buffer at 60°C, permeabilized with PBS-T buffer, and incubated with H_2O_2, followed by incubation with 5% horse serum in PBS buffer for 2 h at 25°C. Then, tissue sections were incubated with anti-mouse Bcl-2 and anti-mouse-Ki67 antibodies (Santa Cruz Biotechnology, Santa Cruz, CA, USA) with a ratio of 1:100 in PBS buffer containing 0.2% horse serum for 24 h at 25 C. The slides were washed three times with PBST buffer, followed by incubation with the secondary antibody (1:500) in PBS (anti-mouse immunoglobulin G (IgG) biotinylated; Vector Labs) for 1 h at 25 C. Antibody reaction was developed using the Vectastain Elite ABC horseradish peroxidase

(HRP) kit (Vector Labs, Inc., Burlingame, CA, USA). In case of frozen tissue, tissue sections of 7 µm were obtained with a cryostat Hyrax C25, Carl Zeiss, Göttingen, Germany, at −20 °C. Images were acquired with a contrast phase inverted-fluorescence microscope (Leica DM IL080 equipped with a digital CDD, Leica Biosystems Inc., Buffalo Grove, IL, USA). In addition, tumor cells treated with rhodamine 123 (Sigma-Aldrich Co. St. Louis, MO, USA) were observed directly using a confocal microscope (Olympus FV1000, Center Valley, PA, USA); the emission signal of fluorescence was monitored at 533 to 563 nm for rhodamine 123 probe.

Antibody Array Assay

Melanoma tissue from three to six mice (~3 g) were cut into small pieces on ice and homogenized by sonication in 300 µL of phosphorylation buffer (HEPES 50 mM pH 7.6 containing sodium-pyrophosphate 50 mM, sodium orthovanadate 1 mM, sodium molybdate 1 mM, EDTA 20 mM, EGTA 20 mM, benzamidine 1 mM, NaF 20 mM, PMSF 0.2 mM, β-glycerophosphate 20 mM, mannitol 200 mM, and protease inhibitor cocktails 5 µL/mL). Then, we used three cycles of sonication at low intensity (20 kHz, 5 W) for 30 s each at 4 °C with 5 min of resting between sonication cycles (Bioblock-LS2d Ultrasound Technology, Ringwood, NJ, USA). Cell-free protein extracts were obtained by centrifugation (12,500 g, 4 °C for 15 min). Protein concentration was determined using the Bradford reagent (BioRad, Hercules, CA, USA) and 50 µg of total protein were added to each well with glass slides of antibody array kit (PathScan Cancer Phenotype Antibody Array Kit #14,821 and PathScan IntraCellular Signaling Array Kit #7,323; Cell Signaling Technology, Danvers, MA, USA). The array glass slides were incubated overnight at 4 °C on an orbital shaker. Following immunoreactions and washes, slides were incubated with a biotinylated-antibody cocktail and HRP-linked streptavidin for 1 h at room temperature. To detect immunoreactivity, LumiGlo® Peroxide reagent was added and the image immediately captured using a digital imaging chemiluminescent system, ChemiDoc™ MP System (BioRad, Hercules, CA, USA). Determination of spot intensity from the microarray was carried out by densitometry analysis using ImageJ software (NIH Image).

Western Blot Analysis

Proteins from tumor extracts were separated under denaturing conditions using polyacrylamide gel electrophoresis at 10–12% [sodium dodecyl sulfate (SDS)]. Thirty micrograms of protein extracts were typically loaded per lane. Protein mixtures were mixed with 10 µL of denaturing buffer [Tris-HCl 0.06 M, pH 6.8, 5% glycerol, 4% SDS, 4% β mercaptoethanol, and 0.0025% bromophenol blue] and incubated for 5 min at 95 °C. Gels were stained with Coomassie blue and proteins from replicate gels transferred to polyvinylidene difluoride (PVDF; Millipore, Billerica, MA, USA) membranes for immunodetection assays. Briefly, PVDF membranes were incubated with TBS-T [Tris-HCL 10 mM; NaCl 0.9%; tween-20 0.1%, dry milk 5%, pH 7.8]. Polyvinylidene difluoride membranes were cut according to range of molecular weight markers and incubated with the indicated antibodies at the concentration suggested by the manufacturer: anti-CD44, anti-Cx43/4, anti-C-Myc, anti-Ras, anti-SNAIL, anti-MMP-1, anti-E-Cad, anti-vimentin, anti-cytokeratin 1 (CK-1), anti-α-tubulin, anti-Akt (C-20), anti-Akt-phosphorylated 1/2/3 (S–473), anti-mTOR, anti-phosphorylated-mTOR-(S2448), anti-β-actin, and anti-α-tubulin (all from Santa Cruz Biotechnology, Santa Cruz, CA, USA) antibodies. Following 12 h of incubation (4 °C) for the primary antibody, membranes were washed and incubated with goat anti-rabbit IgG HRP-conjugate (1:60,000, BioRad, Hercules, CA, USA), in blocking medium for 4 h at 4 °C; the membranes were washed twice with TBS-T buffer and developed using hydrogen peroxide and Supersignal West Pico Luminol (Pierce) Thermo Fisher Scientific, Waltham, MA, USA). Then images were captured using a ChemiDoc™ MP System (BioRad, Hercules, CA, USA). Assays were conducted at least three times, and representative images are shown. Band intensities in gel images or films were quantified using the ImageJ software (NIH Image).

Docking Analysis

Data of the protein structure of mice, rat, and human were obtained from the protein data bank [accession no. AKT (3CQU), HIPK2 (6P5S), AMPK (5UFU), MET (3QTI), JNK (2G01), CD44 (2JCR), and HIF-1α (5JWP)]. The three-dimensional models of CDPs used in the study were obtained from https://pubchem.ncbi.nlm.nih.gov/compound/ and as previously described [18]. Docking analysis was carried out using the software Autodock 4.2.6.1 (available at http://autodock.scripps.edu/). After docking, 100 conformations for each compound were obtained and then clustered for analysis using ADT 1.5.2 software. The conformations selected were within the most represented cluster and corresponded to those showing the lowest values of binding energy and Ki. Model analyses and figure drawing were carried out with PYMOL 2.1.0 (The PyMOL Molecular Graphics System, version 2.1.0; Schrödinger, LLC, New York, NY, USA; https://sourceforge.net/p/pymol).

Statistical Analysis

For correlation analysis, data obtained of antibody arrays and Western blots were analyzed by correlation analysis utilized as response variables (treatments) vs. data of signal intensity for each antibody (cases) using the STATISTICA software (Data Analysis Software System 8.0, Stat Soft Inc., Tulsa, OK, USA). Other data were statistically analyzed using GraphPad Prism 6.0 software (GraphPad Software, San Diego, CA, USA).

RESULTS

CDPs From *P. aeruginosa* PAO1 Induce Apoptosis of Murine B16-F0 Melanoma Cells

First, we examined the effect of these compounds on the B16-F0 melanoma line in culture, finding that CDPs decreased viability

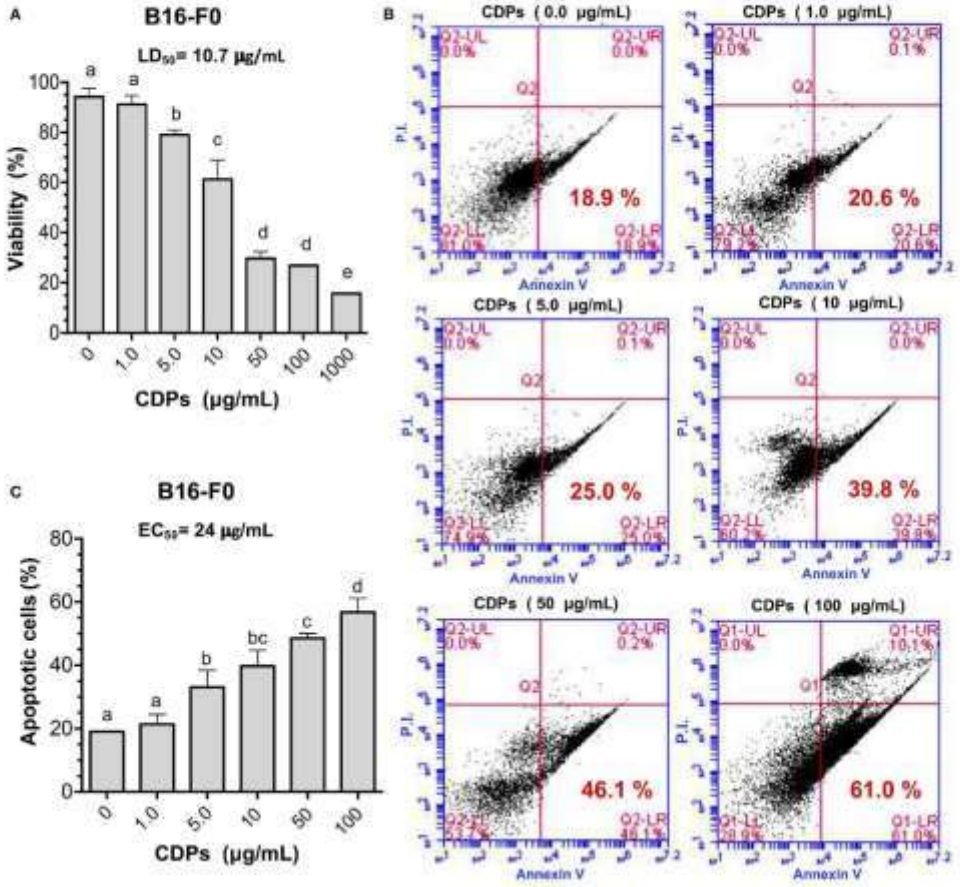

FIGURE 1 | Effects of CDPs on viability and apoptosis of B16 murine melanoma cells. B16-F0 melanoma cells were incubated with CDPs to determine cell viability and apoptosis as described in Materials and Methods. **(A)** Determination of viability of B16-F0 melanoma cells treated with different concentrations of CDPs from *P. aeruginosa* PAO1 by MTT method; LD_{50} of CDPs is shown. **(B,C)** Measurement of apoptosis using annexin V binding and necrosis by propidium iodide (PI) were conducted by flow cytometry using different concentrations of CDPs. **(B)** Representative flow cytometry dot plots show the annexin V and PI cells percentage of CDPs-treated B16-F0 cells. **(C)** Determination of apoptosis induction by CDPs and EC_{50} is shown. Bars represent means ± SE of three independent assays, $n = 3$. One-way analysis of variance (ANOVA) was carried out, with Tukey *post-hoc* test; statistical significance ($P < 0.05$) of differences between treatments is indicated with lowercase letters.

of B16-F0 cells in a dose-dependent manner. Cell cultures showed 75% dead cells with CDPs at 50 µg/mL after 12 h, rendering an LD_{50} of 10.7 µg/mL (**Figure 1A**); remarkably, the LD_{50} data indicated that CDPs were ~5-fold more bioactive in inducing cell death in the B16-F0 murine melanoma line than in the human HeLa line described previously (6). To further support the CDP effect on the B16-F0 melanoma line, we used annexin V binding to determine apoptotic and PI to determine necrotic cells by FACS analysis (**Figures 1B,C**). Whereas, <20% of cells were stained with annexin V in cells incubated with vehicle, ~60% of cells treated with CDPs (50 µg/mL at 4 h) became apoptotic (**Figure 1C**). The EC_{50} of apoptosis induction was ~24 µg/mL at 4 h of treatment (**Figure 1B**). These data indicated that CDPs from *P. aeruginosa* PAO1 were cytotoxic, inducing apoptosis in the B16-F0 melanoma cell line.

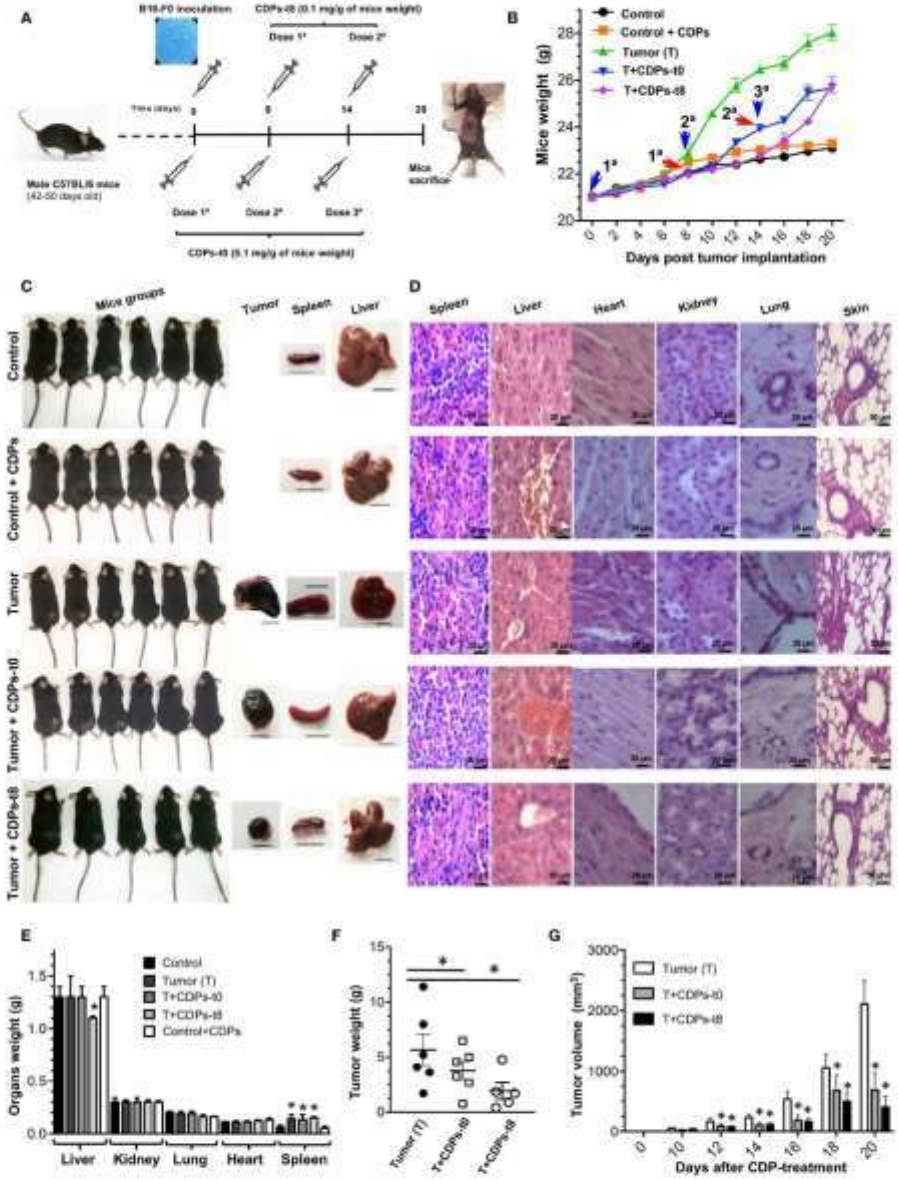

FIGURE 2 | Antitumor effect of CDPs on xenografted tumor melanoma B16-F0 cells in mice. **(A)** Experimental design showing tumor implantation and CDP treatments. Mice of 6 weeks of age were weighed, melanoma was implanted subcutaneously, and treatments were started. Mice (*n* = 6 per group) were treated as

(Continued)

FIGURE 2 | indicated. After 20 days, mice were euthanized, organs dissected, and diverse parameters were determined as described in Materials and Methods. **(B)** Determination of mouse weight over 20 days' period. Arrowheads indicate the CDP administration time and dose number. **(C)** Photograph of mouse groups at the 20th day of experimental procedure before euthanizing. Representative photographs of tumor, spleen, and liver from each mouse group are shown. Scale bar was assigned adjusting the scale with the original ruler corresponding to 10 mm. **(D)** Representative hematoxylin-eosin staining of tissue from spleen, liver, heart, kidney, lung, and skin of the mouse groups. Scale bar in μm is shown. Determination of weight of mouse organs after 20 days **(E)**, tumor weight **(F)**, and tumor volume **(G)**. Bars represent the means ± SE of one experiment, $n = 6$. One-way ANOVA with Bonferroni *post-hoc* test was used to compare treatments with the untreated group (control) or with tumor group (T); significant differences ($P < 0.05$) are indicated with asterisk (*).

Effect of CDPs on Xenografted Melanoma Murine Tumors

To evaluate the antitumorigenic potential of a mixture of bacterial CDPs, we used a subcutaneous xenografted melanoma mouse model (20). Tumors were induced by subcutaneous injection of B16-F0 melanoma cells on male C57BL/6 mice of 10 weeks of age. To determine the effect of CDPs on melanoma development, different mouse groups were tested as described in *Materials and Methods*. Typically, after 8 days, the tumors reached a volume average of 20–50 mm^3. A group of mice was treated with CDP injection from the beginning of cells implantation (T + CDPs-t0) (**Figure 2A**). Another mouse group was treated after the eighth day of melanoma cells implantation [T + CDPs-t8]. To monitor tumor growth, mice were weighed every 2 days for 20 days (**Figure 2B**). The body weight of mice belonging to the tumor (T) group showed a significant increment in weight. Body weight of mice in both the T + CDPs-t0 and T + CDPs-t8 groups were lower than the T group without CDP treatment, suggesting that the weight increment found in the T group could be related to tumor development. Healthy mice treated with CDPs did not show changes in body weight compared to the control group. All mice survived for 20 days, were humanely euthanized, and tumors and organs removed and weighed (**Figure 2C**). There were no significant differences in weights of kidney, lung, and heart organs; however, a 2-fold increase in the weight and volume of the spleen of the T mouse group was observed (**Figures 2C–E**). A decreased liver weight was also observed in the T + CDPs-t8 group (**Figure 2E**).

Data show that CDP treatment caused a significant decrease in mass and volume of tumors (**Figures 2F,G**). We found that the average weight of the tumors in mice without treatment (T) was ~5.5 g, with a tumor volume of ~2,100 mm^3, whereas the tumors from the CDP-treated mouse groups injected immediately with CDPs (T + CDPs-t0), and after the eighth day of melanoma cells implantation [T + CDPs-t8], showed on average ~4 and ~2 g, with volumes of ~70 and ~30 mm^3, respectively, (**Figures 2F,G**). Thus, CDPs decreased size and weight of xenografted tumors formed by B16-F0 melanoma cells in C57BL/6 mice.

Histopathological studies showed no apparent modification of cell size, morphology, and cellular structures from spleen, liver, heart, kidney, lung, and skin in the mice groups (**Figure 2D**). In addition, tissues from the healthy CDP-treated control mouse group were normal; thus, CDP treatments appear to be safe for mice.

Hemoglobin and hematocrit were significantly diminished in the T group (**Figure 3A**). The control mouse group treated with CDPs showed no differences in any of the hematological parameters. Erythrocytes from the T mice group showed characteristic evidence of echinocytes (frequently found in patients with liver disease; **Figure 3B**). We found that the T mouse group had a reduction in the proportion of lymphocytes accompanied by an increment of neutrophils; these effects were less pronounced in mouse groups treated with CDPs (**Figure 3C**).

We also determined the activity of cell damage marker enzymes LDH, AST, and ALT. The T mouse group showed a significant increment in both LDH and AST enzymatic activities (**Figure 3D**), which were diminished in the tumor-induced mice treated with CDPs (T + CDPs-t0 and T + CDPs-t8). The treatment with CDPs in the healthy CDP-treated control mouse group did not alter LDH and AST levels as shown in the control mouse group. Alanine aminotransferase activity did not show significant differences between the mouse groups, except for the T mouse group. Nevertheless, the ALT/LDH ratio showed significant difference with tumor development and CDP treatment. An increased ALT/LDH ratio (~10-fold) was observed in the healthy mouse group administered with CDPs (control + CDPs), whereas a lower value of this ratio was observed in the tumor group without CDP treatment (**Figure 3D**).

Histopathological examination showed strong nuclear fragmentation in cells of tumor tissue from mice treated with CDPs (T + CDPs-t0 and T + CDPs-t8); this effect was not observed in the tissues from the untreated (T) mice group (**Figure 3E**). Bcl-2 and Ki67 tumor markers were significantly diminished in the mouse groups that were CDP treated (**Figure 3E**). Additionally, determination of reactive oxygen species (ROS) on cells dissected from tumor tissues using the rhodamine 123 probe was carried out. Confocal microscopic images showed an exacerbated generation of ROS in the cells from tumors of mice treated with CDPs, as well as a loss of cell morphology (**Figure 3E**), indicating an apoptotic and necrotic status on tumor tissues, induced by CDP treatment.

Cyclodextrins Favor the Antitumor Effect of the CDPs in Xenografted Mouse Melanoma

Because DMSO was the vehicle used to solubilize CDPs, we wondered if the beneficial effect observed on mice with melanoma implantation could be improved by another drug vehicle; we replaced DMSO with a β-cyclodextrin suspension. The CDP–cyclodextrin suspension was administered to the mouse groups with xenografted tumors and compared with treatments where CDPs were dissolved in DMSO. Tumors of the mouse group without treatment (T) showed an average weight of ~9 g with a volume of ~2,200 mm^3. The average weight and volume of tumors from mice treated with CDP-dissolved in DMSO were ~2.5 g and ~900 mm^3, respectively,

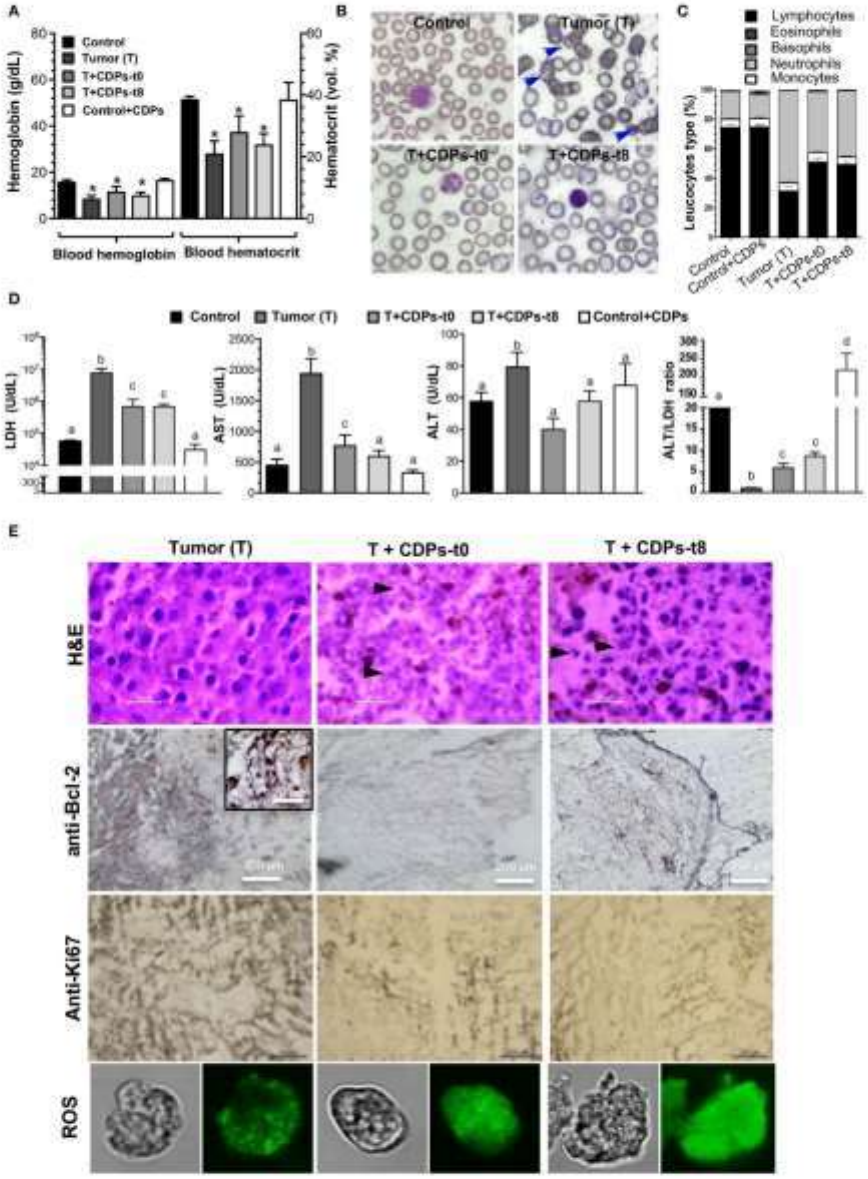

FIGURE 3 | Determination of tumor markers in xenografted tumor melanoma mice treated with CDPs. **(A)** Determination of hemoglobin and hematocrit in the blood of the different mouse groups at 20th day of experimental procedure before euthanizing. **(B)** Morphology of blood cells (echinocytes are indicated with arrowheads).

(Continued)

FIGURE 3 | (C) Leukocyte differential. **(D)** Determination of serum aspartate aminotransferase (AST), and alanine aminotransferase (ALT) activities, and the ALT/AST ratio. Bars represent the means ± SE. $n = 5$. One-way ANOVA test. For *post hoc* test, the Tukey test was used to compare treatments with the untreated group (control). Significant differences ($P < 0.05$) are indicated with asterisks (*) or with lowercase letters. **(E)** Histological analysis of tissue from melanoma tumors by hematoxylin–eosin (H&E) staining. anti-Ki-67 and KI-67-immunoreactivity, and confocal images of tumor cells stained with rhodamine 123 (JC-1) probe. Scale bar is 50 μm. Arrowheads indicate necrotic foci/cavitations. Control, healthy mice; control + CDPs, healthy mice treated with CDPs. Tumor (T), mice with tumor implantation without treatment; T + CDPs-D, mice with tumor implantation and immediately treated after injection; T + CDPs-8D, mice with tumor implantation with CDP treatment at the eighth day of melanoma implantation.

(**Figures 4A,C,D**). The mouse group treated with the CDP-cyclodextrin suspension administered at the eighth day after melanoma cell injection (T + CDPs-cdx8) showed an average tumor weight of ≤0.3 g and a volume of ≤50 mm^3; interestingly, in some mice (20%), the tumor was undetectable (**Figure 4B**). The mouse group treated with CDP-cyclodextrins suspension injected immediately (T + CDPs cdx0) showed a similar tumor weight with DMSO–CDP treatments, but it showed a significant decrease in tumor volume (**Figures 4C,D**). Additionally, the cyclodextrins–CDP treatments significantly decreased spleen size and LDH activity compared to those of DMSO–CDPs treated and untreated mouse groups (**Figures 4A,E**). The lowest LDH activity was observed in the T mouse group treated with CDP-cyclodextrins at the eighth day after tumor implantation (T + CDPs-cdx8). These results indicate that CDPs were more efficient when they were injected with cyclodextrins suspension compared to DMSO.

Modulation of Signaling Pathways by CDPs Treatment in Xenografted Mouse Melanoma

To identify elements dysregulated in cancer and possible cell-signaling pathways targeted by the antitumorigenic effect of the CDPs in the xenografted melanoma mouse model, protein extracts obtained from tumor tissue were used for an immunodetection approach. Results of the cancer and signaling antibody arrays showed that tumors presented a significant increase in the expression of proliferative cell nuclear antigen (PCNA), p27Kip1, N-cadherin, HSP 60, Stat-3, Akt-S473, AMPKa, mTOR-S2448, HSP27, Bad, PRAS40, SAPK/JNK, and caspase-3 (**Figures 5A–C**), which were significantly recovered/diminished in their expression/phosphorylation level by CDP treatment. Additionally, in the T + CDPs mouse group, CDPs caused an increment in the expression of elements such as survivin, Met, and EGF (**Figures 5A–C**).

Because we observed an increment in expression of signaling pathways such as PI3k/Akt/mTOR expression in tumors and its recovery level of expression after CDP treatment, we looked at the activation of Akt-S473, mTOR-S2448, S6k-T389, and other members of signaling pathways such as Xiap, PDK1, NFκB p65, and TNF-α/Fas1. (**Figure 6A**). Phosphorylation of Akt-S473 and S6k-T389 was strongly activated in the tumor mouse group (T), whereas a decrease was observed with CDP treatment, but no difference in activation was observed for mTOR-S2448 (**Figure 6A**). In contrast, Xiap, PDK1, NFκB p65, and TNF-α/Fas1, did not show significant differences in expression level in the CDP treated mouse group with respect to the T group (**Figure 6A**).

We also looked at markers of malignancy (i.e., cancer stem cells, pluripotency, and metastasis). **Figure 6B** shows that the expression of stem cell marker CD44 was decreased to ≤30% in protein extracts of tumors from T + CDPs-D mouse group and was totally depressed in the T + CDPs-8D group; in contrast, the CD24/4 showed low expression levels in the T mice group, with expression levels increased in the T + CDPs-D group. With respect to the oncogenes, c-Myc was decreased, but Ras was increased in the T + CDPs mouse group. Furthermore, the expression of EMT markers such as SNAIL increased in tumors and CDP treated tumors. However, MMP-1, E-cadherin, vimentin, and CK-1 showed a significantly decreased expression in tumors treated with CDPs (**Figure 6B**). These results clearly indicate that, in addition to the PI3k/Akt/mTOR pathway, other signaling pathways are involved in melanoma development as in B16-F0 cells line as in tumor of xenografted melanoma cells, and these also may be targeted by the bacterial CDPs.

DISCUSSION

The quest for novel molecules to target cancer has led investigations to look at microbial metabolites. Cyclic peptides constitute a diverse family of molecules mainly of microbial origin that have antimicrobial, immunomodulator, antioxidant, or anticancerigenic activities (7, 21). Recently, CDPs have attracted attention because of their antiproliferative effects on cancer cell lines (5–6, 22). We recently reported that a mixture of CDPs composed of cyclo(L-Pro-L-Tyr), cyclo(L-Pro-L-Val), and cyclo(1-Pro-L-Phe) isolated from *P. aeruginosa* PAO1 culture inhibited the proliferation of HeLa and CaCo-2 cells (5). In addition, we found that bacterial CDPs are stronger antiproliferative agents compared to chemically synthetized analogs (6). Thus, it appears that CDPs from biological sources are more potent than synthetic CDPs due probably to structural differences in stereospecificity.

Cyclodipeptides affected the viability of B16-F0 cells by inducing apoptosis in cultured cells (**Figure 1**). Although CDP's biological properties have been studied *in vitro*, we now show that CDPs can inhibit melanoma tumor progression in mice. Interestingly, we showed that mice implanted with B16-F0 cells and simultaneously treated with CDPs did not develop tumors, unlike untreated mice. Importantly, in tumors already developed, tumor size was decreased in mice treated with CDPs (**Figures 2–4**). Mice that developed tumors showed diminished blood cell counts, which correlated with an increment in spleen size (**Figures 2, 3**), symptoms that are indicative of an anemic

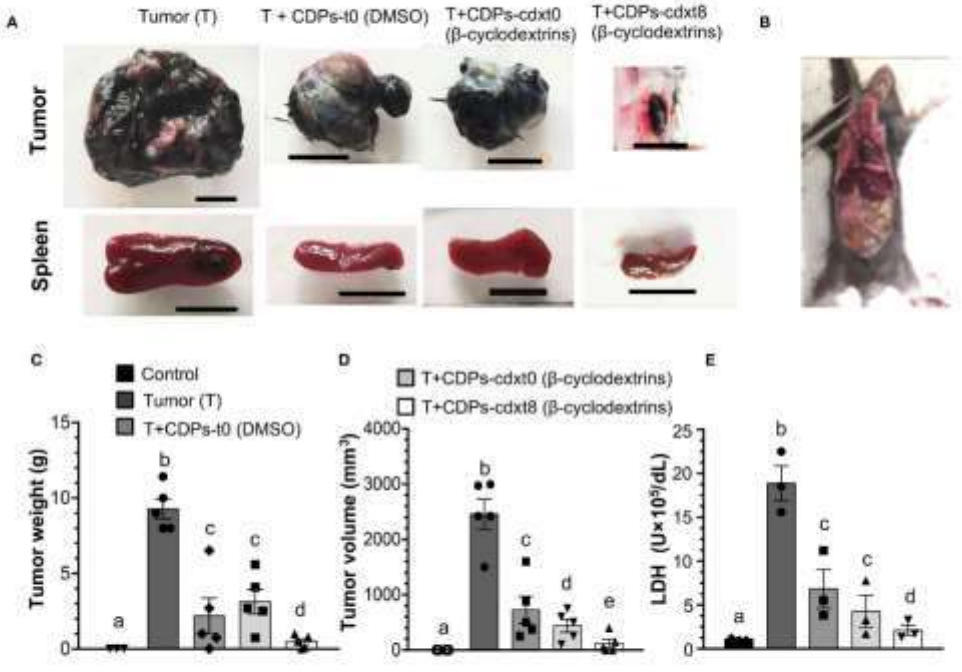

FIGURE 4 | Effects of CDPs suspended in cyclodextrins on xenografted tumor melanoma B16-F0 cells in mice. Mice from the different groups were treated with/without CDPs using as drug vehicle a suspension of cyclodextrins in saline solution. After 20 days of treatment, mice were euthanized, tumors weighed, and LDH activity determined as described in Materials and Methods. **(A)** Representative photographs of tumors and spleens from mouse groups treated with CDPs–cyclodextrins (CDPs-cdx). Scale bar was assigned corresponding to 10 mm. **(B)** Xenografted melanoma mouse that after CDPs–cyclodextrins treatment did not show any tumors. **(C,D)** Tumor weight and volume determination. **(E)** LDH activity in mouse serum. DMSO indicates that CDPs were dissolved in saline solution with DMSO (0.1%), (β-cyclodextrins) indicates that CDPs were dissolved in saline solution with β-cyclodextrins (50 mg/mL). Bars represent means ± SE, mouse groups with $n = 3$–6. One-way ANOVA with Bonferroni post-hoc test was used to compare treatments to the untreated group (control). Significant differences ($P < 0.05$) are indicated with lowercase letters. Control, healthy mice; Tumor (T), mice with tumor implantation without treatment; T + CDPs-t0 (DMSO), mice with tumor implantation with CDPs (DMSO-dissolved) and immediately treated; T + CDPs-cdx-t0 and T + CDPs-cdx-t8, mice with tumor implantation with CDP treatment (β-cyclodextrins-dissolved) immediately after melanoma cell injection and at the eighth day of melanoma implantation, respectively.

status seen in patients with cancer (23). Cyclodipeptide treatment of the tumor-induced mice resulted in a recovery of hematologic parameters (**Figures 3A–C**). Furthermore, LDH, ALT, and AST increased in mice with tumors as described in liver and breast cancers (24, 25), but the levels of these enzymes significantly decreased when mice were treated with CDPs (**Figure 3D**). Interestingly, the control mouse group treated with CDPs did not show altered values of these blood and enzymes levels, suggesting that, at least, the injected amount of CDPs was not toxic to mice. Levels of LDH, ALT, and AST are used as markers of disease evolution of anticancer treatments (25). We observed a recovery of the levels of LDH and AST in mice treated with CDPs similar to those found in healthy mice (**Figure 3D**). This was not observed in the untreated group. These results indicate an improvement in health of mice bearing tumors treated with CDPs. In addition, histological and immunohistochemical data showed strong nuclear fragmentation and decreased Bcl-2 and Ki67 cancer marker levels in tumor tissues from mice treated with CDPs (**Figure 3E**). Images of tissue showed an exacerbated generation of ROS in tumors from CDP-treated mice, confirming the induction of apoptosis, dependent on mitochondrial dysfunction and cytochrome *c* release.

An important issue to consider in therapeutic treatments is the drug bioavailability; in this sense, we improved the bioavailability of the CDPs using a suspension in β-cyclodextrins. Results obtained in our xenografted melanoma mouse model showed that the CDPs dissolved in cyclodextrins were more efficient in inhibiting tumorigenesis than those dissolved in DMSO (**Figure 4**), suggesting that the antitumorigenic effect of the CDPs could be improved by utilization of an appropriate drug vehicle.

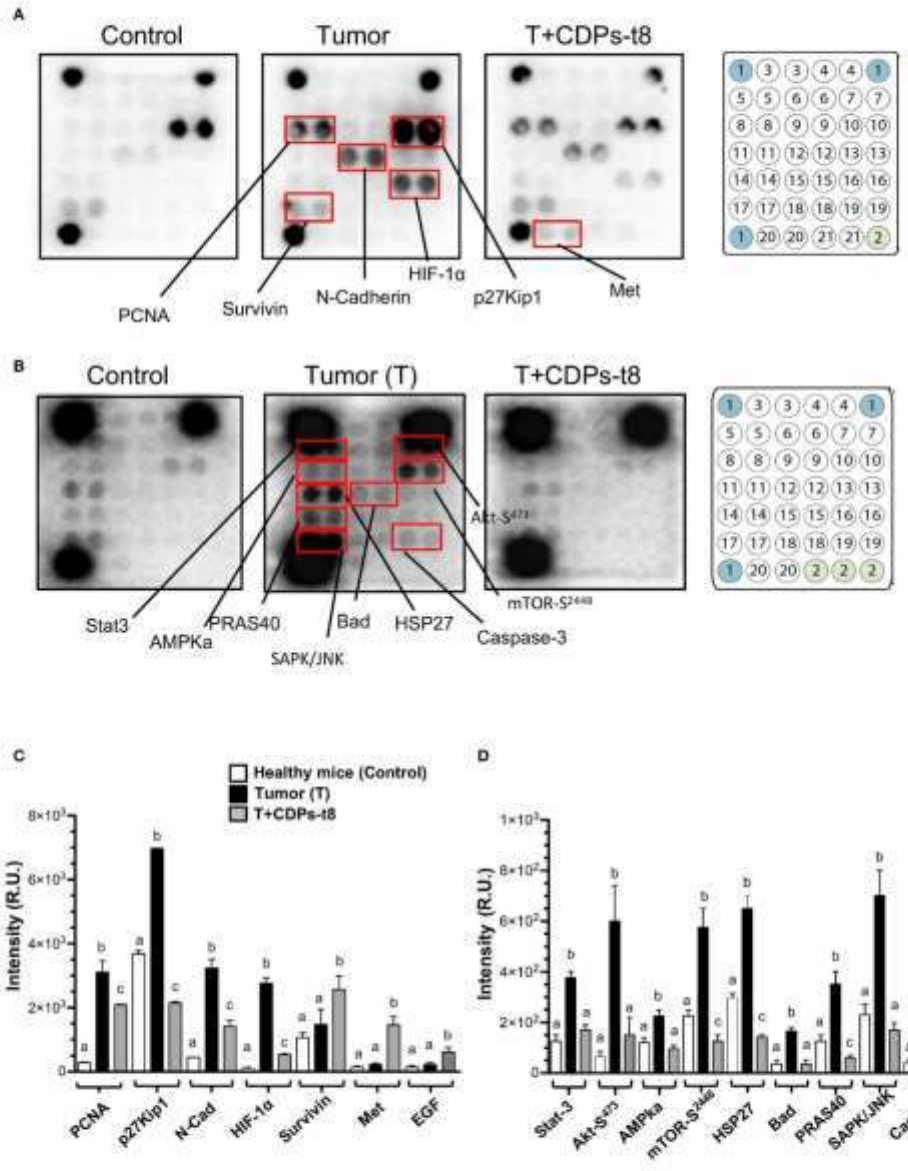

FIGURE 5 | Proteomic analysis of CDPs effect on xenografted tumor melanoma B16-F0 cells in mice. Tumors or healthy skin were homogenized to obtain the tissue lysates used for Western blot assays as described in Materials and Methods. **(A)** Representative images correspond to antibody microarrays (PathScan Cancer

(Continued)

FIGURE 5 | Phosphoprotein Antibody Array. The arrays contained the following antibodies: (1) positive control, (2) negative control, (3) CD31, (4) EpCAM, (5) vimentin, (6) CD44, (7) CD45, (8) PCNA, (9) Ki-67, (10) p27(Kip1), (11) E-cadherin, (12) N-cadherin, (13) VE-cadherin, (14) MUC1, (15) Rb Ser807/811, (16) HIF-1α, (17) survivin, (18) P53, (19) HER2/ErbB2, (20) Met, (21) EGF. (B) Representative images corresponding to antibody microarrays (RayBiotech Human Angiogenesis Array). The array contained the following antibodies: (1) positive control, (2) negative control, (3) ERK1/2 Thr202/Tyr204, (4) Stat1 Tyr701, (5) Stat3 Tyr705, (6) Akt Thr308, (7) Akt-Ser473, (8) AMPKα-Thr172, (9) S6 Ribosomal Protein-Ser235/236, (10) mTOR-Ser2448, (11) HSP27-Ser78, (12) Bad-Ser112, (13) p70S6 Kinase-Thr389, (14) PRAS40-Thr246, (15) p53-Ser15, (16) c-Jun-Ser73, (17) SAPK/JNK-Thr183/Tyr185, (18) PARP-Asp214, (19) caspase-3-Asp175, (20) GSK-3α-Ser21. Proteins that showed differences in expression-phosphorylation levels compared to the control protein extract are indicated. (**C,D**) Determination of signal intensity of spots from microarrays (**A,B**), respectively, was conducted by densitometric analysis software (NIH). Data represent the means ± SE of two independent assays with spot sequencing for each antibody using protein extracts obtained from all assessed mice tumors of each mouse group. Open symbols means ± SE of four densitometry determinations. One-way ANOVA and paired t-test with Bonferroni post hoc test, assessed significance ($P < 0.05$) of differences between treatments is indicated with lowercase letters. Control (healthy mice), Tumor (T) mice with tumor implantation without treatment, T + CDPs-tB, mice with tumor implantation treated with CDPs at the eighth day of implantation (pre-incipient).

To determine the molecular mechanism involved in the antitumorigenic effect of CDPs in the xenografted melanoma murine model, we utilized antibody arrays to screen in tumors, differential expression of proteomic elements related to cancer disease, and intracellular signaling pathways (**Figure 5**). Previously, we found that the CDP mixture from *P. aeruginosa* PAO1 was able to repress phosphorylation of both Akt-S473 and S6k-T389 protein kinases in HeLa cells at short treatment times (6). The PI3K/Akt/mTOR pathway is up-regulated in more than 70% of cancer types (26, 27). In our murine melanoma model, we also found up-regulation of PI3K/Akt/mTOR pathway (**Figure 6**). In this study, also hyperactivation of phosphorylation in melanoma tumors from mice was found, where the level of phosphorylation was decreased in tumors from CDP-treated mice. Thus, it further confirms that CDPs targeted the mTOR pathway, which is critical for cell growth and proliferation. Apoptosis dependent on the Akt-Ser473 inhibition and downstream target proteins by CDPs in our melanoma model indicates the participation of the mTORC1 and mTORC2 complexes in blocking the PI3K/Akt/mTOR signaling pathway, in agree with recent findings described in HeLa cells (28). In agreement with these results, dual inhibition of the mTORC1 and mTORC2 signaling pathways has been proposed as effective therapeutic targets in neoplasias (29, 30). It suggests that CDPs can be considered as potential therapeutic compounds in melanoma by causing dual inhibition of mTORC1 and mTORC2 complexes.

Additionally, we observed an up-regulation of HIF-1α protein in tumors of xenografted melanoma mice (**Figure 5**). The HIF-1 suppressor is a master regulator of elements involved in glycolysis and is dysregulated in tumorigenesis and invasiveness. It is well-known that the regulation of HIF-1 is closely related to the PI3K/Akt/mTOR pathway. Functionally, it has been shown that Akt and HIF-1 interact synergistically during the development of melanoma (31). Our data show that the PI3K/Akt/mTOR and HIF-1 cross-talk pathways are implicated in mouse melanoma development and that CDPs targeted these pathways. Because HIF-1 regulates processes such as survival, apoptosis, glucose metabolism, angiogenesis, and invasiveness by inducing EMT regulators (32–34), it is attractive to postulate that the antitumor effects of CDPs may be mediated by affecting HIF-1 and reflected in the blocking of cell invasion. In addition, the PCNA, which acts during the S and G2 phases of the cell cycle, is considered a marker of cell proliferation, which actively participates in a number of signaling pathways responsible for cell survival (35).

We found that the transcription factor SNAIL is up-regulated in melanoma tumors, whereas expression of CD44 and E-Cad is down-regulated (**Figure 6B**). SNAIL is a prominent inducer of EMT and strongly represses E-cadherin expression. Cyclodipeptides increased SNAIL levels and decreased levels of the hyaluronan receptor CD44, a cell surface adhesion receptor that is highly expressed in many cancers and regulates metastasis by alternative splicing and recruitment of CD44 to the cell surface (36).

Furthermore, important tumorigenic markers were repressed in the CDP-treated mice, such as C-Myc, MMP-9, E-cadherin, vimentin, and CK-1 (**Figure 6B**). These data support the hypothesis that CDPs may promote the activation/repression of the main components of the EMT pathway to induce apoptosis in tumors and probably inhibit tumorigenesis and invasiveness. On the other hand, Xiap, PDK1, NFκB p65, and TNF-α/FasL did not show significant differences in their expression level in the CDP-treated mouse group with respect to the T group (**Figure 6A**), suggesting that these elements play important roles in signaling pathways in which their participation is not affected by the CDPs; however, this does not rule out their involvement.

An approach analysis of the multiple factors and pathways evaluated in our melanoma tumorigenesis model with treatment with bacterial CDPs was conducted using a statistical correspondence analysis (**Figure 7A**). Data show that the cancer factors clearly correlated in up-expressed/activated and down expressed/inactivated as widely described (**Figure 7A**). An important number of proteins are associated with the response variable (control), which were not modified in their expression level in tumors CDPs-treated and untreated groups. A second group of proteins that showed significant changes in their expression levels in the proteomic approach was associated with the response variable Tumor mouse group which developed tumors without treatment. This group of proteins corresponds to oncogenes and tumor suppressors widely associated with tumorigenesis. Finally, a third group of proteins highly implicated in the control of tumorigenesis, invasiveness, and signaling pathways such as PI3K/Akt/mTOR, Ras/ERK, EMT, CSC, and so on, was associated with the CDPs-treated mouse group (**Figure 7A**). From this correlation analysis, some representative proteins of each group were selected and

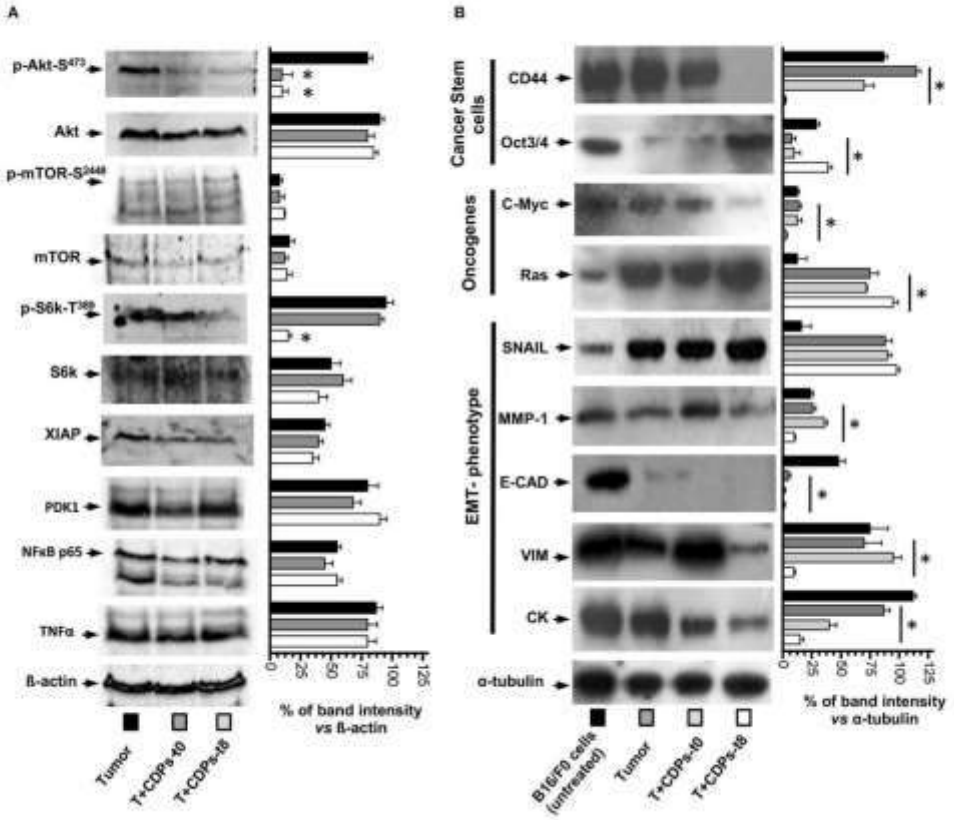

FIGURE 6 | Effects of CDPs on the levels of proteins involved in signaling pathways promoting mouse melanoma growth. Tumor tissue was disrupted, and cell-free protein extracts were used for Western blot assays as described in Materials and Methods. Images correspond to a representative Western blot assay ($n = 3$) using protein extracts of at least three tumors homogenized from the mentioned mouse groups, using the indicated antibodies. **(A)** Antibodies recognized p-Akt-S473, Akt, p-mTOR-S2448, mTOR, pS6K-T389, S6K, XIAP, PDK1, NFκB p65, TNF-α, and β-actin. **(B)** Antibodies used were against CD44, Oct3/4, C-Myc, Ras, SNAIL, MMP-1, E-CAD, VIM, CK-1, and α-tubulin. On the right, graphs correspond to determination of the band intensity from the Western blot assay (left), analyzed by densitometry using the ImageJ software. Data represent the means ± SE of densitometry determinations, $n = 3$ for each antibody, using protein extracts obtained from tumors of each group vs. load control (β-actin or α-tubulin). One-way ANOVA with Bonferroni post-hoc test was used to compare treatments with respect to Tumor group. Significant differences ($P < 0.05$) vs. tumor group are indicated with asterisk (*). B16-F0 mouse cells line untreated; (Tumor) mice with tumor implantation without treatment; (T + CDPs-t0) mice with tumor implantation and CDP treatment immediately after injection; (T + CDPs-t8) mice with tumor implantation and CDP treatment at the eighth day of melanoma implantation.

analyzed by molecular docking using the crystallographic structures with ligands, such as substrate or inhibitors, and evaluated for the feasibility of interaction with the CDPs as modulator molecules (**Figure 7B**). Docking approach showed that the CDPs may interact with protein kinase members of multiple signaling pathways. The cyclo(L-Pro-L-Tyr) and cyclo(L-Pro-L-Phe) showed better predicted interaction values (*Ki* of 2–65 μM and binding energy of −7.8 to −7 kCal/mol), than cyclo(L-Pro-L-Val) (**Table S1**). Docking revealed that the CDPs have the potential to interact in different sites of protein kinases such as substrate-binding site, inhibitor-binding site or co−substrate-binding site. Analysis also predicted a differential affinity for the CDPs, being cyclo(L-Pro-L-Tyr) in general the most potent as inhibitor. Structural images of proteins kinases AKT, HIPK2, AMPK, MET, JNK, HIF-1α, and CD44 with the interaction with the cyclo(L-Pro-Tyr) are shown in **Figure 7B**.

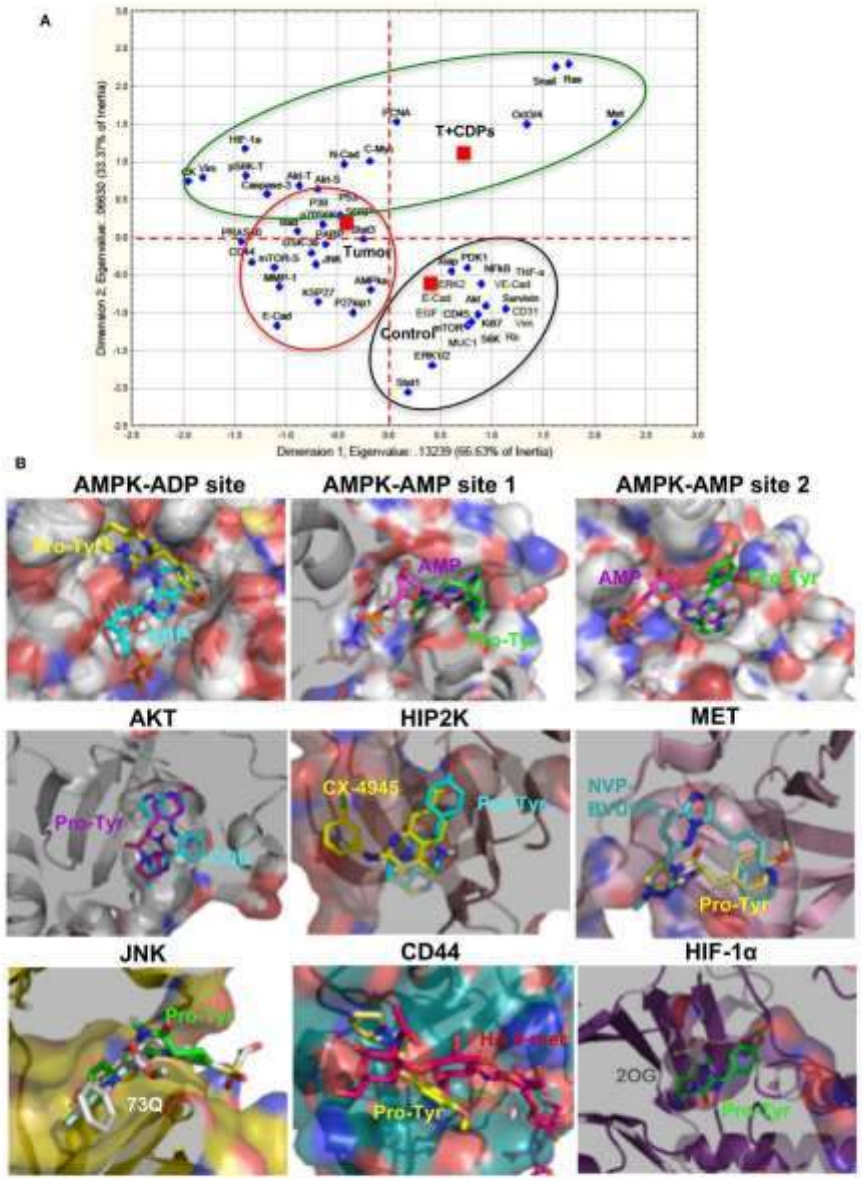

FIGURE 7 | Correlation analysis of proteomic approach on xenografted tumor melanoma B16-F0 cells in mice treated with CDPs and docking analysis. **(A)** Correlation analysis of densitometry data from microarrays and Western blots (**Figures 5**, **6**) were analyzed by multivariate exploratory techniques, using the

(Continued)

FIGURE 7 | Correspondence analysis (CA) of the STATISTICA Software System 8.0 (Stat Soft Inc., Tulsa, OK, USA). Comparison groups are as follows: healthy mice (control), mice with tumor implantation without treatment (Tumor), mice with tumor implantation and CDP treatment (T + CDPs). **(B)** Docking analysis of the CDP cyclo(L-Pro-L-Tyr) in the binding sites of tyrosine-kinases. A view of the protein showing the catalytic or inhibitor binding sites of protein kinases is presented with the orientation of the CDP (Pro-Tyr) in the predicted conformations. The protein is shown as surface with the interior in cartoon. Pro-Tyr and other molecules are shown as sticks colored by elements. Pro-Tyr, cyclo(L-Pro-L-Tyr); CCL4 [illegible]; CX-4945 [illegible]; NVP-BVU972 [illegible]; HA-5 [illegible]; 20G, 2-oxoglutarate. Models were carried out with PyMOL 2.1.0 (The PyMOL Molecular Graphics System, version 2.1.0, Schrödinger, LLC, New York, NY, USA).

In agreement with our results, some reports have described that some melanoma treatments implicate the use of tyrosine kinase inhibitors such as the MAPK pathway, PI3K (16). Thus, we can propose that inhibition or activation of the protein kinases such as AKT, HIPK2, AMPK, MET, JNK, HIF-1α, and CD44 by treatment with CDPs in the mouse melanoma model could involve the blocking of the substrate binding site as a molecular mechanism.

Melanoma tumors in mouse showed a significant decrease in factors involved in survival, proliferation, invasiveness, angiogenesis, and glucose metabolism. Thus, our data suggest that bacterial CDPs suppress the activation of the signaling pathways associated with the onset of tumorigenesis governed by PI3K/Akt/mTOR, Ras-ERK, PI3K/JNK/PKA, p27Kip1/CDK1/survivin, MAPK, HIF-1, EMT, and CSC not actually shown. Although the mode of action of CDPs is not totally elucidated, we propose that CDPs target multiple pathways and processes (oncogenes and tumor suppressors) involved in tumor formation and progression by blocking the catalytic site conserved in the serine-threonine kinase family. Findings indicate that the multiple signaling pathways are implicated in melanoma aggressiveness, showing that bacterial CDPs interfere during melanoma development by a mechanism dependent on protein kinase inhibition. Our data suggest that CDPs have potential antiproliferative properties to be used as antineoplastic drugs.

DATA AVAILABILITY STATEMENT

All datasets generated for this study are included in the article/ **Supplementary Material**.

ETHICS STATEMENT

The animal study was reviewed and approved by the Institutional Committee for Use of Animals of the Universidad Michoacana de San Nicolás de Hidalgo. The study was carried out in accordance with the Mexican Official Regulations for the Use and Care of Animals (NOM-062-ZOO-1999, Ministry of Agriculture, Mexico).

AUTHOR CONTRIBUTIONS

JC-G: conception and design. MD-M, LH-P, JG-P, AD-P, and LM-A: development of methodology. JC-G, JR-Z, GP-R, and JM: analysis and interpretation of data. JC-G, JR-Z, HR, GP-R, and JM: writing, review, and/or revision of the manuscript. JC-G, JR-Z, and HR: administrative, technical, or material support. JC-G, JR-Z, and GP-R: study supervision. All authors read and approved the final manuscript.

FUNDING

This study was funded by the Consejo Nacional de Ciencia y Tecnología (CONACYT) of Mexico (Grant Nos. 256119 and 222405) and the Marcos Moshinsky Foundation and Universidad Michoacana de San Nicolás de Hidalgo/C.I.C.2.14 grants. MD-M and LH-P received a scholarship from CONACYT. GP-R and JM were supported by the Intramural Research Program (National Institutes of Health (NIH), National Heart, Lung, and Blood Institute (NHLBI)).

ACKNOWLEDGMENTS

We thank R. Noriega for the B16-F0 murine melanoma line and Madeline Hernandez for care of animals of the intramural research program.

SUPPLEMENTARY MATERIAL

The Supplementary Material for this article can be found online at: https://www.frontiersin.org/articles/10.3389/fonc.2020.01111/full#supplementary-material

REFERENCES

1. Fischbach MA, Segre JA. Signaling in host-associated microbial communities. *Cell.* (2016) 164:1288–300. doi: 10.1016/j.cell.2016.02.037
2. Martinez KB, Leone V, Chang EB. Microbial metabolites in health and disease: navigating the unknown in search of function. *J Biol Chem.* (2017) 292:8553–9. doi: 10.1074/jbc.R116.752899
3. Shibajit Kumar S, Dileep C, Mohandas C, Nambisan B, Ca J. Cyclo(D-Tyr-D-Phe): a new antibacterial, anticancer, and antioxidant cyclic dipeptide from *Bacillus* sp. N strain associated with a rhabditid entomopathogenic nematode. *J Pept Sci.* (2014) 20:173–85. doi: 10.1002/psc.2594
4. Vazquez-Rivera D, Gonzalez O, Guzman-Rodriguez J, Diaz-Perez AL, Ochoa-Zarzosa A, López-Bucio J, et al. Cytotoxicity of cyclodipeptides from *Pseudomonas aeruginosa* PAO1 leads to apoptosis in human cancer cell lines. *Biomed Res Int.* (2015) 2015:197608. doi: 10.1155/2015/197608
5. Brauns SC, Milne P, Naude R, Van de Venter M. Selected cyclic dipeptides inhibit cancer cell growth and induce apoptosis in HT-29 colon cancer cells. *Anticancer Res.* (2004) 24:1713–9.

6. Hernandez-Padilla L, Vazquez-Rivera D, Sanchez-Briones LA, Diaz-Perez AL, Moreno-Rodriguez J, Moreno-Eutimio MA, et al. The antiproliferative effect of cyclodipeptides from *Pseudomonas aeruginosa* PAO1 on HeLa cells involves inhibition of phosphorylation of Akt and S6k kinases. *Molecules.* (2017) 22:1024. doi: 10.3390/molecules22061024
7. Boyer N, Morrison KC, Kim J, Hergenrother PJ, Movassaghi M. Synthesis and anticancer activity of epipolythiodiketopiperazine alkaloids. *Chem Sci.* (2013) 4:1646–57. doi: 10.1039/c3sc50174d
8. Borders EB, Bivona C, Medina PJ. Mammalian target of rapamycin: biological function and target for novel anticancer agents. *Am J Health Syst Pharm.* (2010) 67:2095–106. doi: 10.2146/ajhp100020
9. Laplante M, Sabatini DM. mTOR signaling in growth control and disease. *Cell.* (2012) 149:274–93. doi: 10.1016/j.cell.2012.03.017
10. Kim YC, Guan KL. mTOR: a pharmacologic target for autophagy regulation. *J Clin Invest.* (2015) 125:25–32. doi: 10.1172/JCI73939
11. Allen-Petersen BL, Risom T, Feng Z, Wang Z, Jenny ZP, Thoma MC, et al. Activation of PP2A and inhibition of mTOR synergistically reduce MYC signaling and decrease tumor growth in pancreatic ductal adenocarcinoma. *Cancer Res.* (2019) 79:209. doi: 10.1158/0008-5472.CAN-18-0717
12. Hanahan D, Weinberg RA. The hallmarks of cancer. *Cell.* (2000) 100:57–70. doi: 10.1016/S0092-8674(00)81683-9
13. Mariotti A, Perotti A, Sessa C, Rüegg C. N-cadherin as a therapeutic target in cancer. *Expert Opin Investig Drugs.* (2007) 16:451–65. doi: 10.1517/13543784.16.4.451
14. Kourtidis A, Yanagisawa M. Cadherin signaling: keeping cells in touch. *F1000Research.* (2015) 4:550. doi: 10.12688/f1000research.6445.1
15. Domingues B, Lopes JM, Soares P, Pópulo H. Melanoma treatment in review. *Immunotargets Ther.* (2018) 7:35–49. doi: 10.2147/ITT.S134842
16. Leonardi GC, Falzone L, Salemi R, Zanghì A, Spandidos DA, McCubrey JA, et al. Cutaneous melanoma: from pathogenesis to therapy (review). *Int J Oncol.* (2018) 52:1071–80. doi: 10.3892/ijo.2018.4287
17. Ortiz-Castro R, Díaz-Pérez C, Martínez-Trujillo M, del Río RE, Campos-García J, López-Bucio J. Transkingdom signaling based on bacterial cyclodipeptides with auxin activity in plants. *Proc Natl Acad Sci USA.* (2011) 108:7253–8. doi: 10.1073/pnas.1006740108
18. González O, Ortiz-Castro R, Díaz-Pérez C, Díaz-Pérez AL, Magaña-Dueñas V, López-Bucio J, et al. Non-ribosomal peptide synthases from *Pseudomonas aeruginosa* play a role in cyclodipeptide biosynthesis, quorum-sensing regulation, and root development in a plant host. *Microb Ecol.* (2017) 73:616–29. doi: 10.1007/s00248-016-0896-4
19. Sharma S, Stolina M, Lin Y, Gardner B, Miller PW, Kronenberg M, et al. T cell-derived IL-10 promotes lung cancer growth by suppressing both T cell and APC function. *J Immunol.* (1999) 163:5020–8.
20. Overwijk WW, Restifo NP. B16 as a mouse model for human melanoma. *Curr Protoc Immunol.* (2001) Chapter 20:Unit 20.1. doi: 10.1002/0471142735.im2001s39
21. Borthwick AD. 2,5-Diketopiperazines: synthesis, reactions, medicinal chemistry, and bioactive natural products. *Chem Rev.* (2012) 112:3641–716. doi: 10.1021/cr200398y
22. Furukawa T, Akutagawa T, Funatani H, Uchida T, Hotta Y, Niwa M, et al. Cyclic dipeptides exhibit potency for scavenging radicals. *Bioorg Med Chem.* (2012) 20:2002–9. doi: 10.1016/j.bmc.2012.01.050
23. Hung N, Shen CC, Hu YW, Hu LY, Yeh CM, Teng CJ, et al. Risk of cancer in patients with iron deficiency anemia: a nationwide population-based study. *PLoS ONE.* (2015) 10:e0119647. doi: 10.1371/journal.pone.0119647
24. Thornburg JM, Nelson K, Clem BF, Lane AN, Arumugam S, Simmons A, et al. Targeting aspartate aminotransferase in breast cancer. *Breast Cancer Res.* (2008) 10:R84. doi: 10.1186/bcr2154
25. Cao R, Wang LP. Serological diagnosis of liver metastasis in patients with breast cancer. *Cancer Biol Med.* (2012) 9:57–62. doi: 10.3969/j.issn.2095-3941.2012.01.011
26. Karbowniczek M, Spittle CS, Morrison T, Wu H, Henske EP. mTOR is activated in the majority of malignant melanomas. *J Invest Dermatol.* (2008) 128:980–7. doi: 10.1038/sj.jid.5701074
27. Song M, Bode AM, Dong Z, Lee MH. AKT as a therapeutic target for cancer. *Cancer Res.* (2019) 79:1019–31. doi: 10.1158/0008-5472.CAN-18-2738
28. Hernández-Padilla L, Reyes de la Cruz H, Campos-García J. Antiproliferative effect of bacterial cyclodipeptides in the HeLa line of human cervical cancer reveals multiple protein kinase targeting, including mTORC1/C2 complex inhibition in a TSC1/2-dependent manner. *Apoptosis.* (2020). doi: 10.1007/s10495-020-01629-z. [Epub ahead of print].
29. Chresta CM, Davies BR, Hickson I, Harding T, Cosulich S, Critchlow SE, et al. AZD8055 is a potent, selective, and orally bioavailable ATP-competitive mammalian target of rapamycin kinase inhibitor with *in vitro* and *in vivo* antitumor activity. *Cancer Res.* (2010) 70:288–98. doi: 10.1158/0008-5472.CAN-09-1751
30. Kawata T, Tada K, Kobayashi M, Sakamoto T, Takiuchi Y, Iwai F, et al. Dual inhibition of the mTORC1 and mTORC2 signaling pathways is a promising therapeutic target for adult T-cell leukemia. *Cancer Sci.* (2018) 109:103–11. doi: 10.1111/cas.13431
31. Sanchez-Hernandez I, Baquero P, Calleros L, Chiloeches A. Dual inhibition of (V600E)BRAF and the PI3K/AKT/mTOR pathway cooperates to induce apoptosis in melanoma cells through a MEK-independent mechanism. *Cancer Lett.* (2012) 314:244–55. doi: 10.1016/j.canlet.2011.09.037
32. Oskarsson T, Batlle E, Massagué J. Metastatic stem cells: sources, niches, and vital pathways. *Cell Stem Cell.* (2014) 14:306–21. doi: 10.1016/j.stem.2014.02.002
33. Zhang S, Zhou X, Wang B, Zhang K, Liu S, Yue K, et al. Loss of VHL expression contributes to epithelial-mesenchymal transition in oral squamous cell carcinoma. *Oral Oncol.* (2014) 50:809–17. doi: 10.1016/j.oraloncology.2014.06.007
34. Soni S, Padwad YS. HIF-1 in cancer therapy: two decade long story of a transcription factor. *Acta Oncol.* (2017) 56:503–15. doi: 10.1080/0284186X.2017.1301680
35. Wang XC. PHB2: a silent housekeeper or a potential therapeutic target? *Trends Pharmacol Sci.* (2014) 35:178–96. doi: 10.1016/j.tips.2014.02.004
36. Senbanjo LT, Chellaiah MA. CD44: a multifunctional cell surface adhesion receptor is a regulator of progression and metastasis of cancer cells. *Front Cell Dev Biol.* (2017) 5:18. doi: 10.3389/fcell.2017.00018

Conflict of Interest: The authors declare that the research was conducted in the absence of any commercial or financial relationships that could be construed as a potential conflict of interest.

11. BIBLIOGRAFÍA

Alison, M. R. (2001). Cancer. Encyclopedia of life sciences. *Nature Publishin g Group*.

Causes and Prevention. National Cancer Institute [Consultado 2020 Mayo 7]. Disponible en: http://www.cancer.gov/about-cancer/causes-prevention

Aldaco-Sarvide, F., Pérez-Pérez, P., Cervantes-Sánchez, G., Torrecillas-Torres, L., Erazo-Valle-Solís, A. A., Cabrera-Galeana, P., & Cárdenas-Cárdenas, E. (2018). Mortalidad por cáncer en México: actualización 2015.*cáncer*, *85*, 1.

Almendro, V., García-Recio, S., & Gascón, P. (2010). Tyrosine kinase receptor transactivation associated to G protein-coupled receptors. *Current drug targets*, *11*(9), 1169-1180.

Al-Othman, N., Ahram, M., & Alqaraleh, M. (2019). Role of androgen and microRNA in triple-negative breast cancer. *Breast disease*, (Preprint), 1-13.

Amit, I., Wides, R., & Yarden, Y. (2007). Evolvable signaling networks of receptor tyrosine kinases: relevance of robustness to malignancy and to cancer therapy. *Molecular systems biology*, *3*(1), 151.

Anaya-Ruiz, M., Vincent, A. K., & Perez-Santos, M. (2014). Cervical cancer trends in Mexico: incidence, mortality and research output. *Asian Pac J Cancer Prev*, *15*(20), 8689-8692.

Arrieta, O., Cardona, A. F., Martín, C., Más-López, L., Corrales-Rodríguez, L., Bramuglia, G.,& Carranza, H. (2015). Updated frequency of EGFR and KRAS mutations in nonsmall-cell lung cancer in Latin America: the Latin-American Consortium for the Investigation of Lung Cancer (CLICaP). *Journal of Thoracic Oncology*, *10*(5), 838-843.

Ashkenazi, A. (2002). Targeting death and decoy receptors of the tumour-necrosis factor superfamily. *Nature Reviews Cancer*, *2*(6), 420-430.

Astrinidis, A., & Henske, E. P. (2005). Tuberous sclerosis complex: linking growth and energy signaling pathways with human disease. *Oncogene*, *24*(50), 7475-7481.

Batool, A., Majeed, S. T., Aashaq, S., Majeed, R., Bhat, N. N., & Andrabi, K. I. (2020). Eukaryotic initiation factor 4E is a novel effector of mTORC1 signaling pathway in cross talk with Mnk1. *Molecular and Cellular Biochemistry*, *465*(1-2), 13-26.

Berdasco, M., & Esteller, M. (2010). Aberrant epigenetic landscape in cancer: how cellular identity goes awry. *Developmental cell*, *19*(5), 698-711.

Bergom, C., Gao, C., & Newman, P. J. (2005). Mechanisms of PECAM-1-mediated cytoprotection and implications for cancer cell survival. *Leukemia & lymphoma*, *46*(10), 1409-1421.

Björkerud, S., & Björkerud, B. (1996). Apoptosis is abundant in human atherosclerotic lesions, especially in inflammatory cells (macrophages and T cells), and may contribute to the accumulation of gruel and plaque instability. *The American journal of pathology*, *149*(2), 367.

Bhowmick, N. A., Neilson, E. G., & Moses, H. L. (2004). Stromal fibroblasts in cancer initiation and progression. *Nature*, *432*(7015), 332-337.

Borders, E. B., Bivona, C., & Medina, P. J. (2010). Mammalian target of rapamycin: biological function and target for novel anticancer agents. *American Journal of Health-System Pharmacy*, *67*(24), 2095-2106.

Bourhis, J., Le, M. G., Barrois, M., Gerbaulet, A., Jeannel, D., Duvillard, P & Riou, G. (1990). Prognostic value of c-myc proto-oncogene overexpression in early invasive carcinoma of the cervix. *Journal of clinical oncology*, *8*(11), 1789-1796.

Bourguignon, L. Y., Wong, G., Earle, C., Krueger, K., & Spevak, C. C. (2010). Hyaluronan-CD44 interaction promotes c-Src-mediated twist signaling, microRNA-10b expression, and RhoA/RhoC up-regulation, leading to Rho-kinase-associated cytoskeleton activation and breast tumor cell invasion. *Journal of Biological Chemistry*, *285*(47), 36721-36735.

Brachmann, S. M., Kleylein-Sohn, J., Gaulis, S., Kauffmann, A., Blommers, M. J., Kazic-Legueux, M., & Romanet, V. (2012). Characterization of the mechanism of action of the pan class I PI3K inhibitor NVP-BKM120 across a broad range of concentrations. *Molecular cancer therapeutics*, *11*(8), 1747-1757.

Cabrita, M. A., & Christofori, G. (2008). Sprouty proteins, masterminds of receptor tyrosine kinase signaling. *Angiogenesis*, *11*(1), 53-62.

Cafferkey, R., Young, P. R., McLaughlin, M. M., Bergsma, D. J., Koltin, Y., Sathe, G. M. & Livi, G. P. (1993). Dominant missense mutations in a novel yeast protein related to

mammalian phosphatidylinositol 3-kinase and VPS34 abrogate rapamycin cytotoxicity. *Molecular and cellular biology*, *13*(10), 6012-6023.

Campbell, P. J. (2012). Telomeres and cancer: from crisis to stability to crisis to stability. *Cell*, *148*(4), 633-635.

Carracedo, A., Ma, L., Teruya-Feldstein, J., Rojo, F., Salmena, L., Alimonti, A., & Papa, A. (2008). Inhibition of mTORC1 leads to MAPK pathway activation through a PI3K-dependent feedback loop in human cancer. *The Journal of clinical investigation*, *118*(9), 3065-3074.

Chandarlapaty, S., Sawai, A., Scaltriti, M., Rodrik-Outmezguine, V., Grbovic-Huezo, O., Serra, V., & Rosen, N. (2011). AKT inhibition relieves feedback suppression of receptor tyrosine kinase expression and activity. *Cancer cell*, *19*(1), 58-71.

Chakrabarty, A., Sánchez, V., Kuba, M. G., Rinehart, C., & Arteaga, C. L. (2012). Feedback upregulation of HER3 (ErbB3) expression and activity attenuates antitumor effect of PI3K inhibitors. *Proceedings of the National Academy of Sciences*, *109*(8), 2718-2723.

Chelimo, C., Wouldes, T. A., Cameron, L. D., & Elwood, J. M. (2013). Risk factors for and prevention of human papillomaviruses (HPV), genital warts and cervical cancer. *Journal of Infection*, *66*(3), 207-217.

Chen, M., Meng, Q., Qin, Y., Liang, P., Tan, P., He, L & Cui, J. (2016). TRIM14 inhibits cGAS degradation mediated by selective autophagy receptor p62 to promote innate immune responses. *Molecular cell*, *64*(1), 105-119.

Chia, S., Gandhi, S., Joy, A. A., Edwards, S., Gorr, M., Hopkins, S., & Dent, S. F. (2015). Novel agents and associated toxicities of inhibitors of the pi3k/Akt/mtor pathway for the treatment of breast cancer. *Current oncology*, *22*(1), 33.

Chiarini, F., Evangelisti, C., McCubrey, J. A., & Martelli, A. M. (2015). Current treatment strategies for inhibiting mTOR in cancer. *Trends in pharmacological sciences*, *36*(2), 124-135.

Chinnaiyan, A. M., O'Rourke, K., Tewari, M., & Dixit, V. M. (1995). FADD, a novel death domain-containing protein, interacts with the death domain of Fas and initiates apoptosis. *Cell*, *81*(4), 505-512.

Chresta, C. M., Davies, B. R., Hickson, I., Harding, T., Cosulich, S., Critchlow, S. E & James, D. (2010). AZD8055 is a potent, selective, and orally bioavailable ATP-competitive mammalian target of rapamycin kinase inhibitor with in vitro and in vivo antitumor activity. *Cancer research*, *70*(1), 288-298.

Christofferson, D. E., & Yuan, J. (2010). Necroptosis as an alternative form of programmed cell death. *Current opinion in cell biology*, *22*(2), 263-268.

Cohen, G. M. (1997). Caspases: the executioners of apoptosis. *Biochemical Journal*, *326*(1), 1-16.

Copp, J., Manning, G., & Hunter, T. (2009). TORC-specific phosphorylation of mammalian target of rapamycin (mTOR): phospho-Ser2481 is a marker for intact mTOR signaling complex 2. *Cancer research*, *69*(5), 1821-1827.

Corona-Sánchez, I., Peña-Uribe, C. A., González-López, O., Villegas, J., Campos-Garcia, J., & de la Cruz, H. R. (2019). Cyclodipeptides from Pseudomonas aeruginosa modulate the maize (Zea mays L.) root system and promote S6 ribosomal protein kinase activation. *PeerJ*, *7*, e7494.

Cory, S., Vaux, D. L., Strasser, A., Harris, A. W., & Adams, J. M. (1999). Insights from Bcl-2 and Myc: malignancy involves abrogation of apoptosis as well as sustained proliferation. *Cancer research*, *59*(7 Supplement), 1685s-1692s.

Cullen, A. P., Reid, R. I. C. H. A. R. D., Campion, M. I. C. H. A. E. L., & Lörincz, A. T. (1991). Analysis of the physical state of different human papillomavirus DNAs in intraepithelial and invasive cervical neoplasm. *Journal of virology*, *65*(2), 606-612.

Cullen, J. M., Page, R., & Misdorp, W. (2002). An overview of cancer pathogenesis, diagnosis, and management. *Tumors in domestic animals*, 1-44.

Dai, L., Liu, Y., Liu, J., Wen, X., Xu, Z., Wang, Z., & Ye, T. (2013). A novel CyclinE/CyclinA-CDK Inhibitor targets p27Kip1 degradation, cell cycle progression and cell survival: Implications in cancer therapy. *Cancer letters*, *333*(1), 103-112.

De Masson, A., Fouchard, N., Mery-Bossard, L., & Dauendorffer, J. N. (2011). Cutaneous and mucosal aphthosis during temsirolimus therapy for advanced renal cell carcinoma: review of cutaneous and mucosal side effects of mTOR inhibitors. *Dermatology*, *223*(1), 4-8.

DeNardo, D. G., Andreu, P., & Coussens, L. M. (2010). Interactions between lymphocytes and myeloid cells regulate pro-versus anti-tumor immunity. *Cancer and Metastasis Reviews*, *29*(2), 309-316.

Dengler, F. (2020). Activation of AMPK under Hypoxia: Many Roads Leading to Rome. *International Journal of Molecular Sciences*, *21*(7), 2428.

Denault, J. B., & Salvesen, G. S. (2002). Caspases: keys in the ignition of cell death. *Chemical reviews*, *102*(12), 4489-4500.

Dienstmann, R., Rodon, J., Serra, V., & Tabernero, J. (2014). Picking the point of inhibition: a comparative review of PI3K/AKT/mTOR pathway inhibitors. *Molecular cancer therapeutics*, *13*(5), 1021-1031.

Dokianakis, D. N., Sourvinos, G., Sakkas, S., Athanasiadou, E., & Spandidos, D. A. (1998). Detection of HPV and ras gene mutations in cervical smears from female genital lesions. *Oncology reports*, *5*(5), 1195-1203.

Doorbar, J. (2006). Molecular biology of human papillomavirus infection and cervical cancer. *Clinical science*, *110*(5), 525-541.

Duenas-Gonzalez, A., Cetina, L., Coronel, J., & Cervantes-Madrid, D. (2012). Emerging drugs for cervical cancer. *Expert opinion on emerging drugs*, *17*(2), 203-218.

Durán-Maldonado, M. X., Hernández-Padilla, L., Gallardo-Pérez, J. C., Díaz-Pérez, A. L., Martínez-Alcantar, L., Rodríguez-Zavala, J. S., & Campos-Garcia, J. (2020). Bacterial cyclodipeptides target signal pathways involved in malignant melanoma. *Frontiers in Oncology*, *10*, 1111.

Düvel, K., Yecies, J. L., Menon, S., Raman, P., Lipovsky, A. I., Souza, A. L & Vander Heiden, M. G. (2010). Activation of a metabolic gene regulatory network downstream of mTOR complex 1. *Molecular cell*, *39*(2), 171-183.

Earnshaw, W. C., Martins, L. M., & Kaufmann, S. H. (1999). Mammalian caspases: structure, activation, substrates, and functions during apoptosis. *Annual review of biochemistry*, *68*(1), 383-424.

Edinger, A. L., & Thompson, C. B. (2004). Death by design: apoptosis, necrosis and autophagy. *Current opinion in cell biology*, *16*(6), 663-669.

Efeyan, A., & Sabatini, D. M. (2010).mTOR and cancer: many loops in one pathway. *Current opinion in cell biology*, *22*(2), 169-176.

Elmore, S. (2007). Apoptosis: a review of programmed cell death. *Toxicologic pathology*, *35*(4), 495-516.

Enari, M., Sakahira, H., Yokoyama, H., Okawa, K., Iwamatsu, A., & Nagata, S. (1998). A caspase-activated DNase that degrades DNA during apoptosis, and its inhibitor ICAD. *Nature*, *391*(6662), 43-50.

Engelman, J. A., & Jänne, P. A. (2008). Mechanisms of acquired resistance to epidermal growth factor receptor tyrosine kinase inhibitors in non–small cell lung cancer. *Clinical Cancer Research*, *14*(10), 2895-2899.

Evan, G., & Littlewood, T. (1998). A matter of life and cell death. *Science*, *281*(5381), 1317-1322.

Ferlay, J., Soerjomataram, I., Dikshit, R., Eser, S., Mathers, C., Rebelo, M. & Bray, F. (2015). Cancer incidence and mortality worldwide: sources, methods and major patterns in GLOBOCAN 2012. *International journal of cancer*, *136*(5), E359-E386.

Finking, R., & Marahiel, M. A. (2004). Biosynthesis of nonribosomal peptides. *Annu. Rev. Microbiol.*, *58*, 453-488.

Fink, S. L., & Cookson, B. T. (2005). Apoptosis, pyroptosis, and necrosis: mechanistic description of dead and dying eukaryotic cells. *Infection and immunity*, *73*(4), 1907-1916.
Elmore, S. (2007). Apoptosis: a review of programmed cell death. *Toxicologic pathology*, *35*(4), 495-516.

Fisher, D. E. (1994). Apoptosis in cancer therapy: crossing the threshold. *Cell*, *78*(4), 539-542.

Fokas, D., Sainis, I., Briasoulis, E., Vareli, K., Tzakos, A. G., & Kounnis, V. (2010). Cyanobacterial Cyclopeptides as Lead Compounds to Novel Targeted Cancer Drugs.

Funk, J. O., Waga, S., Harry, J. B., Espling, E., Stillman, B., & Galloway, D. A. (1997). Inhibition of CDK activity and PCNA-dependent DNA replication by p21 is blocked by interaction with the HPV-16 E7 oncoprotein. *Genes & development*, *11*(16), 2090-2100.

Gao, C., Sun, W., Christofidou-Solomidou, M., Sawada, M., Newman, D. K., Bergom, C., & Newman, P. J. (2003). PECAM-1 functions as a specific and potent inhibitor of mitochondrial-dependent apoptosis. *Blood*, *102*(1), 169-179.

Gewin, L., & Galloway, D. A. (2001). E box-dependent activation of telomerase by human papillomavirus type 16 E6 does not require induction of c-myc. *Journal of virology*, *75*(15), 7198-7201.

González, O., Ortíz-Castro, R., Díaz-Pérez, C., Díaz-Pérez, A. L., Magaña-Dueñas, V., López-Bucio, J., & Campos-García, J. (2017). Non-ribosomal peptide synthases from

Pseudomonas aeruginosa play a role in cyclodipeptide biosynthesis, quorum-sensing regulation, and root development in a plant host. *Microbial ecology*, *73*(3), 616-629.

Goncalves, A., Fabbro, M., Lhomme, C., Gladieff, L., Extra, J. M., Floquet, A., & Viens, P. (2008). A phase II trial to evaluate gefitinib as second-or third-line treatment in patients with recurring locoregionally advanced or metastatic cervical cancer. *Gynecologic oncology*, *108*(1), 42-46.

Gondry, M., Sauguet, L., Belin, P., Thai, R., Amouroux, R., Tellier, C., & Masson, C. (2009). Cyclodipeptide synthases are a family of tRNA-dependent peptide bond–forming enzymes. *Nature chemical biology*, *5*(6), 414-420.

Guan, P., Howell-Jones, R., Li, N., Bruni, L., de Sanjosé, S., Franceschi, S., & Clifford, G. M. (2012). Human papillomavirus types in 115,789 HPV-positive women: a meta-analysis from cervical infection to cancer. *International journal of cancer*, *131*(10), 2349-235

Guertin, D. A., Stevens, D. M., Saitoh, M., Kinkel, S., Crosby, K., Sheen, J. H., & Sabatini, D. M. (2009). mTOR complex 2 is required for the development of prostate cancer induced by Pten loss in mice. *Cancer cell*, *15*(2), 148-159.

Guri, Y., Colombi, M., Dazert, E., Hindupur, S. K., Roszik, J., Moes, S., & Hall, M. N. (2017). mTORC2 promotes tumorigenesis via lipid synthesis. *Cancer cell*, *32*(6), 807-823.

Güner, O. F. (Ed.). (2000). *Pharmacophore perception, development, and use in drug design* (Vol. 2). Internat'l University Line.

Grivennikov, S. I., Greten, F. R., & Karin, M. (2010). Immunity, inflammation, and cancer. *Cell*, *140*(6), 883-899.

Gwinn, D. M., Shackelford, D. B., Egan, D. F., Mihaylova, M. M., Mery, A., Vasquez, D. S., & Shaw, R. J. (2008). AMPK phosphorylation of raptor mediates a metabolic checkpoint. *Molecular cell*, *30*(2), 214-226.

Hanahan, D., & Weinberg, R. A. (2011). Hallmarks of cancer: the next generation.*cell*, *144*(5), 646-674.

Hengartner, M. O., & Horvitz, H. R. (1994). Programmed cell death in Caenorhabditis elegans. *Current opinion in genetics & development*, *4*(4), 581-586.

Hengartner, M. O. (2000). The biochemistry of apoptosis. *Nature*, *407*(6805), 770-776.

Hernández-Padilla, L., Vázquez-Rivera, D., Sánchez-Briones, L. A., Díaz-Pérez, A. L., Moreno-Rodríguez, J., Moreno-Eutimio, M. A. & Campos-García, J. (2017). The antiproliferative effect of cyclodipeptides from Pseudomonas aeruginosa PAO1 on HeLa cells involves inhibition of phosphorylation of Akt and S6k kinases. *Molecules*, *22*(6), 1024

Hers, I., Vincent, E. E., & Tavaré, J. M. (2011). Akt signalling in health and disease. *Cellular signalling*, *23*(10), 1515-1527.

Hirohashi, S. (1998). Inactivation of the E-cadherin-mediated cell adhesion system in human cancers. *The American journal of pathology*, *153*(2), 333-339.

Holler, N., Zaru, R., Micheau, O., Thome, M., Attinger, A., Valitutti, S.& Tschopp, J. (2000). Fas triggers an alternative, caspase-8–independent cell death pathway using the kinase RIP as effector molecule. *Nature immunology*, *1*(6), 489-495.

Hong, S., Moon, B. H., Yong, Y., Shin, S. Y., Lee, Y. H., & Lim, Y. (2008). Inhibitory effect against Akt of cyclic dipeptides isolated from Bacillus sp. *Journal of microbiology and biotechnology*, *18*(4), 682-685.

Hopman, A. H., Smedts, F., Dignef, W., Ummelen, M., Sonke, G., Mravunac, M.& Ramaekers, F. C. (2004). Transition of high-grade cervical intraepithelial neoplasia to micro-invasive carcinoma is characterized by integration of HPV 16/18 and numerical chromosome abnormalities. *The Journal of Pathology: A Journal of the Pathological Society of Great Britain and Ireland*, *202*(1), 23-33.

Huayue, L. I., Byung Cheol, L. E. E., Tae Sung, K. I. M., Kyung Sook, B. A. E., Jongki, H. O. N. G., Sang Ho CHOI, B. B., & JUNG, J. H. (2008). Bioactive cyclic dipeptides from a marine sponge-associated bacterium, Psychrobacter sp. *Biomolecules & Therapeutics*, *16*(4), 356-363.

Hsu, P. P., Kang, S. A., Rameseder, J., Zhang, Y., Ottina, K. A., Lim, D., & Marto, J. A. (2011). The mTOR-regulated phosphoproteome reveals a mechanism of mTORC1-mediated inhibition of growth factor signaling. *Science*, *332*(6035), 1317-1322.

Igney, F. H., & Krammer, P. H. (2002). Death and anti-death: tumour resistance to apoptosis. *Nature Reviews Cancer*, *2*(4), 277-288.

Inoki, K., Li, Y., Zhu, T., Wu, J., & Guan, K. L. (2002). TSC2 is phosphorylated and inhibited by Akt and suppresses mTOR signalling. *Nature cell biology*, *4*(9), 648-657.

Inoki, K., Zhu, T., & Guan, K. L. (2003). TSC2 mediates cellular energy response to control cell growth and survival. *Cell*, *115*(5), 577-590.

Iommarini, L., Porcelli, A. M., Gasparre, G., & Kurelac, I. (2017). Non-canonical mechanisms regulating hypoxia-inducible factor 1 alpha in cancer. *Frontiers in oncology*, *7*, 286.

Jacinto, E., Facchinetti, V., Liu, D., Soto, N., Wei, S., Jung, S. Y.,& Su, B. (2006). SIN1/MIP1 maintains rictor-mTOR complex integrity and regulates Akt phosphorylation and substrate specificity. *Cell*, *127*(1), 125-137.

Jiang, B. H., & Liu, L. Z. (2008). Role of mTOR in anticancer drug resistance: perspectives for improved drug treatment. *Drug resistance updates*, *11*(3), 63-76.

Kang, Y., & Pantel, K. (2013). Tumor cell dissemination: emerging biological insights from animal models and cancer patients. *Cancer cell*, *23*(5), 573-581.

Kang, X. H., Xu, Z. Y., Gong, Y. B., Wang, L. F., Wang, Z. Q., Xu, L., & Liao, M. J. (2013). Bufalin reverses HGF-induced resistance to EGFR-TKIs in EGFR mutant lung cancer cells via blockage of Met/PI3k/Akt pathway and induction of apoptosis. *Evidence-Based Complementary and Alternative Medicine*, *2013*.

Kanoh, k., kohno, s., katada, j., takahashi, j., & uno, i. (1999). (-)-Phenylahistin arrests cells in mitosis by inhibiting tubulin polymerization. *The Journal of antibiotics*, *52*(2), 134-141.

Karar, J., & Maity, A. (2011). PI3K/AKT/mTOR pathway in angiogenesis. *Frontiers in molecular neuroscience*, *4*, 51.

Kakumoto, K., Ikeda, J. I., Okada, M., Morii, E., & Oneyama, C. (2015). mLST8 promotes mTOR-mediated tumor progression. *PloS one*, *10*(4), e0119015.

Karimkhani, C., Green, A. C., Nijsten, T., Weinstock, M. A., Dellavalle, R. P., Naghavi, M., & Fitzmaurice, C. (2017). The global burden of melanoma: results from the Global Burden of Disease Study 2015. *British Journal of Dermatology*, *177*(1), 134-140.

Kawata, T., Tada, K., Kobayashi, M., Sakamoto, T., Takiuchi, Y., Iwai, F., & Sato, H. (2018). Dual inhibition of the mTORC 1 and mTORC 2 signaling pathways is a promising therapeutic target for adult T-cell leukemia. *Cancer science*, *109*(1), 103-111.

Kerr, J. F., Wyllie, A. H., & Currie, A. R. (1972). Apoptosis: a basic biological phenomenon with wideranging implications in tissue kinetics. *British journal of cancer*, *26*(4), 239-257.

Kim, D. H., Sarbassov, D. D., Ali, S. M., Latek, R. R., Guntur, K. V., Erdjument-Bromage, H., & Sabatini, D. M. (2003). GβL, a positive regulator of the rapamycin-sensitive pathway required for the nutrient-sensitive interaction between raptor and mTOR. *Molecular cell*, *11*(4), 895-904.

Kim MK, Kim TJ, Sung CO, et al. (2010).High expression of mTOR is associated with radiation resistance in cervical cancer. J Gynecol Oncol;21:181-185.

Kim, Y. C., & Guan, K. L. (2015).mTOR: a pharmacologic target for autophagy regulation. *The Journal of clinical investigation*, *125*(1), 25-32.

Kurz, S. M., Diebold, S. S., Hieronymus, T., Gust, T. C., Bartunek, P., Sachs, M., & Zenke, M. (2002). The impact of c-met/scatter factor receptor on dendritic cell migration. *European journal of immunology*, *32*(7), 1832-1838.

Kunz, J., Henriquez, R., Schneider, U., Deuter-Reinhard, M., Movva, N. R., & Hall, M. N. (1993). Target of rapamycin in yeast, TOR2, is an essential phosphatidylinositol kinase homolog required for G1 progression. *Cell*, *73*(3), 585-596.

Kuri-Morales, P. A. (2011). La transición en salud y su impacto en la demanda de servicios. *Gac Med Mex*, *147*(6), 451-454.

Kerr, J. F. (2002). History of the events leading to the formulation of the apoptosis concept. *Toxicology*, *181*, 471-474.

Kischkel, F. C., Hellbardt, S., Behrmann, I., Germer, M., Pawlita, M., Krammer, P. H., & Peter, M. E. (1995). Cytotoxicity-dependent APO-1 (Fas/CD95)-associated proteins form a death-inducing signaling complex (DISC) with the receptor. *The EMBO journal*, *14*(22), 5579-5588.

Krajewski, S., Tanaka, S., Takayama, S., Schibler, M. J., Fenton, W., & Reed, J. C. (1993). Investigation of the subcellular distribution of the bcl-2 oncoprotein: residence in the nuclear envelope, endoplasmic reticulum, and outer mitochondrial membranes. *Cancer research*, *53*(19), 4701-4714.

Kurosaka, K., Takahashi, M., Watanabe, N., & Kobayashi, Y. (2003). Silent cleanup of very early apoptotic cells by macrophages. *The Journal of Immunology*, *171*(9), 4672-4679.

Laplante, M., & Sabatini, D. M. (2012).mTOR signaling in growth control and disease. *Cell*, *149*(2), 274-293.

Laplante, M., & Sabatini, D. M. (2013). Regulation of mTORC1 and its impact on gene expression at a glance.

Lane, D. P. (1992). Cancer. p53, guardian of the genome. *Nature*, *358*, 15-16.

Lakshmi, S., Nair, B., Jayaprakash, P. G., Rajalekshmy, T. N., Nair, K., & Pillai, R. (1997).c-erbB-2 oncoprotein and epidermal growth factor receptor in cervical lesions. *Pathobiology*, *65*(3), 163-168.

Leary, A., Auclin, E., Pautier, P., & Lhommé, C. (2013). The PI3K/Akt/mTOR pathway in ovarian cancer: biological rationale and therapeutic opportunities. *Ovarian Cancer-A Clinical and Translational Update*, 275-302.

Lee, D. F., Kuo, H. P., Chen, C. T., Hsu, J. M., Chou, C. K., Wei, Y.,& He, X. (2007). IKKβ suppression of TSC1 links inflammation and tumor angiogenesis via the mTOR pathway. *Cell*, *130*(3), 440-455.

Lengauer, C., Kinzler, K. W., & Vogelstein, B. (1998). Genetic instabilities in human cancers. *Nature*, *396*(6712), 643-649.

Lertkiatmongkol, P., Liao, D., Mei, H., Hu, Y., & Newman, P. J. (2016). Endothelial functions of PECAM-1 (CD31). *Current opinion in hematology*, *23*(3), 253.

Levine, B., & Kroemer, G. (2008). Autophagy in the pathogenesis of disease. *Cell*, *132*(1), 27-42.

Li, B., & Dou, Q. P. (2000). Bax degradation by the ubiquitin/proteasome-dependent pathway: involvement in tumor survival and progression. *Proceedings of the National Academy of Sciences*, *97*(8), 3850-3855.

Li, S., Ogawa, W., Emi, A., Hayashi, K., Senga, Y., Nomura, K.,& Kasuga, M. (2011). Role of S6K1 in regulation of SREBP1c expression in the liver. *Biochemical and biophysical research communications*, *412*(2), 197-202.

Li, J., Ren, J., Liu, X., Jiang, L., He, W., Yuan, W. & Dai, C. (2015). Rictor/mTORC2 signaling mediates TGFβ1-induced fibroblast activation and kidney fibrosis. *Kidney international*, *88*(3), 515-527.

Lin, J., & Ding, D. (2016). Upregulation of miR-150 expression as a poor prognostic marker for cervical cancer patients. *Int J Clin Exp Pathol*, *9*(9), 9491-9496.

Liu, J., Sun, Y., Zhang, H., Ji, D., Wu, F., Tian, H., & Zhang, G. (2016). Theanine from tea and its semi-synthetic derivative TBrC suppress human cervical cancer growth and migration by inhibiting EGFR/Met-Akt/NF-κB signaling. *European journal of pharmacology*, *791*, 297-307.

Liu, X., & Lieberman, J. (2017). A mechanistic understanding of pyroptosis: the fiery death triggered by invasive infection. In *Advances in immunology* (Vol. 135, pp. 81-117). Academic Press.

Llaguno, S. R. A., & Parada, L. F. (2016). Cell of origin of glioma: biological and clinical implications. *British journal of cancer*, *115*(12), 1445-1450.

Lowe, S. W., & Lin, A. W. (2000). Apoptosis in cancer Carcinogenesis 21 (3): 485–495.

Ma, L., Chen, Z., Erdjument-Bromage, H., Tempst, P., & Pandolfi, P. P. (2005). Phosphorylation and functional inactivation of TSC2 by Erk: implications for tuberous sclerosisand cancer pathogenesis. *Cell*, *121*(2), 179-193.

Monk, B. J., Sill, M. W., McMeekin, D. S., Cohn, D. E., Ramondetta, L. M., Boardman, C. H., & Cella, D. (2009). Phase III trial of four cisplatin-containing doublet combinations in stage IVB, recurrent, or persistent cervical carcinoma: a Gynecologic Oncology Group study. *Journal of Clinical Oncology*, *27*(28), 4649.

Moore, K. N., Herzog, T. J., Lewin, S., Giuntoli, R. L., Armstrong, D. K., Rocconi, R. P., & Gold, M. A. (2007). A comparison of cisplatin/paclitaxel and carboplatin/paclitaxel in stage IVB, recurrent or persistent cervical cancer. *Gynecologic oncology*, *105*(2), 299-303.

Manning, B. D., Tee, A. R., Logsdon, M. N., Blenis, J., & Cantley, L. C. (2002). Identification of the tuberous sclerosis complex-2 tumor suppressor gene product tuberin as a target of the phosphoinositide 3-kinase/akt pathway. *Molecular cell*, *10*(1), 151-162.

Maltez, V. I., Tubbs, A. L., Cook, K. D., Aachoui, Y., Falcone, E. L., Holland, S. M., ... & Miao, E. A. (2015). Inflammasomes coordinate pyroptosis and natural killer cell cytotoxicity to clear infection by a ubiquitous environmental bacterium. *Immunity*, *43*(5), 987-997.

Marzban, H., Del Bigio, M. R., Alizadeh, J., Ghavami, S., Zachariah, R. M., & Rastegar, M. (2015). Cellular commitment in the developing cerebellum. *Frontiers in cellular neuroscience*, *8*, 450.

Mathew, R., Karantza-Wadsworth, V., & White, E. (2007). Role of autophagy in cancer. *Nature Reviews Cancer*, *7*(12), 961-967.

Mayer, C., Zhao, J., Yuan, X., & Grummt, I. (2004).mTOR-dependent activation of the transcription factor TIF-IA links rRNA synthesis to nutrient availability. *Genes & development*, *18*(4), 423-434.

McManus, E. J., & Alessi, D. R. (2002). TSC1–TSC2: a complex tale of PKB-mediated S6K regulation. *Nature cell biology*, *4*(9), E214-E216.

Miller, K. D., Nogueira, L., Mariotto, A. B., Rowland, J. H., Yabroff, K. R., Alfano, C. M., & Siegel, R. L. (2019). Cancer treatment and survivorship statistics, 2019. *CA: a cancer journal for clinicians*, *69*(5), 363-385.

Mishra, M. N., Chandavarkar, V., Sharma, R., & Bhargava, D. (2019). Structure, function and role of CD44 in neoplasia. *Journal of oral and maxillofacial pathology: JOMFP*, *23*(2), 267.

Mizushima, N. (2007). Autophagy: process and function. *Genes & development*, *21*(22), 2861-2873.

Mosesson, Y., Mills, G. B., & Yarden, Y. (2008). Derailed endocytosis: an emerging feature of cancer. *Nature Reviews Cancer*, *8*(11), 835-850.

Münz, M., Kieu, C., Mack, B., Schmitt, B., Zeidler, R., & Gires, O. (2004). The carcinoma-associated antigen EpCAM upregulates c-myc and induces cell proliferation. *Oncogene*, *23*(34), 5748-5758.

Naismith, J. H., & Sprang, S. R. (1998). Modularity in the TNF-receptor family. *Trends in biochemical sciences*, *23*(2), 74-79.

Noya, F., Chien, W. M., Broker, T. R., & Chow, L. T. (2001). p21cip1 degradation in differentiated keratinocytes is abrogated by costabilization with cyclin E induced by human papillomavirus E7. *Journal of virology*, *75*(13), 6121-6134.

NCCN Clinical Practice guidelines in Oncology. Cervical Cancer, version 2, 2013. National Comprehensive Cancer Network. Disponible en http://www.nccn.org

Oh, S. T., Kyo, S., & Laimins, L. A. (2001). Telomerase activation by human papillomavirus type 16 E6 protein: induction of human telomerase reverse transcriptase expression through Myc and GC-rich Sp1 binding sites. *Journal of virology*, *75*(12), 5559-5566.

O'Reilly, K. E., Rojo, F., She, Q. B., Solit, D., Mills, G. B., Smith, D.,& Baselga, J. (2006).mTOR inhibition induces upstream receptor tyrosine kinase signaling and activates Akt. *Cancer research*, *66*(3), 1500-1508.

Okuyama, K., Kaida, A., Hayashi, Y., Hayashi, Y., Harada, K., & Miura, M. (2015). KPU-300, a Novel Benzophenone–Diketopiperazine–Type Anti-Microtubule Agent with a 2-Pyridyl Structure, Is a Potent Radiosensitizer That Synchronizes the Cell Cycle in Early M Phase. *Plos one*, *10*(12), e0145995.

Oren, M. (1999). Regulation of the p53 tumor suppressor protein. *Journal of Biological Chemistry*, *274*(51), 36031-36034.

Ortiz-Castro, R., Díaz-Pérez, C., Martínez-Trujillo, M., Rosa, E., Campos-García, J., & López-Bucio, J. (2011). Transkingdom signaling based on bacterial cyclodipeptides with auxin activity in plants. *Proceedings of the National Academy of Sciences*, *108*(17), 7253-7258.

P de Carvalho, M., & Abraham, W. R. (2012). Antimicrobial and biofilm inhibiting diketopiperazines. *Current medicinal chemistry*, *19*(21), 3564-3577.

Papilomavirus humanos (PVH) y cáncer cervicouterino. Organización Mundial de la Salud [Consultado 2020 Mayo 7] Disponible en: https://www.who.int/es/news-room/fact-sheets/detail/human-papillomavirus-(hpv)-and-cervical-cancer

Pasparakis, M., & Vandenabeele, P. (2015). Necroptosis and its role in inflammation. *Nature*, *517*(7534), 311-320.

Pim, D., Collins, M., & Banks, L. (1992). Human papillomavirus type 16 E5 gene stimulates the transforming activity of the epidermal growth factor receptor. *Oncogene*, *7*(1), 27-32.

Potter, C. J., Pedraza, L. G., & Xu, T. (2002). Akt regulates growth by directly phosphorylating Tsc2. *Nature cell biology*, *4*(9), 658-665.

Ponta, H., Sherman, L., & Herrlich, P. A. (2003). CD44: from adhesion molecules to signalling regulators. *Nature reviews Molecular cell biology*, *4*(1), 33-45.

Prasad, C. (1995). Bioactive cyclic dipeptides. *Peptides*, *16*(1), 151-164.

Qu, X., Yu, J., Bhagat, G., Furuya, N., Hibshoosh, H., Troxel, A., & Levine, B. (2003). Promotion of tumorigenesis by heterozygous disruption of the beclin 1 autophagy gene. *The Journal of clinical investigation*, *112*(12), 1809-1820.

Ren, Y., Huang, F., Liu, Y., Yang, Y., Jiang, Q., & Xu, C. (2009). Autophagy inhibition through PI3K/Akt increases apoptosis by sodium selenite in NB4 cells. *Bmb Rep*, *42*(9), 599-604.

Reynoso-Noverón, N., Meneses-García, A., Erazo-Valle, A., Escudero-de Los Ríos, P., Kuri-Morales, P. A., & Mohar-Betancourt, A. (2016). Challenges in the development and implementation of the National Comprehensive Cancer Control Program in Mexico.*salud pública de méxico*, *58*, 325-333.

Rios, J., & Puhalla, S. (2011). PARP inhibitors in breast cancer: BRCA and beyond. *Breast Cancer*, *25*(11).

Ríos, P. R., Rivera, A. G., Cervantes, F. S., & Martínez, P. M. (2015). Trends in mortality from cancer in Mexico: 1990-2012. *Evidencia Médica e Investigación en Salud*, *8*(1), 5-15.

Riou, G., Lê, M., Le Doussal, V., Barrois, M., George, M., & Haie, C. (1987). C-myc proto-oncogene expression and prognosis in early carcinoma of the uterine cervix. *The Lancet*, *329*(8536), 761-763.

Sakahira, H., Enari, M., & Nagata, S. (1998). Cleavage of CAD inhibitor in CAD activation and DNA degradation during apoptosis. *Nature*, *391*(6662), 96-99.

Salvesen, G. S., & Duckett, C. S. (2002). IAP proteins: blocking the road to death's door. *Nature reviews Molecular cell biology*, *3*(6), 401-410.

Sancak, Y., Peterson, T. R., Shaul, Y. D., Lindquist, R. A., Thoreen, C. C., Bar-Peled, L., & Sabatini, D. M. (2008). The Rag GTPases bind raptor and mediate amino acid signaling to mTORC1. *Science*, *320*(5882), 1496-1501.

Sancak, Y., Thoreen, C. C., Peterson, T. R., Lindquist, R. A., Kang, S. A., Spooner, E., & Sabatini, D. M. (2007). PRAS40 is an insulin-regulated inhibitor of the mTORC1 protein kinase. *Molecular cell*, *25*(6), 903-915.

Sarbassov, D. D., Guertin, D. A., Ali, S. M., & Sabatini, D. M. (2005). Phosphorylation and regulation of Akt/PKB by the rictor-mTOR complex. *Science*, *307*(5712), 1098-1101.

Sarbassov, D. D., Ali, S. M., Sengupta, S., Sheen, J. H., Hsu, P. P., Bagley, A. F., & Sabatini, D. M. (2006). Prolonged rapamycin treatment inhibits mTORC2 assembly and Akt/PKB. *Molecular cell*, *22*(2), 159-168.

Savarese, D. M., Savy, G., Vahdat, L., Wischmeyer, P. E., & Corey, B. (2003). Prevention of chemotherapy and radiation toxicity with glutamine. *Cancer treatment reviews*, *29*(6), 501-513.

Schnell, U., Cirulli, V., & Giepmans, B. N. (2013). EpCAM: structure and function in health and disease. *Biochimica et Biophysica Acta (BBA)-Biomembranes*, *1828*(8), 1989-2001.

Schmidt, D. S., Klingbeil, P., Schnölzer, M., & Zöller, M. (2004). CD44 variant isoforms associate with tetraspanins and EpCAM. *Experimental cell research*, *297*(2), 329-347.

Silva, I. D. S. (1999). *Epidemiología del cáncer: principios y métodos*. OPS.

Sinha, S., & Levine, B. (2008). The autophagy effector Beclin 1: a novel BH3-only protein. *Oncogene*, *27*(1), S137-S148.

Sinha, S., Srivastava, R., De Clercq, E., & Singh, R. K. (2004). Synthesis and antiviral properties of arabino and ribonucleosides of 1, 3-dideazaadenine, 4-nitro-1, 3-dideazaadenine and diketopiperazine. *Nucleosides, Nucleotides and Nucleic Acids*, *23*(12), 1815-1824.

Smith, H. O., Tiffany, M. F., Qualls, C. R., & Key, C. R. (2000). The rising incidence of adenocarcinoma relative to squamous cell carcinoma of the uterine cervix in the United States—a 24-year population-based study. *Gynecologic oncology*, *78*(2), 97-105.

Stambolic, V., MacPherson, D., Sas, D., Lin, Y., Snow, B., Jang, Y., & Mak, T. W. (2001). Regulation of PTEN transcription by p53. *Molecular cell*, *8*(2), 317-325.

Sudarsanam, S., & Johnson, D. E. (2010). Functional consequences of mTOR inhibition. *Curr Opin Drug Discov Devel*, *13*(1), 31-40.

Taja-Chayeb L, Chavez-Blanco A, Martínez-Tlahuel J, et al. Expression of platelet derived growth factor family members and the potential role of imatinib mesylate for cervical cancer. Cancer Cell Int 2006;6:22.

Thatte, U., & Dahanukar, S. (1997). Apoptosis. *Drugs*, *54*(4), 511-532.

Thomas, M., & Banks, L. (1998). Inhibition of Bak-induced apoptosis by HPV-18 E6. *Oncogene*, *17*(23), 2943-2954.

Temkin, S. M., Yamada, S. D., & Fleming, G. F. (2010). A phase I study of weekly temsirolimus and topotecan in the treatment of advanced and/or recurrent gynecologic malignancies. *Gynecologic oncology*, *117*(3), 473-476.

Tee, A. R., Manning, B. D., Roux, P. P., Cantley, L. C., & Blenis, J. (2003). Tuberous sclerosis complex gene products, Tuberin and Hamartin, control mTOR signaling by acting as a GTPase-activating protein complex toward Rheb. *Current biology*, *13*(15), 1259-1268.

Tjalma, W., Weyler, J., Goovaerts, G., De Pooter, C., Van Marck, E., & Van Dam, P. (1997). Prognostic value of bcl-2 expression in patients with operable carcinoma of the uterine cervix. *Journal of clinical pathology*, *50*(1), 33-36

Tjalma W, DeCuyper E, Weyler J, et al. Expression of bcl-2 in invasive and in situ carcinoma of the uterine cervix. Am J Obstet Gynecol 1998;178:113-117.

Toker, A. (2012). Achieving specificity in Akt signaling in cancer. *Advances in biological regulation*, *52*(1), 78.

Vajdic, C. M., & van Leeuwen, M. T. (2009). Cancer incidence and risk factors after solid organ transplantation. *International journal of cancer*, *125*(8), 1747-1754.

Vázquez-Rivera, D., González, O., Guzmán-Rodríguez, J., Díaz-Pérez, A. L., Ochoa-Zarzosa, A., López-Bucio, J., ... & Campos-García, J. (2015). Cytotoxicity of cyclodipeptides from Pseudomonas aeruginosa PAO1 leads to apoptosis in human cancer cell lines. *BioMed Research International*, *2015*.

Veldman, T., Horikawa, I., Barrett, J. C., & Schlegel, R. (2001). Transcriptional activation of the telomerase hTERT gene by human papillomavirus type 16 E6 oncoprotein. *Journal of virology*, *75*(9), 4467-4472.

Vogelstein, B., & Kinzler, K. W. (2004). Cancer genes and the pathways they control. *Nature medicine*, *10*(8), 789-799.

Wang, H. G., Pathan, N., Ethell, I. M., Krajewski, S., Yamaguchi, Y., Shibasaki, F., & Reed, J. C. (1999). Ca2+-induced apoptosis through calcineurin dephosphorylation of BAD. *Science*, *284*(5412), 339-343.

Wang, T., Srivastava, S., Hartman, M., Buhari, S. A., Chan, C. W., Iau, P., & Lee, S. C. (2016). High expression of intratumoral stromal proteins is associated with chemotherapy resistance in breast cancer. *Oncotarget*, *7*(34), 55155.

Weinberg, R. A. (1991). Tumor suppressor genes. *Science*, *254*(5035), 1138-1146.

Wertz, I. E., & Dixit, V. M. (2010). Signaling to NF-κB: regulation by ubiquitination. *Cold Spring Harbor perspectives in biology*, *2*(3), a003350.

West, K. A., Castillo, S. S., & Dennis, P. A. (2002). Activation of the PI3K/Akt pathway and chemotherapeutic resistance. *Drug resistance updates*, *5*(6), 234-248.

Wood, L. D., Calhoun, E. S., Silliman, N., Ptak, J., Szabo, S., Powell, S. M.& Kern, S. E. (2006). Somatic mutations of GUCY2F, EPHA3, and NTRK3 in human cancers. *Human mutation*, *27*(10), 1060-1061.

Woodman, C. B., Collins, S. I., & Young, L. S. (2007). The natural history of cervical HPV infection: unresolved issues. *Nature Reviews Cancer*, *7*(1), 11-22.

Yao, T., Ying, X., Zhao, Y., Yuan, A., He, Q., Tong, H & Pu, J. (2015). Vitamin D receptor activation protects against myocardial reperfusion injury through inhibition of apoptosis and modulation of autophagy. *Antioxidants & redox signaling*, *22*(8), 633-650.

Yu, X. N., Zhang, G. C., Sun, J. L., Zhu, H. R., Shi, X., Song, G. Q. & Guo, H. Y. (2020). Enhanced mLST8 expression correlates with tumor progression in hepatocellular carcinoma. *Annals of Surgical Oncology*, 1-12.

Yuan, T. L., & Cantley, L. C. (2008). PI3K pathway alterations in cancer: variations on a theme. *Oncogene*, *27*(41), 5497-5510.

Zagouri, F., Sergentanis, T. N., Chrysikos, D., Filipits, M., & Bartsch, R. (2012). Molecularly targeted therapies in cervical cancer. A systematic review. *Gynecologic oncology*, *126*(2), 291-303.

Zeng, Z., Sarbassov, D. D., Samudio, I. J., Yee, K. W., Munsell, M. F., Ellen Jackson, C., & Konopleva, M. (2007). Rapamycin derivatives reduce mTORC2 signaling and inhibit AKT activation in AML. *Blood*, *109*(8), 3509-3512.

Zhu, J., & Thompson, C. B. (2019). Metabolic regulation of cell growth and proliferation. *Nature reviews Molecular cell biology*, *20*(7), 436-450.